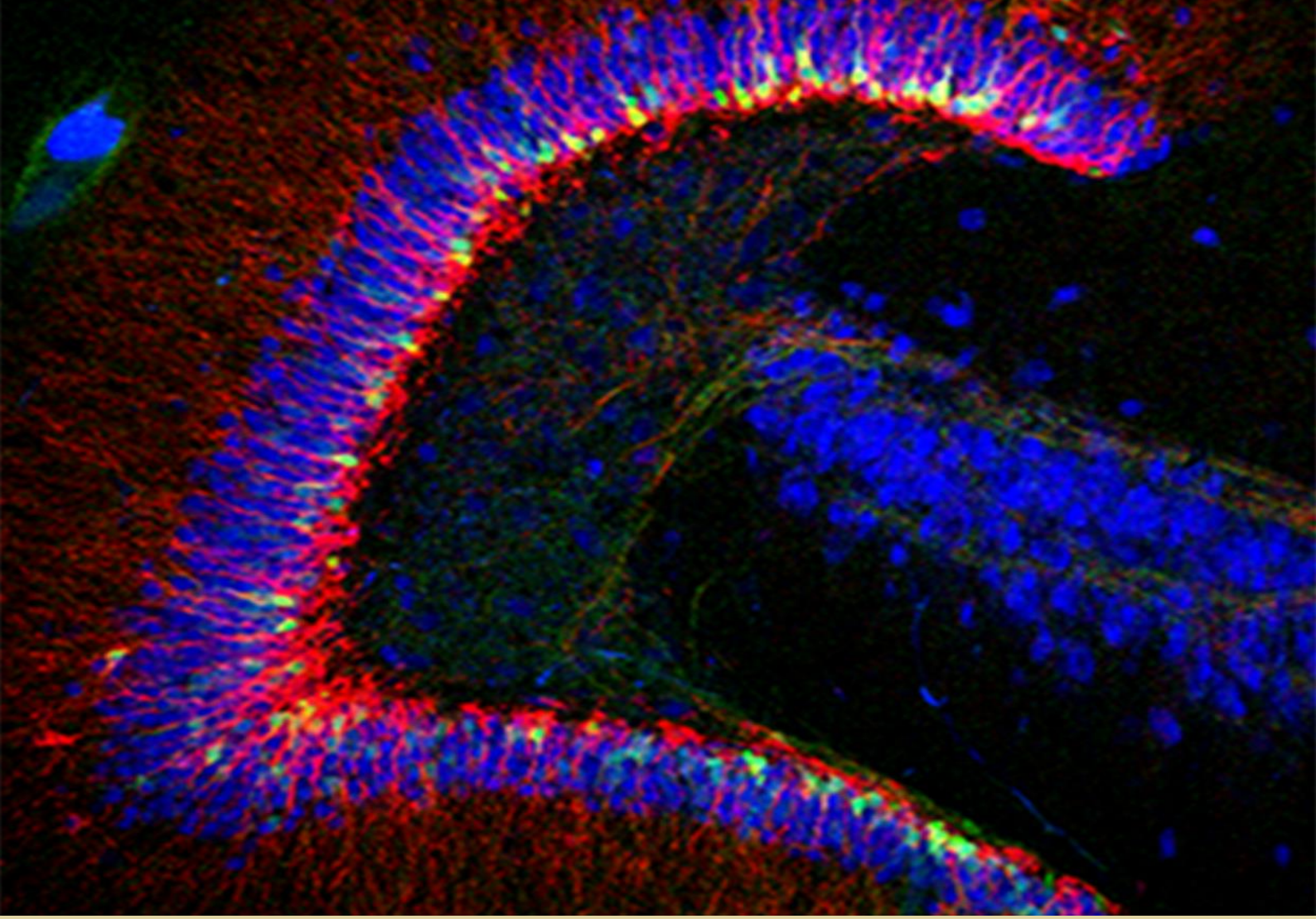

Ana Sofia Simões Bento Baptista

IMPACT OF METHAMPHETAMINE ON DENTATE GYRUS NEUROGENESIS: THE UNDERLYING MECHANISMS AND THE ROLE OF NEUROPEPTIDE Y

Doctoral thesis in Health Sciences (Biomedical Sciences), supervised by Doctor Ana Paula Silva Martins and co-supervised by Doctor Fabienne Agasse, and presented to the Faculty of Medicine of the University of Coimbra

July 2014

· U C ·

Universidade de Coimbra

Cover:

Image of the dentate gyrus expressing green fluorescent protein (green), doublecortin (red) and NeuN (blue) from G42 (GAD67-GFP) mouse hippocampus, obtained by confocal microscopy

Ana Sofia Simões Bento Baptista

O impacto da metanfetamina na neurogénese do giro dentado: estudo dos mecanismos subjacentes e do papel do neuropeptídeo Y

Impact of methamphetamine on dentate gyrus neurogenesis: the underlying mechanisms and the role of neuropeptide Y

UNIVERSIDADE DE COIMBRA

Tese de Doutoramento apresentada à Faculdade de Medicina da Universidade de Coimbra, para prestação de provas de Doutoramento em Ciências da Saúde, no ramo de Ciências Biomédicas.

Este trabalho foi realizado no Laboratório de Farmacologia e Terapêutica Experimental, no Instituto de Imagem Biomédica e Ciências da Vida (IBILI), da Faculdade de Medicina da Universidade de Coimbra, sob orientação da Doutora Ana Paula Silva Martins e co-orientação da Doutora Fabienne Agasse, e no *Institut du Cerveau et de la Moelle épinière*, Paris, França, sob a supervisão do Doutor Alberto Bacci, ao abrigo de uma bolsa de doutoramento financiada pela Fundação para a Ciência e a Tecnologia (SFRH / BD / 63773 / 2009), co-financiada pelo Quadro de Referência de Estratégia Nacional (Fundo Social Europeu).

Agradecimentos

"Agradeço" é a palavra que mais utilizo neste espaço. Nunca poderia chegar até aqui sem o apoio de todos que, de forma diferente, contribuíram para a concretização deste trabalho. Apenas duas palavras: Muito obrigada!

À Doutora Ana Paula Silva quero agradecer por me ter aceitado no seu grupo. Agradeço especialmente as suas críticas construtivas que tanto contribuíram para a concretização deste trabalho. Tenho ainda de salientar a sua clarividência na discussão dos resultados que tanto me ajudaram a evoluir na área da investigação. Não posso deixar de agradecer a sua amizade durante todos estes anos.

À Doutora Fabienne Agasse, agradeço a sua disponibilidade na orientação na bancada e por ter partilhado os seus conhecimento que tanto me ajudaram a evoluir no laboratório. Obrigada pelo companheirismo tanto no laboratório como nas passeatas por Paris. *Merci beaucoup!*

To Doctor Alberto Bacci, I thank the opportunity to do part of my work in his laboratory. I have to express my gratitude for the precious suggestions that helped to improve this thesis. Finally, thank you for the good moments that I spent in the lab. *Grazie mille!*

À Professora Doutora Tice Macedo, ao Professor Doutor Carlos Fontes Ribeiro, ao Doutor Francisco Ambrósio e ao Professor Doutor Frederico Teixeira e, agradeço o apoio prestado e a oportunidade de desenvolver o meu trabalho no Laboratório de Farmacologia e Terapêutica Experimental.

À Joana Gonçalves agradeço tudo o que me ensinou e toda a ajuda que me prestou no laboratório. Mas, mais importante, agradeço a sua amizade e os bons momentos passados fora do lab. Obrigada por tudo.

À Tania, à Vanessa e ao Ricardo, obrigada pela vossa amizade tanto no laboratório como fora dele.

To all people from the Bacci lab, thank you for all the help, support and most importantly for the friendship. A special thanks to Joana, Charlotte, Camille, Giulia, Geeske and Martin for the good moments in and outside the lab.

À Patrícia e ao Zé agradeço a sua amizade, disponibilidade e ajuda durante estes quatro anos de doutoramento.

A todos os colegas e amigos da linha de investigação *Ocular and brain diseases: pharmacology and experimental therapeutics* e do Laboratório de Farmacologia e Terapêutica Experimental, muito obrigada pelo apoio e amizade.

Aos meus pais, quero agradecer o seu amor incondicional, todo o apoio e encorajamento para que este trabalho se tornasse possível. Obrigada por estarem sempre ao meu lado!

À minha irmã quero agradecer todo o seu apoio incondicional e companheirismo. O teu ombro foi importante para mim!

À Palmira, Ângela, Afonso e Ricardo, obrigada pelos bons momentos partilhados, bem como o apoio.

Ao meu tio Tonito, obrigada por te teres preocupado para que nunca estivesse sozinha.

Aos meus amigos que me acompanham durante as férias e em todos os momentos que estou em Portugal!

Agradeço à Fundação para a Ciência e a Tecnologia, a bolsa de doutoramento atribuída (SFRH/BD/63773/2009), financiada pelo POPH - QREN, comparticipado pela União Europeia e Fundo Europeu de Desenvolvimento regional e por fundos nacionais do Ministério da Ciência, Tecnologia e Ensino Superior.

Index

Abbreviations

5-HT1A	Serotonin receptor 1A
Abbreviations	
ACSF	Artificial cerebrospinal fluid
AMPA	α-Amino-3-hydroxy-5-methyl-4-isoxazole propionic acid
AMPH	Amphetamine
AP	Action potential
AraC	Cytosine β-D-arabinofuranoside
ATP	Adenosine triphosphate
Bad	Bcl-2-associated death promoter protein
Bak	Bcl-2 homologous antagonist/killer protein
Bax	Bcl-2-associated X protein
BBB	Blood-brain barrier
Bcl-2	B-cell lymphoma 2 protein
Bclw	Bcl-2-like protein 2
Bcl-X_L	B-cell lymphoma-extra large protein
bFGF-2	basic Fibroblast growth factor 2
Bid	BH3 interacting-domain
BMVEC	Brain microvascular endothelial cell
BrdU	5-bromo-2'-deoxyuridine
CA1	C*ornu ammonis* 1
CA2	C*ornu ammonis* 2
Ca^{2+}	Calcium
CA3	C*ornu ammonis* 3
CaMKII	Calcium/calmodulin-dependent kinase II
cAMP	3'-5'-cyclic adenosine monophosphate
Cdk2	Cyclin-dependent kinase 2
cGMP	cyclic Guanosine monophosphate
C_m	Membrane capacitance
CNS	Central nervous system
CPON	C-flanked peptide of NPY
CuZnSOD	Superoxide dismutase
D1	Dopamine D1 receptor
D2	Dopamine D2 receptor
D3	Dopamine D3 receptor
D4	Dopamine D4 receptor
D5	Dopamine D5 receptor
DA	Dopamine
DAT	Dopamine transporter
DCG-IV	(2*S*,2'*R*,3'*R*)-2-(2',3')-dicarboxycyclopropyl)glycine
DCX	Doublecortin
DG	Dentate gyrus
DGCs	Dentate granule cells
EC	Entorhinal cortex
EGF	Epidermal growth factor
EGFR	Epidermal growth factor receptor
eNOS	Endothelial nitric oxide synthase
EPSCs	Excitatory postsynaptic currents
EPSPs	Excitatory postsynaptic potentials

ERK1/2	Extracellular-signal-regulated kinases 1/2
fEPSPs	field excitatory postsynaptic potentials
FGFR1	Fibroblast growth factor receptor 1
GABA	Gamma-aminobutyric acid
GAD67	Glutamate decarboxylase (67 kDa)
GFAP	Glial fibrillary acidic protein
GFP	Green fluorescent protein
GluA2	AMPA receptor subunit 2
GluN1	NMDA receptor subunit 2A
GluN2A	NMDA receptor subunit 2A
GluN2B	NMDA receptor subunit 2B
GSSG	Glutathione in its oxidized form
HPLC-EC	High performance liquid chromatography with electrochemical detection
IL-1α	Interleukin-1 alpha
IL-1β	Interleukin-1 beta
IL-6	Interleukin-6
K^+	Potassium
KA	Kainate
KCC2	K^+-Cl^- co-transporter
LFS	Low frequency stimulation
LPP	Lateral perforant pathway
LTD	Long-term depression
LTP	Long-term potentiation
MAPK	Mitogen-activated protein kinase
MDA	Malondialdehyde
MDMA	3,4-Methylenedioxymethamphetamine
METH	Methamphetamine
Mg^{2+}	Magnesium
mGlu	metabotropic glutamate receptor
mPFC	medial Prefrontal cortex
MPP	Medial perforant pathway
mRNA	messenger RNA
MWM	Morris water Maze
Na^+	Sodium
NeuN	Neuronal nuclei protein
NeuroD	Neuronal differentiation
NKCC1	Na^+-K^+-$2Cl^-$ co-transporter
NMDA	N-methyl-D-aspartate
nNOS	Neuronal nitric oxide synthase
NO	Nitric oxide
NPY	Neuropeptide Y
PI	Propidium iodide
PKA	Protein kinase A
PKC	Protein kinase C
PP	Pancreatic polypeptide
Prox 1	Prospero-related homeobox 1
PSA-NCAM	Polysialylated-neural cell adhesion molecule
PV	Parvalbumin
PYY	Peptide YY
R_{in}	Input resistance
RMP	Resting membrane potential

SGZ	Subgranular zone
Sox2	SRY (sex determining region Y)-box 2
SVZ	Subventricular zone
TBS	Theta-burst stimulation
TJ	Tight junction
TNF-α	Tumor necrosis factor-alpha
TTX	Tetradotoxin
Tuj1	Neuron-specific class III beta-tubulin
TUNEL	Terminal deoxynucleotidyl transferase dUTP nick-end labeling
VGCCs	Voltage-gated Ca^{2+} channels
VGLUT1	Vesicular glutamate transporter-1
VMAT-2	Vesicular monoamine transporter-2
Z-VAD	z-Val-Ala-DL-Asp (OMe)-fluoromethylketone

Publications

The results presented in Chapter 2 were resubmitted for publication in an international peer-reviewed journal:

Baptista S, Lasgi C, Benstaali C, Milhazes N, Borges F, Fontes-Ribeiro C, Agasse S, Silva AP (2014). Methamphetamine decreases dentate gyrus stem cell self-renewal and shifts the differentiation towards neuronal fate. Stem Cell Res.

The results presented in Chapter 3 were published in an international peer-reviewed journal:

Baptista S, Bento AR, Gonçalves J, Bernardino L, Summavielle T, Lobo A, Fontes-Ribeiro C, Malva JO, Agasse F, silva AP (2012). Neuropeptide Y promotes neurogenesis and protection against methamphetamine-induced toxicity in mouse dentate gyrus-derived neurosphere cultures. Neuropharmacology 62: 2413–2423.

The following reviews also contributed for the present thesis:

Gonçalves J, Martins J, Baptista S, Ambrósio AF, Silva AP (2014). Relevance of the central neuropeptide Y system upon drug of abuse consumption. Addict. Biol. *In revision*

Gonçalves J, Baptista S, Silva AP (2014). Psychostimulants and brain dysfunction: A review of the relevant neurotoxic effects. Neuropharmacology 14.

Malva JO, Xapelli S, Baptista S, Valero J, Agasse F, Ferreira R, Silva AP (2012). Multifaces of neuropeptide Y in the brain--neuroprotection, neurogenesis and neuroinflammation. Neuropeptides 46: 299–308.

Silva AP, Martins T, Baptista S, Gonçalves J, Agasse F, Malva JO (2010). Brain injury associated with widely abused amphetamines: neuroinflammation, neurogenesis and blood-brain barrier. Curr Drug Abuse Rev 3: 239–254.

The results presented in Chapter 2 and Chapter 3 are formatted according to the journal where papers were published or submitted for publication, with minor modifications.

Resumo

A metanfetamina (MET) é uma droga de abuso, cujo consumo tem vindo a aumentar a nível mundial. Vários estudos mostraram que o consumo de MET induz danos irreversíveis a nível cerebral, reflectindo-se em défices cognitivos. Apesar dos mecanismos serem ainda pouco conhecidos, tem sido sugerido que a neurogénese do giro dentado (GD) poderá contribuir para estes défices, uma vez que tem um papel fundamental na cognição. No geral, a MET tem um impacto negativo na neurogénese do GD, nomeadamente na proliferação celular e na diferenciação em neurónios. Por outro lado, tem sido demonstrado que o neuropeptídeo Y (NPY) exibe propriedades protectoras, pró-proliferativas e pró-neurogénicas. Para melhor perceber os mecanismos implícitos nos défices cognitivos induzidos pela MET, o nosso objectivo consistiu em estudar o seu efeito na neurogénese do GD, focando principalmente na capacidade de auto-renovação das células estaminais, na diferenciação em neurónios e nas propriedades funcionais dos neurónios imaturos e maturos. Mais ainda, o papel protector do NPY foi avaliado na tentativa de identificarmos um potencial alvo terapêutico contra os efeitos nefastos provocados pela MET na neurogénese do GD.

Neste trabalho, usámos neuroesferas do GD para estudar o impacto da MET nas propriedades de auto-renovação das células estaminais. Verificámos que a MET (1 nM) retarda a progressão do ciclo celular da fase G0/G1 para a fase S, aumentando o número de células na fase G0, acompanhado pela diminuição da expressão da ciclina E. Em paralelo, a MET diminuiu os níveis de fosforilação do receptor do factor de crescimento da epiderme (*FGFR*) e da proteína cinase regulada por sinal extracelular (*ERK*). Além disso, a MET (10 nM) diminuiu a capacidade de auto-renovação das células estaminais do GD verificado pela diminuição do número de neuroesferas. No entanto, a MET diminuiu a divisão celular no sentido da auto-renovação (pares de células $Sox2^{+}/Sox2^{+}$) aumentando no sentido da diferenciação (pares de células $Sox2^{-}/Sox2^{-}$), tendo sido este efeito mediado por receptores N-metil-D-aspartato (NMDA). Em concordância, verificámos que o fenótipo neuronal foi preferencialmente gerado. Em conclusão, a MET afectou negativamente a proliferação e a auto-renovação das células estaminais, mas levando à sua diferenciação em neurónios.

No presente trabalho, foi também explorado o efeito da MET na morte celular, proliferação e diferenciação neuronal em culturas derivadas de neuroesferas do GD, bem como o papel protector do NPY. Estas culturas foram expostas a diferentes concentrações de MET (1 – 1000 nM) e foi verificado um aumento da morte celular por apoptose e por necrose para concentrações superiores a 10 nM sem, no entanto, afectar a proliferação celular. Mais ainda, a MET aumentou a libertação de glutamato, e a inibição dos receptores NMDA preveniu a morte

celular por apoptose. Curiosamente, a MET diminuiu a diferenciação em neurónios para todas as concentrações testadas, inclusivamente a concentração não tóxica (1 nM). O NPY conseguiu prevenir a morte celular por apoptose induzida pela MET, através da activação dos receptores Y_1 ou Y_2, bem como o aumento da libertação de glutamato induzida pela MET. Por outro lado, o NPY preveniu também a diminuição do número de neurónios maturos provocada pela MET através da activação dos receptores Y_1. É ainda de salientar que, por si só, o NPY promoveu a proliferação e a diferenciação neuronal através da activação dos receptores Y_1. Em resumo, a MET teve um impacto negativo na viabilidade e neurogénese das células do GD, mas o NPY revelou-se uma ferramenta promissora contra estes feitos nefastos.

O efeito da MET na neurogénese e nas propriedades funcionais dos neurónios imaturos e maturos foram avaliados num modelo animal de neurogénese no GD, os murganhos G42 (*GAD67-GFP*), em que os neurónios imaturos são identificados pela expressão da proteína verde fluorescente (*GFP*). Assim, os animais foram administrados com 2 mg/kg de MET, uma vez por dia durante 7 dias. A MET promoveu a diferenciação dos neurónios imaturos sem alterar o seu número. Contudo, a MET não teve qualquer efeito na cinética dos potenciais de acção (PAs) nem nas propriedades passivas de membrana (capacitância, resistência de membrana e potencial de membrana em repouso). As células GFP^+ do grupo 2 e do grupo 3, que geram poucos PAs ou alta frequência de PAs, respectivamente, geraram correntes pós-sinápticas excitatórias (CPSEs), exibindo também potenciação após aplicação de trens de estimulação nas fibras do córtex entorrinal medial. Curiosamente, a MET induziu potenciação de longa duração (PLD) nas células do grupo 3, enquanto nas células maturas aumentou a amplitude da PLD. Em conclusão, a MET induziu diferenciação dos neurónios imaturos, incitou PLD nas células GFP^+ do grupo 3 e gerou maior PLD nas células granulares maturas.

Abstract

Methamphetamine (METH) is a drug of abuse, whose consumption has been increasing worldwide. Several studies reported that METH causes irreversible brain abnormalities that may reflect in cognitive deficits. Despite the fact that the underlying mechanisms are still not well known, it has been suggested that dentate gyrus (DG) neurogenesis may contribute to these deficits, since it plays an essential role in cognition. In general, METH exerts a negative impact in DG neurogenesis. In contrast, several studies evidenced that neuropeptide Y (NPY) displays neuroprotection and enhances proliferation and neurogenesis in the DG. Therefore, we aimed to study the effect of METH in DG neurogenesis, specifically looking to DG stem cell capacities, neuronal differentiation and functional properties of immature neurons. Furthermore, we unraveled if NPY could be a therapeutic target against the injurious effects caused by METH in DG neurogenesis.

In the present work, we took advantage of DG neurosphere cultures to study the impact of METH on DG stem cell self-renewal functions. We observed that METH (1 nM) delayed cell cycle from G0/G1 to S phase transition, increasing the number of cells in the quiescent state (G0). In fact, these data correlated with a decrease in cyclin E expression. Also, METH decreased the phosphorylation levels of the epidermal growth factor receptors (EGFR) and extracellular-signal-regulated kinase 1/2 (ERK1/2) protein levels. Moreover, METH (10 nM) decreased DG stem cell self-renewal as verified by the decrease in the number of secondary neurospheres. However, METH shifted DG cell division from self-renewal ($Sox2^+/Sox2^+$ pairs of daughter cells) to differentiation ($Sox2^-/Sox2^-$ pairs of daughter cells), an effect mediated by N-methyl-D-aspartate (NMDA) receptor activation. In agreement, METH (10 nM) increased immature neurons in DG neurospheres. Overall, METH altered DG stem cell properties by delaying cell cycle and decreasing self-renewal capacities by shifting DG stem cell proliferation or self-renewal to differentiation towards neuronal fate.

We also investigated the effect of METH on cell death, proliferation and differentiation in DG-derived neurosphere cultures, as well as the protective role of NPY. Cultures were exposed to different concentrations of METH (1 – 1000 nM) and an increase in cell death by necrosis and apoptosis was verified to concentrations up to 10 nM. Furthermore, METH (10 nM) increased glutamate release, and inhibition of NMDA receptors prevented cell death by apoptosis. Interestingly, METH decreased neuronal differentiation at all concentrations tested, including at the nontoxic concentration (1 nM). On the other hand, NPY prevented apoptotic cell death *via* activation of Y_1 or Y_2 receptor subtypes, as well as prevented glutamate release induced by METH. Again, the protective effect of NPY *via* Y_1 receptors was verified as it

prevented the decrease of mature neurons induced by METH. Besides, NPY by itself promoted cell proliferation and neuronal differentiation once again through activation of Y_1 receptors. Taken together, METH negatively affects DG cell viability and neurogenesis, and NPY revealed to be a promising protective tool against the deleterious effects of METH on hippocampal neurogenesis.

The effect of METH on the functional properties of new neurons was performed using an animal model of DG neurogenesis, the G42 (GAD67-GFP) mice, where immature neurons express the green fluorescent protein (GFP). Thus, mice were administered with 2 mg/kg METH (i.p.), once a day for 7 days. As a result, we found that METH promoted differentiation of GFP^+ cells without changing their number. However, METH had no effect in action potential (AP) firing kinetics or in passive membrane properties (membrane capacitance, input resistance and resting membrane potential). Furthermore, GFP^+ cells (group 2 and group 3, generating few or high frequency APs, respectively) generated excitatory postsynaptic currents (EPSCs) as well as potentiation upon medial perforant pathway (MPP) fiber stimulation. Interestingly, METH induced long-term potentiation (LTP) in group 3 cells, whereas generated a stronger LTP in mature DG neurons. In conclusion, METH leads to immature neurons differentiation, induces LTP in group 3 GFP^+ cells and strengths LTP in mature DG neurons.

Chapter 1

Introduction

1. Introduction

1.1. Methamphetamine

1.1.1. General properties of methamphetamine

Methamphetamine (METH) belongs to the family of the amphetamine-like drugs, which also include amphetamine (AMPH) and 3,4-Methylenedioxymethamphetamine (MDMA, ecstasy). The structure of these drugs is very similar with the neurotransmitter dopamine (DA) (Fleckenstein et al., 2007; Figure 1.1) and, indeed, amphetamines exert their psychoactive action by mainly affecting the dopaminergic system (Neve et al., 2004).

METH is easily manufactured due to the easy access and low cost of reagents, resulting in an increase use worldwide (United Nations Office on Drugs and Crime, 2011). This drug is commonly known as *crystal*, *meth*, *speed*, *crank* or *ice*, and can be found in powder, tablets, paste or crystalline form (Figure 1.1), being administered intravenously, orally, by inhalation or smoked. The physiological and behavioral alterations observed in METH abusers may include hypertension, hyperthermia, cerebrovascular hemorrhage, stroke, seizures, renal and liver failure (Albertson et al., 1999; Perez et al., 1999), cognitive deficits, agitation, aggressiveness, paranoia, and psychosis (reviewed by Cadet and Krasnova, 2009). Also, cessation of regular METH use induces sleep disturbance, anxiety, hyperphagia and craving (Cruickshank and Dyer, 2009).

METH is a lipophilic molecule with a low molecular weight (149.24 g/mol), and has weak base properties and low protein binding ability, which allows its passive diffusion into the brain, cells and vesicular compartments (de la Torre et al., 2004). In fact, our group characterized the time-course changes of METH levels in plasma and brain from mice administered with 30 mg/kg METH (i.p.), and we concluded that within 1 h, METH diffused fast to circulation and rapidly reached the brain (Martins et al., 2011). Moreover, METH can be metabolized in the human liver microsomes through the activation of the cytochrome P450 2D6, yielding the formation of two metabolites: AMPH, which results from the N-demethylation of METH, and 4-hydroxymethamphetamine, resulting from its aromatic hydroxylation (Lin et al., 1997; Cruickshank and Dyer, 2009). In the rat, METH can be excreted in urine as METH (30-50%) and as several metabolites, such as 4-hydroxymethamphetamine, AMPH, 4-hydroxynorephedrine and 4-hydroxyamphetamine. Noteworthy, intraperitoneal (i.p.) injection of METH leads to a faster excretion than oral administration (Caldwell et al., 1972). In fact, our group observed that 1 h after METH administration (30 mg/kg, i.p.), AMPH was also significantly detectable in both plasma and brain (Martins et al., 2011).

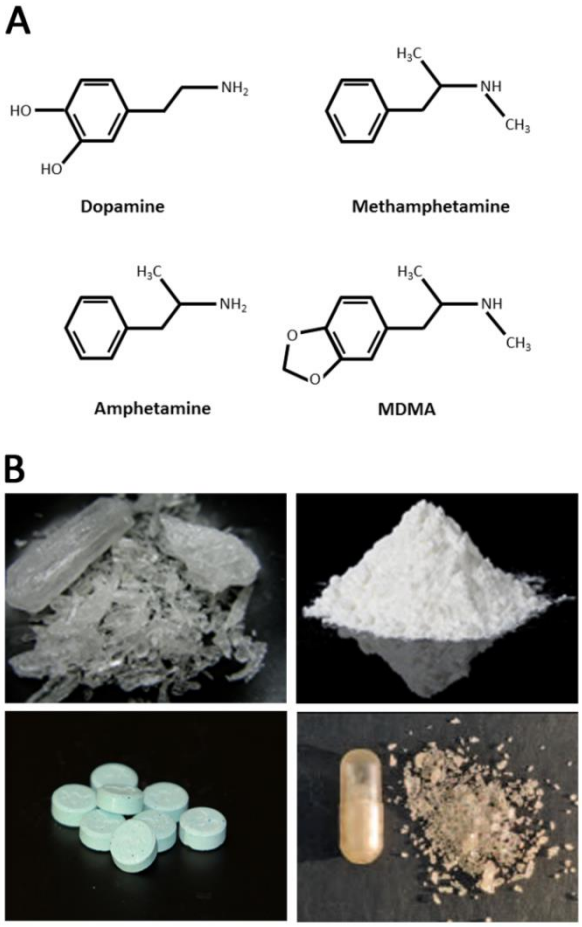

Figure 1.1 – (A) Chemical structure of DA and amphetamine-like drugs such as AMPH, METH and MDMA (ecstasy). (B) Methamphetamine can be found as crystals, powder, tablets or capsules. Adapted from Fleckenstein et al., 2007.

1.1.2. Methamphetamine neurotoxicity

Dopaminergic deregulation

DA is a neurotransmitter that, upon binding and activation of D1, D2, D3, D4 and D5 receptors, plays a major role in motor control, motivation, cognition and reward behavior (Schultz, 2007). In addition, DA autorreceptors localized presynaptically function as modulators in the control of neuronal firing rating and neurotransmitter release (Beaulieu and Gainetdinov, 2011). DA action is terminated by uptake from the extracellular space into presynaptic terminals *via* dopamine transporter (DAT) and then stored in synaptic vesicles *via* the vesicular monoamine transporter-2 (VMAT-2; Riddle et al., 2006; Figure 1.2 A). In fact, due to its similar structure to DA, METH has the particularity to have high affinity to DAT and VMAT-2 (Yamamoto et al., 2010). Accordingly, METH promotes the release of DA from nerve endings, increasing its

extracellular levels (Kish, 2008), therefore, inhibiting DA uptake *via* VMAT-2 (Brown et al., 2000) and DAT (Fleckenstein et al., 1997; Figure 1.2 B). Specifically, Sandoval and collaborators (2000) demonstrated that METH (4x 5 or 10 mg/kg, 2 h apart, s.c.) decreases DAT activity in mice striatal synaptosomes that persists after synaptosome wash (Sandoval et al., 2000). METH-induced alterations in dopaminergic neurons is not restricted to DAT as this drug is also able to decrease VMAT-2 immunoreactivity in striatal synaptosomes, enhancing monoaminergic deficits (Hadlock et al., 2010).

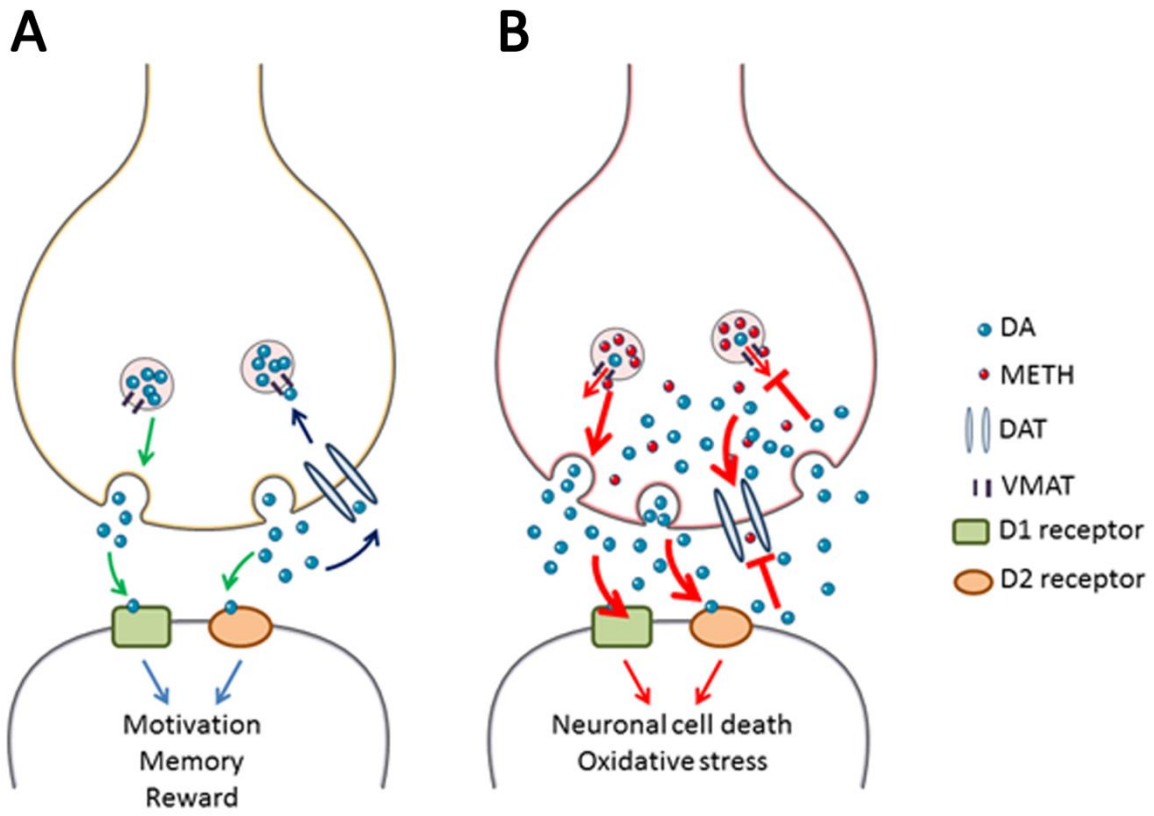

Figure 1.2 – METH-induced alterations on dopaminergic system. In the absence of METH (A), DA is released from the presynaptic terminals and will activate DA receptors (green arrows), which activation is involved in motivational, memory and reward processes. Afterwards, cytoplasmic uptake of DA is mediated by DAT, whereas vesicular uptake occurs *via* VMAT-2 (dark blue arrows). In the presence of METH (B), DA release from vesicles, presynaptic terminals, and by DAT and VMAT-2 reverse transport is increased (red arrows) while DA uptake is inhibited, resulting in overactivation of DA receptors and long-term METH intake will lead to dopaminergic deficits.

The activation of DA receptors upon METH exposure induced dopaminergic deficits as described by O'Dell and collaborators (1993). Indeed, inhibition of D1 or D2 receptors prevented DA depletion in rat striatum after a binge administration of METH (4x 4 mg/kg, 2 h apart, s.c.). Furthermore, the inhibition of the same receptors was able to prevent the increased release of

DA induced by METH administration (O'Dell et al., 1993). Additionally, METH-induced loss of VMAT-2 by activation of D2 receptors, through a mechanism that involved astrocytic activation (Hadlock et al., 2010). Besides, the activation of neuronal nitric oxide synthase (nNOS) may be a reliable mechanism of METH-induced DA depletion, since its inhibition (Di Monte et al., 1996) or deletion (Itzhak et al., 1998) can prevent these effects.

Overall, METH changes dopaminergic homeostasis in the central nervous system (CNS) by enhancing the release of DA from nerve terminals, inhibiting its uptake and overactivating DA receptors that will trigger neurotoxic events (Figure 1.2 B).

Glutamatergic dysfunction and excitotoxicity

Glutamate is the main excitatory neurotransmission in the CNS. Glutamatergic transmission occurs *via* activation of ionotropic N-methyl-D-aspartate (NMDA), α-amino-3-hydroxy-5-methyl-4-isoxazole propionic acid (AMPA) and kainate (KA) receptors, or metabotropic G protein-coupled receptors (Tata and Yamamoto, 2007).

In addition to the afore-mentioned effects on dopaminergic system, several pieces of evidence indicate that METH interferes with the glutamatergic system in several brain regions (reviewed by Silva et al., 2010; Gonçalves et al., 2014). Indeed, Yamamoto and colleagues (1999) showed that glutamatergic transmission is decreased by METH due to presynaptic hypoactivity in behaviorally sensitized rats, an effect that could be mediated by NMDA receptor activation. Furthermore, binge administration of METH (4x 10 mg/kg every 2 h, i.p.) increased glutamate release in rat lateral striatum that was maintained for 24 h after the last METH injection (Mark et al., 2007). Importantly, this finding was corroborated with up-regulation of vesicular glutamate transporter-1 (VGLUT1) mRNA in the cortex and VGLUT1 protein in the striatum, suggesting enhanced glutamatergic neurotransmission (Mark et al., 2007). In the hippocampus, METH (3x 7.5 mg/kg, 2 h apart, i.p.) increased extracellular glutamate after each administration that persisted 7 h after the last drug injection (Rocher and Gardier, 2001).

One of the mechanisms underlying METH-induced excitotoxicity involves calcium (Ca^{2+}) release from intracellular stores. Indeed, inhibition of Ca^{2+} release from the endoplasmic reticulum prevented METH excitotoxicity in hippocampal cultures, which was dependent on NMDA receptor activation (Smith et al., 2010). Other possible mechanisms may include alterations in the expression of glutamate receptor subunits. Indeed, Simões and collaborators (2007) observed that a single dose of METH (30 mg/kg, i.p.) increased GluN2A and GluA2 subunit protein levels in rat hippocampus. Importantly, alterations in glutamatergic receptors may contribute to spatial memory deficits observed in these animals. In agreement with the above-

mentioned effects in the hippocampus, cortical and striatal GluA2 subunit levels were increased, together with a decrease and increase levels of GluN1 and GluN2A, respectively (Simões et al., 2007). These and others studies have suggested that brain regions react differently under METH exposure. Noteworthy, not only may the glutamatergic system be involved in the development of excitotoxic events, but also could play a role in mechanisms of addiction (Crawford et al., 2013). Indeed, activation of group II metabotropic glutamate receptor (mGluR) by LY379268 (0.3 or 1 mg/kg, i.p.), whose activation decreases glutamate release, attenuated the motivation for METH self-administration (0.05 mg/kg/infusion, 6 h/day for 14 days).

In conclusion, alterations of glutamatergic transmission (glutamate release and receptor subunit expression) depend on the frequency of METH exposure, and can induce excitotoxicity.

Mitochondrial dysfunction and oxidative stress

Mitochondria are the cellular organelles mainly responsible for energy production (adenosine triphosphate, ATP, production), regulation of cellular metabolism, and maintenance of Ca^{2+} homeostasis (Picard et al., 2011). METH was able to interfere with the mitochondrial electron transport chain, specifically the complex I (Klongpanichapak et al., 2006), complex II-III (Brown et al., 2005) and complex IV, which could slow the production of ATP (Burrows et al., 2000). Regarding *in vitro* studies, Tian and collaborators (2009) verified that METH (100 or 300 µM) induced severe damage to mitochondria (mitochondrial fragmentation) in rat hippocampal progenitor cells. Indeed, mitochondria are tightly involved in apoptotic events and these can be enhanced by a high dose of METH (40 mg/kg, i.p.) as demonstrated by Jayanthi and collaborators (2001). Specifically, it was shown that METH up-regulates the pro-apoptotic proteins Bax, Bad, Bak and Bid in mice cortex (Jayanthi et al., 2001). On the other hand, the same authors observed that the anti-apoptotic proteins Bcl-2, Bcl-X_L and Bclw were down-regulated in the same brain region (Jayanthi et al., 2001). Moreover, it was proposed that METH activates apoptotic mediators in the mitochondria, leading to their translocation into the nucleus, thus resulting in DNA fragmentation (Jayanthi et al., 2004). Interestingly, our group showed that METH triggers apoptotic cell death to subventricular zone (SVZ) stem/progenitor cells, in agreement with the increase of caspase-3 activity (Bento et al., 2011).

METH use or exposure increases the release of vesicular and cytoplasmic DA towards the cytoplasm and the extracellular space (Iversen, 2006). In fact, due to their acidic pH, synaptic vesicles maintain DA to its reduced state and, when DA is outside the vesicular-reducing environment is oxidized to 5-cystein-DA and DA quinones, becoming reactive (LaVoie and Hastings, 1999; Krasnova and Cadet, 2009). Other oxidative mechanisms include lipid

peroxidation, which was verified by elevated levels of malondialdehyde (MDA, product resulted from lipid peroxidation) after METH administration in several brain areas, including striatum (Yamamoto and Zhu, 1998), caudate putamen, substantia nigra, ventral tegmental area, cortex and hippocampus (Horner et al., 2011). Accordingly, *post-mortem* brain analysis from METH users revealed that both lipid peroxidation and 4-hydroxynonenal (a product resulted from lipid peroxidation) are increased in the caudate nucleus and frontal cortex (Fitzmaurice et al., 2006). Moreover, protein carbonyls resulted from protein oxidation are increased in the hippocampus 24 h after a binge-administration of METH to Swiss mice (4x 10 mg/kg, i.p.; Gluck et al., 2001). Also, up-regulation of total glutathione was verified in mice striatum, frontal cortex and hippocampus, whereas an increase of glutathione peroxidase activity was only observed in the striatum and frontal cortex after a single dose of METH (10 mg/kg, i.p.; Flora et al., 2002). Interestingly, mice that overexpress superoxide dismutase (CuZnSOD), an enzyme that catalyses the breakdown of superoxide radicals, are protected against METH-induced toxicity (Cadet et al., 1994; Krasnova and Cadet, 2009). Additionally, increased activity of CuZnSOD and up-regulation of glutathione in its oxidized form (GSSG) were observed in caudate nucleus from METH users (Mirecki et al., 2004).

Overall, oxidative stress resulted from DA, lipid and protein oxidation, or by mitochondrial dysfunction induced by METH contributes to neuronal dysfunction and toxicity.

Hyperthermia

It is well documented that METH induces hyperthermia and that increase of body temperature contributes to METH-induced toxicity (reviewed by Silva et al., 2010; Gonçalves et al., 2014). Indeed, increase of environment temperature exacerbated striatal DA depletion triggered by METH (4x 5 mg/kg every 2 h, i.p.; Bowyer et al., 1994). On the other hand, DA and serotonin (5-HT) depletion caused by METH administration was attenuated when rats were placed in a cooled environment (5°C). Accordingly, blockade of METH-induced hyperthermia by maintaining rats in a cold room (5°C) completely prevented DA oxidation (LaVoie and Hastings, 1999). Also, hyperthermia induced by METH (9 mg/kg, s.c.) was the main contributor to the increase of blood-brain barrier (BBB) permeability (Kiyatkin ey al., 2007). Despite these data, some authors have highlighted that METH-induced toxicity can be independent of hyperthermia as, by itself, does not induce DA depletion (Bowyer, 1995). Nevertheless, it seems unquestionable that at least hyperthermia aggravates brain dysfunction triggered by METH.

Neuroinflammation and inflammatory mediators

In response to injury, the brain can trigger an inflammatory response also known as neuroinflammation. In fact, it has been suggested that glia and inflammatory mediators may contribute to METH-induced neuropathology (reviewed by Silva et al., 2010; Gonçalves et al., 2014). Importantly, our group demonstrated that an acute high dose of METH (30mg/kg, i.p.) induces a robust gliosis and up-regulation of tumor necrosis factor-alpha (TNF-α) and TNF receptor 1 protein levels, which can justify METH-induced neuronal dysfunction in the hippocampus (Gonçalves et al., 2010). Others have also shown that METH increases the levels of interleukin-1 alpha (IL-1α) and interleukin-6 (IL-6) mRNA in the striatum (Sriram et al., 2006), and IL-1β mRNA in the hypothalamus (Yamaguchi et al., 1991). Accordingly, our group showed that METH (30 mg/kg, i.p.) up-regulated TNF-α and IL-6 mRNA levels in mice hippocampus, but without changing IL-1β (Gonçalves et al., 2008). *In vitro* studies demonstrated that METH induced microglial cell death followed by increased expression of TNF- α and IL-6 protein levels and, interestingly, low concentrations of exogenous TNF-α was able to prevent the toxic effects mediated by METH through the activation of IL-6 signaling (Coelho-Santos et al., 2012). Moreover, METH-induced neuroinflammation in mouse hippocampal organotypic slice cultures was characterized by a marked microglial activation, which was further prevented by the activation of neuropeptide Y (NPY) Y_2 receptor subtype (Gonçalves et al., 2012a).

Overall, several studies have demonstrated that METH is able to trigger the activation of microglia cells and astrocytes, that will lead to the release of pro-inflammatory mediators and, therefore, contributing to neuronal dysfunction and toxicity.

Blood-brain barrier

More recently, it has been suggested that METH neurotoxicity may also result from its capacity to change blood-brain barrier (BBB) integrity (reviewed by Silva et al., 2010; Gonçalves et al., 2014). Indeed, some studies showed that METH increases BBB permeability in rodents, specifically in the cerebral cortex (Sharma and Ali, 2006), hippocampus, amygdala (Bowyer and Ali, 2006) and caudate-putamen (Bowyer et al., 2008). Also, our group observed that METH (30 mg/kg, i.p.) transiently increases BBB permeability in mice hippocampus, an effect that could be explained by the decrease of tight junction (TJ) proteins, such as the zonula occludens 1, claudin-5 and occludin, that are involved in the integrity maintenance of the BBB (Martins et al., 2011). Moreover, an increased activity of the metalloproteinase 9 could contribute to these alterations of the BBB function, probably due to the extracellular matrix degradation (Martins et al., 2011). Besides these animal studies, *in vitro* approaches demonstrated that METH can have a direct

effect on endothelial cells since it is able to alter human brain microvascular endothelial cell (BMVEC) properties followed by down-regulation of TJ proteins (Ramirez et al., 2009). On the other hand, our group observed that a low concentration of METH increases barrier permeability across BMVECs *via* eNOS/NO-mediated transcytosis but not involving alterations on TJ proteins (Martins et al., 2013). Thus, METH can alter BBB function through different mechanisms, which turns the brain more vulnerable to external factors including pathogens.

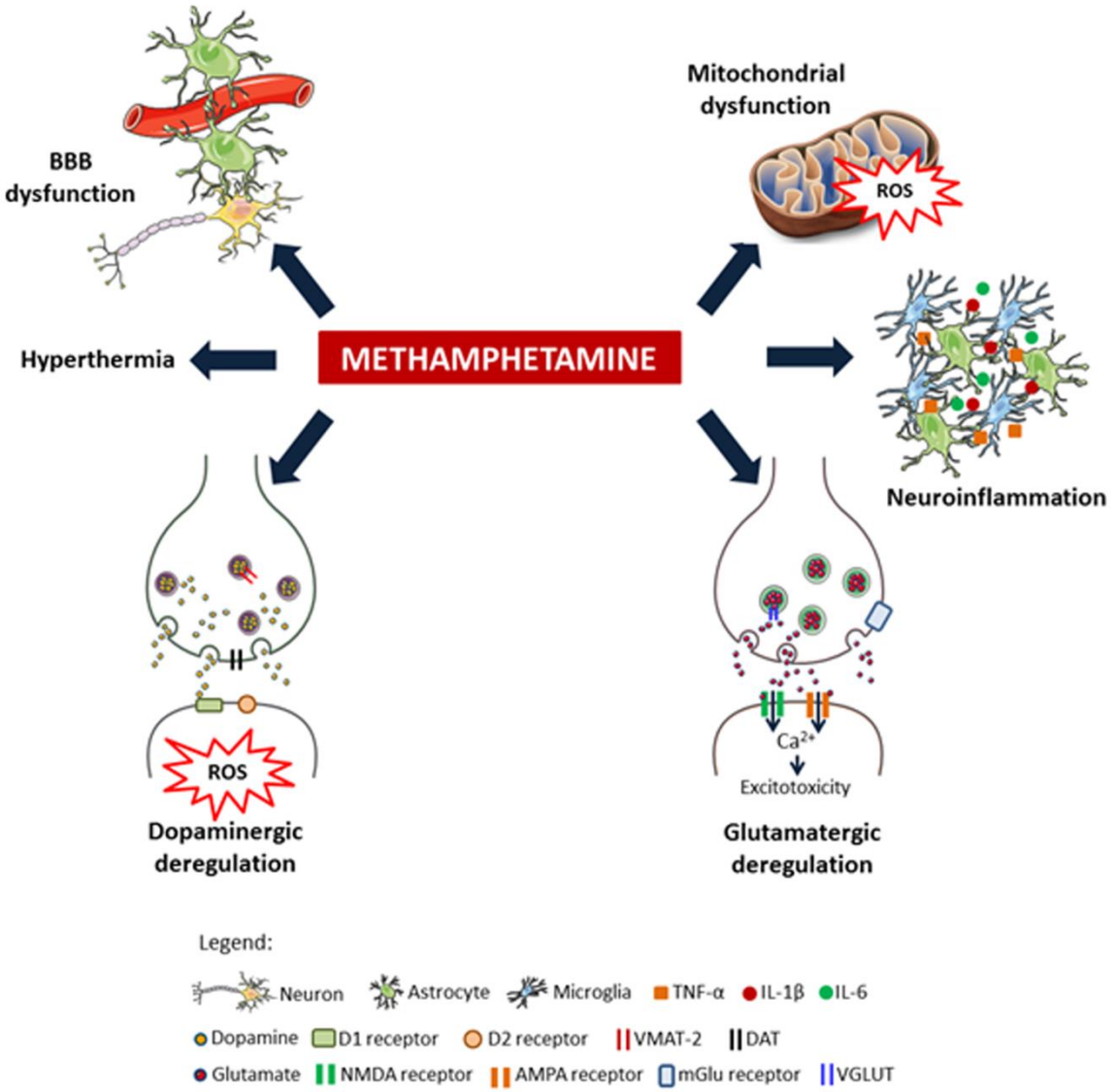

Figure 1.3 – Schematic representation of neurotoxicity induced by METH. Adapted from Gonçalves et al., 2014.

In summary, METH interferes with dopaminergic transmission that can trigger oxidative stress. Furthermore, METH induces changes in glutamatergic transmission, an effect that seems to be correlated with memory deficits observed in METH abusers. Besides, mitochondrial dysfunction, hyperthermia, neuroinflammation and BBB dysfunction can also contribute to METH-induced toxicity (Figure 1.3).

1.2. The hippocampus

The hippocampus was named due to its resemblance to the seahorse, *i.e.*, derives from the Greek *hippos* that means horse and *kampos*, meaning sea monster. The hippocampus is part of the forebrain, is located in the medial temporal lobe under the cerebral cortex and plays a crucial role in learning and memory as well as in the formation of new episodic memories (Li et al., 2009).

The hippocampus has a highly stereotypical connection pattern: information from the layer II of the entorhinal cortex (EC) enters the hippocampus forming the perforant pathway that passes the subiculum and establishes synaptic connections on the dentate gyrus (DG) and *cornu ammonis* 3 (CA3) areas (Neves et al., 2008; Figure 1.4). The perforant pathway can be distinguished in the medial (MPP) and lateral (LPP) perforant pathways whose axonal projections terminate specifically in the middle and outer third of the molecular layer of the DG, respectively. Dentate granule cells (DGCs) project their dendrites towards the molecular layer to receive synaptic inputs from both MPP and LPP, whereas the axons, or mossy fibers, reach the proximal dendrites of CA3 pyramidal cells (Deng et al., 2010; Figure 1.4). In turn, CA3 pyramidal cells project to other cells of the CA3 through commissural connections and to CA1 pyramidal cells through the Schaffer collateral projections. In addition, CA1 pyramidal neurons receive direct synaptic inputs from layer III of the EC and send axonal outputs towards the subiculum and the deep layers of the EC (Neves et al., 2008; Figure 1.4).

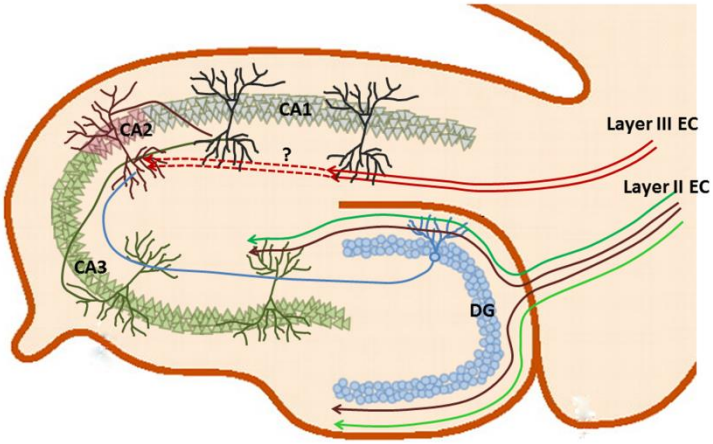

Figure 1.4 – Schematic representation of the cytoarchitecture of the hippocampus. The DG receives inputs from axons of the perforant path (in purple) that derive from layer II of the EC. DGCs project their axons or mossy fibers to the proximal apical dendrites of CA3 and CA2 pyramidal neurons. CA3 neurons, in turn, project into the ipsilateral CA1 pyramidal layer through the Schaffer collaterals. Also, projections from layer II and layer III of the EC contact directly with CA3 and CA1 pyramidal neurons, respectively.

In addition to this well-known trisynaptic pathway, other excitation circuits have been recently found, involving a population of larger pyramidal neurons that reside between the CA3 and CA1 areas, named CA2. Indeed, this region receives inputs from the supramammilary nucleus of the hypothalamus (Haglund et al., 1984; Maglóczky et al., 1994), and mossy fibers from the DG (Kohara et al., 2014). Still, it is controversial whether CA2 cells receive projections from layer III EC (Chevaleyre et al., 2010; Kohara et al., 2014), but form functional glutamatergic synapses with CA1 pyramidal neurons (Kohara et al., 2014).

1.2.1. Synaptic plasticity in the hippocampus

Long-term potentiation

The hippocampus plays an important role in learning and memory mainly due to a high level of synaptic plasticity (Neves et al., 2008). The DG of the hippocampus receives synaptic inputs from the MPP and the LPP characterized by different short-term plasticity properties. Indeed, paired-pulse stimulation of MPP results in short-term depression, whereas stimulation of the LPP shows short-term facilitation, suggesting high and low transmitter release probability, respectively (Colino and Malenka, 1993). On the other hand, DG neurons can experience long-lasting increase of synaptic strength in response to specific pre- and postsynaptic firing pattern, an effect identified as long-term potentiation (LTP; Bliss and Lømo, 1973). The mechanism for LTP induction in the DG may rely on an increase in neurotransmitter release, an increase in

postsynaptic response, or a combination of both (Bliss et al., 2003). In fact, an increase in glutamate release onto DG neurons resulted from high frequency stimulation of the perforant pathway will induce LTP (Dolphin et al., 1982). Also, several pieces of evidence demonstrated that LTP in DG cells are dependent on postsynaptic NMDA receptor activation (Colino and Malenka, 1993; Ge et al., 2007a; Kannangara et al., 2014). Specifically, blocking NMDA receptors impair LTP in the DG (Colino and Malenka, 1993; Ge et al., 2007a) and postsynaptic NMDA receptor-containing GluN2A subunits were shown to be important for synaptic plasticity and spatial memory performance (Kannangara et al., 2014). Also, plasticity of synapses between CA3 and CA1 pyramidal neurons have been object of intensive study. Indeed, CA3 and CA1 pyramidal neurons generate LTP in response to firing pattern at mossy fibers (Harris and Cotman, 1986; Yeckel et al., 1999) and Schaffer collaterals (Zakharenko et al., 2001; Bayazitov et al., 2007), respectively.

LTP induction in the hippocampus is induced by repetitive release of glutamate from the presynaptic terminals that leads to the activation of postsynaptic AMPA receptors followed by cell depolarization. The resulting postsynaptic neuron depolarization leads to removal of magnesium (Mg^{2+}) ions that block NMDA receptors, and Ca^{2+} ions are allowed to enter the cell. Also, voltage-gated Ca^{2+} channels (VGCCs) can be recruited for LTP induction (Lamprecht and LeDoux, 2004). Ca^{2+} influx through NMDA receptors or VGCCs trigger the delivery of new AMPA receptors into postsynaptic sites (process known as spine AMPAfication). This results in enhanced synaptic responses which last for several hours. Spines enriched with new AMPA receptors, in turn, can undergo structural changes through rearrangement of cytoskeletal microfilaments composed by F-actin (Fukazawa et al., 2003). In addition to the mechanism outlined above, other intracellular signaling pathways may ensure synaptic efficacy, such as the phosphorylation of calcium/calmodulin-dependent kinase II (CaMKII). Indeed, Ca^{2+} binds to CaMKII promoting the translocation from the cytoplasm to the synapse, which binds to GluN2B subunit of NMDA receptors (Barria and Malinow, 2005). This CaMKII activity results in the recruitment of AMPA receptors into the surface of dendritic spines (Hayashi et al., 2000). Indeed, the recruitment of AMPA is responsible for synaptic strengthening.

Long-term depression

Long-term depression (LTD) is defined as long-lasting decrease of synaptic plasticity strength. It has been suggested that hippocampal LTD is important for the processing of relevant information by deleting or inhibiting irrelevant information. Indeed, in the hippocampus, inhibition of NMDA receptor-dependent LTD impairs reversal learning (Nichols et al., 2008).

LTD induction at MPP synapses requires activation of all groups of mGlu receptors (group I, II and III mGlu receptors). In detail, activation of group I mGlu receptor induces LTD in a mechanism independent of NMDA receptor activation (Camodeca et al., 1999), but requires activation of Src family of non-receptor tyrosine kinases (Luttrell et al., 1999), which further activates p38 MAPK (Rush et al., 2002). These kinases, in turn, will phosphorylate transcription and translation factors, thereby regulating gene expression and protein synthesis (Kelleher et al., 2004; Thomas and Huganir, 2004). Moreover, activation of Group II mGlu receptors induces a rapid and prolonged depression of MPP-evoked excitatory postsynaptic potentials (EPSPs) after low frequency stimulation (LFS) (Pöschel and Manahan-Vaughan, 2005), and reversible depression of field EPSPs (fEPSPs) accompanied by a reduction of paired-pulse depression, suggesting a decrease of presynaptic neurotransmitter release (Huang et al., 1999). However, induction of LTD mediated by these receptors not only is dependent on presynaptic decrease of neurotransmitter release, but also is dependent on NMDA receptor activation. In the same context, activation of protein kinase A and C (PKA and C) seems to be downstream targets for LTD induction (Huang et al., 1999).

In addition to the abovementioned induction of LTD upon mGlu receptor activation, LTD can be also induced by a prolonged train of LFS (1-2 Hz) at the MPP (Huang et al., 1999) and LPP (Christie and Abraham, 1992). LFS-induced LTD requires postsynaptic elevation of intracellular Ca^{2+} concentration (O'Mara et al., 1995), specifically resulting from the activation of the nitric oxide (NO)-cyclic guanosine monophosphate (cGMP) pathway at postsynaptic sites followed by activation of PKG (Wu et al., 1998). Additionally, activation of low voltage-activated Ca^{2+} channels, or T-type Ca^{2+} channels, is also involved in LTD induction at MPP-DG synapses (O'Mara et al., 1995).

1.2.2. Methamphetamine and synaptic plasticity in the hippocampus

It has been shown that METH induces memory deficits (Thomson et al., 2004) and that cognition is dependent on LTP induction (Neves et al., 2008). Accordingly, rats administered with METH (5 mg/kg, i.p., for 12 days) present lower membrane potential and input resistance in CA1 pyramidal neurons, correlated with neuronal injury (Hori et al., 2010). Moreover, both chronic regimen and prenatal exposure to METH reduced LTP in CA1 pyramidal cells (Hori et al., 2010). In addition, METH perfusion (30 μM) to hippocampal slices was able to increase glutamatergic synaptic transmission observed by the increase of fEPSPs without tetanic stimulation and, interestingly, this effect seems to be NMDA-independent (Swant et al., 2010). This enhanced baseline synaptic transmission was proposed to be mediated by activation of dopaminergic D1

and serotonergic 5-HT1A receptors. Besides, administration with 10 mg/kg (i.p.) twice a day for 5 days decreased LTP amplitude in CA1 pyramidal neurons (Swant et al., 2010). On the other hand, chronic administration of METH (24 mg/kg, i.p.) for 14 days did not induce any effect in LTP magnitude of CA1 pyramidal cells. However, LTP was decreased after 21 days of drug abstinence, which was correlated with poorer spatial memory performance (North et al., 2013). Moreover, the medial prefrontal cortex (mPFC) receives excitatory inputs from the hippocampus, but repeated METH administration (4 mg/kg, i.p., for 4 days) impairs LTP in the hippocampal-mPFC and D1 receptor activation seems to contribute to this effect (Ishikawa et al., 2005).

To date, little is known regarding the effect of METH on hippocampal synaptic plasticity, but the few studies available show that METH decreases LTP in CA1 pyramidal neurons that could be correlated with memory deficits. On the other hand, the effect of this psychostimulant on the plasticity of the DG is far from being accomplished, including the effect of METH on synaptic plasticity and integration of young neurons resulted from the differentiation of resident stem cells.

1.3. Adult neurogenesis

In the adult rodent brain, new neurons are continually generated throughout life and they become functionally integrated in the preexistent circuitries (Lledo et al., 2006). In fact, neurogenesis occurs in restricted brain regions and the best described niches are the subventricular (SVZ) and subgranular zone (SGZ). Regarding the SVZ, stem/progenitor cells lay adjacent to the ependymal layer, which lines the lateral ventricles. The resulting neuroblasts derived from stem/progenitor cells migrate through the rostral migratory stream towards the olfactory bulb. There, neuroblasts move radially into the granular and periglomerular layers and differentiate into mature interneurons participating in odor discrimination (Zhao et al., 2008). In humans, SVZ neurogenesis ceases by the eighteenth month of life, however quiescent stem cells remain in the SVZ area (Sanai et al., 2004). Noteworthy, neurogenesis can occur in other brain areas, including the hypothalamus (Kokoeva et al., 2005, 2007), cerebral cortex, cerebellum and olfactory bulb (Decimo et al., 2012). SGZ neurogenesis of the hippocampus will be further described in detail due to the importance of this structure for the present thesis.

1.3.1. Neurogenesis in the subgranular zone of the dentate gyrus

DGCs continue to be generated throughout adulthood in the SGZ of the DG, a thin layer localized in the innermost part of the granule cell layer right adjacent to the hilus (Ehninger and Kempermann, 2008). Resident stem and progenitor cells of the SGZ have the ability to self-renew, *i.e.*, maintain stem cell identity after cell division (Gage, 2000). Self-renewal properties can be demonstrated *in vitro* in the presence of growth factors (epidermal and fibroblast growth factors) by using the neurosphere assay: generation of secondary/tertiary neurosphere colonies derived from a stem cell prevenient from a primary/secondary passage neurosphere colony (Babu et al., 2007). Importantly, Suh and collaborators (2007) demonstrated that cells expressing the stem cell marker SRY (sex determining region Y)-box 2 (Sox2) can self-renew, generating two $Sox2^+$ cells, identical to the initial one. Stem/progenitor cells exhibit multipotency, verified both *in vitro* (Babu et al., 2007) and *in vivo* (Suh et al., 2007; Chetty et al., 2014).

Within the SGZ, type 1 cells, or radial glia-like cells, are the precursor cells of DGCs and can be identified by the expression of the astroglial marker glial fibrillary acidic protein (GFAP), Sox2 and nestin, which is an intermediate filament highly expressed in stem and progenitor cells. Particularly, these cells extend long apical processes into the molecular layer (Filippov et al., 2003; Figure 1.5). Radial glia-like cells give rise to transient amplifying cells, or type 2 cells, which can be distinguished from their precursor cells as they do not express GFAP and lack processes towards the molecular layer, being horizontally orientated in the SGZ (Filippov et al., 2003; Figure 1.5). Type 2 cells undergo cell division and can be subgrouped in type 2a and type 2b cells (Kronenberg et al., 2003). Type 2a cells express nestin, lack doublecortin (DCX, a microtubule-associated protein expressed in precursor and immature neurons) and some may express the prospero-related homeobox 1 (Prox1, DGC marker; Steiner et al., 2008). Conversely, type 2b cells express DCX, polysialylated-neural cell adhesion molecule (PSA-NCAM, role in cell-cell adhesion), neuronal differentiation factor (NeuroD, transcription factor involved in neuronal differentiation) and Prox1 (Filippov et al., 2003; Ehninger and Kempermann, 2008; Steiner et al., 2008). Further differentiation of type 2 cells gives rise to type 3 cells that show low proliferative activity. Similarly to type 2 cells, these cells also express DCX, PSA-NCAM, NeuroD and Prox1, but lack nestin expression (Kronenberg et al., 2003; Ehninger and Kempermann, 2008). Type 3 cells are postmitotic neurons and begin to project dendrites vertically towards the molecular layer and axons towards the hilus (Brandt et al., 2003). Indeed, further differentiation of type 3 cells generates postmitotic immature granule neurons, which develop more extensive dendrites (Zhao et al., 2006) and axons (Toni et al., 2008) towards the molecular layer and hilus/CA3

subfield, respectively (Figure 1.5). The functional properties of DGCs are described in the next section.

An important tool to identify stem, progenitor or immature DGCs is the use of retroviruses expressing fluorescent proteins. Retroviruses infect replicating cells and, therefore, allow the identification and manipulation of newborn neurons driving adult neurogenesis. Indeed, this procedure permits morphological analyses and characterization of synaptic integration during neuronal maturation (Espósito et al., 2005; Zhao et al., 2006; Ge et al., 2007a; Toni et al., 2008). Using this technique, it has been shown that 10-day-old neurons have dendrites reaching the inner molecular layer, whereas dendrites of 14-day-old neurons reach the middle molecular layer (Zhao et al., 2006). Moreover, these dendrites present varicosities instead of spines, which are defined as swelled dendritic proportions. Additionally, 21-day-old neurons which dendrites already reach the outer molecular layer exhibit spines, the main postsynaptic sites that receive glutamatergic inputs (Zhao et al., 2006). Regarding axonal development, immature DGC mossy fibers begin to form synapses with postsynaptic targets in the CA3 subfield 17 days after cell division, and continue to mature thereafter (Toni et al., 2008). These immature DGCs form functional glutamatergic synapses and establish synaptic connections with mossy cells, interneurons and CA3 pyramidal neurons (Toni et al., 2008). Moreover, along with this differentiation process, immature DGCs migrate out the SGZ towards the granule cell layer.

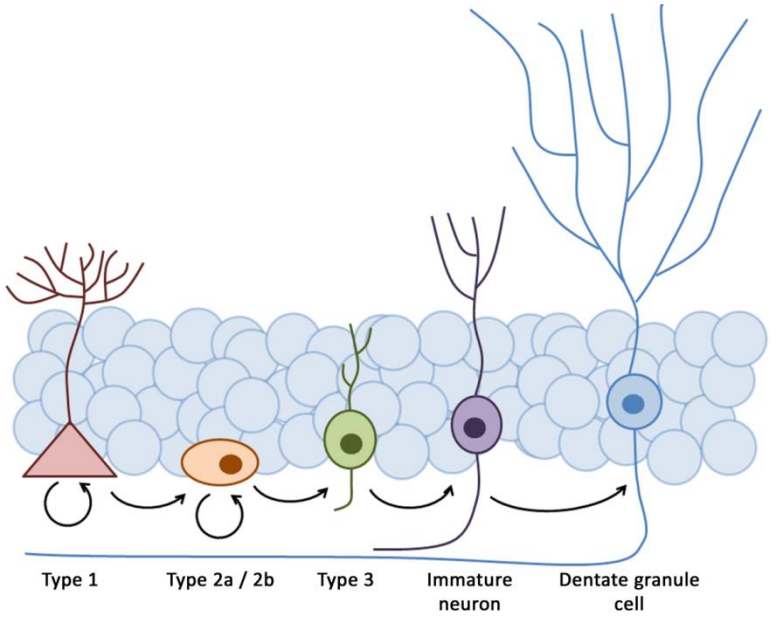

Figure 1.5 – Schematic representation of the SGZ neurogenesis. Radial glia-like cells (type 1) are stem cells of the SGZ with self-renewal capacities. These cells give rise to transient amplifying cells (type 2) that present a different morphology from type 1 cells, but maintaining the ability to self-renew. Type 3 cells, or neuroblasts, result from the differentiation of type 2 cells, and maturation proceeds with dendritic and axonal development, giving rise to mature dentate granule neurons that will integrate into the preexistent neuronal circuitries.

In brief, stem and progenitor cells from the SGZ proliferate and differentiate into DGCs that are fully integrated into the preexistent neuronal circuitries of the DG (van Praag et al., 2002).

1.3.2. Functional properties of dentate granule cells: young *versus* mature dentate granule cells

Excitability

Action potentials (APs) are brief sharp electrical events that permit communication between nerve cells. APs are generated by the abrupt and selective membrane permeability to sodium (Na^+) followed by potassium (K^+) ions (Kandel et al., 1991). An AP is triggered by a depolarization of the plasma membrane that reaches the voltage threshold for opening of voltage-gated Na^+ channels. During the opening of Na^+ channels, their conductance increases, resulting in a rapid inward Na^+ flow. This causes more depolarization, resulting in the opening of more Na^+ channels and the membrane sharply depolarizes towards Na^+ reversal potential (E_{Na}), at which the electrochemical gradient of Na^+ ions across the membrane is zero. The drop of Na^+ channel driving force, their voltage-dependent inactivation and the opening of voltage-gated K^+ channels lead sharp membrane repolarization due to increase of K^+ conductance and K^+ outward flow (Kandel et al., 1991). Importantly, this mechanism of AP generation and waveform was nicely described by the classical Hodgkin-Huxley model (Kandel et al., 1991). Young DGCs have a relative low AP threshold, but during maturation both AP amplitude and firing dynamics (frequency) increases (Mongiat et al., 2009). Furthermore, voltage-dependent inward Na^+ and outward K^+ conductances increase during development of young DGCs (Espósito et al., 2005). Interestingly, Schimdt-Hieber and collaborators (2004) showed that early low threshold APs are Na^+ channel-independent, as they are insensitive to tetradotoxin (TTX), but are generated by T-type Ca^{2+} channels. Accordingly, immature DGCs exhibit large amplitudes of inward Na^+ and outward K^+ conductances, and repetitive spikes only after the fourth week of age (Espósito et al., 2005) before which low threshold Ca^{2+}-dependent spikes dominate (Mongiat et al., 2009).

Passive membrane properties

Young and mature DGCs have different resting membrane potential (RMP). In particular, young neurons are characterized by a more depolarizing potential that will gradually become more hyperpolarized during maturation (Espósito et al., 2005; Spampanato et al., 2012). Indeed, a correlation between RMP and AP firing has been made by Spampanato and colleagues (2012)

showing that cells with RMP around -30 mV fire one or few mini-spikelets in response to depolarizing current injections. In addition, immature DGCs that fire few AP during the depolarization step present RMP around -50 mV. In contrast, mature neurons with RMP of -80 mV exhibit repetitive fully-blown AP during the current step (Spampanato et al., 2012).

The input resistance (R_{in}) of a neuron depends on the density of ion channels opened at any given time (Espósito et al., 2005). In fact, Liu and collaborators (2000) classified the maturation stage of DG cells by their R_{in}, by showing that DG cells with highest values of R_{in} have more depolarizing RMP and small dendritic length (Liu et al., 1996). Also, Schmidt-Hieber and co-workers (2004) used this parameter to identify young DGCs and immature neurons since these cells exhibit high R_{in} in the gigaohm (GΩ) range that is gradually decreased as DG cells mature. In fact, cells showing this high R_{in} also fire APs with short amplitude, whereas neurons with a more mature AP firing profile have lower R_{in} (Espósito et al., 2005).

Another characteristic of immature DGCs is the lower membrane capacitance (C_m), which is proportional to cell surface. Indeed, immature neurons have a smaller soma than mature DGCs, correlated with a lower C_m. Accordingly, cells with small C_m present high R_{in} and depolarized RMP. As DGCs mature, a gradual increase of C_m is paralleled by R_{in} decreases and RMP hyperpolarization (Espósito et al., 2005; Vivar et al., 2012).

Synaptic transmission and plasticity

The main role of SGZ neurogenesis is to give rise to neurons from stem/progenitor cells that will then integrate into DG circuitry. Indeed, these new-incorporating cells must be able to receive inputs and send outputs. Noteworthy, during some stages of neuronal development of type 1, or radial glia-like cells, neither GABAergic nor glutamatergic synaptic transmission has been detected (Tozuka et al., 2005). However, although radial glia-like cells do not show fast synaptic responses, they present GABA signaling (Song et al., 2012). Indeed, GABA released from fast-spiking interneurons (parvalbumin-positive interneurons) maintains radial glia-like cells quiescence, and γ_2-containing $GABA_A$ receptors mediate this effect (Song et al., 2012).

Type 2 cells (transient amplifying cells) have no afferent synaptic connection, but express both glutamate and GABA receptors (Zhao et al., 2006). In fact, neither perforant pathway stimulation (Ge et al., 2006) nor NMDA or AMPA receptors activation (Tozuka et al., 2005) induce postsynaptic responses in type 2 cells. However, these cells show GABA-evoked currents after focal application of GABA *via* $GABA_A$ receptor activation (Tozuka et al., 2005). Also, stimulation of the hilar region evokes GABA currents but not after stimulation of the MPP, suggesting that GABA is released from local interneurons (Tozuka et al., 2005).

As dendrites develop in young DGCs, not only do they receive inhibitory inputs from local GABAergic interneurons, but also they receive glutamatergic synapses from mossy cells and perforant path in the molecular layer (Ge et al., 2006). At this stage, GABA is excitatory in contrast to what is observed in mature DGCs. Indeed, immature neurons have high intracellular chloride (Cl^-) concentration due to high expression of Na^+-K^+-$2Cl^-$ co-transporter (NKCC1), a Cl^- importer (Ge et al., 2007b; Figure 1.6). In these cells, NKCC1 drive Cl^- ions into the cell and, as a consequence, the activation of $GABA_A$ receptors leads to the efflux of Cl^-, depolarizing the membrane (Ge et al., 2007b). As DGCs mature, the expression of NKCC1 is down-regulated giving place to the K^+-Cl^- co-transporter (KCC2), a Cl^- exporter, and switching GABA from excitatory to inhibitory (Ge et al., 2007b; Figure 1.6).

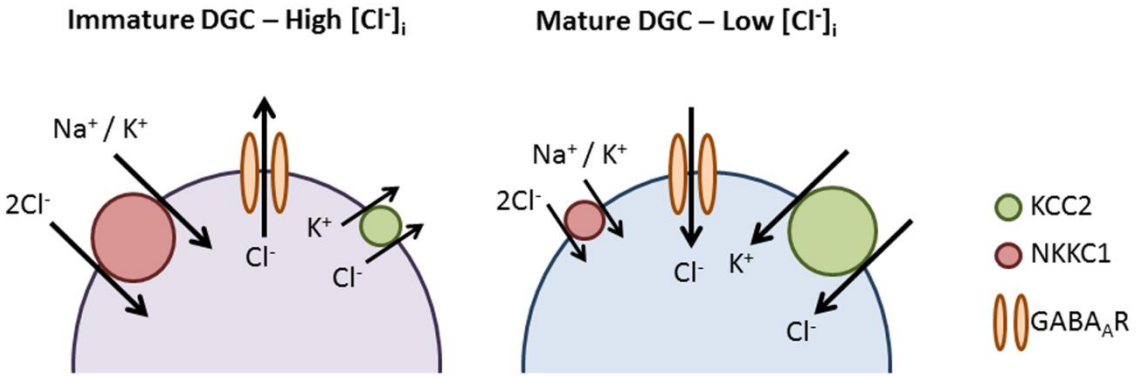

Figure 1.6 – Schematic representation showing the effect of GABA on immature and mature dentate granule cells (DGCs). In immature DGC, the Na^+-K^+-$2Cl^-$ co-transporter (NKCC1) is highly expressed, whereas the K^+-Cl^- co-transporter (KCC2) is poorly expressed, resulting in high chloride concentration inside the cell ($[Cl^-]_i$). Therefore, $GABA_A$ receptor activation leads to Cl^- outflow and membrane depolarization. During maturation, KCC2 is up-regulated and NKCC1 down-regulated, switching GABA from depolarizing to hyperpolarizing action.

The first glutamatergic excitatory inputs occur in parallel with dendritic development and elongation towards the molecular layer (Espósito et al., 2005; Zhao et al., 2006). Indeed, 19 day-old immature DGCs exhibit already excitatory postsynaptic currents (EPSC) induced by stimulation of the MPP, despite the low amplitude. However, DGCs reach its maximal amplitude around 49 day-old (Mongiat et al., 2009). Indeed, the growth and development of newborn DG neuronal dendrites (Zhao et al., 2006) correspond to the increase of EPSC amplitudes (Mongiat et al., 2009). Interestingly, neurons generated in adulthood remarkably present similar responses of short-term plasticity from the afferents inputs of LPP and MPP as neurons generated during development (Laplagne et al., 2006). Meanwhile, morphological studies show

that immature neurons extend axons towards the hilus (Zhao et al., 2006; Toni et al., 2008; Gu et al., 2012) and transmit outputs to CA3 area with development and extension of axonal mossy fibers. Indeed, thin axonal fibers can be seen in the hilus in 10 day-old neurons (Zhao et al., 2006) and maturation from 17 to 75 day-old DG neurons show a gradual increase in presynaptic vesicles (Toni et al., 2008). In addition, adult-born neurons elicit postsynaptic currents in interneurons, mossy cells and CA3 pyramidal cells, being fully integrated in the existent circuitry (Toni et al., 2008).

In addition to synaptic integration into existent circuitries, synaptic plasticity has also been demonstrated in developing DGCs. Indeed, Ge and collaborators (2007a) found that neurons older than 2 weeks exhibit LTP in response to theta-burst stimulation (TBS). Importantly, the authors also observed a critical period for enhanced synaptic plasticity that corresponds to one month-old young DGC and this LTP enhancement was dependent on the activation of GluN2B-containing NMDA receptors (Ge et al., 2007a). Moreover, the same group used an optogenetic method to excite adult-born DG and, simultaneously, investigate the evoked postsynaptic currents in CA3 area. Noteworthy, 1 week-old neurons (post-retroviral infection) do not induce any postsynaptic responses at CA3 pyramidal cells, indicating that mossy fibers had not reached the CA3 area yet (Gu et al., 2012). On the other hand, at 2 week of age, excitation of newborn DG neurons produces EPSCs in CA3 pyramidal cells, reaching the maximum amplitude at one month-old (Gu et al., 2012) that corroborates with enhanced LTP in these immature neurons.

In summary, new DG neurons develop from resident stem/progenitor cells that integrate into preexistent synaptic circuitries through dendritic and axonal morphological changes, allowing them to receive inputs from EC and send outputs to CA3 pyramidal cells, respectively.

1.3.3. Function of adult dentate gyrus neurogenesis

It is well established that the hippocampus is essential for the formation of new episodic memories as well as for long-term memory storage (Neves et al., 2008). In fact, this was assessed by elimination of synaptic transmission through deletion of NMDA receptors specifically in the CA1 area, which was correlated with poor memory performance in the Morris water Maze (MWM; Tsien et al., 1996). Accordingly, it has been proposed that DG adult neurogenesis gives its major contribution to the formation of new memories. Indeed, the importance of neurogenesis on spatial memory was demonstrated by Garthe and collaborators (2009) by showing that ablation of neurogenesis for several weeks induce learning and memory

deficits. Furthermore, a critical period for enhanced synaptic plasticity was verified in four week-old immature neurons (Ge et al., 2007a) since these were preferentially recruited into spatial memory networks (Kee et al., 2007). Accordingly, inactivation of these same immature neurons disrupted hippocampal memory retrieval (Gu et al., 2012). Importantly, the correct timing at initial stages of neuronal differentiation is crucial for the proper integration into existent circuitries and consequently to memory performance (Farioli-Vecchioli et al., 2008).

The hippocampus is also responsible in forming new associative memories by storing memories independently of each other, retrieving memories from partial cues and flexibly applying stored memories to novel situations (Yassa and Stark, 2011). Indeed, this brain region allows the formation of distinct memories from similar episodes that are stored in a distinct non-overlapped manner, a phenomenon identified as pattern separation. Pattern completion, on the other hand, is involved in the recall of previously acquired memories from partial information cues (Yassa and Stark, 2011). Interestingly, it seems that hippocampal neurogenesis facilitates pattern separation as demonstrated by Nakashiba and colleagues (2012). These authors showed that mature DGCs are not very important for pattern separation between similar environments, but are required for achieving a rapid pattern completion. Additionally, the same authors observed that adult born DGCs are essential for proper acquisition and discrimination of similar contexts (Nakashiba et al., 2012). Interestingly, increasing neurogenesis promotes a higher level of discrimination between two similar contexts, which strongly reveal the importance of neurogenesis on hippocampal pattern separation (Sahay et al., 2011). Importantly, immature DG neurons presenting NMDA receptor-containing GluN2B subunits seem to be essential to facilitate pattern separation (Kheirbek et al., 2012). In agreement, GluN2B subunits are required for the induction of LTP in young DG neurons during the critical period of enhanced synaptic plasticity (Ge et al., 2007a).

In summary, incorporation of newborn neurons into the preexistent neuronal circuitries plays a crucial role in the formation of new memories as well as in the discrimination of two similar contexts, known as pattern separation.

1.3.4. Modulation of adult subgranular zone neurogenesis

SGZ is a dynamic neurogenic niche that can be easily susceptible to intrinsic and extrinsic factors. Indeed, neurogenesis can be positively modulated by astrocytes that recruit stem cells to differentiate into neurons (Song et al., 2002), an effect that involve ephrin-B2 signaling (Ashton et al., 2012; Figure 1.7), which has been shown to regulate neuronal spine morphogenesis and synaptogenesis of adult hippocampal neurons (Xu et al., 2011).

Neurotransmitters can also modulate neurogenesis as demonstrated by Tozuka and collaborators (2005) where GABA-induced depolarization to type 2 cells increase the expression of NeuroD. Moreover, glutamate mediates NMDA-induced excitation to neural progenitor cells, leading to differentiation of neural progenitor cells (Deisseroth et al., 2004). Extrinsic factors such as voluntary exercise confirmed to increase the number of proliferating cells, neuronal differentiation and survival (Bruel-Jungerman et al., 2009; Snyder et al., 2009). Moreover, enriched environment (home cages that enhance sensory, cognitive and motor stimulation) contributes to the survival of proliferating precursor cells and the neuronal phenotype is preferentially generated (Kempermann et al., 1997; Figure 1.7). On the other hand, injuries such as temporal lobe epilepsy transiently increases the number of DCX-expressing immature granule neurons, but the development of these neurons is compromised since granule cells born after status epilepticus present abnormal dendrites with high spine density that project into the hilus (Jessberger et al., 2007). Furthermore, some newborn DGCs migrate into the hilus instead the granule cell layer, which results in the generation of aberrant circuitries (Jessberger et al., 2007).

In contrast, rodent neurogenesis can be negatively modulated by ageing, verified by the reduced number of radial glia-like and progenitor cells, as well as the number of postmitotic immature granule neurons (Rao et al., 2006; Gebara et al., 2013; Figure 1.7). Interestingly, hippocampal neurogenesis in humans continues throughout life with only a minor decrease during ageing (Spalding et al., 2013). Also, stress and glucocorticoid exposure/administration reduce rodent proliferation (Boku et al., 2009) and differentiation into neurons (Chetty et al., 2014), but enhances hippocampal oligodendrogenesis (Chetty et al., 2014; Figure 1.7). In the same context, the decrease of hippocampal neurogenesis by chronic stress is known to contribute to the onset of depression (Dagytè et al., 2011; Snyder et al., 2011). Regarding the effect of neurodegenerative diseases in neurogenesis, a mouse model of Parkinson disease shows a reduced number of proliferating cells as well as newborn neurons (Kohl et al., 2012). Similarly, animal models of Alzheimer disease carrying a mutated form of the amyloid precursor protein, a membrane protein that originates β-amyloid protein after proteolysis, present decreased proliferation, neuronal differentiation or survival (Haughey et al., 2002; Donovan et al., 2006). Additionally, in a mouse model of Huntington disease, dendritic arborization was reduced as well as long-term survival of newborn DG neurons (Pla et al., 2014). Another feature with a negative impact in neurogenesis is neuroinflammation (Figure 1.7), since proinflammatory cytokines (IL-6 and TNF-α) were shown to impair neurogenesis (Ekdahl et al., 2003; Monje et al., 2003).

In general, chronic exposure to drugs of abuse has a negative impact on cell proliferation, on immature neurons or survival of newborn DGCs, verified to several drugs as follows: MDMA (Hernández-Rabaza et al., 2006), cocaine (Yamaguchi et al., 2004), nicotine (Abrous et al., 2002), heroin (Eisch et al., 2000) and alcohol (Richardson et al., 2009; Taffe et al., 2010; Figure 1.7). An interplay between impairment of neurogenesis and memory deficits induced by cocaine was pointed by Sudai and co-workers (2011), showing that the decrease in newborn neurons was correlated with the poorer memory performance in the water T-maze. On the other hand, chronic administration of a low dose of AMPH increased neuronal differentiation as well as the survival of newborn neurons (Dabe et al., 2013). Similarly, MDMA increased cell proliferation after intermittent administration of MDMA (5 mg/kg, every 2 days; Catlow et al., 2010).

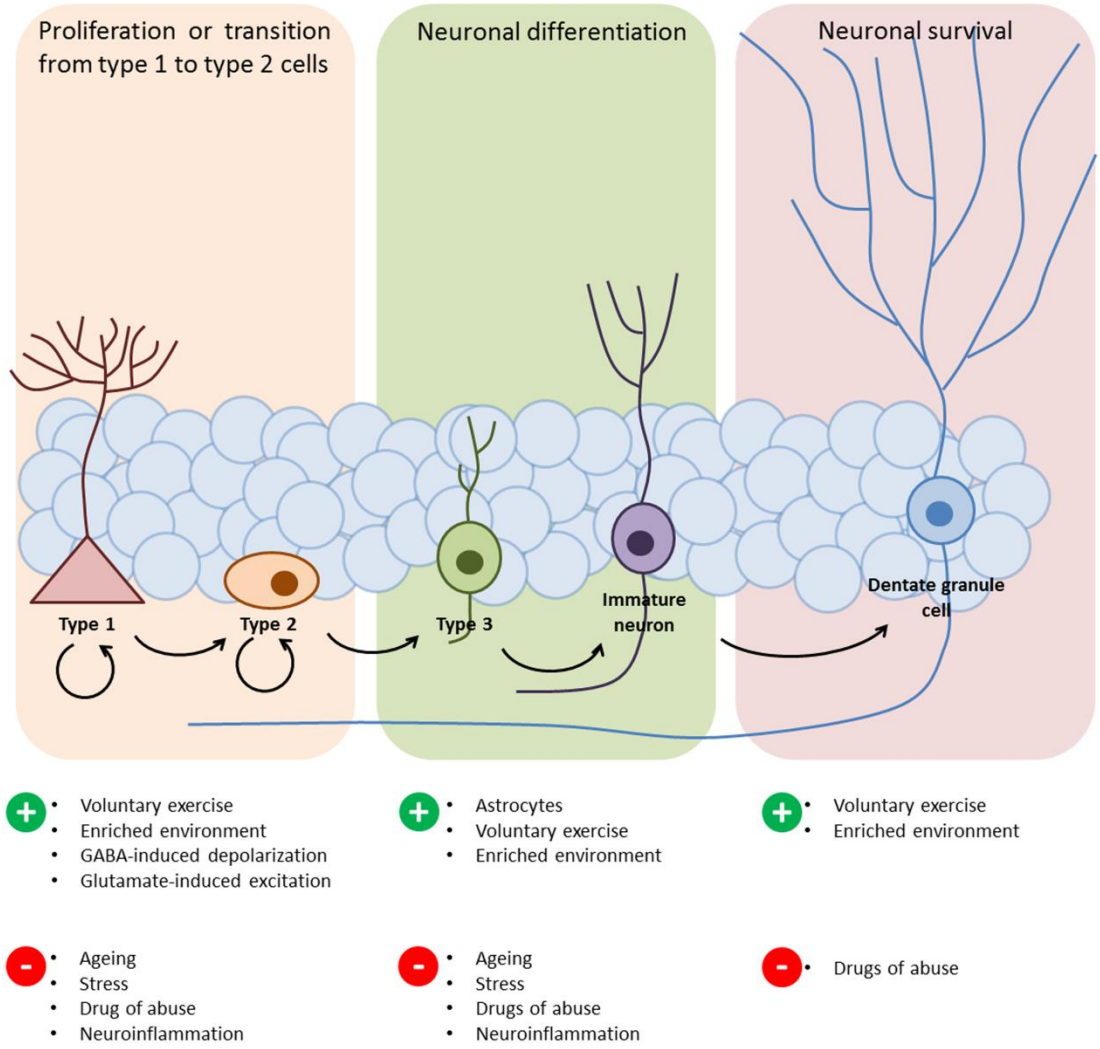

Figure 1.7 – Modulation of SGZ neurogenesis. Summary of some of the effects that positively or negatively modulates cell proliferation, neuronal differentiation and neuronal survival of stem/progenitor cells of the SGZ.

1.3.5. Neurogenesis and methamphetamine

As briefly pointed to other psychostimulants, METH can also alter the homeostasis of neurogenesis, effects that also dependent on the dose and frequency of exposure to the drug (reviewed by Silva et al., 2010; Gonçalves et al., 2014). Indeed, it has been first demonstrated by Hildebrandt and colleagues (1999) that a single dose of 50 mg/kg METH (i.p.) for 15 days decreases the number of BrdU-positive cells in the DG of gerbils. Accordingly, a single administration of 25 mg/kg METH (i.p.) to gerbils induced a transient decrease of proliferation in the SGZ (Teuchert-Noodt et al., 2000). On the other hand, mice administered with 1 mg/kg METH (s.c.) for 14 days showed no effect on DG cell proliferation (Maeda et al., 2007). Moreover, Mandyam and collaborators (2008) used different paradigms of self-administration to correlate with human patterns of METH abuse as follows: recreational, chronic and dependence. Indeed, self-administration for 1 h/day, twice weekly, of 0.05 mg/kg/infusion METH (i.v.) to Wistar rats (intermittent short-access, recreational pattern) increased proliferating cells in the SGZ (Mandyam et al., 2008; Recinto et al., 2012) as well as DCX-positive cells, with no effect on cell survival, neuronal and astroglial differentiation (Mandyam et al., 2008). However, METH administered 6 h/day for 22 days (Recinto et al., 2012) or 49 days (Mandyam et al., 2008, chronic and dependence paradigms) decreased the number of proliferating and DCX-positive cells, as well as the survival and differentiation into neuron and astrocytes (Mandyam et al., 2008).

An interesting analysis of cell cycle in rats self-administering METH demonstrated that this drug (0.05 mg/kg/injection, i.v., 6 h daily access for 13 days) decreases the population of cells in the S phase of the cell cycle, without changing, however, its length (Yuan et al., 2011). In fact, the different response of DG cells to METH stimuli depends on the maturational state as observed by Yuan and collaborators (2011), showing that METH (0.05 mg/kg/injection, i.v., 1 h daily access for 13 days) increased the number of radial glia-like cells (type 1 cells) in the rat DG. On the other hand, METH (0.05 mg/kg/injection, i.v., 1 or 6 h daily access for 4 or 13 days) decreased the number of proliferating neuroblasts (type 2a cells) and increased the number of late precursor cells (type 3 cells; Yuan et al., 2011). Interestingly, Recinto and collaborators (2012) showed that decreased hippocampal proliferation in self-administered rats is correlated with poorer working memory performance, and withdrawal increased the survival of the progenitors. *In vitro* studies also point that METH impairs proliferation of hippocampal precursors as observed by Tian and collaborators (2009), where the authors showed that METH (300 μM) decreases the number of proliferating cells in rat hippocampal neural progenitor cell cultures, due to mitochondrial fragmentation-triggering apoptotic events. Additionally, Venkatesan and collaborators (2011) argued that METH (100 μM) decreases the number of

proliferating cells in neural progenitor cell cultures in part due to an increase of oxidative and nitrosative stress. In the SVZ, our group demonstrated that METH increases the number of $Sox2^{+}/TUNEL^{+}$ cells, meaning that SVZ stem/progenitor cells are also a target for METH-induced toxicity. Additionally, METH decreased cell proliferation, neuronal differentiation and axonogenesis in SVZ neurosphere cultures (Bento et al., 2011).

As a result, METH induces changes in hippocampal neurogenesis, depending on the dose/concentration and/or frequency of exposure. Interestingly, different stages of DG neuron development react differently upon METH exposure. Therefore, little is known regarding the effect of METH on DG stem cell dynamics as well as the underlying mechanisms of METH-induced toxicity. Importantly, how METH affects the functional properties and integration of preexistent circuitries of young DG neurons needs further consideration.

1.4. Neuropeptide Y in the central nervous system

Neuropeptide Y (NPY) is a 36 amino acid peptide and was first isolated and characterized by Tatemoto and colleagues from the porcine brain extracts (Tatemoto et al., 1982a, Tatemoto, 1982b). Furthermore, this neuropeptide belongs to the neuropeptide tyrosine family that also comprises peptide YY (PYY) and pancreatic polypeptide (PP; Michel et al., 1998).

NPY is widely expressed in the CNS, specifically in the cerebral cortex, nucleus accumbens, amygdala, entorhinal cortex, hypothalamus and hippocampus (Schwartzberg et al., 1990). Indeed, NPY can be expressed in cell bodies, axons and terminals in the cerebral cortex, corpus callosum, caudate putamen, hippocampus and hypothalamus (Chronwall et al., 1985). Specifically, this peptide is expressed by somatostatin-positive interneurons in the cerebral cortex (Papadopoulos et al., 1987) and, in the hippocampus, there is a wide distribution being found in the hilus of the DG, CA1, CA2 and CA3 subfields (Chronwall et al., 1985; De Quidt and Emson, 1986).

NPY participates in many physiological functions in the CNS such as feeding (Gao et al., 2004) and anxiety-/depression-like behaviors (Broqua et al., 1995; Sajdyk et al., 1999). Also, this neuropeptide modulates neurotransmitter release (Malva et al., 2012) and neurogenesis in both SGZ (Howell et al., 2003, 2005) and SVZ (Agasse et al., 2008), as well as neuroprotection against excitotoxic insult (Silva et al., 2003a) and drugs of abuse administration (Thiriet et al., 2005).

1.4.1. Biosynthesis and structure

The human NPY gene is located on chromosome 7 at the locus 7p15.1 (Baker et al., 1995) and NPY cDNA consists of 291 bases, suggesting that the prepro-NPY has 97 amino acids

long with a molecular weight predicted to about 11 kDa (Minth et al., 1984). In detail, the NPY gene presents four exons separated by three introns. The first exon includes the 5'-nontranslated segment of NPY, the second exon comprises the signal peptide and the majority of NPY sequence, the third exon contains the terminal tyrosine, the sequence GKR (glycine, lysine and arginine) and the first 23 amino acids of the C-flanked peptide of NPY (CPON), and the fourth exon includes the terminal heptapeptide of the CPON and the 3'-nontranslated sequence (Minth et al., 1986; Allen, 1990). In fact, prepro-NPY comprises a hydrophobic 28 amino acid N-terminal signal peptide sequence followed by NPY sequence, the GKR and a 30-amino acid terminal peptide at the C-terminal peptide, CPON (Minth et al., 1984; Figure 1.8 A). As reviewed by Cerdá-Reverter and Larhammar (2000) the enzyme signal peptidase removes the signal peptide located at the N-terminal of the prepro-NPY, which will generate the pro-NPY. Moreover, the removal of C-terminal CPON from pro-NPY by the prohormone convertase, results in the NPY_{1-39}. Then, the enzyme carboxypeptidase removes the lysine and the arginine residues from the GKR sequence at the COOH terminal from NPY_{1-39} peptide, resulting in NPY_{1-37}. Afterwards, the G residue is removed by the amidating enzyme, resulting in the final amino acid sequence of the active NPY molecule, NPY_{1-36} (Cerdá-Reverter and Larhammar, 2000; Figure 1.8 A).

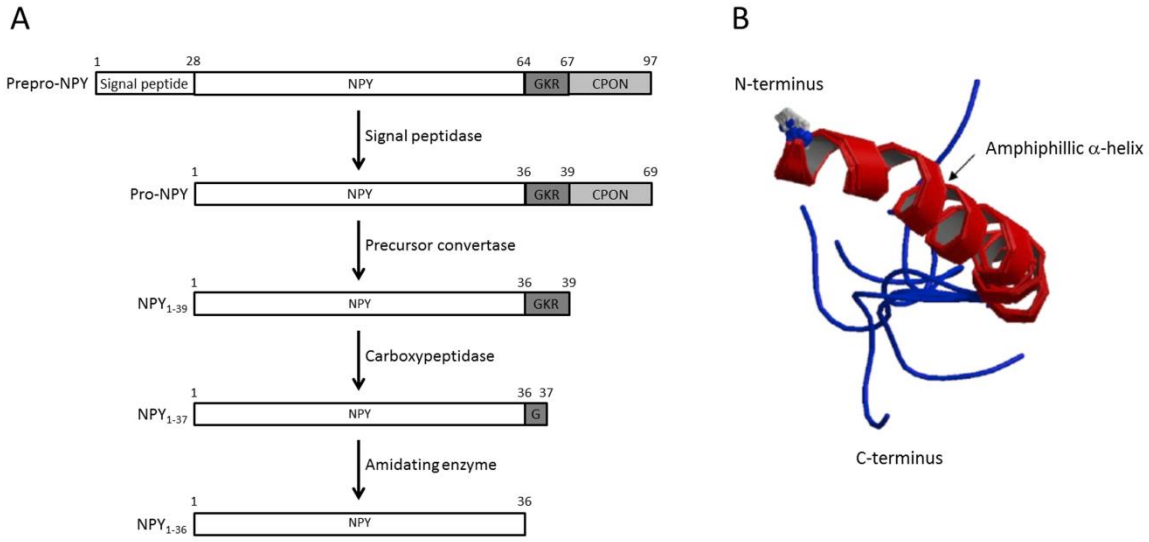

Figure 1.8 – NPY biosynthesis (A) and three dimensional structure (B). Adapted from Cerdá-Reverter and Larhammar, 2000; Silva, 2003; Baptista, 2009; Dyzma et al., 2010.

After complete biosynthesis of NPY, the resultant neuropeptide molecule consists in a total of 36 amino acids with a high content of tyrosine residues. In fact, comparing the primary

structures of NPY with PYY and PP, this neuropeptide contains a N-terminal tyrosine similar to PYY and the same C-terminal tyrosine as PP (Tatemoto, 1982b). Indeed, an extensive analysis revealed that the tertiary structure of NPY crystals has globular and compact structure, due to stabilized interactions between a poly-proline helix and an α-helix separated by a type I β-turn, creating a hairpin-like loop that makes closer the N-terminal with the C-terminals (Allen et al., 1987). Specifically, the residues 13-32 from the amphiphilic α-helix are stabilized by hydrophobic interactions with the amphiphilic poly-proline helix in residues 1-8 (Minakata et al., 1989; Figure 1.8 B).

1.4.2. Neuropeptide Y receptors

NPY receptors belong to the family of G-protein coupled receptors (Michel, 1991; Benarroch, 2009) and modulate the inhibition of adenylate cyclase activity followed by inhibition of cAMP generation (Michel et al., 1991). Moreover, NPY receptors inhibit intracellular Ca^{2+} influx at both synaptic and nonsynaptic terminal areas (Toth et al., 1993; Silva et al., 2003b). Moreover, NPY receptor activation is able to activate the mitogen-activated protein kinase (MAPK) pathway (Howell et al., 2005) and enhance G-protein coupled inwardly rectifying potassium channels (GIRK channels; Paredes et al., 2003).

Y_1 receptor

Y_1 receptors are glycoproteins with molecular weight around 70 kDa (Wan and Lau, 1995). Also, Y_1 receptor gene is grouped together with Y_5 receptor in mice chromosome 8B3-C2 and in human chromosome 4q31 (Eva et al., 2006). In fact, the C-terminal of NPY is essential for Y_1 receptor recognition and a full NPY sequence is necessary for Y_1 receptor to be fully activated (Wan and Lau, 1995). The first Y_1 receptor agonist to be described was [Leu^{31},Pro^{34}]NPY, obtained by the replacement of Ile^{31} and Gln^{34} for Leu^{31} and Pro^{34} (Fuhlendorff et al., 1990). Indeed, this agonist has high affinity to Y_1 receptor, whereas low affinity is observed to Y_2 receptors (Fuhlendorff et al., 1990). Regarding Y_1 receptor antagonists, the most used are non-peptides, which includes BIBP3226 (Vanderheyden et al., 1997), LY357897 (Hipskind et al., 1997) and BIBO3304 (Wieland et al., 1998).

The main physiological functions of Y_1 receptors are the regulation of food intake (Kask et al., 1998; Kanatani et al., 2000; Gao et al., 2004), anxiety and stress (Broqua et al., 1995; Sajdyk et al., 1999), seizure threshold (Gariboldi et al., 1998), ethanol dependence (Bhisikar et al., 2009; Sparrow et al., 2012) and GABAergic transmission (Molosh et al., 2013).

These receptors are widely distributed in both central and peripheral nervous systems. Hence, in the CNS, Y_1 receptor mRNA expression is highly expressed in the cerebral cortex, amygdala, hypothalamus and spinal cord (Kishi et al., 2005). Furthermore, Y_1 receptor immunoreactivity is evident in the nucleus accumbens, caudate putamen, ventral tegmental area, hypothalamus and cerebellum (Wolak et al., 2003). In the rat and mice hippocampus, Y_1 receptor mRNA is highly expressed in the granule cell layer of the DG (Kishi et al., 2005) and in pyramidal layers, whereas moderate density hybridization was found in the ventral and intermediate subiculum (Kishi et al., 2005). Furthermore, Wolak and collaborators (2003) observed that Y_1 receptors are highly expressed within the cell bodies and fibers of CA1, CA2 and CA3 subfields of Sprague-Dawley rats, but in the DG the only immunoreactivity observed was in fibers from the molecular layer. Regarding human hippocampus, the granule cell layer of the DG express high levels of Y_1 receptor mRNA, whereas almost undetectable levels was found in the subiculum, and CA1 and CA3 subfields (Caberlotto et al., 1997).

Y_2 receptor

NPY Y_2 receptor subtype is a 7 transmembrane protein with a molecular weight of 50 kDa (Parker and Williams, 1990) and is confined in the human chromosome 4q31 like Y1 receptor subtype and in mice chromosome 3 (Ammar et al., 1996). In fact, this receptor has higher affinity to NPY and PYY (Rose et al., 1995) and can be activated by NPY(3-36) and NPY(13-36), which have more affinity for this receptor than for Y_1 receptors (Grandt et al., 1996). Regarding Y_2 receptor antagonists, the first to be synthesized was T4-[NPY(33-36)] (Grouzmann et al., 1997), followed by the non-peptide BIIE0246 (Doods et al., 1999) and, more recently, the JNJ-31020028, a non-peptide that can cross the BBB (Shoblock et al., 2010; Swanson et al., 2011).

Y_2 receptor main physiological functions involve the regulation of neurotransmitter release, specifically the inhibition of glutamate release (Silva et al., 2003b), and reduction of neuronal excitability, *i.e.*, the duration of epileptic activity and the number of seizure episodes in mice hippocampus (El Bahh et al., 2005). Noteworthy, overexpression of Y_2 receptors alone, or in combination with NPY overexpression, suppresses seizures in the hippocampus and slowed the progression of kindling (Woldbye et al., 2010). Besides, these receptors mediate spatial and nonspatial working memory processing (Redrobe et al., 2004), anxiety-/depression-like behaviors (Tasan et al., 2010), and circadian rhythm (Soscia and Harrington, 2005). Furthermore, Y_2 receptors are also involved in food intake as demonstrated by Ortiz and colleagues (2007), which inhibition increased food intake, whereas activation increased insulin levels in diet-

induced obese mice (Ortiz et al., 2007). Regarding ethanol abuse, central blockade of Y_2 receptor subtype suppresses ethanol self-administration (Rimondini et al., 2005).

Y_2 receptor mRNA is expressed throughout the brain, exhibiting high expression in the hippocampus, hypothalamus and amygdala, whereas moderate levels can be found in substantia nigra and ventral tegmental area (Parker and Herzog, 1999). Besides, Y_2 receptor protein is expressed in several brain areas, specifically in the olfactory bulb, the layers 2/3 and 6 of the cerebral cortex, amygdala, hypothalamus and hippocampus (Stanić et al., 2011). Specifically in the DG, Y_2 receptor localization is mainly presynaptic since high levels are found in the mossy fibers, whereas in CA1 and CA2, Y_2 receptor is mainly localized in cell bodies (Stanić et al., 2006).

Y_3 receptor

Y_3 receptors are considered as putative because this receptor has not been cloned yet and no specific agonists or antagonists have been found (Michel et al., 1998). However, Glaum and collaborators (1997) suggested that the positions 13 and 14 of NPY are important for Y_3 receptor recognition. Also, this receptor subtype has high affinity to NPY, but poorly recognizes PYY and PP in the rat cardiac myocytes (Balasubramaniam et al., 1990).

This receptor subtype is present in the heart and chromaffin cells (Balasubramaniam et al., 1997) however, little is known about the presence and distribution of Y_3 receptors in the CNS. In fact, Monnet and collaborators (1992) reported its expression in the rat CA3 dorsal hippocampus. Other pieces of evidence pointed that Y_3 receptors are expressed in the nucleus tractus solitarius (NTS) and, upon NPY activation, modulates bradychardia, hypotension and inhibition of glutamate responses (Grundemar et al., 1991). Moreover, NPY, but not PYY and PP, through activation of Y_3 receptors, inhibits EPSCs of NTS neurons and suppresses inhibitory postsynaptic currents evoked from local GABAergic interneurons of the NTS in the brain stem (Glaum et al., 1997).

Y_4 receptor

Human Y_4 receptor gene is localized in the region 10q11.2 of the chromosome 10, whereas in mice is confined to the chromosome 14 (Darby et al., 1997). Furthermore, human Y_4 receptor is a 7-transmebrane protein, with a 60 kDa molecular weight, and is coupled to an adenylyl cyclase, which results in the inhibition of the second messenger cAMP (Voisin et al., 2000). In addition, Berglund and collaborators (2003) observed that human Y_4 receptor subtype forms a 160 kDa homodimer, and this complex dissociates upon PP or 1229U91 (agonist) binding. In fact, PP binds to the receptor with high affinity and selectivity (Berglund et al., 2001),

whereas NPY and PYY have lower and similar affinities between them (Zou et al., 2008). Regarding Y_4 receptor ligands, the Y_1 receptor antagonist, GW1229 (also known as 1229U91 or GR121118), is an Y_4 receptor agonist, and UR-AK49 is a non-peptide antagonist for this receptor (Ziemek et al., 2007).

In the CNS, Y_4 receptor mRNA is highly expressed in the brainstem and hypothalamus, but moderate expression is observed in the entorhinal cortex, hippocampus (DG, CA1, CA2 and CA3) and subiculum (Parker and Herzog, 1999; Berglund et al., 2003). Similarly, Y_4 receptor immunoreactivity can be observed in the cortex and hypothalamus, specifically in the lateral hypothalamic area where orexin neurons highly express this receptor (Campbell et al., 2003). The fact that Y_4 receptor is expressed in orexin-expressing neurons in the hypothalamus may closely be correlated with food intake control. Indeed, selective activation of Y_4 receptors in the lateral hypothalamic area of freely moving rats induces strong dipsogenic and moderate food intake responses (Campbell et al., 2003). In addition, it was suggested that centrally activation of Y_4 receptor may be involved in both luteinizing hormone, hormone responsible for triggering ovulation and production of testosterone, and follicle-stimulating hormone release that regulates development, growth and pubertal maturation of the body (Raposinho et al., 2000). Also, Y_4 mRNA can be found in whole rat retina and retina endothelial cell line (Álvaro et al., 2007), where was shown to inhibit KCl-evoked increase of intracellular Ca^{2+}, and so to have a neuroprotective role (Álvaro et al., 2009).

Y_5 receptor

Y_5 receptor is a 7 transmembrane protein with a molecular weight of 57 kDa (Campbell et al., 2001) and the gene resides in human chromosome 4q, approximately 20 kb away from Y_1 receptor gene and in an opposite orientation (Gerald et al., 1996; Herzog et al., 1997; Larhammar and Salaneck, 2004). Furthermore, human Y_5 receptor shares only 30-33% of the amino acid sequence with Y_1, Y_2 and Y_4 receptor subtypes, and 88% with rat Y_5 receptor (Hu et al., 1996). Also, Y_5 receptors are preferentially activated by NPY and PYY (Gerald et al., 1996); however some specific and selective agonists have been developed, such as the agonist [^{125}I][cPP(1-7),NPY(19-23),Ala^{31},Aib^{32},Gln^{34}]hPP that has high affinity and specificity for Y_5 receptors, contrarily to what is observed in Y_1, Y_2 or Y_4 receptors (Cabrele et al., 2000; Dumont et al., 2004). Cabrele and collaborators (2000) observed that NPY or PP/NPY chimeras provided with key motif Ala^{31}-Aib^{32} show to be highly selective and to have high affinity with Y_5 receptors. Regarding Y_5 receptor antagonists, the non-peptide L-152,804 is potent and highly selective to this receptor, but not to Y_1, Y_2 or Y_4 receptors (Kanatani et al., 2000). Moreover, a new Y_5

receptor antagonist has been described, the trans-N-[1-(2-fluorophenyl)-3-pyrazolyl]-3-oxospiro-[6-azaisobenzofuran-1(3H),1'-cyclohexane]-4'-carboxamide, which efficiently inhibits these receptors when taken orally and is metabolically stable (Haga et al., 2009).

In the human brain, high expression of Y_5 receptor mRNA is found in the hypothalamus, stratum granulosum of the DG, and a lower expression in CA1 and CA3 subfields of the hippocampus (Jacques et al., 1998). However, discrete expression of Y_5 receptor mRNA can be observed in the frontal and temporal cortices (Jacques et al., 1998). In the rat, Y_5 receptor mRNA (Hu et al., 1996) and immunoreactivity (Wolak et al., 2003) are distributed in the cortex, hippocampus (highest expression in the DG and CA3), caudate putamen, nucleus accumbens and hypothalamus.

The main function of Y_5 receptor is the control of food intake. Indeed, the activation of this receptor seems to stimulate hyperphagia and increase of body weight (Criscione et al., 1999; Mashiko et al., 2003). Furthermore, Y_5 receptor activation is involved in the control of neuronal excitability (Woldbye et al., 1997), as well as in the inhibition of glutamate release from hippocampal synaptosomes (Silva et al., 2005). Moreover, activation of this receptor subtype induces neuroprotection in the DG and CA3 hippocampal subfields of organotypic slice cultures exposed to an excitotoxic insult (Silva et al., 2003a). Regarding drugs of abuse, inhibition of Y_5 receptors decreases cocaine-induced self-administration, increases DA release in the nucleus accumbens and leads to hyperactivity (Sørensen et al., 2012).

y_6 receptor

y_6 receptor gene is localized in the region 5q31 of the human chromosome 5 and mRNA was found in cardiac and skeletal muscle tissues (Gregor et al., 1996). Moreover, *y_6* receptor expression in primates has never been found (Matsumoto et al., 1996), thus no physiological function has been addressed yet, leading to the interesting hypothesis that, in primates, is believed that the *y_6* gene became nonfunctional during evolution (Gregor et al., 1996; Michel et al., 1998). Furthermore, mRNA of this receptor subtype was found in the murine brain, including the hippocampus and hypothalamus, and has high affinity to PP (Gregor et al., 1996).

1.4.3. Neuropeptide Y and methamphetamine

The first study available that explored the effect of METH on NPYergic system points to an increase of NPY release in the paraventricular nucleus (PVN) after METH administration (5 mg/kg, i.p.) to Wistar rats (Yoshihara et al., 1996). In fact, PVN receives NPY projection from the hypothalamus (Broberger et al., 1999), an important region for the feeding behavior control, and

METH has been shown to decrease food intake (Ginawi et al., 2005). Therefore, the link between METH use and food behavior alterations may not rely on changes in NPY release, but may interfere with Y_1 receptor signaling as it has been suggested to regulate food intake in this region. Furthermore, NPY mRNA levels are augmented in the arcuate nucleus of the hypothalamus after METH injection (7.5 mg/kg, i.p.; Crowley et al., 2005). Regarding the striatum, a single dose of METH (15 mg/kg, i.p.) or multiple doses of 10 mg/kg METH (i.p.) managed to decrease NPY immunoreactivity in the posterior nucleus accumbens and caudate nucleus, an effect caused by activation of D1 receptors (Westwood and Hanson, 1999). However, Horner and collaborators (2006) verified that the expression of prepro-NPY mRNA is upregulated in the striatum an effect that also involved D1 receptor activation (Horner et al., 2006). Moreover, METH addiction revealed no changes on NPY levels in the caudate nucleus, caudate putamen, nucleus accumbens or thalamus, but a decrease was observed in the Brodmann's cortical area 9 and 22 (Frankel et al., 2007). Apart from this, Okahisa and collaborators (2009) link the Y_1 receptor gene to the susceptibility to METH dependence and METH use disorders, by pointing that the genotypic distribution of rs7687423 of Y_1 receptor gene was different in METH users when compared to controls (non-users).

The neuroprotective properties of NPY have been raised as an important feature under several pathological conditions. At the cellular level, it is well known that NPY modulates neurotransmitter release and Ca^{2+} homeostasis (Silva et al., 2001; Malva et al., 2012). Contrarily to NPY, METH administration increases intracellular Ca^{2+} verified by the activation of calpain, a mediator of endoplasmic reticulum-dependent cell death (Jayanthi et al., 2004), and alterations of neurotransmitter homeostasis (Mark et al., 2004, 2007). In fact, Thiriet and collaborators (2005) found that NPY (10 µg, i.c.v.), through activation of Y_2 receptors and to a less extend Y_1 receptors, lowers hyperthermia and protects mice striatum injected with a binge regimen of METH (4x 10 mg/kg every 2 h, i.p.). Also, a very interesting finding from our group revealed that Y_2 receptors are involved in METH-induced memory deficits, demonstrating that blockade of Y_2 receptor subtype completely prevented METH-induced deficits in spatial and recognition memory performance in mice injected with 30 mg/kg METH (i.p.; Gonçalves et al., 2012a). Indeed, these findings are positively correlated with high expression of Y_2 receptors in the DG, CA1 and CA3 subfields of the hippocampus in METH-injected mice (Gonçalves et al., 2012a). In fact, Y_2 receptors seem to have a dual effect: its inhibition protects against METH-induced memory deficits, but on the other hand, its activation protects against METH-induced cell death in mice hippocampus (Gonçalves et al., 2012b).

1.4.4. Neuropeptide Y and neurogenesis of the hippocampus

New neurons are produced throughout life, but the regulation of neurogenesis is far to be unraveled. Nevertheless, some studies have highlighted the impact of NPYergic system on neurogenesis. Howell and collaborators (2003) showed that incubation with NPY (1 μM) for 3, 5 or 7 days increases the number of proliferating cells ($BrdU^+$), progenitor cells ($Nestin^+$) and committed neurons. Furthermore, these proproliferative and proneurogenic effects induced by NPY are mediated by Y_1 receptor subtype since SGZ cultures derived from Y_1 receptor KO mice and incubated with NPY did not exhibit any changes neither on proliferation nor on neuronal differentiation (Howell et al., 2003). Also, the same group showed that Y_1 homozygous KO 129/SvJ mice present lower cell proliferation in the SGZ, however without affecting newborn neurons survival (Howell et al., 2005). Additionally, NPY-induced proliferation requires extracellular-signal-regulated kinase 1/2 (ERK1/2) activation since the phosphorylated state of ERK1/2 was up-regulated after NPY incubation (Howell et al., 2005). Another mechanism intrinsic to NPY-induced SGZ cell proliferation is the up-regulation of fibroblast growth factor receptor 1 (FGFR1) levels, whose activation induces clonal development of neural stem/progenitor cells, and together with NPY potentiates proliferation in SGZ cell cultures (Rodrigo et al., 2010). Additionally, SGZ cell cultures incubated with NPY showed an increase of FGFR1 mRNA and protein levels in proliferating cells *via* activation of Y_1 receptor (Rodrigo et al., 2010). Moreover, the proliferative effect induced by NPY through Y_1 receptors in SGZ cell cultures seems to be mediated by NO since the inhibition of nNOS reduced cell proliferation and the proportion of $Nestin^+/BrdU^+$ cells to control levels (Cheung et al., 2012). An interesting finding was that only the intracellular NO is able to contribute to the proliferative effect induced by NPY *via* activation of the cGMP-PKG pathway followed by downstream activation of ERK1/2 pathway (Cheung et al., 2012). Similarly, animal studies demonstrated that NPY (2.5 pmol, i.c.v.) through Y_1 receptors specifically enhanced proliferation of transient amplifying neural progenitor cells and neuroblasts, and stimulated neuronal differentiation in the DG (Decressac et al., 2011). Noteworthy, as described in section 1.3.4, age down-regulates neurogenesis (Couillard-Després, 2012) and Hattiangady and collaborators (2005) observed that in middle-aged (12-21 month-old) and aged (up to 22 month-old) Fisher 344 rats the number of NPY-positive interneurons in the DG is decreased by half when compared to young rats (3-6 month-old).

1.5. Objectives

It has been shown that chronic exposure to METH induces structural alterations in the hippocampus as well as hippocampal-dependent memory deficits (Thompson et al., 2004). Furthermore, METH can have a dual and opposite effects on DG neurogenesis depending on the dose and frequency of exposure to the drug (Mandyam et al., 2008). Indeed, simulating recreational use of METH was possible to observe an increase in the number of proliferating cells and newborn neurons, whereas addiction administration protocols develop the opposite effect. Despite these studies, little information is available regarding the mechanisms underlying METH-induced alteration of neurogenesis. Therefore, this study presents three major aims regarding the effect of METH on DG neurogenesis: 1 – investigate the impact of this drug of abuse on DG stem cell self-renewal capacities; 2 – explore a possible therapeutic strategy taking advantage of the protective and proneurogenic properties of NPY; and 3 – study alterations on synaptic plasticity of both immature and mature DGCs.

Stem cells have the ability to self-renew and differentiate into the major three neural cell types: neurons, astrocytes and oligodendrocytes (Pastrana, 2011). In fact, it has been recently shown that METH self-administration increases the number of radial glia-like cells, but decreases the number of neuroblasts (Yuan et al., 2011). In the present work, we explored the effect of METH on DG stem cell self-renewal assessed by the neurosphere assay, as well as cell proliferation focusing on cell cycle alterations and the possible contribution of MAPK pathway (Heo et al., 2006). Furthermore, we aim to analyze the effect of METH on DG stem cell division, characterized by cell fate after cell division: if towards self-renewal or towards differentiation.

The second aim consists on the possible protective and proneurogenic role of NPY against the toxicity induced by METH. Here, we explored the mechanisms underlying METH-induced cell death of DG stem/progenitor cells under differentiation. Meantime, the effect of METH on neuronal differentiation will be also taken into consideration. Moreover, NPY will be tested to counteract the possible toxic effect induced by this drug, since it was described by others to protect striatal cells from METH-induced toxicity (Thiriet et al., 2005). Besides the protective effect of NPY, this neuropeptide can also enhance cell proliferation and neuronal differentiation to both SGZ (Howel et al., 2003, 2005; Decressac et al., 2011) and SVZ (Agasse et al., 2008; Decressac et al., 2009). Here, we will test if NPY is also able to prevent the negative effects of METH on neurogenesis.

Synaptic changes are verified in the DG following learning and can be represented as LTP (Neves et al., 2008). In fact, immature DG neurons have a critical period where they exhibit enhanced synaptic plasticity (Ge et al., 2007a), which could be correlated with activation and

recruitment of these cells during learning acquisition (Kee et al., 2009). Therefore, we addressed weather a chronic regimen of METH induces changes in DG neurogenesis and how it could be correlated with synaptic plasticity. We will take advantage of the G42 (GAD67-GFP) mice as a model of neurogenesis, which was previously described to label immature neurons in the DG with a transient GABAergic phenotype (Cabezas et al., 2012).

Chapter 2

Methamphetamine decreases dentate gyrus stem cell self-renewal and shifts the differentiation towards neuronal fate

2.1. Abstract

Methamphetamine (METH) is a highly addictive psychostimulant drug of abuse that negatively interferes with neurogenesis. In fact, we have previously shown that METH triggers stem/progenitor cell death and decreases neuronal differentiation in the dentate gyrus (DG). Still, little is known regarding its effect on DG stem cell properties. Herein, we investigate the impact of METH on mice DG stem/progenitor cell self-renewal functions. METH (10 nM) decreased DG stem cell self-renewal, while 1 nM delayed cell cycle in the G0/G1-to-S phase transition and increased the number of quiescent cells (G0 phase), which correlated with a decrease in cyclin E, pEGFR and pERK1/2 protein levels. Importantly, both drug concentrations (1 or 10 nM) did not induce cell death. In accordance with the impairment of self-renewal capacity, METH (10 nM) decreased $Sox2^{+}/Sox2^{+}$ while increased $Sox2^{-}/Sox2^{-}$ pairs of daughter cells. This effect relied on N-methyl-D-aspartate (NMDA) signaling, which was prevented by the NMDA receptor antagonist, MK-801 (10 μM). Moreover, METH (10 nM) increased doublecortin (DCX) protein levels consistent with neuronal differentiation. In conclusion, METH alters DG stem cell properties by delaying cell cycle and decreasing self-renewal capacities, mechanisms that may contribute to DG neurogenesis impairment followed by cognitive deficits verified in METH consumers.

2.2. Introduction

Methamphetamine (METH) is a highly addictive drug whose consumption has been increasing worldwide and turned to be a public health problem (Silva et al., 2010). Several studies have extensively described the negative effects of METH in the Central Nervous System (Gonçalves et al., 2014; Krasnova and Cadet, 2009), concluding that METH abusers exhibit smaller hippocampal volume, which was positively correlated with poorer memory performance (Thompson et al., 2004). Accordingly, animal studies have clearly demonstrated hippocampal neuronal dysfunction (Gonçalves et al., 2010), as well as cognitive deficits induced by this psychostimulant (Simões et al., 2007). Nevertheless, the mechanisms of METH-induced memory deficits are still poorly understood, but pieces of evidence show that neurogenesis is tightly related to memory. In fact, reduction in the number of immature neurons induces deficits in long-term retention of spatial cognitive functions (Deng et al., 2009), and ablation of hippocampal neurogenesis impairs memory performance related to pattern separation functions (Clelland et al., 2009).

The information available regarding the effect of METH on neurogenesis describes that, in the dentate gyrus (DG), cell proliferation is decreased in gerbils (postnatal day 30) administered once with the drug at postnatal day 14-20 (50 mg/kg) (Hildebrandt et al., 1999). On the other hand, a lower dose of METH (25 mg/kg) transiently decreased cell proliferation in the same region (Teuchert-Noodt et al., 2000). Furthermore, a chronic METH administration (1 mg/kg/day for 14 days) had no effect on the number of proliferating cells in mice DG (Maeda et al., 2007). Interestingly, Wistar rats self-administered with METH (0.05 mg/kg/infusion, 1 h intermittent access, 2x a week during 28 days) displayed an increase in DG cell proliferation as well as in neuronal differentiation, whereas both short (1 h/day) and long (6 h/day) access decreased proliferation and differentiation followed by a reduced number of DG granule cell neurons (Mandyam et al., 2008). Furthermore, self-administration of METH (1 h/day access METH for 13 days) increased the number of radial glia-like cells (type 1 cells), but decreased the proportion of preneuronal neuroblasts (type 2a cells; Yuan et al., 2011) showing that at different maturation stages cells respond differently to an external stimuli (Tashiro et al., 2007). Also, daily access to METH (6 h/day for 4 or 13 days) decreased the number of proliferating cells in the DG without changing, however, the length of S-phase of the cell cycle (Yuan et al., 2011). *In vitro* studies also point that METH reduced proliferation of rat hippocampal neural progenitor cells (Tian et al., 2009; Venkatesan et al., 2011). Additionally, our group recently verified that a nontoxic concentration of METH (1 nM for 7 days) decreased the number of mature neurons in DG-derived neurosphere cultures (Chapter 3, Figure 3.7). Concerning the subventricular zone (SVZ), we have also shown that METH decreases cell proliferation, neuronal differentiation and maturation of stem/progenitor cells (Bento et al., 2011).

Overall, it seems clear that METH interferes with hippocampal neurogenesis, but many questions remain unanswered. In fact, the direct effect of this drug on stem cell self-renewal capacities has never been addressed before. Herein, we show that METH delays cell cycle progression from G0/G1-to-S phase. This effect could be due to the down-regulation of cyclin E, a cyclin involved in the progression through the G1 phase and initiation of DNA replication in the S phase, and to the decrease of epidermal growth factor receptor (EGFR) and extracellular-signal-regulated kinases 1/2 (ERK1/2) phosphorylation, mediators in the MAPK signaling pathway involved in cell proliferation progression. Also, METH decreases DG stem cell self-renewal capacities, which seems to involve NMDA receptors. In conclusion, the present work reveals a negative impact of METH on DG stem cell capacities that can contribute to memory deficits upon METH consumption.

2.3. Material and methods

2.3.1. Dentate gyrus neurosphere cultures

Post-natal 1-3-day-old C57BL/6J mice were sacrificed by decapitation and brains were placed in sterile saline solution. Afterwards, meninges were removed and DG fragments were dissected from 450 µm-thick brain coronal sections, digested in 0.025% trypsin and 0.265 mM EDTA (both from Life Technologies, Carlsbad, CA, USA), and single cells were obtained by gentle trituration. Then, cells were diluted in serum-free culture medium (SFM) composed of Dulbecco's modified Eagle's medium/Ham's (DMEM) F-12 medium GlutaMAX-I supplemented with 100 U/ml penicillin, 100 µg/ml streptomycin, 1% B27 supplement, 5 ng/ml epidermal growth factor (EGF) and 2.5 ng/ml basic fibroblast growth factor (bFGF-2) (all from Life Technologies). Afterwards, cells were plated in uncoated Petri dishes and neurospheres were allowed to develop for 6 days in a 95% air-5% CO_2 humidified atmosphere at 37°C. At 6 days, the neurospheres mean diameter was 90.22 ± 2.24 µm (measurements performed on 2 independent cultures).

Experimental procedures were performed according to the guidelines of the European Communities Council Directives (2010/63/EU) and the Portuguese law for the care and use of experimental animals (DL nº 129/92). All efforts were made to minimize animal suffering and to reduce the number of animals.

2.3.2. Cell death assay

DG neurospheres were exposed to 10 or 100 nM METH (Department of Chemistry and Biochemistry, Faculty of Sciences, University of Porto, Portugal) for 24 h (Figure 2.1 A) and then dissociated with NeuroCult® chemical dissociation Kit (Stem Cell Technologies, Grenoble, France). Cells were adhered to SuperFrost Plus glass slides (Thermo Scientific, Menzel GmbH & Co KG, Braunscheweig, Germany) by centrifugation (360 x*g*, 5 min; Cellspin I, Tharmac GmbH, Waldsoms, Germany), and fixed in 4% paraformaldehyde (PFA). Afterwards, terminal deoxynucleotidyl transferase dUTP nick-end labeling (TUNEL) assay was performed to label apoptotic nuclei. Briefly, cells were rinsed 3x 10 min with 0.01 M phosphate-buffered saline (PBS) and permeabilized in 0.25% Triton X-100 for 30 min at room temperature. Cells were then incubated with terminal deoxynucleotidyl transferase buffer (0.25 U/µl terminal transferase, 6 µM biotinylated dUTP, pH 7.5; Roche, Basel, Switzerland) for 1 h at 37°C in a humidified chamber. Afterwards, cells were rinsed with a termination buffer solution (300 mM NaCl and 30 mM sodium citrate) for 15 min, followed by PBS for 5 min and incubated with Fluorescein

(1:100; Vector Laboratories, Burlingame, USA) for 1 h. Additional SRY (sex determining region Y)-box 2 (Sox2) immunostaining was performed (as described in the immunocytochemistry section) to identify stem cells. Finally, nuclei were counterstained with 4 µg/ml Hoechst 33342 (Sigma-Aldrich) for 5 min and mounted in Dako fluorescence mounting medium (Dako, Glostrup, Denmark). Cell counts were obtained from 6 microscope fields of each coverslip, from 3 independent cultures performed in triplicate.

2.3.3. Immunocytochemistry

DG cell cultures or neurospheres were fixed in 4% PFA for 30 min, permeabilized in 1% Triton X-100 and 3% bovine serum albumin (BSA; all from Sigma-Aldrich, St Louis, MO, USA) in PBS, followed by overnight incubation at 4°C with the following antibodies: goat polyclonal anti-Sox2 (1:200; Santa Cruz Biotechnology, Heidelberg, Germany), goat anti-doublecortin (DCX, 1:500; Santa Cruz Biotechnology) and rabbit polyclonal anti-glial fibrillary acidic protein (GFAP, 1:500; Sigma-Aldrich). Then, cells were rinsed with PBS and incubated for 1 h with the appropriate secondary antibodies: donkey anti-goat Alexa Fluor 594 or donkey anti-rabbit Alexa Fluor 488 (both 1:200; Life Technologies). Afterwards, nuclei were stained with 4 µg/ml Hoechst 33342 (Sigma-Aldrich) and slides were mounted in Dako Fluorescence images for cells counts were recorded using a fluorescence microscopy (Leica DMIRE200, Wetzler, Germany).

2.3.4. Cell cycle analysis

Six-day-old DG primary neurospheres were exposed to 1 nM METH for 24 h or 72 h (Figure 2.2 A), dissociated and fixed in 70% ethanol for 20 min at 4°C. Then, cells were centrifuged at 550 x*g* for 5 min and ressuspended in a solution containing 2% Fetal Bovine Serum (FBS; Life Technologies) in PBS. Afterwards, 10^6 cells/ml were incubated with 10 µM Vybrant® Dye Cycle Orange (Life Technologies), which is a DNA-selective and membrane permeant probe that binds stoichiometrically to DNA and becomes fluorescent upon binding, in the presence of 0.1% Triton X-100 for 45 min at 37°C. Afterwards, cells in suspension were centrifuged at 550 x*g* for 5 min and resuspended in 2% FBS in PBS. Approximately 30000 events were analyzed on a FACS Calibur flow cytometer (Becton Dickinson, San Jose, CA, USA) and cell cycle was analyzed using the ModFit software.

Cell quiescence was assessed in DG neurospheres treated with 1 nM METH for 24 h (Figure 2.2 A). Neurospheres were dissociated to single cells (NeuroCult®) and incubated for 15 min at 37°C with 1 µg/ml Hoechst 33342 (Life Technolgies) and 1 µg/ml pyronin-Y (Sigma-Aldrich), a fluorescent probe that binds to RNA, in culture medium supplemented with 0,1%

Triton. Then, cells were centrifuged for 5 min at 550 x*g*, resuspended in culture medium and analyzed on a FACS Aria III (Becton Dickinson). In detail, pyronin-Y was excited at 488 nm and red fluorescence was collected at 545/35 nm, and Hoechst 33342 was excited at 355 nm (UV) and blue fluorescence was recorded at 450/50 nm. A total of 10000 cells were analyzed per sample at a velocity of 400 events/second. Proper controls consisting of cells incubated with either Hoechst 33342 or Pyronin-Y were performed to calibrate the cytometer. Also, to exclude dead cells, DG cells were incubated with 2 µg/ml propidium iodide (Sigma-Aldrich). Data were analyzed using the flowJo software.

To clarify the behavior of these cells during time, the number of cell divisions within 24 h was analyzed. For that, we took advantage of the tracing dye carboxyfluorescein diacetate succinimidyl ester (CellTrace™ CFSE; Life Technologies), a cell-permeable non-fluorescent ester that once inside the cell, the esterase cleaves the acetyl groups and the molecule becomes markedly fluorescent. The succinimidyl ester group covalently binds to amino groups on intracellular macromolecules, anchoring the dye. As cells divide, each daughter cell receives half the fluorescent label of the parent and fluorescence intensity can be measured, allowing the quantification of the number of generations. Thus, DG neurospheres were incubated with the CFSE (10 µM) for 24 h and a total of 10000 cells were analyzed on a FACS Aria III (Becton Dickinson) with a 488 nm laser. Control conditions were performed by incubating DG cells with the tracing dye for 30 min. Data were analyzed using the flowJo software.

2.3.5. Western blot analysis

To evaluate cyclin A, D1 and E protein levels, 6-day-old neurospheres were exposed to 1 nM METH or to 10 nM METH for cyclin E protein levels determination during 24 h (Figure 2.4 A). Moreover, phospho-epidermal growth factor receptor (pEGFR), epidermal growth factor receptor (EGFR), phospho-fibroblast growth factor receptor 1 (pFGFR1), phospho-extracellular-signal-regulated kinases 1/2 (pErk1/2) and extracellular-signal-regulated kinases 1/2 (ERK1/2) protein levels were analyzed in DG neurospheres exposed to 1 or 10 nM METH for 6 or 24 h (Figure 2.5 A). Regarding DCX and GFAP protein levels, DG cells were exposed to 1 or 10 nM METH for 6 days (Figure 2.8 A) and the resulting neurospheres were harvested. Then, DG neurospheres were homogenized in RIPA buffer containing 150 mM NaCl, 5 mM EGTA, 50 mM Tris, 1% (v/v) Triton X-100, 0.1% SDS and 0.5% sodium deoxycholate, supplemented with a protease inhibitor cocktail tablet (Roche, Amadora, Portugal) in the ratio of 1 tablet/10 ml RIPA buffer. Afterwards, cells were centrifuged at 17000 x*g* for 15 min and protein concentration was determined using the bicinchoninic acid (BCA) Protein Assay (Thermo Fisher Scientific,

Northumberland, UK). Then, 10 µg or 30 µg of protein samples were separated by electrophoresis in a 8% or 12% SDS-PAGE, respectively, transferred to a polyvinylidene dofluoride (PVDF) membrane (Millipore, Algés, Portugal) and blocked in a solution of 5% non-fat dried milk or 4% BSA in PBS-0.5% Tween (PBS-T; Sigma-Aldrich) for 1 h. Membranes were probed overnight at 4°C with mouse monoclonal anti-cyclin A (1:200; Abcam, Cambridge, UK), mouse monoclonal anti-cyclin D1 (1:100), mouse monoclonal anti-cyclin E (1:100), rabbit polyclonal anti-p21 (1:200), mouse monoclonal anti-p27 (1:200) (all from Santa Cruz Biotechnology), mouse monoclonal anti-phospho-epidermal growth factor receptor (pEGFR; 1:500; Millipore), rabbit polyclonal anti-EGFR (1:200; Abcam), rabbit monoclonal anti- pFGFR1 (1:200; Abcam), rabbit monoclonal anti-pERK1/2 (Thr202/Tyr204; 1:200; Cell Signaling Technology, Beverly, MA, USA), rabbit monoclonal anti-ERK1/2 (1:200; Cell Signaling Technology), rabbit polyclonal anti-GFAP (1:1000; Sigma-Aldrich), goat polyclonal anti-DCX (1:200; Santa Cruz Biotechnology), mouse monoclonal anti-β-actin (1:10000; Sigma-Aldrich) and rabbit polyclonal anti-GAPDH (1:500; Sigma-Aldrich). Then, membranes were rinsed in PBS-T and incubated for 45 min with alkaline phosphatase-conjugated secondary antibodies as follows: anti-rabbit IgG, (1:20000; GE Healthcare Europe GmbH, Freiburg, Germany), anti-mouse (1:10000, GE Healthcare Europe GmbH) and anti-goat IgG, (1:10000, Zymax, California, USA). Densitometric analysis was performed using the ECF reagent (GE Healthcare Europe GmbH), visualized on the Typhoon 9000 system (GE Healthcare Europe GmbH), and band intensities were quantified using the ImageQuant 5.0 software.

2.3.6. Neurosphere self-renewal assay

Self-renewal capacity of DG stem/progenitor cells was assessed using the neurosphere assay. In detail, DG cells were seeded at clonal density of 10 cells/µl (Coles-Takabe et al., 2008; Pastrana et al., 2011) into uncoated 24-well plates and incubated with 1 or 10 nM METH for 6 days and the total number of primary neurospheres in each well was determined (Figure 2.6 A). Afterwards, primary neurospheres were dissociated (NeuroCult® chemical dissociation kit, Stem Cell Technologies) and cells were reseeded as aforementioned without treatments for 6 additional days (Figure 2.6 A). The total number of resulting secondary neurospheres was determined in each well. Results are expressed as percentage of the control (untreated) in both primary and secondary neurospheres from at least 3 independent cultures and performed in triplicate (3 wells per condition within the 24-well plate).

2.3.7. Cell-fate studies: cell pair assay

Uncommitted stem cells can divide symmetrically into two stem cells ($Sox2^+/Sox2^+$) or into two progenitor cells ($Sox2^-/Sox2^-$), or asymmetrically into one uncommitted cell and one committed progenitor cell ($Sox2^+/Sox2^-$). Taking advantage of these properties, we analyzed if METH interferes with cell-fate division. For that, cell pair assay was performed as previously described (Bernardino et al., 2012; Santos et al., 2012; Xapelli et al., 2013) with some modifications. Hence, stem cells were directly isolated from mice DG and 10000 cells (8840 cells/cm^2) were plated onto poly-D-lysine-coated (Sigma-Aldrich) glass coverslips. After seeding, cells were pre-incubated with 10 μM (5R,10S)-(–)-5-Methyl-10,11-dihydro-5H-dibenzo[a,d]cylcohepten-5,10-imine maleate (MK-801; Tocris) for 15 min and then co-exposed with 1 or 10 nM METH for 24 h (Figure 2.7 A). Then, immunocytochemistry to Sox2 was performed (section 2.3.3). A total of 40 pairs of daughter cells that resulted from the division of one stem cell was characterized according to its symmetric cell division towards self-renewal ($Sox2^+/Sox2^+$) and differentiation ($Sox2^-/Sox2^-$), or asymmetric cell division ($Sox2^+/Sox2^-$). Results are expressed as percentage of control (untreated) from at least 2 independent cultures performed in triplicate.

2.3.8. Data analysis

Statistical analysis was determined from at least two independent cultures and by using an analysis of variance (one-way ANOVA) followed by Dunn's multiple comparison or Mann Whitney post-hoc tests, as indicated in the figure legends. Data are expressed as mean + standard error of the mean (SEM) from at least 2 independent cultures in which each condition was performed in duplicate or triplicate, and statistical significance level was set for $P < 0.05$.

2.4. Results

2.4.1. Methamphetamine can induce dentate gyrus stem cell death

Several studies have previously shown that METH can be toxic to different brain cells (Deng et al., 2002; Genc et al., 2003; Mandyam et al., 2007), but the direct effect of this drug on DG stem cells has never been addressed before. Thus, in the present study we started by evaluating the toxic effect of METH on DG stem cells by quantifying the number of positive cells for TUNEL and Sox2 (Figure 2.1 B and C). We observed that 10 nM METH did not induce cell death to Sox2-positive cells (111.00 + 24.51% of control; Figure 2.1 C). However, 100 nM METH

was toxic to DG neurospheres observed by the significant increase of Sox2- and TUNEL-positive cells (196.20 + 26.26% of control; $P < 0.01$; Figure 2.1 C).

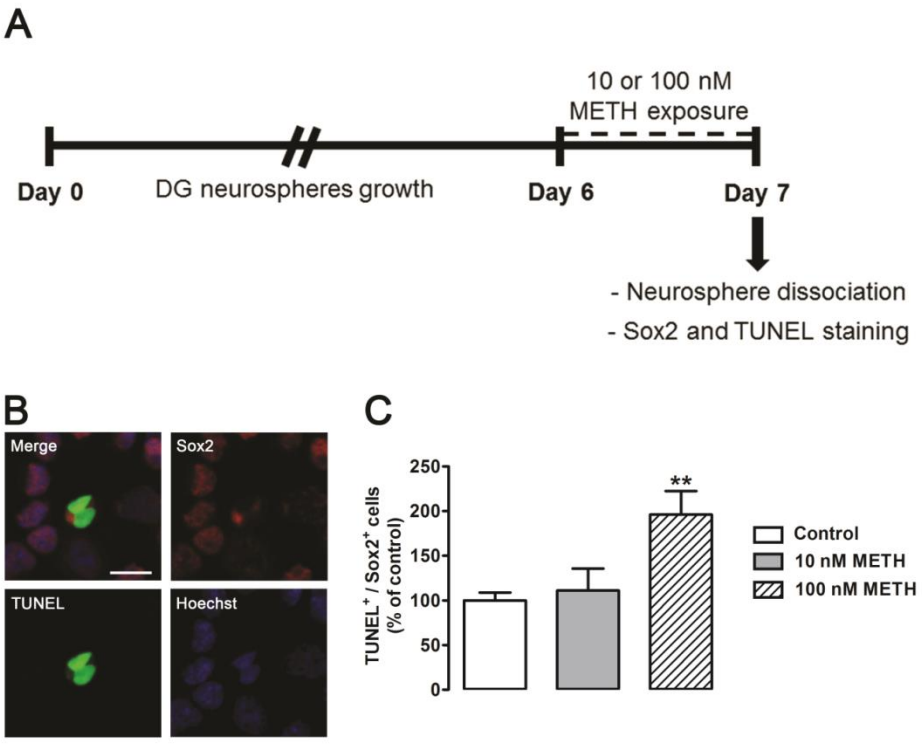

Figure 2.1 – METH can induce DG stem/progenitor cell death. (A) Schematic representation of the experimental design to assess DG cell death. DG neurospheres were exposed to METH (10 or 100 nM) for 24 h and the number of TUNEL- and Sox2-positive cells was determined to evaluate apoptotic cell death of stem cells. (B) Representative fluorescence images of a TUNEL-positive nucleus (green) of a Sox2-positive stem cell (red). Scale bar: 10 µm. (C) Quantification of TUNEL- and Sox2-positive cells in the presence of 10 or 100 nM METH. Only the highest concentration was toxic to stem cells. Data are expressed as % of control + SEM from at least 2 independent cultures where each condition was performed in duplicate. $^{**}P < 0.01$, significantly different from control, using Kruskal-Wallis test followed by Dunn's multiple comparison post-hoc test.

2.4.2. Methamphetamine delays dentate gyrus cell cycle

Based on our previous results (Figure 2.1 C) and in order to select drug concentrations more similar to those frequently present in the brain of METH users, we decided to use 1 or/and 10 nM of METH in the following studies. Noteworthy, both concentrations did not induce stem cell death. Thus, we analyzed the effect of METH (1 nM) on cell cycle progression and, after 24 h, there was an increase in the population of cells in the G0/G1 phase (61.59 + 2.77%, $P < 0.01$) when compared to the control (48.91 + 2.12%; Figure 2.2 B). Furthermore, METH induced a decrease in the percentage of cells in the S phase (control: 36.86 + 2.81%; METH: 27.72 + 1.69%, $P < 0.01$; Figure 2.2 B). Regarding the G2/M phases, no differences were observed between

METH and control conditions (control: 15.04 + 0.77%; METH: 13.42 + 1.08%; Figure 2.2 B). To further clarify if METH induces cell cycle inhibition or delay, neurospheres were exposed to 1 nM METH for 72 h (Figure 2.2 A). We concluded that METH no longer interfered with G0/G1 (control: 86.82 + 0.57%; METH: 85.41 + 0.92%), S (control: 9.37 + 0.16%; METH: 10.94 + 0.83%) or G2/M phases (control: 3.81 + 0.72%; METH: 3.64 + 0.42%; Figure 2.2 C), indicating that METH delays cell cycle progression rather than inhibiting it.

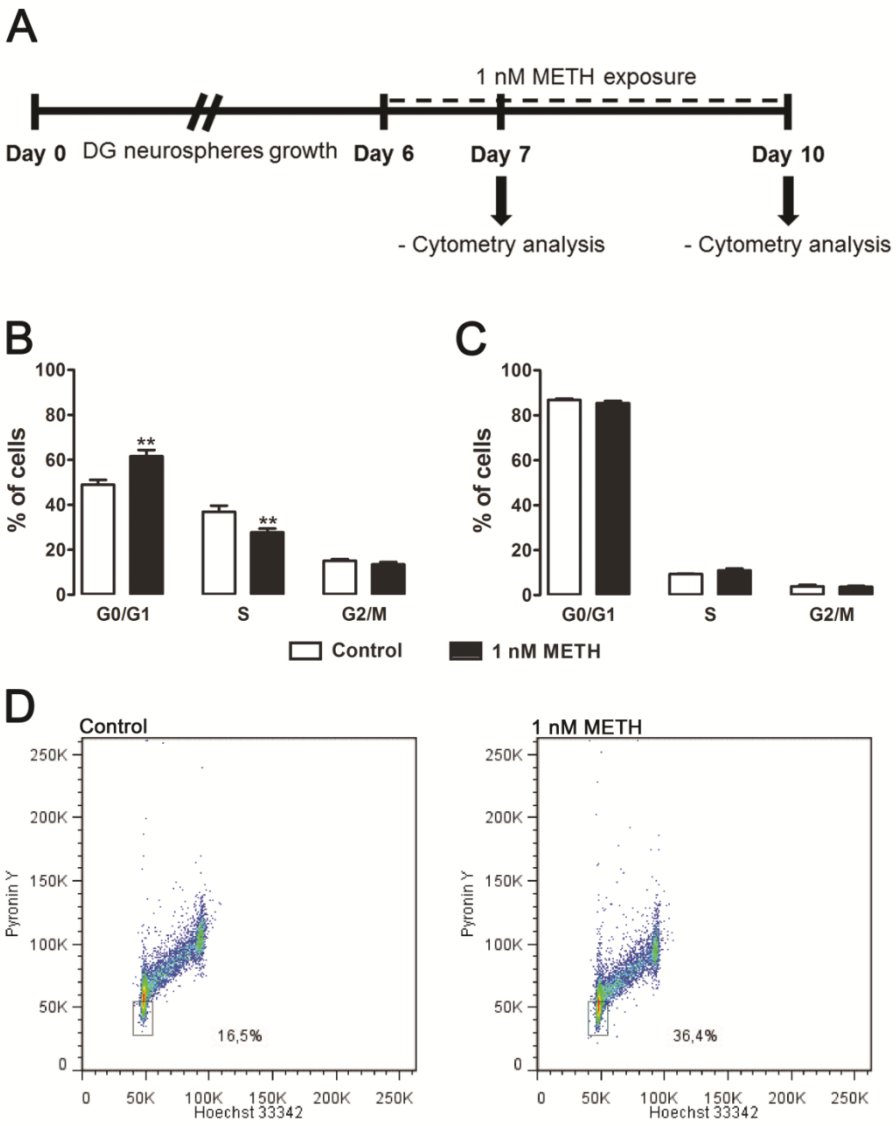

Figure 2.2 – METH delays DG neurosphere cell cycle in the transition from G0/G1 to S phase and induces stem/progenitor cell quiescence. (A) Schematic representation of the experimental protocol for cytometry analysis. (B and C) Quantification of cells present in different phases of the cell cycle after (B) 24 h or (C) 72 h of METH exposure. (B) METH increases the population of cells in the G0/G1 phase while decreasing the S phase. (C) In contrast, METH does not induce any alterations in cell cycle at 72 h exposure. Data are expressed as % of cells + SEM from at least 2 independent cultures and each condition was performed in duplicate. $^{**}P < 0.01$, significantly different from control using Mann Whitney post-hoc test. (D) METH (1 nM for 24 h) increases the number of cells in quiescent phase (G0) as showed by the representative dot plots (representative experiment of 3 independent cultures).

To disclose whether delay in the cell cycle is due to entry in quiescence (G0), DG neurospheres were exposed to 1 nM METH for 24 h (Figure 2.2 A) and then incubated with Hoechst 33342 and pyronin Y to label DNA and mRNA, respectively. Quiescent cells possess less mRNA than actively cycling cells and therefore display low levels of pyronin Y-emitted fluorescence. As represented in Figure 2.2 D, METH increased in about 20% the cell population that rests in G0 (control: 16.5%; METH: 36.4%).

Furthermore, after analyzing the number of cell divisions within DG cells, we verified a decrease in the number of cells with comparable fluorescence when compared to the control (30 min of incubation; Figure 2.3 A). In conclusion, two cell divisions in 24 h were observed as the fluorescence intensity decreased in comparison to the 30 min-probe exposure in control (Figure 2.3 B).

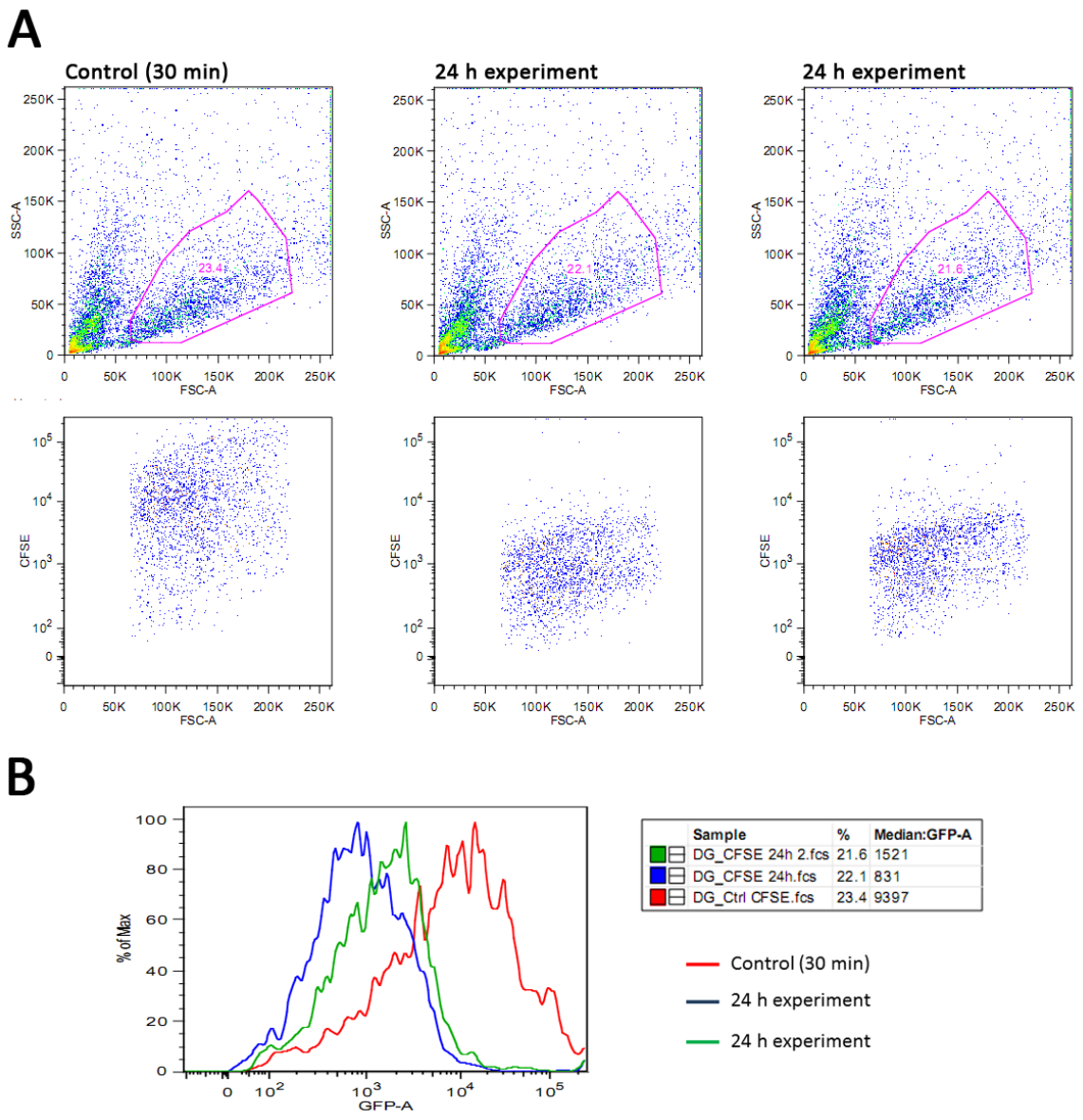

Figure 2.3 – DG cells undergo two cell divisions in 24 h. (A) Representative dot plots from a control condition and 24 h-time course experiment. (B) Fluorescence analysis histogram showing a decrease of GFP fluorescence in both 24 h-time course experiments (green and blue) when compared to the control condition (red).

After demonstrating that METH impairs the progression of DG stem cells from G0/G1 to S phase of the cell cycle, we further investigated possible alterations of cyclins D1, E and A, since these proteins are involved in the cell cycle progression. It was possible to conclude that METH (1 nM) did not induce alterations of cyclin D1 (control: 100.00 + 17.06%; METH: 94.40 + 10.10% of control; Figure 2.4 B) or cyclin A protein levels (control: 100.00 + 12.04%; METH: 104.60 + 13.93% of control; Figure 2.4 E). On the other hand, the expression of cyclin E was down-regulated by this drug (control: 100.00 + 4.36%; METH: 90.20 + 1.52% of control; $P < 0.05$; Figure 2.4 C). A similar down-regulation of cyclin E was observed with 10 nM METH (control: 100.00 + 12.74%; 10 nM METH: 49.46 + 8.18% of control; $P < 0.05$; Figure 2.4 D). Afterwards, we assessed the protein levels of both p21 and p27, the main inhibitors of the complexes cyclin D1/Cdk4/6 and cyclin E/Cdk2, respectively. Thus, METH neither altered the protein levels of p21 (control: 100.00 + 13.38%; METH: 102.60 + 7.34% of control; Figure 2.4 F) nor of p27 (control: 100.00 + 11.64%; METH: 101.40 + 5.93% of control; Figure 2.4 G).

Additionally, since activation of ERK1/2 is highly involved in cell proliferation through the upstream activation of EGFR (Gampe et al., 2011) or FGFR1 (Xiao et al., 2007), we determined the effect of METH on the phosphorylation levels of FGFR1, EGFR and ERK1/2. Indeed, METH (1 nM) did not change the protein levels of pFGFR1 (control: 100.00 + 9.44%; METH: 86.02 + 12.00% of control; Figure 2.5 B) at 6 h of drug exposure, whereas decreased protein levels of pEGFR (control: 100.00 + 9.77%; METH: 48.60 + 13.37% of control; $P < 0.05$; Figure 2.5 C) and pERK1/2 (control: 100.00 + 3.95%; METH: 82.02 + 2.11% of control, $P < 0.05$; Figure 2.5 D) in DG neurospheres at 6 h post-METH exposure. However, after 24 h of METH (1 nM) treatment, pERK1/2 protein levels were similar to control (101.60 + 5.52% of control; Figure 2.5 D). The same effect was observed with 10 nM METH (control: 100.00 + 2.68%; METH 6 h: 77.68 + 5.66% of control, $P < 0.05$; METH 24 h: 123.70 + 13.78% of control; Figure 2.5 E).

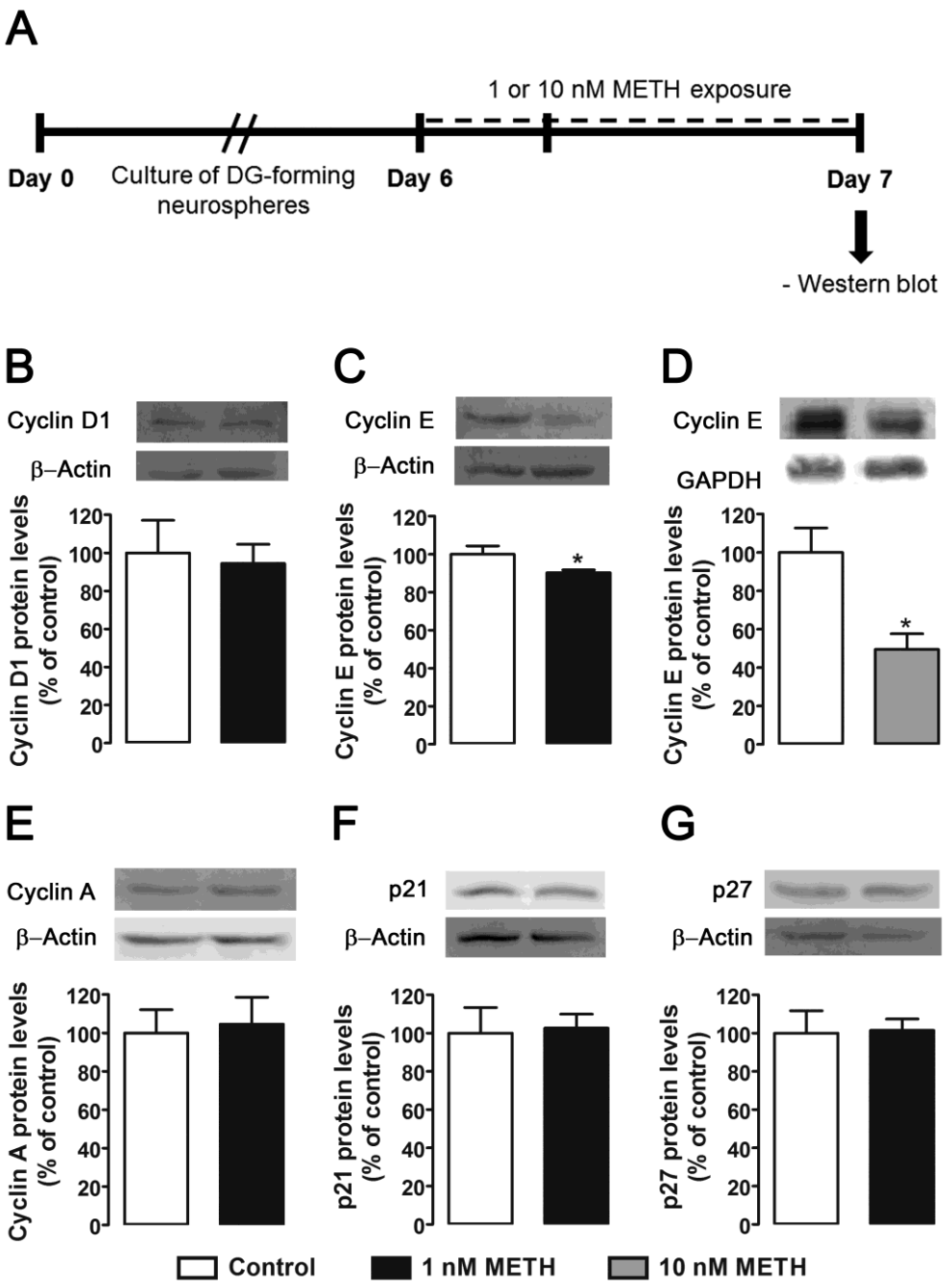

Figure 2.4 – METH down-regulates cyclin E protein levels in DG neurospheres. (A) Schematic representation of the experimental design for western blot studies. METH (1 nM) does not induce alterations in (B) cyclin D1 (37 kDa) or (E) cyclin A (60 kDa) protein expression, but (C) down-regulates cyclin E (53 kDa) expression, which is also observed at (D) 10 nM METH. Additionally, METH (1 nM) does not interfere with (F) p21 (21 kDa) and (G) p27 (27 kDa) expression, the main inhibitors of the complexes cyclin D1/Cdk4/6 and cyclin E/Cdk2, respectively. Above the bars, representative western blot images of the different proteins are shown, including the housekeeping gene β-actin (42 kDa) or GAPDH (36 kDa). Data are expressed as % of control + SEM from at least 4 independent cultures. **P* < 0.05, significantly different from control using Mann Whitney post-hoc test.

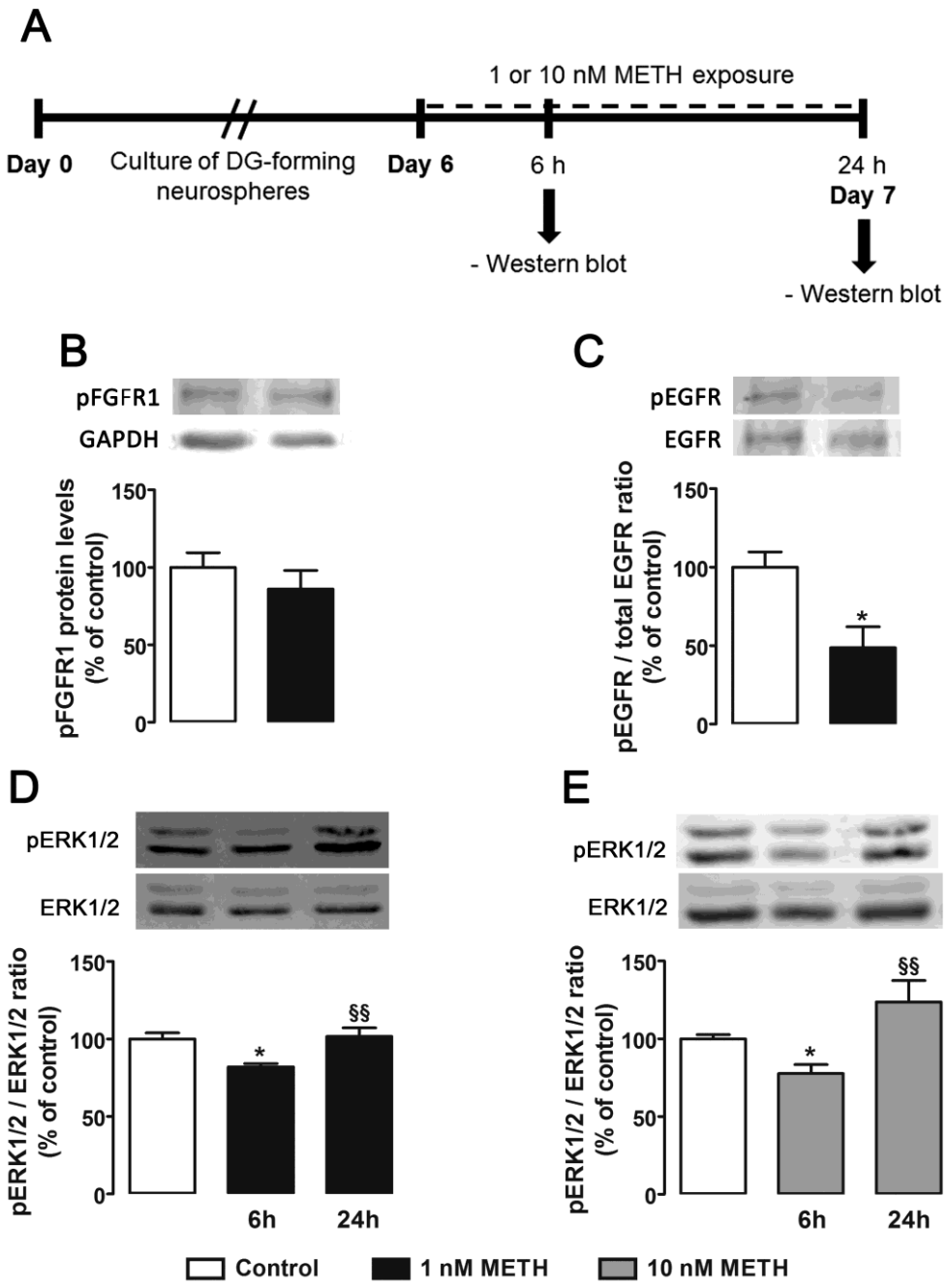

Figure 2.5 – METH down-regulates the phosphorylation form of EGFR and ERK1/2. (A) Schematic representation of the experimental design for western blot studies. Exposure to METH (1 nM) for 6 h does not induce any effect in (B) pFGFR1 (130 kDa), but (C) down-regulates the phosphorylation levels of EGFR (175 kDa). In addition, (D) 1 nM or (E) 10 nM METH decreases the phosphorylation form of ERK1/2 (42/44 kDa) after 6 h of drug exposure, but no alterations were observed after 24 h. Data are expressed as % of control + SEM from at least 4 independent cultures. *$P < 0.05$, significantly different from control using Mann Whitney or Kruskal-Wallis test followed by Dunn's Multiple comparison post-hoc tests. $^{§§}P < 0.01$, significantly different from METH 6 h-exposure using Kruskal-Wallis test followed by Dunn's Multiple comparison post-hoc test.

2.4.3. Methamphetamine decreases dentate gyrus neurosphere self-renewal

DG stem cells have the ability to self-renew and this capacity was assessed using the neurosphere assay (Coles-Takabe et al., 2008; Pastrana et al., 2011). Thus, METH (1 nM) decreased the number of primary neurospheres (control: 100.00 + 5.29%; METH: 76.77 + 5.29% of control, $P < 0.01$; Figure 2.6 B). However, no differences in the number of secondary neurospheres were observed (control: 100.00 + 6.05%; METH: 96.79 + 8.56% of control; Figure 2.6 B) indicating that 1 nM METH did not interfere with self-renewal capacity of DG stem/progenitor cells. In parallel, a higher concentration of METH (10 nM) also decreased the number of primary neurospheres (72.37 + 2.06% of control, $P < 0.05$; Figure 2.6 C). Interestingly, the number of secondary neurospheres was also decreased (control: 100.00 + 4.97%; METH: 76.47 + 3.57% of control, $P < 0.01$; Figure 2.6 C) showing that METH at 10 nM decreases self-renewal capacity.

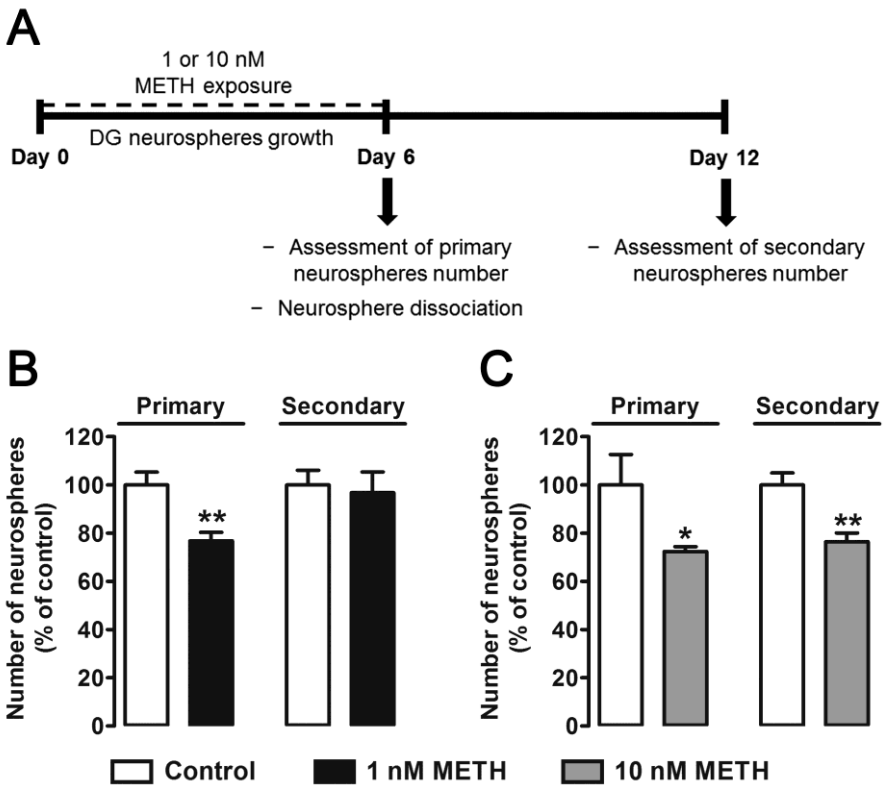

Figure 2.6 – METH decreases DG neurosphere self-renewal. (A) Schematic representation of the experimental design to evaluate the impact of METH on self-renewal capacity of DG stem/progenitor cells. (B) METH (1 nM) decreases the number of primary neurospheres, but does not induce any effect on the number of secondary neurospheres. (C) However, 10 nM METH is able to decrease both the number of primary and secondary neurospheres. Data are expressed as % of control + SEM from 3 independent cultures and each condition was performed in triplicate. *$P < 0.05$; **$P < 0.01$, significantly different from control using Mann-Whitney post-hoc test.

2.4.4. Methamphetamine shifts cell fate towards differentiation *via* activation of NMDA receptors

DG stem cells can self-renew, *i.e.*, one stem cell can divide and give rise at least to one identical cell to itself and/or generate progenitors that undergo differentiation (Gage, 2000). Herein, we observed that 1 nM METH had no effect on DG symmetric cell division towards self-renewal ($Sox2^+/Sox2^+$: 87.01 + 6.60% of control; Figure 2.7 B). Similarly, no effect was verified on symmetric cell division towards differentiation ($Sox2^-/Sox2^-$: 110.90 + 4.63% of control) or on asymmetric cell division ($Sox2^+/Sox2^-$: 99.07 + 7.00% of control; Figure 2.7 B). However, 10 nM METH decreased the number of $Sox2^+/Sox2^+$ pairs of cells (53.74 + 4.69% of control; $P < 0.01$), and the blockade of NMDA receptors with MK-801, completely prevented the effect induced by METH (99.34 + 10.52% of control, $P < 0.05$ compared to METH alone; Figure 2.7 C). Furthermore, METH induced an increase of $Sox2^-/Sox2^-$ pairs of cells and MK-801 also prevented this effect (METH: 191.10 + 8.20%, $P < 0.01$; METH + MK-801: 78.57 + 9.82% of control, $P < 0.001$ compared to METH alone; Figure 2.7 C). On the other hand, 10 nM METH did not affect asymmetric cell division ($Sox2^+/Sox2^-$; Figure 2.7 C).

2.4.5. Methamphetamine increases doublecortin expression in DG neurospheres

As METH directs cell division towards differentiation, we further evaluated neuronal and astroglial differentiation in DG cells treated for 6 days with METH (Figure 2.8 A). Protein levels of DCX, a marker for immature neurons, and of GFAP, an astrocytic marker, were determined by western blot. We observed that 1 nM METH did not interfere with both DCX (105.60 + 7.69% of control; Figure 2.8 B) and GFAP (94.14 + 14.08% of control; Figure 2.8 C) protein levels. However, at a higher concentration (10 nM) METH was able to up-regulate DCX expression (133.70 + 6.83% of control; $P < 0.05$; Figure 2.8 B and D), whereas no changes were observed in GFAP protein levels (93.05 ± 4.29% of control, Figure 2.8 C and D). Overall, these results demonstrate that 10 nM METH directs DG stem/progenitor cell differentiation towards the neuronal fate.

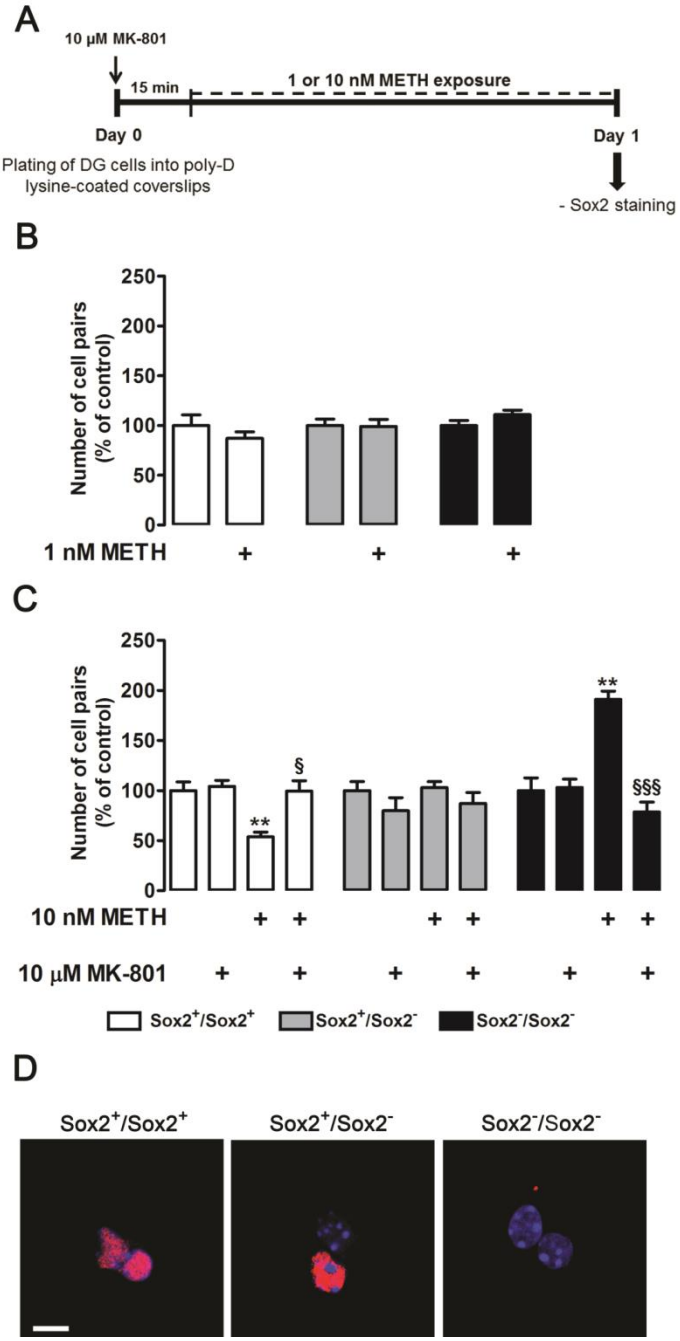

Figure 2.7 – METH triggers DG cell-fate division towards differentiation *via* activation of NMDA receptors. (A) Schematic representation of the experimental design to evaluate how METH interferes with cell fate. (B) METH (1 nM) does not induce any alterations in DG cell-fate division. (C) Nevertheless, a higher concentration of the drug (10 nM METH) decreases the number of $Sox2^+/Sox2^+$ pairs of daughter cells, which was completely prevented by the NMDA receptor inhibitor, MK-801 (10 µM), and increases the number of $Sox2^-/Sox2^-$ pairs of cells without altering asymmetric cell division ($Sox2^+/Sox2^-$). Data are expressed as % of control + SEM from at least 2 independent cultures where each condition was performed in triplicate. $^{**}P < 0.01$, significantly different from control using Kruskal-Wallis test followed by Dunn´s Multiple comparison test. $^{§}P < 0.05$; $^{§§§}P < 0.001$, significantly different from 10 nM METH using Kruskal-Wallis test followed by Dunn´s Multiple comparison test. (D) Representative fluorescence images showing $Sox2^+/Sox2^+$ (symmetric self-renewing cell division), $Sox2^+/Sox2^-$ (asymmetric cell division), and $Sox2^-/Sox2^-$ (symmetric differentiation division) pairs of cells. Scale bar: 5 µm.

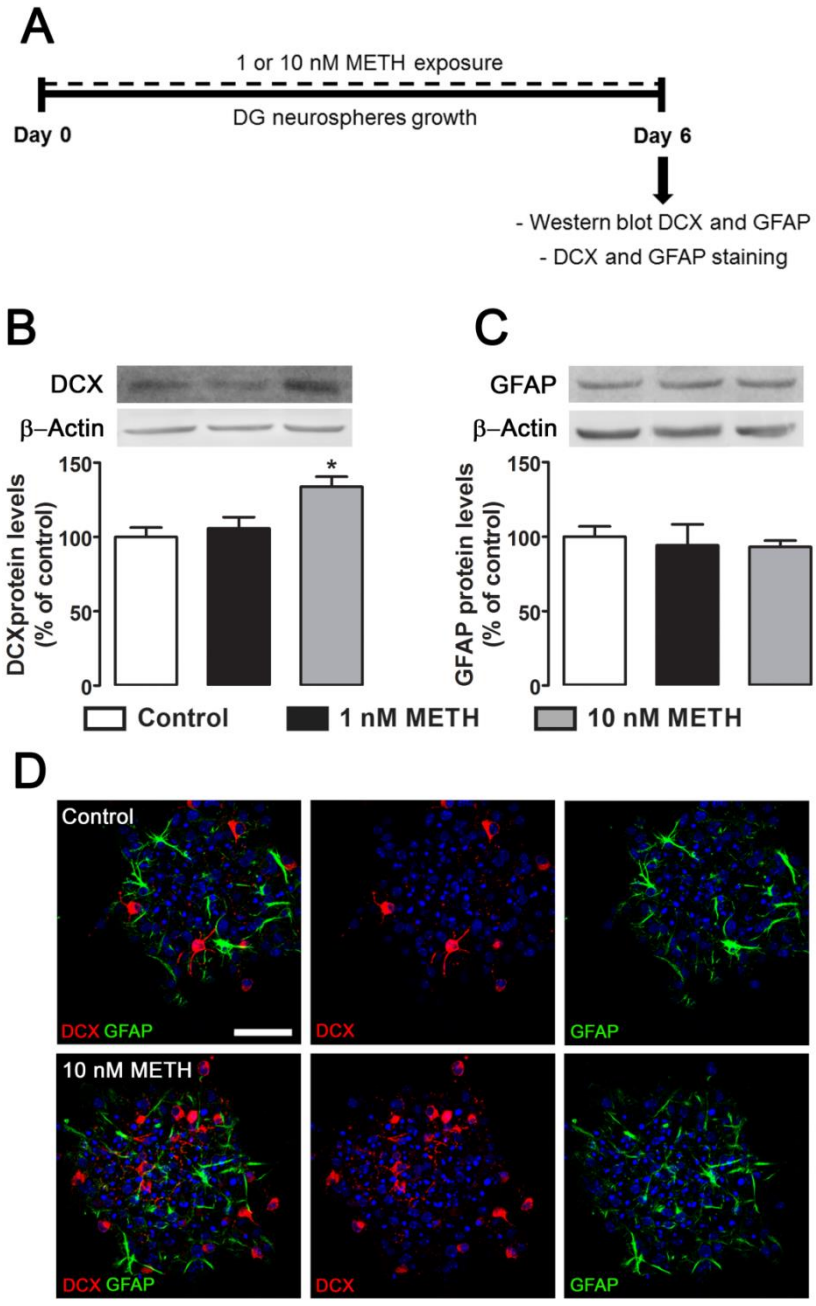

Figure 2.8 – METH increases immature neurons in DG neurospheres. (A) Schematic representation of the experimental design of DG cells to evaluate the effect of METH on DG neurospheres growth. (B) METH (10 nM) increases DCX (40 kDa) protein levels, but without an effect on (C) GFAP (50 kDa) expression. Data are expressed as % of control + SEM from at least 2 independent cultures. **P* < 0.05, significantly different from control using Kruskal-Wallis test followed by Dunn´s Multiple comparison test. (D) Representative fluorescence images of DG neurospheres showing increased DCX (red) immunoreactivity in DG cells exposed to 10 nM METH, without inducing significant alterations in GFAP (green) expression. Nuclei were stained with Hoechst 33342 (blue). Scale bar: 50 µm.

2.5. Discussion

The present work addresses the effect of METH on DG stem cell properties. Indeed, our results show that METH at nontoxic concentrations impaired stem cell properties, specifically by decreasing self-renewal capacity, delaying cell cycle progression and directing cell fate division towards differentiation. Firstly, we verified that METH (100 nM) induced cell death of $Sox2^+$ DG stem/progenitor cells from free floating neurospheres, having no effect at a lower concentration (10 nM). Interestingly, we have shown that exposure to 10 nM METH for 24 h induced cell death on plated DG-derived neurosphere cultures (Chapter 3, Figure 3.1). Thus, we may conclude that neurospheres plated on poly-D-lysine and in a medium devoid of growth factors initiate differentiation and are more sensitive to METH toxicity as compared to free floating $Sox2^+$ neurospheres cultured in the presence of growth factors. This difference may rely on differential abilities to repair DNA damages (Fernando et al., 2011), to counteract oxidative stress (Le Belle et al., 2011) or/and METH-induced apoptosis mechanisms displayed by stem/progenitor cells *versus* committed progenitors.

Herein, we also explored for the first time the impact of METH on the cell cycle in DG stem cells. It was possible to observe a delay in the transition from G0/G1 to the S phase, an increase of cell population in the quiescence state (phase G0), and a down-regulation of cyclin E protein, which forms a complex with cyclin-dependent kinase 2 (Cdk2) being involved in the progression through the G1 phase and initiation of DNA replication in the S phase (Mazumder et al., 2004). Accordingly, to confirm that METH delays cell cycle progression, the doubling time for cell division was assessed and we observed that DG cells undergo two cell divisions in 24 h. On the other hand, METH did not induce any alterations in both cyclin D1 and cyclin A protein levels, which lead us to conclude that METH specifically impairs G1-to-S transition. In fact, little information is available regarding the effect of METH in cell cycle. Nevertheless, Yuan and collaborators (2011) assumed that hippocampal proliferating cells may be arrested in the G1 phase by METH (self-administration of 0.05 mg/kg/injection, 6 h/daily for 13 days) since they observed not only a decreased number of cells in the S phase, but also of cells that enter and exit the S phase without changing, however, its length. In fact, other psychostimulants like cocaine (10 or 100 μM, nontoxic concentrations) also interfere with the transition from G1-to-S phase in AF5 progenitor cells (a rat mesencephalic cell line), confirmed by the down-regulation of cyclin A2 (Lee et al., 2008). Indeed, the authors demonstrated that this effect was triggered by oxidative endoplasmic reticulum stress (Lee et al., 2008). Additionally, Hu and colleagues (2006) observed that cocaine inhibited proliferation in human fetal neural progenitor cells with simultaneous increase of the cyclin-dependent kinase inhibitor, p21. Moreover, very recently

Blanco-Calvo and collaborators (2014) showed that acute administration of cocaine (10 mg/kg) decreases the number of proliferating cells in the subgranular zone, which was prevented by the inhibition of cannabinoid CB1 or CB2 receptors. Cannabinoid receptor blockade was also able to prevent hippocampal-dependent contextual memories induced by cocaine (Blanco-Calvo et al., 2014).

On the other hand, with the present study we verified that METH did not alter protein expression of cyclin inhibitors, p21 and p27, which suggests the involvement of other mechanisms in METH-induced cyclin E down-regulation. In fact, Heo and collaborators (2006) showed that blockade of MAPK pathway with PD-98059 (MEK1 inhibitor) decreased both cyclins D1 and E protein levels. These authors investigated the involvement of MAPK pathway activation in cell proliferation by stimulating mouse embryonic stem cells with EGF, which induced an increase in the phosphorylate state of ERK1/2 and cyclin E proteins (Heo et al., 2006). Furthermore, homocysteine, a sulfur-containing intermediate of methionine metabolism, decreases phosphorylation of ERK1/2 and cyclin E protein expression in mice SVZ cells incubated with FGF-2 (Rabaneda et al., 2008). Based on our results, we may suggest that METH acts upstream to ERK1/2 by decreasing the phosphorylation levels of EGFR, which will interfere with the MAPK pathway through down-regulation of pERK1/2 followed by a decrease in cyclin E expression, that in turn will affect cell cycle progression and resulting in the impairment of DG stem cell self-renewal. In fact, little is known regarding the effect of METH on EGFR, but it was previously demonstrated that neonatal EGF administration increased METH-induced locomotor responses (Mizuno et al., 2004). Still, it was shown that EGFR plays an active role in promoting cell proliferation and neuronal differentiation in the SGZ, as well as in rescuing neurogenesis in aged rats (Jin et al., 2003). Additionally, in a Parkinson's disease animal model, EGFR expression is down-regulated in proliferating cells in the SVZ (Höglinger et al., 2004). Furthermore, it was demonstrated that EGFR expression and signaling was reduced in the SVZ of aged mice, which resulted in a decrease of cell proliferation and neurogenesis (Enwere et al., 2004). Consistent with this finding, we suggest that METH decreases the expression of pEGFR, which down-regulates MAPK signaling as verified by a transient decrease of ERK1/2 phosphorylation, which could lead to down-regulation of cyclin E and, consequently, a decrease in DG stem cell proliferation and self-renewal.

Although MAPK pathway can mediate cell proliferation, it can also be involved in memory performance. Indeed, depending on the frequency of METH exposure, an acute (Cao et al., 2013) or chronic (Ito et al., 2007) administration can improve or decline memory performance, accompanied with an increase or decrease in the phosphorylation levels of

ERK1/2, respectively. Furthermore, ERK1/2 activation leads to the activation of the downstream transcription factor cyclic adenosine monophosphate response element-binding protein (CREB) followed by increased expression of c-fos, which in the DG identifies neurons processing spatial information (Sweatt, 2001). Noteworthy, activation of ERK1/2 is necessary to generate long-term potentiation in DG immature neurons (Darcy et al., 2014). Interestingly, Kee and collaborators (2007) verified that immature neurons present increased c-fos expression, which strongly suggest that these cells are recruited to integrate spatial memory circuitries. Accordingly, in the present study we demonstrate that METH transiently decreased pERK1/2 protein levels in DG stem cells and increased immature neurons, which allow us to hypothesize that these neurons can be synaptically active and though participate in memory processes.

Other important characteristic of neural stem cells is the ability to self-renew. Thus, we further explored for the first time the effect of METH on DG stem cell self-renewal. METH, at nontoxic concentrations (1 nM or 10 nM), was able to decrease the number of primary neurospheres, showing that this drug has a negative effect on stem cell proliferation. In fact, the findings obtained in cell cycle analysis can be correlated with the decreased number of primary neurospheres. Specifically, METH delayed G0/G1-to-S phase progression which decreased the proliferative capacity of DG stem cells and, consequently, could decrease the number of neurospheres. Also, at the highest nontoxic concentration (10 nM), METH decreased the number of secondary neurospheres proving that it affects DG stem cell self-renewal. Some studies addressed the effect of METH on DG neurogenesis and focused mainly on cell proliferation. In detail, it has been described that METH (25 mg/kg) transiently decreases the number of BrdU-positive cells in gerbil dentate gyrus (Teuchert-Noodt et al., 2000). Moreover, Mandyam and collaborators (2008) observed that this drug (0.05 mg/kg/infusion) administered 1 h/day and 6 h/day decreases the number of proliferating cells, characterized by the decreased number of Ki-67-positive cells, a protein expressed during the active phases of the cell cycle. Also, METH induces long-term effects in SGZ stem/progenitor cell proliferation, as described by Schaefers and colleagues (2009) showing that a single METH administration (50 mg/kg) to 14-day-old gerbils decreases the number of BrdU-positive cells, 45 days post-administration. In addition, our group demonstrated that 100 µM METH (48 h of exposure) reduced proliferation in SVZ cultures (Bento et al., 2011).

As METH impairs self-renewal capacity, we also explored the influence of METH in DG stem cell-fate division, a suitable method to characterize the phenotype of cells that are derived from the division of one DG stem cell. Indeed, a stem cell can undergo symmetric cell division towards self-renewal, where the two resulting cells are both stem cells ($Sox2^+/Sox2^+$ pairs of

daughter cells), and towards differentiation, resulting two cells that are committed to differentiate ($Sox2^-/Sox2^-$ pairs of daughter cells). Moreover, one stem cell can divide asymmetrically, originating one pair of cells consisting in one $Sox2^+$ and one $Sox2^-$ cell. Accordingly, we found that METH (10 nM) decreased self-renewal symmetric cell division ($Sox2^+/Sox2^+$ pairs of daughter cells), directing division towards $Sox2^-/Sox2^-$ pairs of daughter cells consistent with cell commitment. In fact, an animal study showed that Sox2-positive cells in the SGZ are able to undergo symmetric or asymmetric cell division, in which one Sox2-positive cell can give rise to one neuron and one astrocyte, or to one neural stem cell and one neuron, respectively (Suh et al., 2007). Also, we observed that these alterations could be, in part, due to the activation of NMDA receptor signaling because inhibition of these receptors prevented the shift of cell division towards differentiation. Moreover, we had previously demonstrated that METH induces an increase of glutamate release from DG neurospheres and the inhibition of NMDA receptors protects DG cells from METH toxicity (Chapter 3, Figure 3.3). In fact, several brain injuries, such as status epilepticus (Sugaya et al., 2010), cerebral ischemia (Choi et al., 2012) and traumatic brain injury (Zheng et al., 2013) can increase neurogenesis, and glutamate seems to play a central role upon activation of NMDA receptors (Arvidsson et al., 2001; Urbach et al., 2008). Indeed, Nacher and colleagues (2003) observed that a single injection of NMDA receptor antagonist (CGP-43487, 5 mg/kg) prevents age-induced decrease of SGZ cell proliferation and neurogenesis in both middle-aged (10 month-old) and aged (20 month-old) Fisher F344 rats. Moreover, administration of NMDA (30 mg/kg) to Sprague-Dawley rats decreased the population of proliferating cells in the DG, whereas administration of MK-801 or CGP37849 resulted in the opposite effect (Cameron et al., 1995). Also, MK-801 administration (3 mg/kg) to NMDA-infused (2 mg/ml) Wistar rats increases the phosphorylated levels of ERK in newly generated neurons (Okuyama et al., 2004), which strengths the involvement of NMDA receptors in decreasing cell proliferation through regulation of the MAPK pathway. Moreover, Deisseroth and collaborators (2004) demonstrated that NMDA receptors play an active role in neuronal differentiation, showing that excitatory stimuli induced by NMDA receptor activation enhances expression of NeuroD, a downstream regulator of neuronal differentiation, and consequently increases neurogenesis in neural progenitor cells culture.

The present study also reveals that METH (10 nM) enhanced differentiation into immature neurons in DG neurospheres, verified by the increase of DCX protein levels. This effect correlates with the fact that METH increases the pairs of cells that did not express Sox2 ($Sox2^-/Sox2^-$ cell pairs), *i.e.*, differentiating cells. Furthermore, cell cycle alterations induced by METH suggest a differentiation shift. In fact, the length of G1 phase may influence the decision for a

neural stem cell to proliferate or differentiate as reviewed by Salomoni and Calegari (2010). Furthermore, METH did not induce any alterations in GFAP expression, indicating that immature neurons are preferentially generated rather than astrocytes. In accordance to our findings, it was described by Mandyam and collaborators (2008) that METH self-administration (0.05 mg/kg/infusion, 1 h/day, 2 days/week for 49 days) increases neuronal differentiation and maturation of hippocampal progenitor cells.

Our results show that METH interferes with DG stem cell proliferation, an effect due to a delay on cell cycle G0/G1-to-S transition involving down-regulation of pEGFR, cyclin E and pERK1/2. Additionally, METH impairs DG cell self-renewal capacity *via* NMDA signaling. These effects could be useful to elucidate the impairment of hippocampal neurogenesis and memory deficits in METH abusers.

Chapter 3

Neuropeptide Y promotes neurogenesis and protection against methamphetamine-induced toxicity in mouse dentate gyrus-derived neurosphere cultures

3.1. Abstract

Methamphetamine (METH) is a psychostimulant drug of abuse that causes severe brain damage. However, the mechanisms responsible for these effects are poorly understood, particularly regarding the impact of METH on hippocampal neurogenesis. Moreover, neuropeptide Y (NPY) is known to be neuroprotective under several pathological conditions. Here, we investigated the effect of METH on dentate gyrus (DG) neurogenesis, regarding cell death, proliferation and differentiation, as well as the role of NPY by itself and against METH-induced toxicity. DG-derived neurosphere cultures were used to evaluate the effect of METH or NPY on cell death, proliferation or neuronal differentiation. Moreover, the role of NPY and its receptors (Y_1, Y_2 and Y_5) was investigated under conditions of METH-induced DG cell death. METH induced cell death by both apoptosis and necrosis at concentrations above 10 nM, without affecting cell proliferation. Furthermore, at a nontoxic concentration (1 nM), METH decreased neuronal differentiation. NPY's protective effect was mainly due to the reduction of glutamate release, and it also increased DG cell proliferation and neuronal differentiation *via* Y_1 receptors. In addition, while the activation of Y_1 or Y_2 receptors was able to prevent METH-induced cell death, the Y_1 subtype alone was responsible for blocking the decrease in neuronal differentiation induced by the drug. Taken together, METH negatively affects DG cell viability and neurogenesis, and NPY is revealed to be a promising protective tool against the deleterious effects of METH on hippocampal neurogenesis.

3.2. Introduction

Methamphetamine (METH) is an addictive psychostimulant drug of abuse highly toxic to different brain regions, including the hippocampus, and it was previously shown to induce working memory deficits (Simon et al., 2000; Thompson et al., 2004; Simões et al., 2007). Moreover, oxidative stress (Mirecki et al., 2004; Fitzmaurice et al., 2006), increase of glutamate release (Mark et al., 2004; Tata and Yamamoto, 2008), mitochondrial dysfunction (Jayanthi et al., 2004; Brown et al., 2005; Wu et al., 2007; Tian et al., 2009), neuroinflammation (Thomas et al., 2004; Gonçalves et al., 2008, 2010), hyperthermia (Bowyer et al., 1994) and disruption of the blood-brain barrier (BBB; Bowyer et al., 2008; Ramirez et al., 2009; Silva et al., 2010; Martins et al., 2011) are some of the well-known neurotoxic features of this drug. However, the mechanisms underlying METH toxicity are still poorly understood, particularly its effect(s) on adult brain neurogenesis.

Adult hippocampal neurogenesis is an important modulator of brain plasticity (Prickaerts et al., 2004; Lledo et al., 2006) and plays a key role in learning and memory functions (Garthe et

al., 2009; Clelland et al., 2009; Jessberger et al., 2009). This is a process that persists throughout life but several factors may impair the formation of new functional neurons. In fact, drugs of abuse generally have a negative impact on neurogenesis (Mandyam et al., 2008; Silva et al., 2010; Bento et al., 2011). Chronic exposure to cocaine decreases proliferation in the subgranular zone (SGZ), but has no effect on immature cell survival or cell death (Domínguez-Escribà et al., 2006). Furthermore, a binge alcohol administration to adolescent nonhuman primates decreases both proliferation and neurogenesis with an increase in neural degeneration (Taffe et al., 2010). On the other hand, 3,4-methylenedioxymethamphetamine (MDMA) administered to adolescent Sprague-Dawley rats increases proliferation, whereas neuronal differentiation is compromised (Catlow et al., 2010). Chronic administration of morphine and chronic self-administration of heroin impair cell proliferation and neurogenesis (Eisch et al., 2000). Concerning METH, the little information available points to a negative effect on cell proliferation (Teuchert-Noodt et al., 2000; Tian et al., 2009), neuronal differentiation, migration and survival of hippocampal neuronal cells (Mandyam et al., 2008). Additionally, we recently demonstrated that METH is toxic to stem/progenitor cells and decreases proliferation, neuronal differentiation and maturation in the subventricular zone (SVZ) (Bento et al., 2011).

Neuropeptide Y (NPY) is a 36 amino acid peptide widely distributed in both central and peripheral nervous systems (Dumont and Quirion, 2006). In fact, NPY regulates several physiological functions, such as feeding, anxiety, circadian rhythms, body temperature, sexual behavior and cognition (reviewed by Silva et al., 2005a), and has also an important neuroprotective role under pathological conditions (Woldbye et al., 2005; Silva et al., 2005b, 2007). Previously, Thiriet and collaborators (2005) demonstrated that METH-induced cell death in mouse striatum was prevented by NPY. Furthermore, this neuropeptide is able to increase proliferation and neuronal differentiation in the SGZ (Howell et al., 2003; Decressac et al., 2010), in the olfactory epithelium and in the SVZ through Y_1 receptors activation (Hansel et al., 2001; Agasse et al., 2008; Decressac et al., 2009; Thiriet et al., 2011).

The present study aimed to characterize the effects of METH on DG stem/progenitor cell survival, proliferation and neuronal differentiation, as well as to evaluate the protective role of NPY system. Overall, our results demonstrate that NPY is protective against METH-induced DG cell death and prevents the decrease of neurogenesis induced by this drug of abuse.

3.3. Materials and Methods

3.3.1. Animals

Post-natal 1-3-day-old C57BL/6J mice were used in the present study. Experimental procedures were approved by the Institutional Review Board of Faculty of Medicine, University of Coimbra, and were performed according to the guidelines of the European Communities Council Directives (86 / 609 / EEC) and the Portuguese law for the care and use of experimental animals (DL nº 129/92). All efforts were made to minimise animal suffering and to reduce the number of animals.

3.3.2. Dentate gyrus-derived neurosphere cultures

Mice were sacrificed by decapitation and brains were removed and placed in sterile saline solution. DG fragments were dissected out from 450 μm-thick brain coronal sections, digested in 0.025% trypsin and 0.265 mM EDTA (both from Gibco, Rockville, MD, USA) and single cells were obtained by gentle trituration. Cells were diluted in serum-free culture medium (SFM) composed of Dulbecco's modified Eagle's medium/Ham's F-12 medium GlutaMAX-I supplemented with 100 U/ml penicillin, 100 μg/ml streptomycin, 1% B27 supplement, 10 ng/ml epidermal growth factor (EGF) and 5 ng/ml basic fibroblast growth factor (FGF-2) (all from Gibco). Then, cells were plated in uncoated Petri dishes and neurospheres were allowed to develop for 6 days in a 95% air-5% CO_2 humidified atmosphere at 37°C. Afterwards, neurospheres were plated onto poly-D-lysine (Sigma-Aldrich, St Louis, MO, USA) glass coverslips in SFM devoid of growth factors for 24 h in order to form a pseudo-monolayer.

3.3.3. Drug treatments

Methamphetamine [(+)-Methamphetamine hydrochloride, Sigma-Aldrich] was added to SFM devoid of growth factors at the concentrations of 1, 10, 100 or 1000 nM for 24 h, 48 h or 7 days to evaluate cell death, proliferation and differentiation, respectively. The concentrations of METH used were chosen in accordance with the physiological range found in blood, urine, or tissue samples, including the brain, of METH abusers (Takayasu et al., 1995; Kalasinsky et al., 2001; Klette et al., 2006; Melega et al., 2007), and with those that have been successfully used in prior studies (Ramirez et al., 2009; Bento et al., 2011; Lee et al., 2001; Tocharus et al., 2010; Aizenman et al., 2010).

To investigate the effect of NPY in cell proliferation and neuronal differentiation, DG-derived neurosphere cultures were incubated with 1 μM NPY (Bachem, Bubendorf, Switzerland)

for 48 h and 7 days, respectively. Moreover, to study the protective role of NPY and its receptors, DG-derived neurosphere cultures were pre-incubated with 1 μM BIBP3226 (Y_1 receptor antagonist, Bachem) or 1 μM BIIE0246 (Y_2 receptor antagonist, Tocris, Bristol, UK,) for 15 min, followed by co-incubation with 1 μM NPY, 1 μM [Leu^{31},Pro^{34}]NPY, 300 nM NPY13-36 or 1 μM (Gly^{1},$Ser^{3\cdot22}$,$Gln^{4\cdot34}$,Thr^{6},Arg^{19},Tyr^{21},$Ala^{23\cdot31}$,Aib^{32})-PP (Y_1, Y_2 and Y_5 receptor agonists, respectively; all from Bachem) for 1 h, and then co-exposed with 10 nM METH for 24 h or 1 nM METH for 7 days for cell death and differentiation studies, respectively. In attempt to better clarify the cellular mechanisms involved in NPY-induced protection, DG-derived neurosphere cultures were pre-incubated with 1 μM NPY and the N-methyl-D-aspartate (NMDA) receptor antagonist, MK-801 (10 μM, Tocris), for 1 h and 15 min, respectively, and then co-exposed with METH (10 nM) for 24 h. Regarding the NPY system, the concentrations used in the present study were chosen based on previous works where we showed that NPY and its receptor agonists inhibited glutamate release from hippocampal synaptosomes (Silva et al., 2001) and intracellular Ca^{2+} concentration in cultured rat hippocampal neurons (Silva et al., 2003b), as well as prevented hippocampal excitotoxicity (Silva et al., 2003a).

To investigate the role of NPY on neuronal differentiation, DG-derived neurosphere cultures were co-incubated with 10 μM cytosine β-D-arabinofuranoside (AraC, Sigma-Aldrich) plus 1 μM NPY for 7 days. AraC is a nucleoside analogue which incorporates the C sites of the DNA strand, blocking the cells in the S phase of the cell cycle which results in the inhibition of cell proliferation (Azuma et al., 2001).

3.3.4. Immunocytochemistry

DG-derived neurosphere cultures were fixed in 4% paraformaldehyde (PFA), permeabilized in 1% Triton X-100, 3% bovine serum albumine (BSA; all from Sigma-Aldrich) in 0.1 M phosphate-buffered saline (PBS), followed by overnight incubation at 4°C with mouse monoclonal anti-NeuN (1:100, MAB377, Chemicon, Temecula, CA), rabbit monoclonal anti-NPY (1:200, N9528, Sigma-Aldrich), sheep polyclonal anti-NPY Y_1 receptor (1:200, 6732-0150, AbD Serotec, Oxfordshire, UK), rabbit polyclonal anti-NPY Y_2 receptor (1:100, ANR-022, Alomone Labs, Jerusalem, Israel), mouse polyclonal anti-Tuj1 (1:500, MMS-435P, Covance, Emeryville, California, USA), mouse monoclonal anti-GFAP (1:500, #3670, Cell Signaling Technology, Danvers, MA) and mouse monoclonal anti-O4 (1:100, MAB345, Chemicon) in 0.1% Triton X-100, 0.3% BSA in PBS. Cells were rinsed and incubated for 1 h with the appropriate secondary antibodies: goat anti-mouse Alexa Fluor 488, donkey anti-rabbit 488, donkey anti-sheep 488 and goat anti-mouse 594 (1:200; all from Invitrogen). Nuclei were stained with 4 μg/ml Hoechst

33342 (Sigma-Aldrich) and slides were mounted in Dako fluorescence medium (Dako, Carpinteria, CA). To confirm antibody specificity, negative controls were performed for each immunocytochemical assay, and the antibodies used for the NPY system were also chosen based on previous studies (Ruscheweyh et al., 2007; Price et al., 2009; Ferreira et al., 2010; Thiriet et al., 2011). Fluorescence images for cell counts were recorded using an Axioskop 2 Plus fluorescent microscope, while representative images were recorded using a LSM 710 Meta confocal microscope (all from Carl Zeiss, Göttingen, Germany).

3.3.5. Cell death assays

To evaluate necrotic cell death, propidium iodide (PI; 3,8-diamino-5-(3-(diethylmethylamino)propyl)-6-phenyl phenanthridinium diiodide; Sigma-Aldrich) was applied in DG-derived neurosphere cultures. PI is a polar non-toxic compound that in normal conditions does not cross the plasma membrane (Bernardino et al., 2005). Instead, PI only enters dying or dead cells, where membranes have lost their integrity, and then binds to DNA. In the present study, 3 µg/ml PI was applied to DG-derived neurosphere cultures for the last 40 min of the 24 h culture session. Afterwards, cells were fixed with 4% PFA. Then, terminal deoxynucleotidyl transferase dUTP nick-end labeling (TUNEL) assay was performed to label apoptotic nuclei, as described previously (Bernardino et al., 2008; Bento et al., 2011). To confirm that METH triggers apoptosis in DG-derived neurosphere cultures, cells were also co-incubated for 24 h with 100 nM METH plus 25 µM z-Val-Ala-DL-Asp (OMe)-fluoromethylketone (Z-VAD; Calbiochem EMD4 Biosciences, Nottingham, UK), a general pan-caspase inhibitor that irreversibly binds to caspases. In control conditions, Z-VAD was also shown to decrease basal apoptosis in SVZ cultures as described previously (Bernardino et al., 2008; Bento et al. 2011).

To evaluate total cell death, the number of necrotic (PI-positive and TUNEL-negative) and apoptotic cells (TUNEL-positive/PI-negative and TUNEL-/PI-positive, representing cells in early and late phases of apoptosis, respectively) were counted and expressed as percentages of total cells stained with Hoechst 33342.

3.3.6. Cell proliferation studies

Cell proliferation was evaluated by 5-bromo-2'-deoxyuridine (BrdU, Sigma-Aldrich) incorporation based on our previous work (Bento et al., 2011). DG cells were treated for 48 h with METH (1–1000 nM) and 10 µM BrdU was added in the last 4 h of the culture session. According to Nowakowski et al. (1989), the estimated duration of the S-phase is 8 h, so the 4 h pulse with BrdU will allow the identification of cells that entered the S-phase of cell cycle.

Afterwards, cells were fixed in 4% PFA, rinsed in PBS and BrdU was unmasked following successive passages in 1% Triton X-100 for 30 min, ice-cold 0.1 M HCl for 20 min, and 2 M HCl for 40 min at 37°C. Following the neutralization in sodium borate buffer (0.1 M $Na_2B_4O_7$.10 H_2O, pH 8.5; Sigma-Aldrich) for 15 min, cells were rinsed in PBS and incubated in 3% BSA (Sigma-Aldrich), 0.3% Triton X-100 in PBS for 30 min. DG-derived neurosphere cultures were incubated with mouse monoclonal anti-BrdU antibody conjugated with Alexa Fluor 594 (1:100, B35132, Invitrogen) in PBS containing 0.3% Triton X-100 and 0.3% BSA, overnight at 4°C. Nuclei were counterstained with Hoechst 33342 and cell preparations were mounted as previously described. Representative fluorescence images were recorded as described above.

3.3.7. Western blot analysis

Non-treated DG-derived neurosphere cultures were homogenized in RIPA buffer containing 150 mM NaCl, 5 mM EGTA, 50 mM Tris, 1% (v/v) Triton X-100, 0.1% SDS and 0.5% sodium deoxycholate, supplemented with a protease inhibitor cocktail tablet (Roche). Afterwards, cells were centrifuged at 17000 x*g* for 15 min and protein concentration was determined using the Bicinchoninic Acid (BCA) Protein Assay (Thermo Fisher Scientific, Northumberland, UK). Then, 50 or 80 µg of protein samples were separated by electrophoresis in a 8% or 12% SDS-PAGE, transferred to a polyvinylidene fluoride (PVDF) membrane (Millipore, Madrid, Spain) and blocked in 5% non-fat dried milk in PBS-0.5% Tween (PBS-T; Sigma-Aldrich) for 1 h. Afterwards, membranes were probed overnight at 4°C with rabbit monoclonal anti-NPY (1:1000; Sigma-Aldrich), sheep polyclonal anti-NPY Y_1 receptor (1:10,000, AbD Serotec), rabbit polyclonal anti-NPY Y_2 receptor (1:200; Alomone Labs) or rabbit polyclonal anti-GluN1 (1:500; Tocris) antibodies and were re-probed with rabbit anti-β-actin (1:5000; Sigma-Aldrich) overnight at 4°C. Membranes were rinsed in PBS-T and incubated for 45 min with alkaline phosphatase-conjugated secondary antibodies as follows: anti-rabbit IgG, (1:20000, Amersham Biosciences, GE Healthcare Europe GmbH) and anti-sheep IgG, (1:1000, Sigma-Aldrich). Densitometric analysis was performed using the enhanced *chemifluorescence* (ECF) reagent (Amersham Biosciences) and visualized on the Typhoon 9000 system (GE Healthcare Europe GmbH). Band intensities were quantified using the ImageQuant 5.0 software.

3.3.8. High Performance Liquid Chromatography

Levels of glutamate release from DG-derived neurosphere cultures exposed to 10 nM METH during several time points (30 min, 1 h, 6 h or 24 h) in the absence or presence of 1 µM NPY were analyzed by high performance liquid chromatography with electrochemical detection

(HPLC-EC) using a Gilson instrument (Gilson, Inc., Middleton, WI, USA). For that, samples were diluted 1:1 in the following solution: 0.4 mM sodium disulfite, 0.9 mM EDTA and 0.4 N perchloric acid. Afterwards, samples were filtered (0.2 µm nylon filter, Costar, Corning, NY) and derivatized by adding 100 µl of NaOH 0.1N and 15 µl OPA (10 mg/mL of OPA, 45.4 M sodium sulphite, 4.5% absolute ethanol in 327 mM borate buffer at pH 10.4) to 50 µl of sample. Samples were allowed to react at room temperature in the dark for a period of 10 min. The mobile phase containing 0.06 M sodium dihydrogen phosphate, 0.06 mM EDTA and 20 % methanol (pH 4.4) was filtered and degassed with an isocratic protocol (0.8 mL/min) passing through a Supercosil LC18 (25 cm x 4.6 mm x 5 mm, Supelco, Bellefonte, PA, USA) analytical column. The potential was set at 0.85 V relative to an Ag/AgCl reference electrode. Concentrations of glutamate were calculated using a standard curve generated with a glutamate standard purchased from Sigma (St. Louis, MO, USA).

3.3.9. Data analysis

Cell quantifications were performed in the border of the neurospheres where migrating cells emerged, forming a pseudo-monolayer. All the experimental conditions were performed in three different wells obtained from at least two independent cultures. Number of TUNEL, PI, BrdU and NeuN were obtained as percentage of total Hoechst-positive cells from the total of five independent microscopic fields in each coverslip. Statistical analysis was determined by using an analysis of variance (one-way ANOVA) followed by Dunnett's, Bonferroni's or Mann Whitney post-hoc tests, as indicated in the figure legends. Data are expressed as mean ± SEM, and statistical significance level was set for $P < 0.05$.

3.4. Results

3.4.1. Methamphetamine induces dentate gyrus cell death

It is well established that METH induces neural dysfunction or/and death and that the hippocampus is particularly affected by this drug (Thompson et al., 2004; Simões et al., 2007; Gonçalves et al., 2010). To determine the toxic effect of METH on DG-derived neurosphere cultures, we evaluated total cell death (PI-positive and TUNEL-positive cells), and also discriminated between necrotic-like (PI-positive and TUNEL-negative cells) and apoptotic-like cell death (TUNEL-positive cells). No significant differences were observed in total cell death when cells were exposed to 1 nM METH (Figure 3.1 A; control: 26.18±1.59%; 1 nM: 23.34±2.70%). However, total cell death increased in the presence of 10, 100 or 1000 nM METH as follows: 45.36±6.04%, $P < 0.05$; 49.95±6.53%, $P < 0.001$; 59.37±3.73%, $P < 0.001$, respectively (Figure 3.1

A). Moreover, the increase in total cell death was due to an increase in both necrotic- and apoptotic-like cell death (Figures 3.1 B and C, respectively). METH at 1 nM had no effect on the number of PI-positive cells (12.57±1.40%) when compared to control (11.68±1.02%; Figure 3.1 B) but did induce an increase when METH was applied at 10, 100 or 1000 nM (22.45±1.41%, 29.38±4.94% or 28.14±2.22%, respectively; $P < 0.001$ for all concentrations; Figure 3.1 B). Similarly, the number of TUNEL-positive cells in DG-derived neurosphere cultures exposed to 1 nM METH (8.19±1.10%) was not significantly different from control (8.12±0.31%; Figure 3.1 C) but increased in cultures exposed to 10, 100 or 1000 nM METH (16.67±1.08%, 18.88±2.47% or 22.94±2.20%, respectively; $P < 0.001$ for all concentrations; Figure 3.1 C). Furthermore, in order to confirm that METH triggers apoptosis, DG-derived neurosphere cultures were co-incubated with the pan-caspase inhibitor, Z-VAD (25 µM), which completely prevented METH-induced apoptosis (100 nM METH+Z-VAD: 4.00±0.63%; Z-VAD: 3.69±0.59%, $P < 0.05$; Figure 3.1 C).

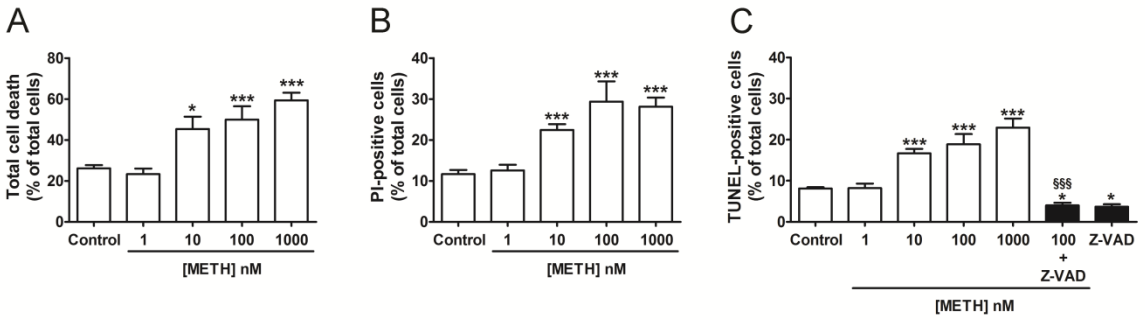

Figure 3.1 – METH induces cell death to DG-derived neurosphere cultures. (A) METH, at concentrations above 10 nM for 24 h, increases total cell death by both necrosis and apoptosis. (B and C) METH increases the number of (B) PI-positive cells (necrosis) and (C) TUNEL-positive cells (apoptosis). In order to confirm that METH triggers apoptosis, DG cells were incubated with the pan-caspase inhibitor, Z-VAD (25 µM), which prevents METH-induced increase of apoptosis. Data are expressed as mean percentage of total cells ± SEM, $n = 4–14$ coverslips. *$P < 0.05$, ***$P < 0.001$, significantly different from control using Dunnett's post hoc test. $^{§§§}P < 0.001$, significantly different from 100 nM METH using Bonferroni's post hoc test.

3.4.2. Neuropeptide Y is protective against methamphetamine-induced dentate gyrus cell death by inhibiting glutamate release.

It is well known that NPY is neuroprotective under several pathological conditions (Woldbye et al. 2005, Silva et al., 2005b and 2007). Thus, we aimed to evaluate a possible protective role of this neuropeptide in DG-derived neurosphere cultures exposed to a toxic concentration of METH (10 nM; Figure 1). We concluded that NPY (1 µM), which is itself not toxic, completely prevented apoptotic cell death induced by 10 nM METH (control: 8.10±0.32%;

NPY: 8.49±0.48%; METH: 16.67±1.08%, $P < 0.001$; METH+NPY: 8.72± 0.70%, $P < 0.001$ *vs.* 10 nM METH; Figure 3.2 A). To identify which NPY receptor mediates this protective effect, selective antagonists for Y_1 and Y_2 receptors (1 µM BIBP3226 and 1 µM BIIE0246, respectively) were used. We observed that both antagonists were able to block the protective effect induced by 1 µM NPY under conditions of METH-induced apoptosis (METH+NPY+Y_1 receptor antagonist: 14.24±1.78%, $P < 0.01$; METH+NPY+Y_2 receptor antagonist: 15.08±1.16%, $P < 0.001$; Figure 3.2 A). Accordingly, the selective activation of Y_1 or Y_2 receptors by the respective agonists (1 µM [Leu^{31},Pro^{34}]NPY or 300 nM NPY13-36, respectively) completely prevented METH-induced apoptosis (control: 8.10±0.32%; METH+Y_1 receptor agonist: 7.41±0.39%; METH+Y_2 receptor agonist: 7.84±0.46%, $P < 0.001$ *vs.* 10 nM METH; Figure 3.2 B). Moreover, our results demonstrate that the Y_5 receptor did not play any protective role since the number of TUNEL-positive cells were similar to the ones observed in the presence of METH alone (METH: 16.67±1.08%; METH+Y_5 receptor agonist: 13.43±0.90%, $P < 0.001$; Figure 3.2 B). Additionally, the Y_1, Y_2 or Y_5 receptor agonists by themselves did not affect apoptotic cell death (control: 8.43±0.65; Y_1 receptor agonist: 6.75±0.79%; Y_2 receptor agonist: 7.73±0.63%; Y_5 receptor agonist: 7.59±0.63%; Figure 3.2 B). We further evaluate if NPY could also prevent necrosis induced by METH. Interestingly, we observed that NPY (1 µM) did not protect DG-derived neurosphere cultures from METH-induced necrosis (Figure 3.2 C). Specifically, the number of PI-positive cells in DG-derived neurosphere cultures was as follows: control, 11.68±1.02%; METH, 22.45±1.41%, $P < 0.001$; NPY, 14.74±0.92%; METH+NPY, 23.36±1.31%, $P < 0.001$ (Figure 3.2 C).

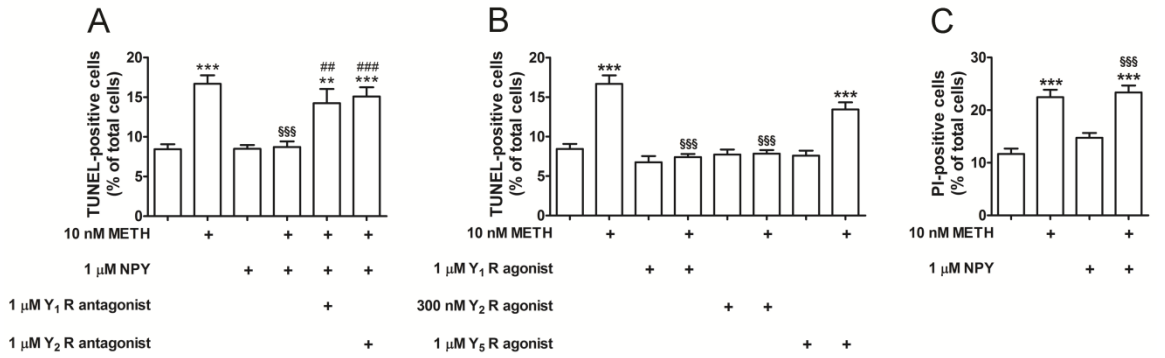

Figure 3.2 – NPY prevents METH-induced apoptosis through activation of both Y_1 and Y_2 receptors. (A) Pre-incubation with NPY (1 µM; 1 h) followed by co-exposure to METH (10 nM) for 24 h prevents drug-induced increase of TUNEL-positive cells in DG-derived neurosphere cultures, and 1 µM BIBP3226 or 1 µM BIIE0246 (Y_1 or Y_2 receptor antagonists, respectively) inhibit the protective effect of NPY. (B) Pre-incubation (1 h) with 1 µM [Leu^{31},Pro^{34}]NPY or 300 nM NPY13-36 (Y_1 and Y_2 receptor agonists, respectively) followed by co-exposure with METH (10 nM) for 24 h reduces the increase of apoptotic DG cell death induced by METH. However, NPY Y_5 receptor agonist (1 µM Gly^{1},Ser$^{3.22}$,Gln$^{4.34}$,Thr^{6},Arg^{19},Tyr^{21},Ala$^{23.31}$,Aib^{32})-PP) did not protect DG cells from METH-induced cell death. (C) NPY (1 µM) did not prevent the increased number of PI-positive

cells induced by 10 nM METH. Data are expressed as mean percentage of total cells ± SEM, n = 5–14 coverslips. $^{**}P < 0.01$, $^{***}P < 0.001$, significantly different when compared to control using Dunnett's post hoc test. $^{§§§}P < 0.001$, significantly different when compared to 10 nM METH using Bonferroni's post hoc test. $^{\#\#}P < 0.01$, $^{\#\#\#}P < 0.001$, significantly different when compared to 10 nM METH plus 1 µM NPY using Bonferroni's post hoc test.

One of the well-known mechanisms of METH-induced neurotoxicity is the abnormal increase of glutamate release (Mark et al., 2004), which leads to the hyperactivation of ionotropic glutamate receptors that may culminate in cell death (Schinder et al., 1996; reviewed by Riddle et al., 2006). Furthermore, we demonstrated that NPY inhibits glutamate release in rat hippocampal cultures (Silva et al., 2001, 2003a). Thus, we hypothesized that the protective role of NPY in DG-derived neurosphere cultures could involve the modulation of glutamatergic system. To clarify this issue, we started by showing that these cultures express the GluN1 subunit of the NMDA receptors, since this is an obligatory subunit of these receptors (Figure 3.3 A). Our results also show that METH (10 nM) did not interfere with GluN1 protein levels (Figure 3.3 A). Then, we analyzed the involvement of NMDA receptors in METH-induced DG-derived neurosphere cultures apoptosis, and we concluded that the blockade of NMDA receptors by MK-801 (10 µM) completely prevented cell death induced by METH (control: 5.06±0.54%; MK-801: 5.36±0.42%; METH+MK-801: 5.57±0.60%; Figure 3.3 B). Interestingly, this protective effect was very similar to that induced by NPY (METH+NPY: 5.03±0.56%) or in the presence of both MK-801+NPY (4.94±0.40%; Figure 3.3 B). Thus, since NMDA receptors are involved in METH-induced cell death and NPY is able to prevent this toxic effect, we further evaluated the modulation of glutamate release by both METH and NPY. In fact, we concluded that 10 nM METH increases glutamate release by DG-derived neurosphere cultures at all time points analyzed (30 min: 134.60±12.76%; 1 h: 121.70±3.30%; 6 h: 157.40±21.33%; 24 h: 124.0±9.89% of control; Figure 3.3 C). Regarding the effect of NPY, we observed that at 30 min this peptide did not interfere with the levels of glutamate release (133.40±5.12% of control; Figure 3.3 C). However, NPY prevented METH-induced increase of glutamate release at 1 h, 6 h and 24 h after METH exposure (1 h: 84.79±8.62%, $P < 0.05$; 6 h: 100.10±3.63%, $P < 0.01$; 24 h: 87.42±9.46%, $P < 0.01$; Figure 3.3 C).

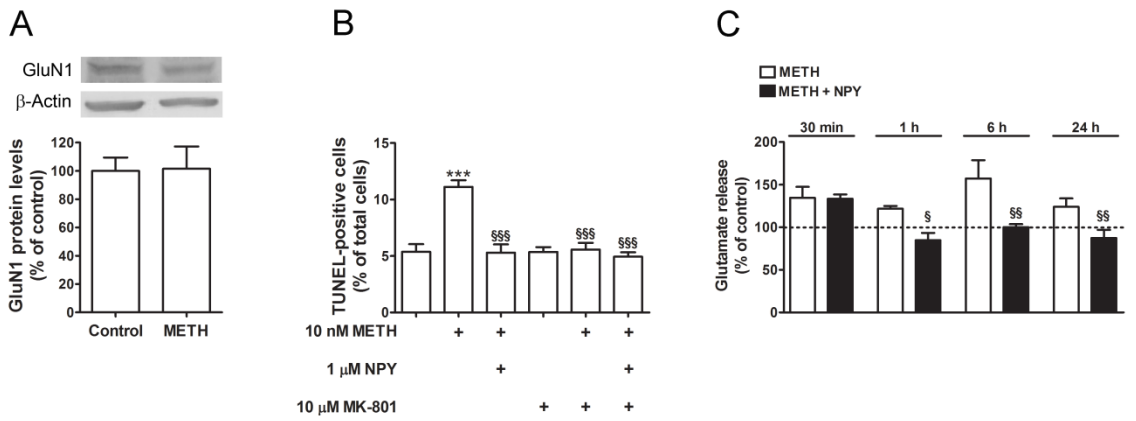

Figure 3.3 – METH induces apoptotic cell death through activation of NMDA receptors and increases glutamate release, which is prevented by NPY. (A) DG-derived neurosphere cultures express the GluN1 subunit (120 kDa) of NMDA receptors, and exposure to METH (10 nM) for 24h had no effect on its protein levels. (B) Inhibition of NMDA receptors by MK-801 (10 μM) completely prevents METH-induced increase of TUNEL-positive cells. (C) METH (10 nM) increases glutamate release at all time points analyzed (30 min, 1 h, 6 h and 24 h), and NPY (1 μM) inhibits this increase at 1 h, 6 h and 24 h post-drug exposure. Data are expressed as mean percentage of total cells ± SEM or percentage of control ± SEM, n = 4–9. ***P < 0.001, significantly different when compared to control using Dunnett's post hoc test. $^{§}P$ < 0.05, $^{§§}P$ < 0.01, $^{§§§}P$ < 0.001, significantly different when compared to 10 nM METH using Bonferroni's or Mann Whitney post hoc tests.

As abovementioned, NPY proved to protect DG-derived neurosphere cultures from METH-induced cell death. Thus, we further evaluated the expression of NPY as well as both Y_1 and Y_2 receptors by western blot (Figure 3.4 A–C) and immunocytochemistry (Figure 3.4 D–L) in DG-derived neurosphere cultures. In fact, NPY-positive cells (green, Figure 3.4 D–F) were found in DG cells, including in Tuj1- (Figure 3.4 D), GFAP- (Figure 3.4 E) and O4-positive cells (Figure 3.4 F), as referring to neurons, astrocytes and oligodendrocytes, respectively (red; Figure 3.4 D–F). Furthermore, both Y_1 (green, Figure 3.4 G–I) and Y_2 receptors (green, Figure 3.4 J–L) are also expressed in neurons (Figure 3.4 G and J), astrocytes (Figure 3.4 H and K) and oligodendrocytes (Figure 3.4 I and L) from DG-derived neurosphere cultures.

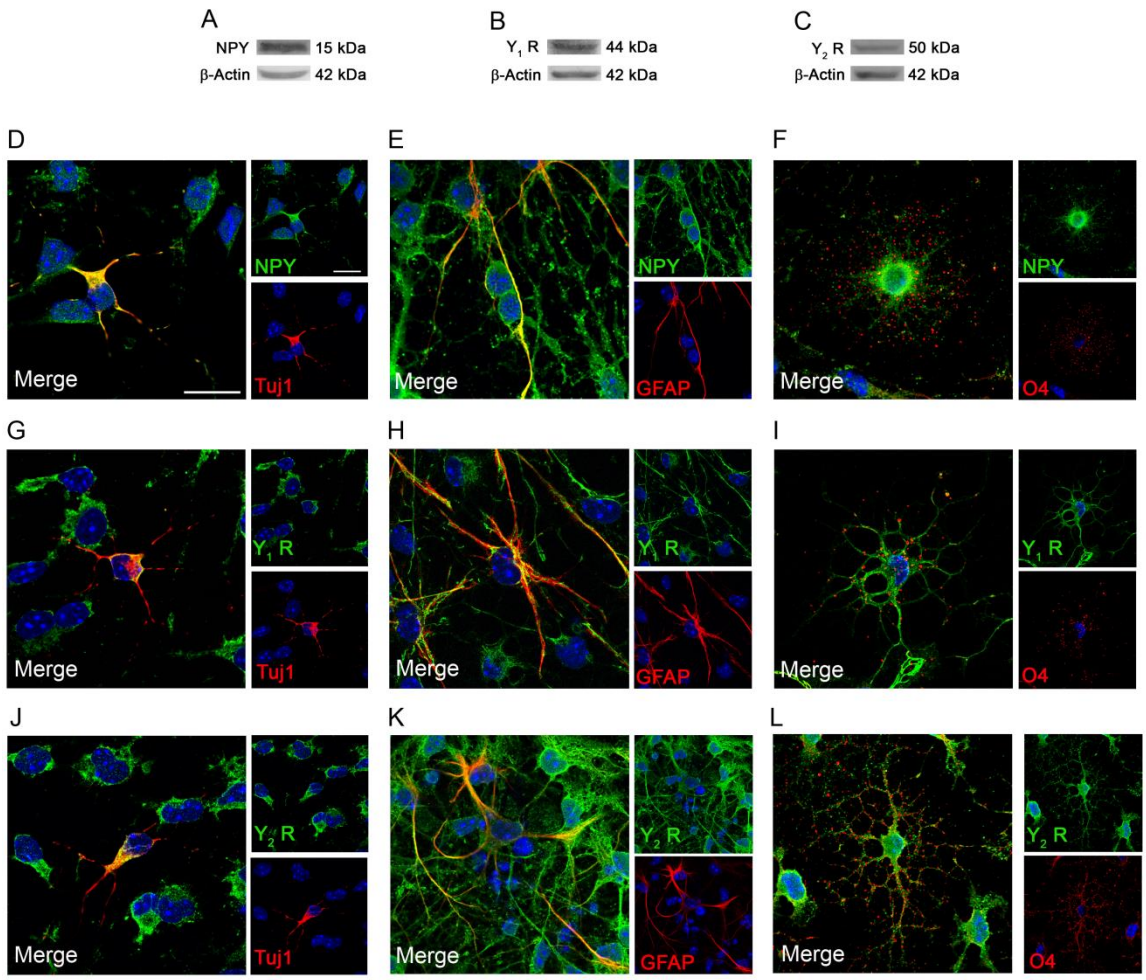

Figure 3.4 – Cells from DG-derived neurosphere cultures express (A, D–F) NPY, (B, G–I) Y_1 and (C, J–L) Y_2 receptor subtypes. The expression of (A) NPY (15 kDa), (B) Y_1 (44 kDa) and (C) Y_2 (50 kDa) receptor proteins in DG neurosphere-derived cultures was evaluated by western blot. Accordingly, representative fluorescence images of (D–F) NPY, (G–I) Y_1 and (J–L) Y_2 receptors (all green) show a clear co-localization with Tuj1, GFAP and O4 (all red) showing that neurons, astrocytes and oligodendrocytes, respectively, express these proteins. Scale bar: 50 µm.

3.4.3. Methamphetamine does not affect dentate gyrus cell proliferation

We have previously shown that METH inhibits SVZ progenitor cell proliferation (Bento et al., 2011). Here, we also investigated the concentration-dependent effect of METH (1-1000 nM) on proliferation in DG-derived neurosphere cultures by assessing BrdU incorporation. At low concentrations, METH had no effect on the number of BrdU-positive cells (control: 4.52±0.18%; 1 nM: 4.28±0.54%; 10 nM: 4.61±0.44%; Figure 3.5). However, exposure to 100 and 1000 nM METH decreased the number of BrdU-positive cells to 2.28± 0.17% ($P < 0.001$) and 2.63±0.40% ($P < 0.01$), respectively (Figure 3.5). Since METH decreases BrdU-labeled cells at the same concentrations that increases cell death (100 and 1000 nM), we further evaluated BrdU incorporation under co-exposure to 100 nM METH and Z-VAD (25 µM). In the presence of Z-VAD,

the number of BrdU-positive cells was similar to control (Z-VAD: 3.71±0.27%; METH+Z-VAD: 4.08±0.47%, $P < 0.01$ *vs.* 100 nM METH; Figure 3.5) indicating that decrease in BrdU incorporation was due to cell death rather than to the inhibition of cell proliferation.

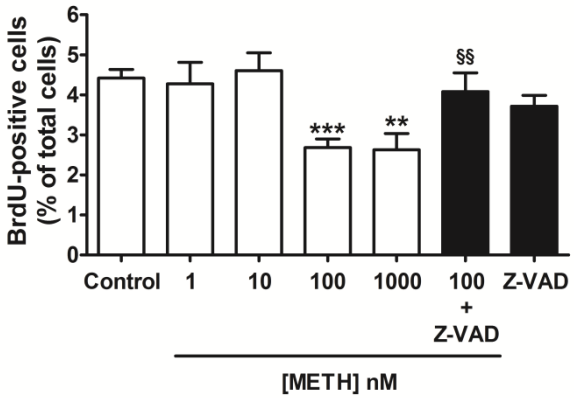

Figure 3.5 – METH decreases BrdU incorporation in DG cultures. Bar graph representing BrdU incorporation in DG-derived neurosphere cultures treated with METH (1–1000 nM) for 48 h, showing a decrease in the number of BrdU-labeled cells in cultures exposed to 100 and 1000 nM METH. Co-incubation with Z-VAD (25 µM) prevented METH-induced decrease in the number of BrdU-positive cells. Data are expressed as mean percentage of total cells ± SEM, n = 4–12 coverslips. $^{**}P < 0.01$, $^{***}P < 0.001$, significantly different when compared to control using Dunnett's post hoc test. $^{§§}P < 0.01$, significantly different when compared to 100 nM METH using Bonferroni's post hoc test.

3.4.4. Neuropeptide Y is proproliferative, proneurogenic and prevents methamphetamine-induced decrease of neuronal differentiation

Several studies have demonstrated that NPY increases proliferation and neuronal differentiation in SGZ (Howell et al., 2003; Decressac et al., 2011) and SVZ (Agasse et al., 2008; Decressac et al., 2009) cell cultures. In the present study, we evaluated the proproliferative effect of NPY on DG-derived neurosphere cultures and found that NPY (1 µM) increased proliferation as assessed by counting BrdU-positive cells (control: 3.64±0.10%; NPY: 5.30±0.25%; $P < 0.001$; Figure 3.6 A–F). Moreover, the proproliferative effect of NPY was completely blocked by the Y_1 receptor antagonist (3.17±0.40%, $P < 0.001$ *vs.* 1 µM NPY; Figure 3.6 F), whereas the Y_2 receptor antagonist had no effect (5.01±0.13%, $P < 0.01$; Figure 3.6 F). By themselves, the Y_1 or Y_2 receptor antagonists did not affect proliferation (3.29±0.19%, or 3.33±0.24%, respectively; Figure 3.6 F).

We also evaluated the effect of the selective activation of different NPY receptor subtypes, and concluded that 1 µM [Leu^{31},Pro^{34}]NPY increased the number of BrdU-positive cells (control: 3.64±0.10%; Y_1 R agonist: 6.55±0.66%, $P < 0.001$; Figure 3.6 G), an effect blocked by the

Y_1 receptor antagonist (3.69±0.24%, $P < 0.001$ *vs.* 1 μM Y_1 receptor agonist; Figure 3.6 G). Moreover, the selective activation of Y_2 or Y_5 receptors with 300 nM NPY13-36 or 1 μM (Gly^{1},Ser^{3}·^{22},Gln^{4}·^{34},Thr^{6},Arg^{19},Tyr^{21},Ala^{23}·^{31},Aib^{32})-PP, respectively, had no effect on the number of BrdU-positive cells when compared to control (3.91±0.40% or 4.67±0.21%, respectively; Figure 3.6 G).

Rats administered METH have been reported to show a decrease in neuronal differentiation (Mandyam et al., 2008). Consistent with this, our fluorescent images clearly show that METH decreased the number of NeuN-labeled cells in DG-derived neurosphere cultures (Figure 3.7 A and B). In contrast, NPY proved to be proneurogenic (Figure 3.7 C and H) by increasing the number of NeuN-positive cells, and was also able to prevent the decrease in the number of NeuN-stained cells induced by 1 nM METH (Figure 3.7 D, J and K). Specifically, DG-derived neurosphere cultures incubated with 1 μM NPY showed an increase in NeuN-positive cells (control: 6.85±0.12%; NPY: 11.64±0.72%, $P < 0.001$; Figure 3.7 H). Furthermore, the proneurogenic effect of NPY was inhibited by the Y_1 receptor antagonist (6.34±0.57%, $P < 0.001$ *vs.* 1 μM NPY; Figure 3.7 H), but the blockade of the Y_2 receptor had no effect (11.09±0.87%, $P < 0.01$ *vs.* control; Figure 3.7 H). The Y_1 and Y_2 receptor antagonists by themselves did not interfere with the number of NeuN-positive cells (5.52±0.93% or 6.16±0.62%, respectively; Figure 3.7 H). In addition, to eliminate the proproliferative effect of NPY in neuronal differentiation, an anti-mitotic agent (AraC) was used. We first concluded that AraC was not toxic to DG cells since there was no effect on PI- and TUNEL-positive cells when compared to the control (Figure 3.8). Furthermore, AraC had no effect on the number of NeuN-positive cells relative to control (6.38±0.41%, Figure 3.7 H). Moreover, NPY in the presence of AraC, was able to increase the number of NeuN-positive cells (10.32±0.72%), which allow us to conclude that NPY increases both cell proliferation and neuronal differentiation (Figure 3.7 H). Also, the selective activation of Y_1 receptors increased the number of NeuN-positive cells (1 μM [Leu^{31},Pro^{34}]NPY: 13.07±0.94%, $P < 0.001$) when compared to control (7.12±0.15%), whereas the activation of Y_2 or Y_5 receptors had no significant effect on neuronal differentiation (8.42±0.49% or 7.75±0.62%, respectively; Figure 3.7 I).

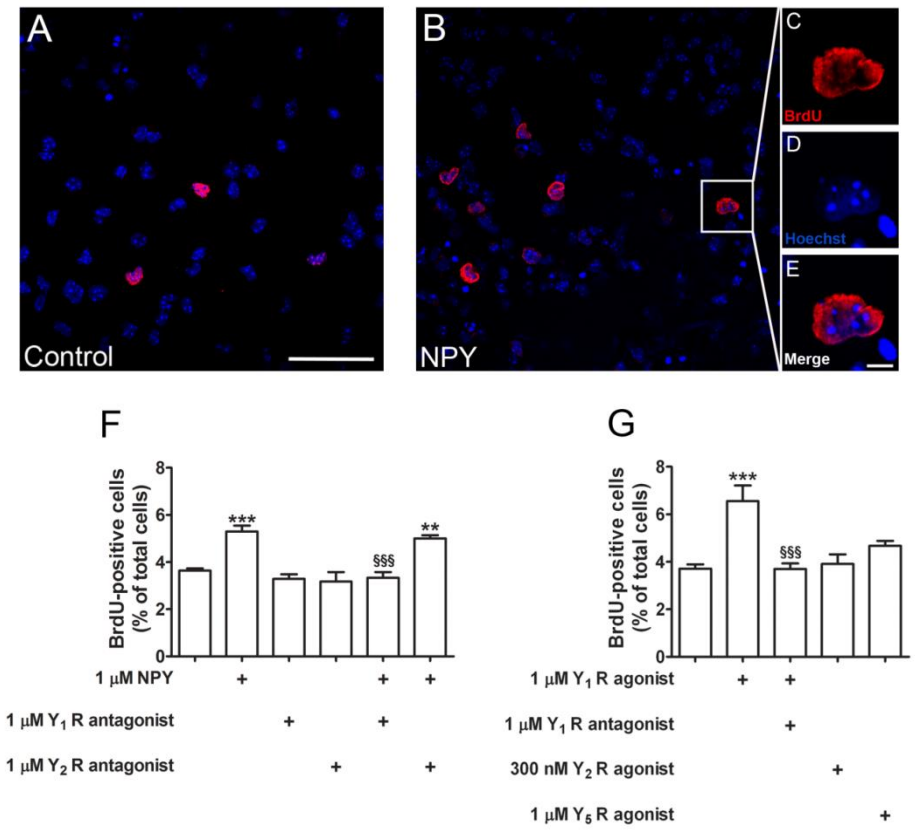

Figure 3.6 – NPY increases DG cell proliferation through the activation of NPY Y_1 receptor subtype. (A–E) Representative fluorescence images of DG-derived neurosphere cultures immunolabeled for BrdU (red) in (A) control conditions or (B–E) in the presence of 1 µM NPY for 48 h. Nuclei were identified by Hoechst 33342 staining (blue). Scale bars: 50 µm (A and B) and 5 µm (C–E). (F) The number of BrdU-positive cells in DG-derived neurospheres cultures is increased by 1 µM NPY (48 h exposure), which was prevented by the Y_1 receptor antagonist (1 µM BIBP3226). (G) Selective activation of Y_1 receptor by [Leu^{31},Pro^{34}]NPY (1 µM) increases the number of BrdU-positive cells, while activation of Y_2 or Y_5 by NPY13-36 (300 nM) or (Gly^{1},Ser^{3}·^{22},Gln^{4}·^{34},Thr^{6},Arg^{19},Tyr^{21},Ala^{23}·^{31},Aib^{32})-PP (1 µM), respectively, have no effect on DG cell proliferation. Data are expressed as mean percentage of total cells ± SEM, *n* = 6–12 coverslips. ***P* < 0.01 and ****P* < 0.001, significantly different when compared to control using Dunnett's post hoc test. $^{§§§}P$ <0.001, significantly different when compared to (B) 1 µM NPY or (C) 1 µM Y_1 receptor agonist using Bonferroni's post hoc test.

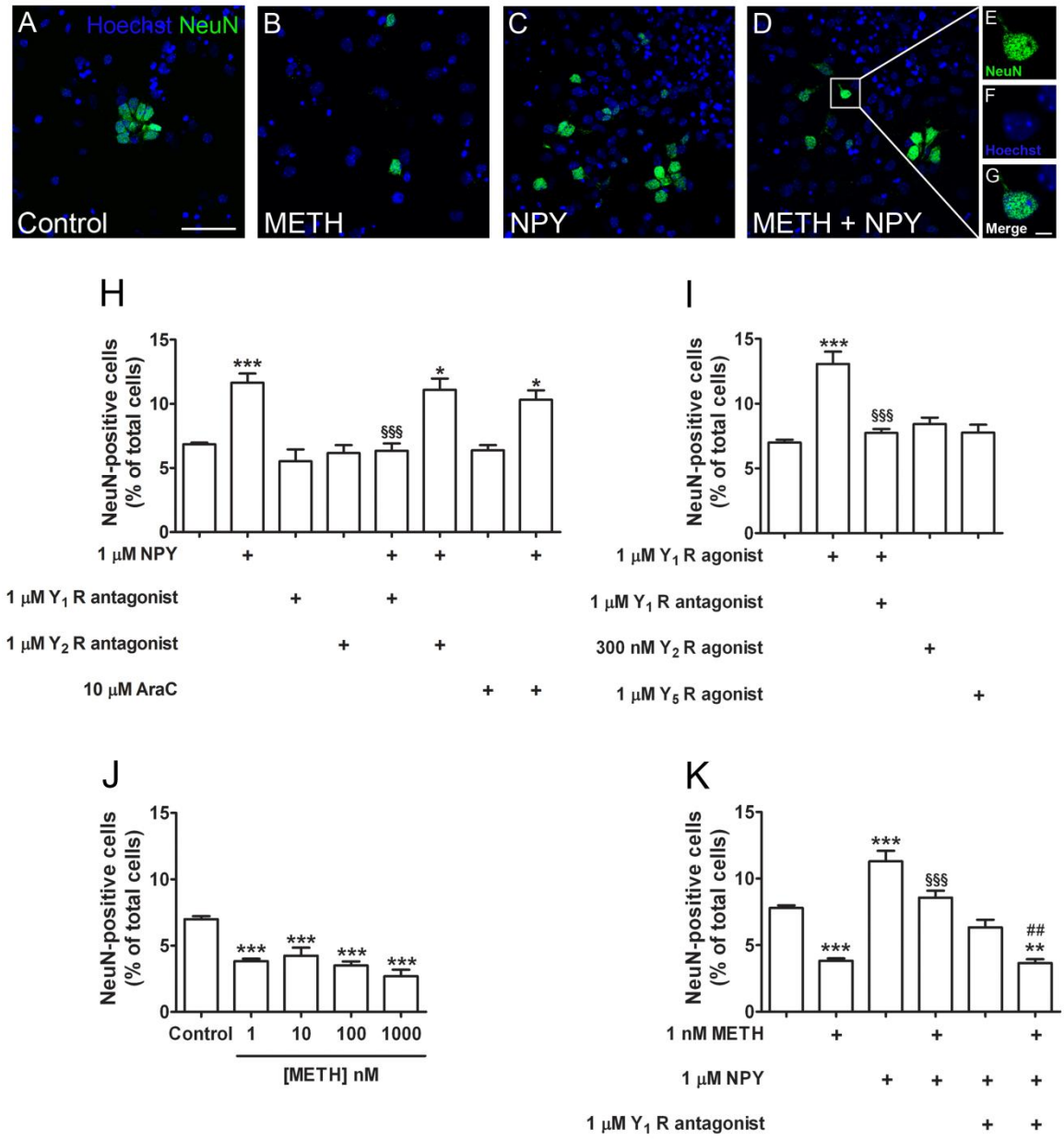

Figure 3.7 – Neuropeptide Y (NPY) increases neuronal differentiation through the activation of NPY Y_1 receptor subtype and prevents the decrease of neuronal differentiation induced by METH. (A–G) Representative fluorescence images of DG cells immunolabeled for NeuN (green) and nuclei staining by Hoechst 33342 staining (blue) in (A) control conditions, (B) exposed to 1 nM METH, (C) 1 µM NPY or (D) exposed to METH plus NPY all for 7 days. (E –G) Higher magnification of a (E) NeuN-positive cell (green), (F) stained with Hoechst (blue) and (G) merge from cultures exposed to METH plus NPY for 7 days. Scale bar: 50 µm (A–D) and 5 µm (E–G). (H) NPY (1 µM) triggers neuronal differentiation through the activation of Y_1 receptor subtype, even in the presence of the anti-mitotic agent, AraC (10 µM). (I) NPY Y_1 receptor subtype activation triggers neuronal differentiation in DG-derived neurosphere cultures. (J) METH decreases neuronal differentiation in DG-derived neurosphere cultures at all concentrations tested (1–1000 nM), including the nontoxic concentration of 1 nM. (K) NPY prevents METH-induced decrease in neuronal differentiation *via* activation of Y_1 receptor subtype. Data are expressed as mean percentage of total cells ± SEM, n = 3–28 coverslips. *P < 0.05, **P < 0.01 and ***P < 0.001, significantly different when compared to control using Dunnett's post hoc test. $^{§§§}P$ < 0.001, significantly different when compared to (H) 1 µM NPY, (I) 1 µM [Leu^{31},Pro^{34}]NPY or (K) 1

nM METH using Bonferroni's post hoc test.$^{###}P < 0.001$, significantly different when compared to 1 µM NPY plus 1 nM METH (K) using Bonferroni's post hoc test.

To investigate the effect of METH on neuronal differentiation, DG-derived neurosphere cultures were exposed to METH (1–1000 nM). A decrease in the number of NeuN-positive cells was observed at all concentrations tested (control: 6.96±0.10%; 1 nM: 3.83±0.18%; 10 nM: 4.24±0.61%; 100 nM: 3.50±0.31%; 1000 nM: 2.70±0.48%; $P < 0.001$ for all concentrations; Figure 3.7 J). It was previously described that METH increases cell death at concentrations above 10 nM (Figure 3.1), which suggest that the decrease in the number of NeuN-positive cells observed at 10, 100 and 1000 nM is probably due to cell death rather than to an inhibition of neuronal differentiation. However, at the nontoxic METH concentration (1 nM), there was a significant decrease in the number of NeuN-positive cells, which demonstrates that METH also inhibits neuronal differentiation in this system (Figure 3.7A, B and J).

Since NPY has an important protective role under METH exposure (Thiriet et al., 2005), we further investigated its effect in preventing the decrease of neuronal differentiation in DG-derived neurosphere cultures. Interestingly, we demonstrated that NPY prevented METH-induced decrease in the number of NeuN-positive cells (8.57±0.52%, $P < 0.001$ *vs.* 1 nM METH; Figure 3.7 K). Also, the Y_1 receptor antagonist was able to inhibit the effect mediated by the activation of Y_1 receptor.

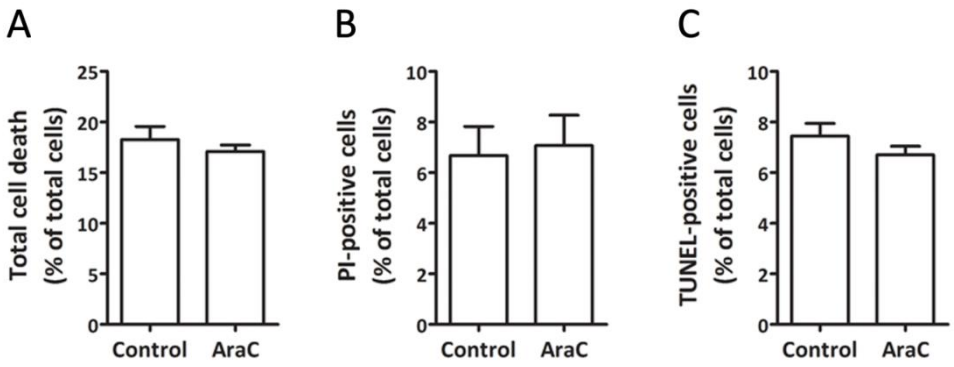

Figure 3.8 – AraC does not induce cell death to DG-derived neurosphere cultures. (A) Incubation with AraC (10 µM) for 24 h has no effect on total cell death, as well as on the number of (B) PI-positve (necrosis) or (C) TUNEL-positive (apoptosis) cells.

3.5. Discussion

The present study demonstrates that METH is toxic and decreases neurogenesis in DG-derived neurosphere cultures without affecting cell proliferation. Furthermore, we also show

that NPY displays effective proproliferative, proneurogenic and protective roles against METH-induced toxicity.

Several studies have shown that METH is toxic to different cell types, such as striatal neurons (Deng et al., 2002), astrocytes (Mandyam et al., 2007), microglia (Tocharus et al., 2010) and oligodendrocytes (Genc et al., 2003). The neurogenic niches have been overlooked, but recently we showed for the first time that METH triggers SVZ cell death (Bento et al., 2011). Accordingly, here we demonstrate that DG cells are highly sensitive to METH since it induced DG cell death by both necrosis and apoptosis, even at low concentrations. To clarify the underlying mechanisms of METH toxicity in DG-derived neurosphere cultures, we looked for the involvement of the glutamatergic system. Glutamate is the major excitatory neurotransmitter in the CNS and is responsible for many physiological functions, such as cognition and sensation (reviewed by O'Connor et al., 2010), but can also be involved in several pathological conditions. This neurotransmitter may act *via* different receptors, and NMDA ionotropic glutamate receptors have been shown to have a crucial role in many brain conditions (Kitayama et al., 2004; reviewed by Hardingham and Bading, 2010). Thus, in the present work, we demonstrated that DG cells express the GluN1 subunit, which is an obligatory subunit of NMDA receptors; however, METH did not induce alterations of GluN1 protein levels. Consistent with this, our group has also shown no alterations in GluN1 protein levels in the hippocampus of rats acutely administrated with 30 mg/kg METH (Simões et al., 2007). Additionally, we concluded that inhibition of NMDA receptors in our cultures by MK-801 prevented apoptotic cell death induced by METH. Afterwards, we demonstrated that METH increases glutamate release from DG-derived neurosphere cultures until, at least, 24 h post-drug exposure. In fact, our work corroborates other studies showing that METH provokes an increase of extracellular glutamate in the rat lateral striatum (Mark et al., 2004; Tata and Yamamoto, 2008) and in the hippocampus (Rocher and Gardier, 2001), and that inhibition of NMDA receptors results in blockade of METH-induced neurotoxicity (Farfel et al., 1992; Gross et al., 2011). Nevertheless, here we address for the first time the involvement of NMDA receptors in METH-induced toxicity in DG-derived neurosphere cultures, which may have interesting implications for the understanding of the impact of drugs of abuse on brain neurogenic niches.

Relatively, little is known about the effect of METH on proliferation of neural progenitor cells. Tian and collaborators (2009) observed a decreased number of proliferating cells in rat hippocampal neural progenitor cell (rhNPC) cultures exposed to METH (300 μM) for 24 h, and this effect was due to reactive oxygen species production. Similarly, Venkatesan and colleagues (2011) recently showed that METH decreases BrdU-positive cells in a concentration-dependent

manner. Moreover, Teuchert-Noodt and co-workers (2000) showed that a single dose of METH (25 mg/kg; i.p.) decreases proliferation, in a transient manner, in the SGZ of adult gerbils. On the other hand, chronic 1 mg/kg METH (s.c.) administration once daily for 14 days had no effect on DG proliferation in mice (Maeda et al., 2007). Concerning self-administration procedures, 0.05 mg/kg/infusion METH (i.v.) taken 1 h/daily, 2 days per week, increases cell division, whereas 1 h/day and 6 h/day decreases cell proliferation (Mandyam et al., 2008). Here, we report that METH does not affect cell proliferation since at 1 nM (nontoxic concentration) and 10 nM (toxic concentration) there were no changes on the number of BrdU-positive cells. Moreover, at higher concentrations there was a decrease in the number of BrdU-positive nuclei, but this effect was prevented by the caspase inhibitor, Z-VAD. These observations strongly indicate that the decreased number of BrdU-stained cells was due to the significant increase of cell death induced by METH. In contrast, we previously demonstrated that METH decreases SVZ cell proliferation (Bento et al., 2011). Thus, according to the neurogenic niche and METH concentration, this drug can have opposite effects on cell proliferation.

METH was found to decrease the number of mature neurons in DG-derived neurosphere cultures at nontoxic concentrations showing a direct and negative effect of METH on neurogenesis. We previously observed the same effects in SVZ cultures (Bento et al., 2011). On the other hand, Venkatesan and collaborators (2011) showed no effect in neuronal and glial differentiation, which can be justified by the fact that the authors used a dramatically higher METH (250 µM) concentration and different experimental conditions (24 h exposure with METH). *In vivo* studies have also demonstrated that 1 h/day (2 days per week) access to METH (0.05 mg/kg/infusion, i.v.) for 49 days increases differentiation and maturation of hippocampal progenitors, consistent with the increased numbers of proliferating cells (Mandyam et al., 2008). However, 1 or 6 h/day access to METH decreased neuronal differentiation, maturation and survival of the progenitor cells (Mandyam et al., 2008).

After identifying that METH is toxic to cells in DG-derived neurosphere cultures, we further aimed to look for a possible therapeutic strategy. We showed that NPY prevented METH-induced apoptotic cell death in DG-derived neurosphere cultures and that this protection is mediated *via* activation of Y_1 and Y_2 receptors both expressed by DG cells. Interestingly, by inhibiting only one of the receptors, NPY completely loses its protective function, suggesting that the pathways triggered by Y_1 and Y_2 receptor activation are similar and both confer cell protection. In fact, little is known about the role of NPYergic system against METH-induced toxicity, but in accord with our findings, Thiriet and collaborators (2005) observed that NPY (10 µg, i.c.v.) administered 1 h before, 24 and 48 h after the first METH injection, as well as the

selective activation of Y_1 or Y_2 receptors, decreased the number of TUNEL-positive cells in mice striatum administered with METH (4x 10 mg/kg every 2 h, i.p.). Furthermore, we aimed to uncover the mechanism(s) responsible for NPY protection in DG-derived neurosphere cultures. We clearly show that NPY blocked the glutamate release triggered by METH. NPY's protective effect was not potentiated in the presence of the NMDA receptor antagonist (MK-801), suggesting that METH induces DG apoptotic cell death by increasing glutamate release that in turn overactivates NMDA receptors. Thus, cell death was completely abolished either by inhibiting glutamate release with NPY or directly blocking NMDA receptors. Consistent with this, we have previously shown that NPY inhibits KCl-evoked glutamate release in rat hippocampal synaptosomes *via* Y_2 receptors (Silva et al., 2003a), and that activation of both Y_1 and Y_2 receptors is neuroprotective against rat hippocampal excitotoxicity (Silva et al., 2003b; Xapelli et al., 2007). Additionally, our results show that NPY did not prevent the increase in necrosis induced by METH. As reviewed by Barros et al. (2001), necrosis involves energy depletion by concurrent ATP hydrolysis by ion pumps and defective ATP production, resulting in cell swelling and lysis. This metabolic depletion leads to Ca^{2+} deregulation, which activates degradative enzymes occurring mitochondrial disruption. Despite the fact that NPY is able to prevent neuronal cell death by both apoptosis and necrosis in other pathological experimental models (Silva et al., 2003a; Xapelli et al., 2007), the only paper available in the literature regarding METH insult (Thiriet et al., 2005) reports only protection against apoptosis. Thus, in the present work we suggest that the pathways that mediate necrosis and apoptosis can be divergent, where we observed that NPY had no protective effect on METH-induced necrosis.

In addition to its protective, NPY also induces an increase in proliferation and neuronal differentiation *via* Y_1 receptors. These findings are consistent with previous studies performed in SGZ cell cultures (Howell et al., 2003 and 2005) where incubation with 1 µM NPY for 3 days increased cell number, BrdU incorporation, nestin and class III β-tubulin immunoreactive cells. Also, NPY (1 µM) is a proproliferative factor for neuroblasts in the DG through the activation of ERK1/2 (Howell et al., 2005). Agasse and co-authors (2008) demonstrated that SVZ cells exposed to 1 µM NPY for 48 h or 7 days showed an increase in proliferation or neuronal differentiation, respectively, *via* Y_1 receptor activation and MAPK pathway. Others verified that administration of 2.5 pmol/µl NPY (i.c.v.) for 48 h or 7 days to in C57BL/6 adult mice induces an increase in proliferation or neuronal differentiation, respectively, and that this increase is due to the activation of Y_1 receptor subtype (Decressac et al., 2010).

It is well accepted that memory deficits are closely related to neuronal dysfunction or/and loss (Simon et al., 2000; Thompson et al., 2004). In fact, our group has previously

evaluated the effect of METH on working memory and revealed mnemonic deficits in Sprague-Dawley rats injected with an acute subcutaneous dose of 30 mg/kg METH (Simões et al., 2007). Likewise, Simon and collaborators (2000) verified that METH abusers display cognitive deficits, which was correlated with a significant decrease in hippocampal volume (Thompson et al., 2004). Furthermore, it is known that deficits in brain adult neurogenesis can contribute to cognitive deficits. In fact, Madsen et al. (2003) verified that the impairment of neurogenesis in rats subjected to fractionated brain irradiation, lead to cognitive deficits. Thus, to prevent the impairment of neurogenesis induced by METH, we also challenged DG-derived neurosphere cultures with NPY and we observed that it completely prevented the decrease of neurogenesis induced by METH. Also, we observed that the selective activation of Y_1 receptor completely prevented this effect. Importantly, taking into consideration the results reported here and by others showing that NPY is a protective, proneurogenic and proproliferative factor, we still cannot unambiguously determine if this preventive effect under conditions of METH-induced decrease of neuronal cells is due to mechanisms of protection, proliferation or/and neuronal differentiation. However, it is clear that NPY, *via* Y_1 receptors, is able to prevent the toxic effect of METH on DG cells.

Taken together, the present work allows us to better understand how METH affects the cell dynamics in hippocampal neurogenesis. Moreover, it was also demonstrated that the NPYergic system plays an important protective role against the destructive effects of this drug of abuse on hippocampal neurogenesis.

Chapter 4

Methamphetamine promotes neuronal differentiation and strengthens long-term potentiation of glutamatergic synapses onto immature dentate granule neurons in G42 (GAD67-GFP) mice

4.1. Abstract

Some studies have suggested that methamphetamine (METH) is harmful to DG neurons and neuronal development, which can in part justify memory deficits observed in METH abusers. Moreover, changes in synaptic strength originating from the entorhinal cortex seem to underlie cognitive deficits, similar to those seen by METH abuse. However, little is known about the effects of METH on synaptic plasticity of the dentate gyrus (DG). Here, we investigate the impact of METH on neurogenesis and synaptic plasticity. To do so, we used a transgenic mouse (GAD67-GFP, line G42), in which GFP is transiently expressed in maturing newborn neurons, and has been previously used as a model of adult neurogenesis. In this mouse line, GFP^+ cells show different firing profile as follows: group 1 cells fire a single action potential (AP), group 2 cells fire few APs, and group 3 fire APs repeatedly, similarly to mature neurons. Accordingly, dendrites complexity increased from group 1 to group 3. Also, group 1 GFP^+ cells does not produce excitatory postsynaptic currents (EPSCs) upon medial perforant pathway (MPP) fiber stimulation, in contrast to group 2 and group 3 cells, whose EPSCs can undergo potentiation. Taking this into consideration, mice were administered with 2 mg/kg METH (i.p.), once a day for 7 days, and we found that METH enhanced the differentiation of GFP^+ cells shifting from DCX- to a more mature NeuN-expressing GFP^+ cells, without changing the number of GFP^+ cells. However, METH had no effect on either AP firing or passive membrane properties. Interestingly, METH induced LTP in group 3 cells in contrast to the control group (saline-treated), in which only a medium-term potentiation could be observed. In mature (GFP^-) cells, METH generated a stronger long-term potentiation (LTP) in comparison to control. In conclusion, METH promotes the differentiation of immature neurons, induces LTP in group 3 GFP^+ cells and strengthens LTP in mature DG neurons. These effects of METH can justify the enhancement of memory performance during short-term administration.

4.2. Introduction

Methamphetamine (METH) is a psychostimulant drug of abuse, highly addictive and toxic to the human brain (reviewed by Silva et al., 2010; Gonçalves et al., 2014). Many studies indicated that METH abuse induces cognitive deficits, specifically by reducing the rate of psychomotor speed, attention capacity, lower ability to manipulate information, and deficits in working memory (Simon et al., 2000). METH abusers under abstinence exhibit poorer performance in attention and psychomotor speed, learning and memory, or in fluency tests (Kalechstein et al., 2003). Indeed, Thompson and collaborators (2004) associated memory

performance with alterations in tissue volume and observed that the hippocampus is the most affected region, showing a correlation between hippocampal tissue atrophy with poorer word-recall test. In rodents, hippocampal-dependent memory performance may depend on the dose of METH administered where a high dose (30 mg/kg, i.p.) induces hippocampal neuronal dysfunction (Gonçalves et al., 2010) and memory deficits (Simões et al., 2007; Gonçalves et al., 2012b), whereas a lower dose (1 mg/kg, i.p.) improved spatial memory consolidation (Cao et al., 2013). Nevertheless, it is noteworthy that METH (Desoxyn®) is FDA approved to the treatment of Attention Deficit Disorder with Hyperactivity (ADHD).

Adult neurogenesis occurs throughout life and subgranular zone of the dentate gyrus (DG) and subventricular zone are the main neurogenic niches (Lledo et al., 2006). Moreover, a link between hippocampal neurogenesis and memory performance was observed by Kee and colleagues (2007) where they show that immature DG neurons are preferentially activated and recruited into spatial memory networks. In contrast, long-term ablation of neurogenesis induces memory and learning impairments and spatial flexibility deficits (Garthe et al., 2009). These authors also observed reduced long-term potentiation (LTP) in the DG after ablation of neurogenesis (Garthe et al., 2009). Interestingly, Green and collaborators (1990) demonstrated that exploratory behavior (learning) is linked with an increase in evoked field excitatory postsynaptic potential (EPSP) in the DG, suggesting a role of LTP in acquisition of new memories.

It is well known that neurogenesis is affected by several insults, and drugs of abuse are not an exception. Indeed, METH can induce alterations in hippocampal neurogenesis, which depends on the dose and frequency of exposure. One single injection of METH (50 mg/kg) decreased cell proliferation in gerbils (Hildebrandt et al., 1999), whereas a smaller dose (25 mg/kg) transiently decreased proliferation (Teuchert-Noodt et al., 2000). On the other hand, a low dose of METH (1 mg/kg, i.p.) chronically administered to mice had no effect in the number of proliferating cells (Maeda et al., 2007). Interestingly, a study that relates self-administration protocol with human patterns of METH abuse (recreational, chronic and dependence) revealed that intermittent access (recreational) to METH (0.05 mg/kg/infusion, 2x/week for 28 days) displayed an increase in DG cell proliferation as well as in neuronal differentiation. On the other hand, both short (1 h/day, chronic) and long (6 h/day, dependence) access decreased proliferation and differentiation followed by a reduced number of DG granule cell neurons (Mandyam et al., 2008). Moreover, DG cells react differently to METH as demonstrated by Yuan and colleagues (2011), where METH self-administration (6 h/day for 4 or 13 days) increased the number of radial glia-like cells (type 1 cells), but decreased the population of type 2a cells, which suggests that METH impairs the transition from type 1 to type 2a cells.

Overall, METH can improve or impair neurogenesis depending on the dose and frequency of exposure, but whether METH affects functional properties of immature and mature DG cells remains unknown. In the present work, we explored the effects of chronic METH administration in DG neurogenesis and its influence in synaptic plasticity of both newborn and mature neurons. Here, we show that METH enhances maturation of immature neurons, but neither affects passive membrane properties nor action potential kinetics. However, METH induces LTP in immature neurons and strengthened LTP in mature DGCs. In conclusion, we predict that chronic administration with a low dose of METH may result in improved memory performance.

4.3. Materials and methods

4.3.1. G42 transgenic (GAD67-GFP) mice

We used G42 (GAD67-GFP) mice, which were designed to express GFP in inhibitory GABAergic neurons. Indeed, GFP is present in parvalbumin-expressing, fast-spiking interneurons in the neocortex (Chattopadhyaya et al., 2004). In the hippocampus, however, GFP is sparsely expressed by inhibitory interneurons, and in the DG immature granule cells in the DG is selectively labeled (Cabezas et al., 2012, 2013). Indeed, these cells are postmitotic immature neurons, showing a transient GABAergic phenotype and expressing specific markers related to neuronal development: DCX, a microfilament protein that is specifically expressed in postmitotic neurons and used as a marker for immature neurons; calretinin, a calcium-binding protein that is transiently expressed in immature DGCs; some cells express NeuN, a marker for mature DGCs; and Prox1, a marker that specifically identifies DGCs (Cabezas et al., 2013).

G42 mice were continuously backcrossed on a C57BL/6 background, were weaned at postnatal day 21 (P21) and only males were used for the experiments. Although hydrocephaly has been described in this mouse strain (http://jaxmice.jax.com/007677.html), all hydrocephalus animals were discarded from experiments.

Animals were housed on a 12-h light/dark cycle in a temperature-controlled room with access to food and water *ad libitum*. All procedures were performed in accordance with the European Communities Council Directive (2010/63/EU) for care and use of experimental animals. All efforts were made to minimize suffering and reduce the number of animals.

4.3.2. Methamphetamine injection protocol

Methamphetamine hydrochloride was provided by Profs Nuno Milhazes from the Institute of Health Sciences-North, Gandra PRD, Portugal, and Fernanda Borges from the Faculty of Sciences, University of Porto, Portugal. METH was dissolved in 0.9% NaCl in a concentration of 0.8 mg/ml and P20-24 G42 mice were injected chronically with 2 mg/kg METH (i.p.), or saline solution (control, vehicle animals), once a day for 7 days. Afterwards, both immunohistochemical, morphological and electrophysiological experiments were performed 24 h after the last injection (Figure 4.1). The dose was chosen based on previous works showing that one administration of 2 mg/kg METH (i.p.) reduces $GABA_BR$-GIRK slow inhibitory postsynaptic currents in GABAergic neurons of the ventral tegmental area 24 h or 7 days after METH injection (Padgett et al., 2012).

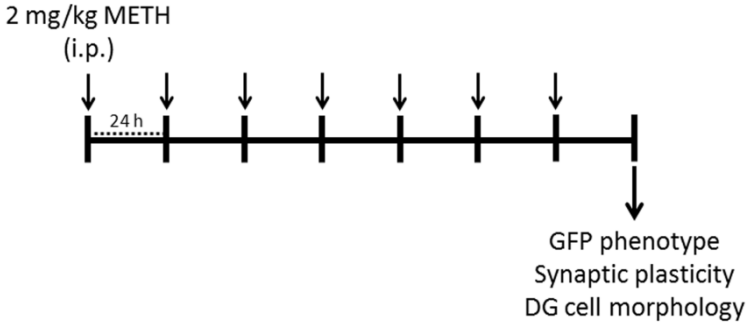

Figure 4.1 – METH injection protocol. G42 mice were injected with 2 mg/kg METH (i.p.) once a day for 7 consecutive days. Immunohistochemical, electrophysiological and DG cell morphology experiments were performed 24 h after the last METH administration.

4.3.3. Immunohistochemistry

G42 mice were anesthetized with a solution consisting of ketamine (80 mg/kg, i.p.) and xylazine (20 mg/kg, i.p.) and were transcardially perfused with 4% (w/v) paraformaldehyde (PFA, Sigma-Aldrich, Saint-Quentin Fallavier, France) in phosphate-buffer saline solution (PBS; Sigma-Aldrich). Afterwards, brains were post-fixed overnight in 4% PFA, rinsed with PBS and cryoprotected in 30% sucrose (Sigma-Aldrich) in PBS for 48 h. Then, brains were horizontally cut in 40-µm thick slices in a cryotome (Microm HM450). Slices were rinsed in PBS (3x 10 min) and were incubated in a blocking solution consisting of 10% bovine serum albumin (BSA) and 0.3% Triton (both from Sigma-Aldrich) in PBS for 2 h at room temperature. Slices were then incubated overnight at 4°C with 0.1% normal donkey serum (Sigma-Aldrich), 0.3% Triton in PBS and primary antibodies as follows: chicken anti-green fluorescent protein (1:1000; Millipore), rabbit anti-doublecortin (DCX; 1:2000; Cell Signaling, Danvers, MA) and mouse anti-NeuN (1:250; Millipore).

Slices were rinsed in PBS (3x 10 min) and incubated with the respective secondary antibodies in 0.3% Triton for 3.5 h at room temperature as follows: donkey anti-mouse IgG Cy3 (1:400), donkey anti-chicken IgG Cy2 (1:500), donkey anti-rabbit IgG Cy3 (1:600) and Alexa Fluor® 647 donkey anti-mouse (1:400; all from Jackson ImmunoResearch Laboratories, Suffolk, England). Slices were rinsed in PBS (3x 10 min) and then mounted in Fluoromount-G (Southern Biotech, Birmingham, USA).

4.3.4. Acquisition and analysis of confocal images

To determine GFP cell density in the DG, tiled images were acquired in an inverted confocal microscope (SP2 Leica, Germany), using a 40x/1.25 N.A objective from horizontal slices marked for NeuN and GFP. The number of GFP cells was counted in each tiled image from one DG plan, and the correspondent DG area was determined due to NeuN staining, obtained from the combination of all tiled images. Analysis of the total number of GFP cells and DG area was performed using Image J from 5 mice each group, 4 horizontal slices per animal.

The level of neuronal maturation of GFP^+ cells was assessed from images obtained from horizontal slices that were stained for GFP, DCX and NeuN. Images were obtained from stacks of 10-17 sections, 2.5 µm apart, using a 63x/1.32 N.A objective. Images were acquired from four slices/animal of five saline- or METH-treated mice. Cell counts were determined using Image J software. Results are expressed as percentage of total GFP cells expressing DCX and/or NeuN.

4.3.5. Electrophysiology

G42 mice were anesthetized with halothane (Sigma-Aldrich) and were immediately decapitated. Brains were quickly removed into ice-cold solution containing in mM: 248 sucrose, 26 $NaHCO_3$, 1 KCl, 1 $CaCl_2$, 5 $MgCl_2$ and 10 glucose (all from Sigma-Aldrich). Then, 350 µm-thick horizontal slices were obtained using a vibratome (Leica VT 1200 S, Nanterre, France) and transferred to a chamber containing artificial cerebrospinal fluid solution (ACSF; in mM: 126 NaCl, 2.5 KCl, 1.25 NaH_2PO_4, 26 $NaHCO_3$, 2 $CaCl_2$, 1 $MgCl_2$ and 16 glucose, all from Sigma-Aldrich), bubbled with 95% O_2 / 5% CO_2 at 34°C for 30 min, followed by incubation at room temperature for at least 1 h before recording.

Slices were perfused with ACSF containing the $GABA_AR$ antagonist gabazine (10 µM; Tocris, Lille, France) and the chamber temperature was set for 32-34°C as described by Ge et al. (2006, 2007a). For the electrophysiological experiments, slices were transferred to a submerged chamber and neurons were visualized using infrared videomicroscopy, with a microscope equipped with epifluorescence. GFP^+ and mature GFP^- cells were characterized by their action

potential (AP) firing. Microelectrodes with 3-4 MΩ tip-resistance were pulled from borosilicate glass capillaries (World Precision Instruments, WPI, Florida 34240, USA) using a Flaming/Brown Micropipette puller P-97 (Sutter Instruments, USA).

Intracellular solution consisted in (in mM) 130 potassium gluconate, 10 KCl, 10 HEPES, 2 $MgCl_2$, 5 Phosphocreatine, 4 MgATP, 0.3 NaGTP and 0.2 EGTA (all from Sigma-Aldrich), pH 7.3, with reversal potential set at -70 mV and osmolarity approximately 290 mOsm. DGCs were whole-cell patch-clamped and recorded both in current- and voltage-clamp modes as will be further indicated in each experiment.

Action potential firing of dentate gyrus neurons

GFP^+ and GFP^- cells were characterized in current-clamp mode. AP firing was evoked by injecting 1 second-long depolarizing steps of increasing amplitude, starting at -25 pA and with a 10 pA increment. Cells were recorded both at resting membrane potential and at a holding potential of -70 mV, by injecting a holding current. AP peak amplitude, half-width and peak area were analyzed off-line.

GFP^+ cells were identified in terms of their AP firing profile as follows: Group 1: GFP^+ cells that fire a single AP; Group 2: GFP^+ cells that fire more than one, but could not sustain repetitive firing; and Group 3: GFP^+ cells that fired repeatedly.

Synaptic plasticity

DGCs (both GFP^+ and GFP^-) were kept in voltage-clamp mode at a holding potential of -70 mV. A bipolar stimulating electrode fabricated from a theta capillary (WPI) and filled with ACSF was placed in the middle third of the molecular layer in order to orthodromically stimulate the MPP (Figure 4.2). EPSCs were evoked by short (0.2 ms) pulses of 5 V. Short-term plasticity was assessed by evoking pairs of responses separated by 200-ms inter-pulse intervals (Figure 4.2 B).

LTP was induced by applying the theta-burst stimulation (TBS) paradigm consisting of 5 bursts of extracellular stimulations at 100 Hz, repeated at 5 Hz and paired with postsynaptic depolarization at -30 mV. These bursts were delivered 16 times at 0.1 Hz (Figure 4.2 C). Recordings were discarded if series resistance was above 30 MΩ or changed more than 20%.

Selective MPP stimulation was verified by the presence of paired-pulse depression of EPSCs in response to two stimuli, closely separated in time (200 ms), as opposed to paired-pulse facilitation, typical of LPP stimulation (Colino and Malenka, 1993). Activation of MPP was further confirmed by functional expression of metabotropic glutamate receptor 2 ($mGlu_2$), which are

absent at LPP terminals (Macek et al., 1996; Chiu and Castillo, 2008; Shigemoto et al., 1997). Indeed, slices were perfused with the mGlu2 agonist (2*S*,2'*R*,3'*R*)-2-(2',3')-dicarboxycyclopropyl)glycine (DCG-IV; 1 µM), 30 min after LTP induction and reduction of EPSC amplitude was monitored (Figure 4.11).

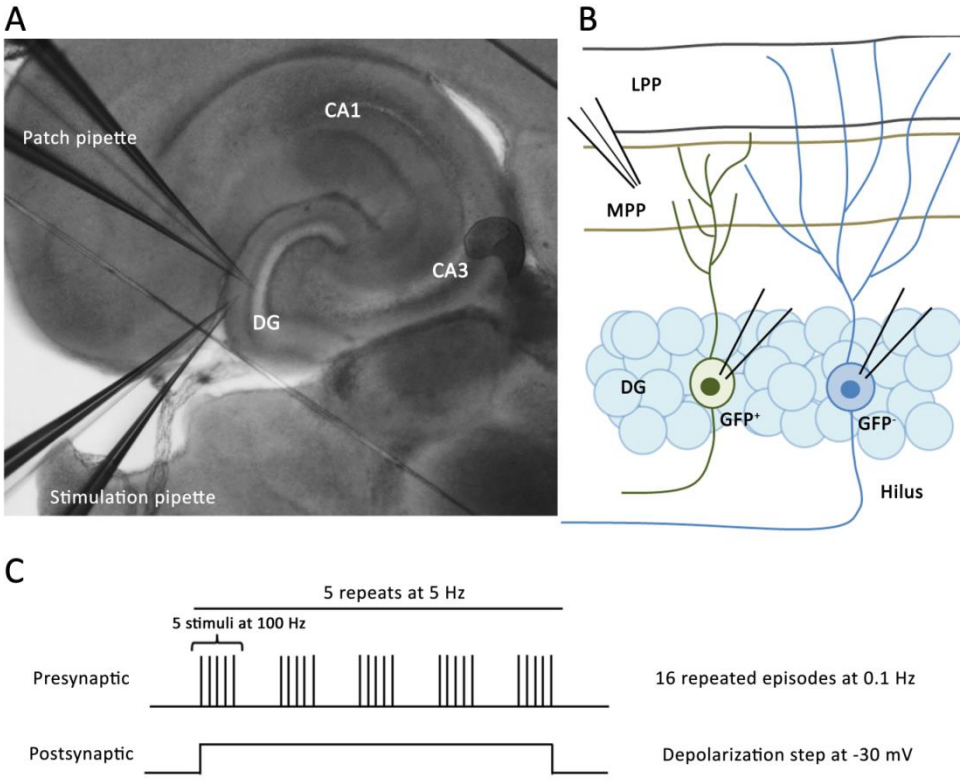

Figure 4.2 – Evoked EPSCs from GFP^+ and GFP^- cells were recorded through MPP stimulation and LTP was induced by TBS. (A) Transmission image from a live horizontal slice showing the stimulation pipette at the MPP and the recording patch pipette in the granule cell layer. (B) Schematic representation of the protocol to evoke EPSCs in GFP^+ (green) and GFP^- (blue) cells. (C) TBS protocol. DG: Dentate gyrus; LPP: Lateral perforant pathway; MPP: Medial perforant pathway.

Dentate granule cell morphology

Neurobiotin (3 mg/ml; Vector Labs) was dissolved in the intracellular solution and cells were filled during recordings. At the end of electrophysiological experiments, pipettes were gently pulled and slices fixed overnight in 4% PFA. Slices were then rinsed in PBS followed by incubation for 5 min with a solution consisted of 3% H_2O_2 and 10% methanol in PBS (all from Sigma-Aldrich). Slices were then rinsed twice with PBS (10 min each) and were permeabilized in 2% Triton in PBS for 1 h. Slices were incubated for 2 h with ABC reagent (Avidin and biotinylated horseradish peroxidase [HRP] complex, Vector Labs) according to the manufacturer and rinsed in

PBS as follows: 2x 10 min, 1x 15 min and 1x 1 h. Slices were reacted with 3,3'-diaminobenzidine (DAB, Vector Labs) until the stain was visualized by using a stereotaxic microscope and were immediately rinsed twice with PBS. Slices were then mounted in 85% glycerol (Sigma-Aldrich) in PBS. Neurons were reconstructed using the Neurolucida software (MicroBrightField) using a 40× objective.

Differential interference contrast images were acquired with a macroscope (AZ100 Nikon) from stacks of 11 sections, 2 µm apart, using a 5x objective.

4.3.6. Data analysis

AP parameters, passive membrane properties and EPSCs were analyzed in Clampfit software (pClamp). LTP magnitude was determined by comparing the mean amplitude of EPSCs in the last 5 min of the plasticity in relation to the 5 min of baseline. Dendritic constructions were analyzed in Neurolucida explorer.

Statistical significance was assessed using analysis of variance (one-way ANOVA) followed by Bonferroni's multiple comparison or Mann Whitney post-hoc tests, as indicated in the figure legends. Data are expressed as mean ± standard error of the mean (SEM) and statistical significance level was set for $P < 0.05$.

4.4. Results

4.4.1. Methamphetamine does not change body weight

G42 mice were injected with 2 mg/kg METH or saline (i.p.) once a day for 7 days (Figure 4.1) and body weight was monitored. Mice were weighted in the first day of injection and then every two days, and finally in the day of the experiment. Within the saline group, there was an increase of body weight through time as follows: in the first day of injection mice weighted 10.00 + 0.39 g followed by 11.33 + 0.40 g, 12.76 + 0.43 g, 14.36 + 0.41 g, and in the experimental day 14.98 + 0.40 g (n = 24 animals; Figure 4.3). Regarding the METH group, in the first day of injection mice weighted 10.03 + 0.40 g followed by 11.05 + 0.45 g, 12.61 + 0.43 g, 14.22 + 0.50 g, and at the experimental day 14.61 + 0.49 g (n = 22 animals; Figure 4.3). Our findings show that METH did not induce alterations in body weight at each time points when compared to saline-injected mice (Figure 4.3).

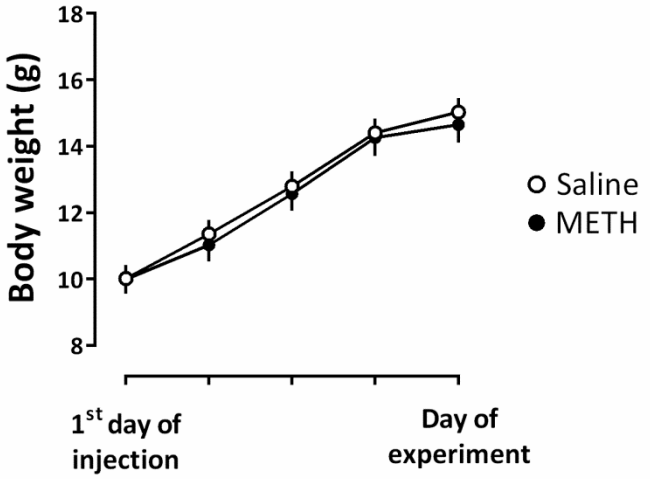

Figure 4.3 – Chronic administration of METH has no effect in G42 mice body weight. G42 mice were weighted in the first day of injection, every two days afterwards and on the experiment day. Data are expressed as mean ± SEM (n = 24 in saline and n = 22 in METH group).

4.4.2. Methamphetamine accelerates immature dentate granule cell maturation

METH interferes with stem and progenitor cell proliferation and maturation depending on the dose and frequency of exposure (Teuchert-Noodt et al 2000; Mandyam et al., 2008; Yuan et al., 2011). In the present work, we used G42 mice as a model of DG neurogenesis, whose GFP^+ expression is transient and specific for immature dentate granule neurons (Cabezas et al., 2012, 2013). Therefore, we tested if METH treatment changes the density of GFP^+ cells in the DG of G42 mice (Figure 4.4). We observed that chronic administration of METH (2 mg/kg, i.p.) did not significantly change the number of GFP^+ cells over a DG horizontal section as follows: Saline: 1.09 + 0.35 GFP^+ cells/mm^2 (Figure 4.4 A and C) and METH: 1.53 + 0.47 GFP^+ cells/mm^2 (Figure 4.4 B and C).

According to Cabezas and collaborators (2012, 2013), GFP^+ cells in this mouse line can have different stages of neuronal maturation, as they express only DCX (open arrows), co-express DCX and NeuN (filled arrows), or only NeuN (arrow heads) (Figure 4.6 A-D). Chronic administration of METH decreased the number of GFP^+ cells that expressed only DCX (Saline: 42.59 + 3.33%; METH: 31.24 + 2.17% of total GFP cells; $P < 0.05$) and increased the number of GFP^+ cells expressing only NeuN (Saline: 51.58 + 3.88%; METH: 66.78 + 2.55% of total GFP cells; $P < 0.01$), without interfering with GFP^+ cells co-expressing DCX and NeuN (Saline: 17.68 + 3.33%; METH: 16.59 + 1.56% of total GFP cells) (Figure 4.5 E; n = 5 animals each group).

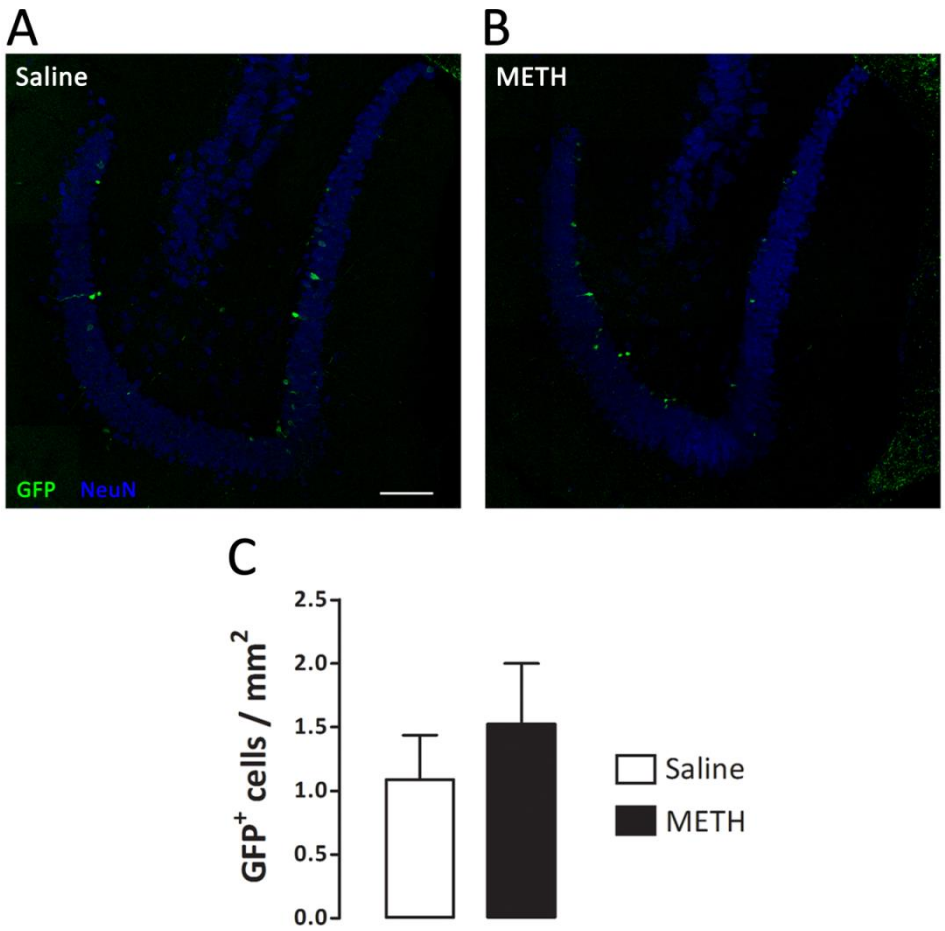

Figure 4.4 – METH does not change the number of GFP^+ cells. (A and B) Representative confocal images of DG expressing GFP^+ (green) and $NeuN^+$ (blue) cells from G42 mice injected with (A) saline or (B) METH. (C) Bar graph depicting the density of GFP cells in the DG from saline- or METH-injected mice, showing that METH has no effect in GFP^+ cell density. Data are expressed as mean + SEM from 5 animals injected with saline or METH, using Mann-Whitney post-hoc test. Scale bar: 100 µm.

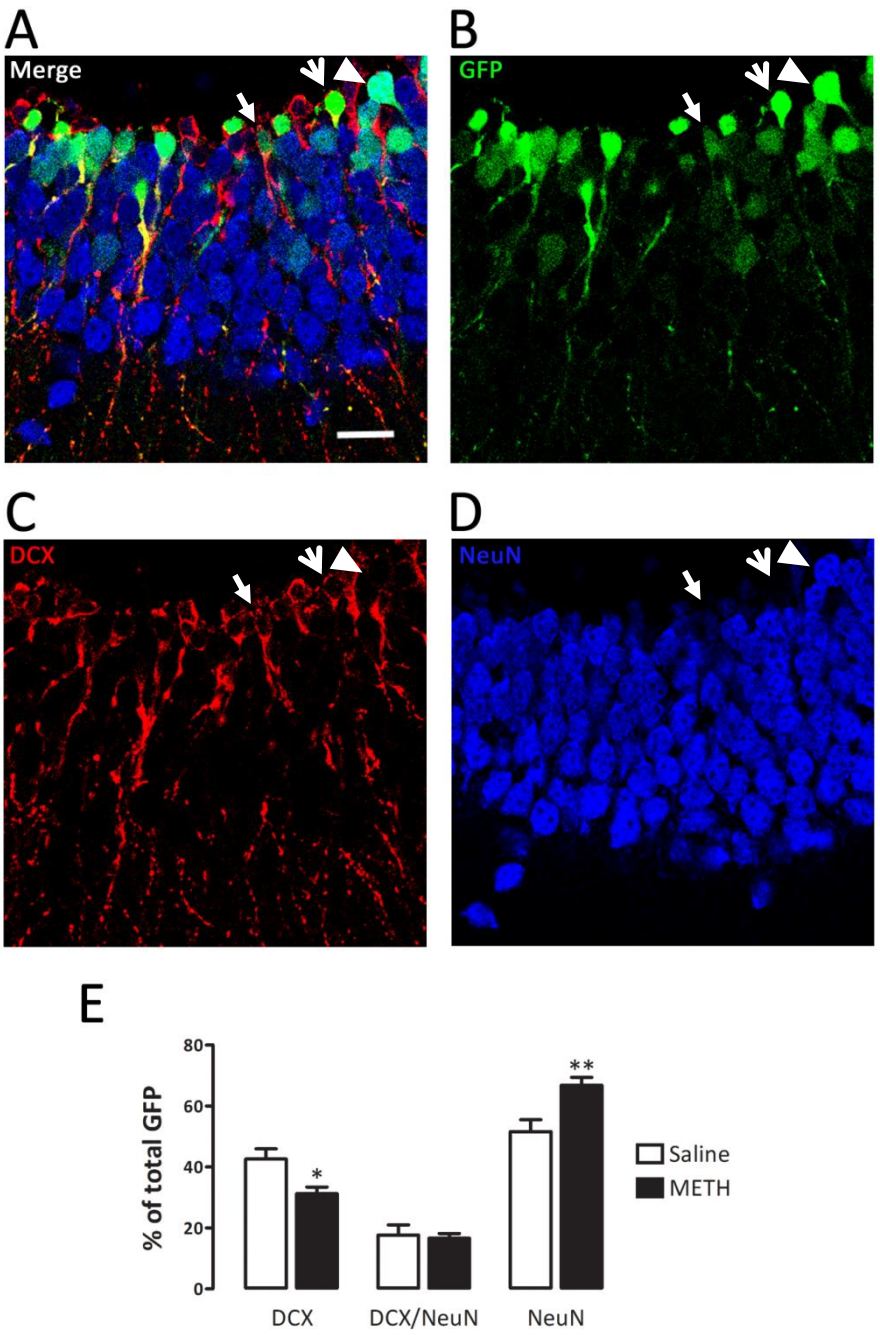

Figure 4.5 – METH triggers differentiation of immature DG neurons. (A–D) Representative confocal images exhibiting the different phenotypes of immature cells, GFP^+ DGCs. Immature neurons were identified as GFP^+ cells (B) and different phenotypes were characterized by co-expression with (C) DCX and/or (D) NeuN. Indeed, at least three different development stages of maturation were identified as follows: 1 – a more immature developmental stage, in which GFP^+ cells express only DCX (open arrows); 2 – an intermediary stage where GFP^+ cells express both DCX and NeuN (close arrows); and 3 – a more matured stage showing GFP^+ cells expressing only NeuN, (arrow heads). (E) Chronic injection of METH enhances differentiation of GFP^+ cells by decreasing the population of GFP^+ cells that express DCX (open arrows) while increasing those that express NeuN (arrow heads), without changing the number of GFP^+ neurons co-expressing both DCX and NeuN (close arrows). Data are expressed as percentage of total GFP^+ cells + SEM from 4 horizontal slices/animal of five animals per condition. $^*P < 0.05$ and $^{**}P < 0.01$, significantly different from saline using Mann-Whitney post hoc test.

4.4.3. Methamphetamine treatment neither alters action potential waveform nor membrane passive properties of developing dentate gyrus neurons.

METH treatment enhances the differentiation of GFP^+ cells. Therefore, we tested if METH alters the functional properties of these cells. GFP^+ neurons of G42 mice display three different patterns of AP firing in response to a depolarizing current pulse (Figure 4.6 A). Group 1 neurons represent GFP^+ cells that fire a single AP irrespective of the intensity of stimulation (Figure 4.6 B); group 2 includes GFP^+ cells that could generate few APs during the depolarizing current step. APs of group 2 DG neurons tended to become smaller in amplitude during the step. (Figure 4.6 C); group 3 includes GFP^+ cells that exhibit AP firing pattern, more similar to mature neurons (GFP^-), *i.e.* multiple APs with little or no changes of spike amplitude during the train (Figure 4.6 D).

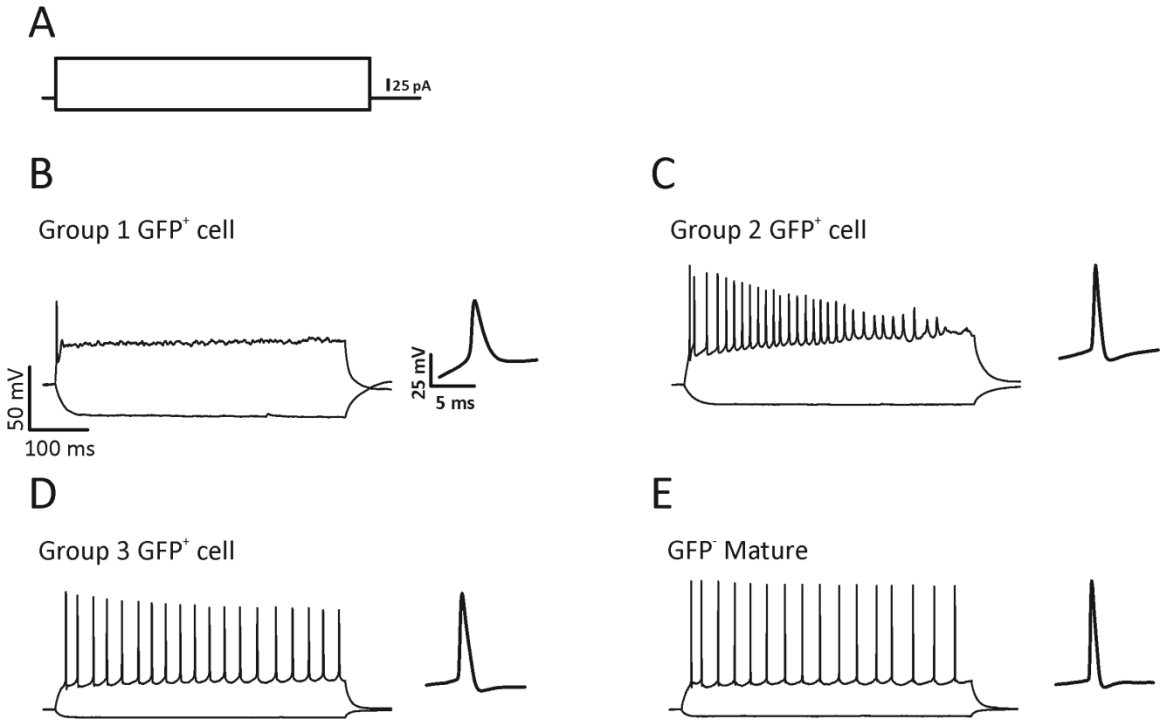

Figure 4.6 – DG immature neurons from G42 mice have different AP firing profiles. (A) Current pulses of -25 and 85 pA with 1 s duration were applied to DG cells under current-clamp configuration. GFP^+ cells present different behavior upon a depolarizing current step: (B) GFP^+ cells that only exhibit one AP (Group 1), (C) GFP^+ cells that do not sustain high frequency firing (Group 2), and (D) GFP^+ cells that fire during the entire depolarizing step (Group 3). (E) AP firing from a GFP^- or mature cell.

Accordingly, immature GFP^+ cells also differed in dendritic development: group 1 GFP^+ cells have few and short ramifications, mostly confined in the inner dentate granule layer (Figure

4.7 A). Group 2 cells have longer dendrites and more branching points than group 1 cells (Figure 4.7 B) and complexity is more prominent as GFP^+ cells matures into group 3 cells (Figure 4.7 C). DG neurons belonging to groups 2 and 3 share the same region of the DG, whereas group 1 neurons tended to localize more internally, at the border with the hilus. Finally, mature neurons present the most elaborated dendritic arborization of all cells, with dendrites reaching the outer molecular layer (Figure 4.7 D).

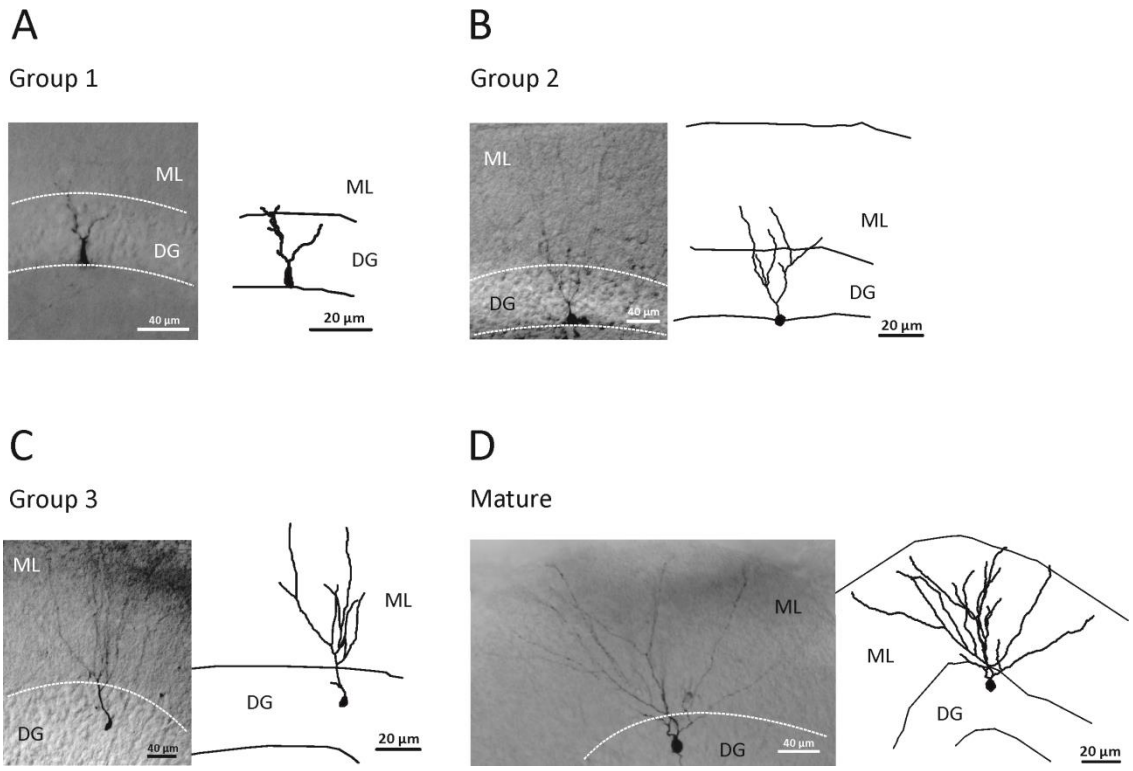

Figure 4.7 – DG immature neurons have different morphologies. Left panels show neurobiotin-filled GFP^+ and mature cells that were reconstructed for anatomical analysis (right panels). (A) Group 1 GFP^+ cells present modest dendritic development, whereas development of dendrites are more complex in (B) group 2 and (C) group 3 GFP^+ cells. (D) Mature neurons show more complex dendritic tree when compared to GFP^+ cells. DG: Dentate gyrus; ML: Molecular layer.

In electrophysiological experiments the incidence of GFP^+ cells of group 3 was the highest in both saline and METH groups (Figure 4.8). In particular, 24% of GFP^+ patched cells were identified as belonging to group 1, 18% to group 2 and 58% to group 3 cells in saline-injected animals (n = 76 total cells from 24 animals). However, no significant effect was observed in METH-injected animals as follows: 19% of GFP^+ patched cells belonged to group 1 cells, 26% to group 2 and 55% to group 3 (n = 74 total cells from 22 animals; Figure 4.8).

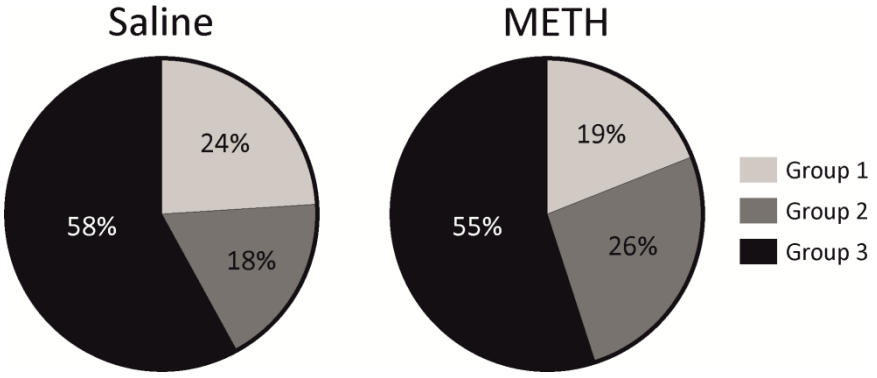

Figure 4.8 – Distribution of GFP$^+$ cells according to group 1, 2 and 3 in both control (saline) and METH condition. Group 3 GFP$^+$ cells are more prevalent than groups 1 and 2 cells in both saline and METH groups.

We tested whether METH treatment changed AP waveform and/or passive membrane properties of GFP$^+$ cells. METH treatment did not change AP amplitude, peak, area, half-width or threshold (P > 0.05 in all cases; Figure 4.9, Table 1). Moreover, drug treatment did not alter passive membrane properties, such as resting membrane potential, membrane capacitance and membrane resistance (P > 0.05 in all cases Figure 4.9, Table 1). Importantly, however, in both saline- and METH-treated animals GFP$^+$ DG neurons belonging to groups 1-3 displayed different values for AP peak and amplitude as well as for passive membrane properties neurons (Figure 4.9, Table 1). This was consistent with the functional changes of developing DG neurons, as previously described (Mongiat et al., 2009).

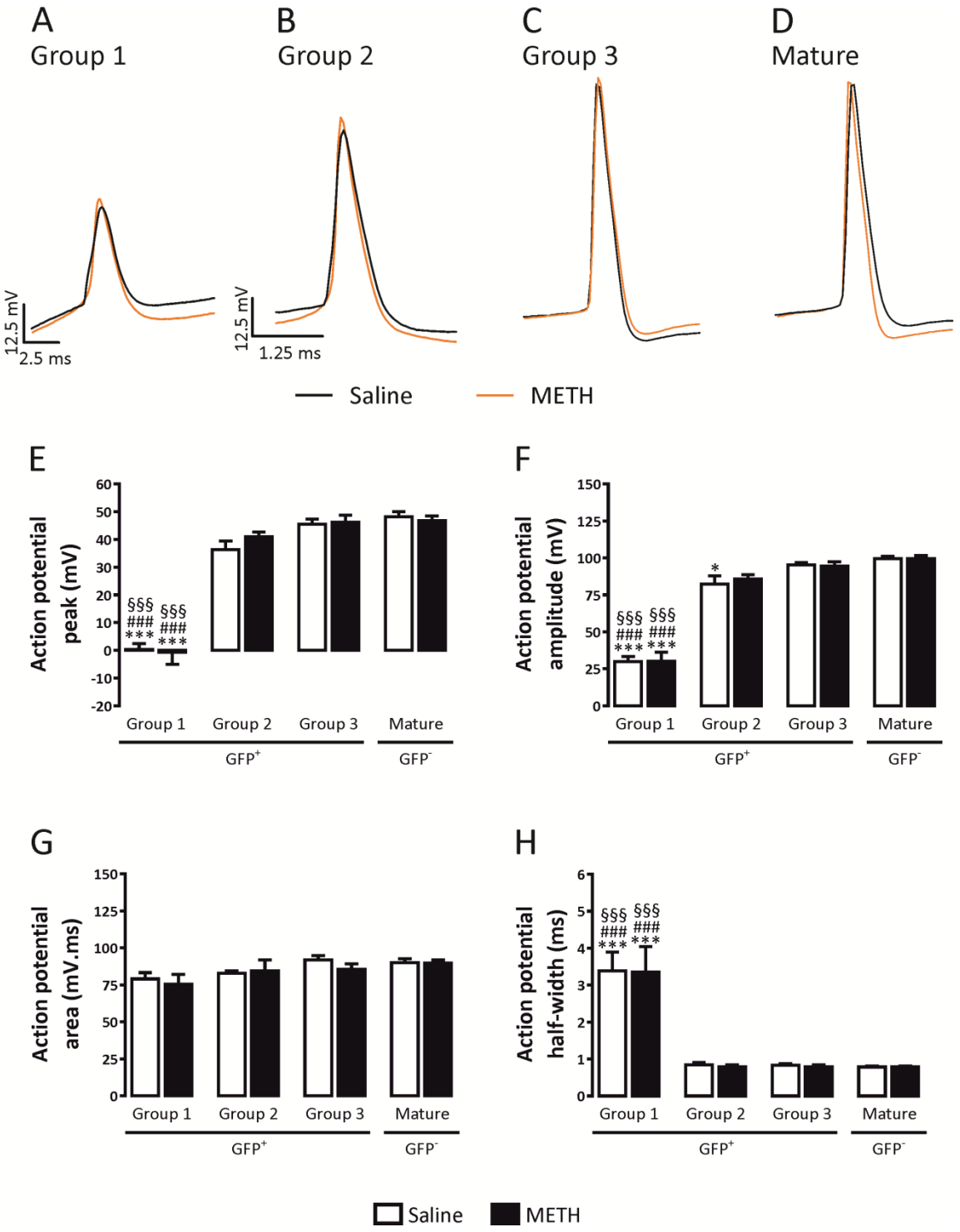

Figure 4.9 – METH has no effect on AP waveform. Representative single AP traces from (A) group 1, (B) group 2, (C) group 3 GFP$^+$ cells and mature neurons (D). METH has no effect in (E) AP peak, (F) AP amplitude, (G) AP area or (H) AP half-width. Data are expressed as mean + SEM (n = 6 – 23). *P < 0.05 and ***P < 0.001, significantly different from the corresponding mature group using Bonferroni's multiple comparison post-hoc test. $^{###}P$ < 0.001, significantly different from group 2 GFP$^+$ cells using Bonferroni's multiple comparison post-hoc test. $^{§§§}P$ < 0.001, significantly different from group 3 GFP$^+$ cells using Bonferroni's multiple comparison post-hoc test.

Table 1 – AP waveform values of GFP⁺ cells and mature neurons from figures 4.9 and 4.10

	GFP⁺						GFP⁻	
	Group 1		Group 2		Group 3		Mature	
	Saline	METH	Saline	METH	Saline	METH	Saline	METH
AP peak (mV)	0.24±2.17	-0.72±4.28	36.31±3.08	40.95±1.70	45.50±1.78	46.18±2.50	48.19±1.79	46.75±1.70
AP amplitude (mV)	29.89±3.45	30.25±5.99	82.33±5.63	85.83±2.81	95.27±1.53	94.43±2.94	99.60±1.51	99.44±2.09
AP area (mV.ms)	79.07±4.15	75.44±6.68	82.80±1.72	84.50±7.36	91.87±2.91	85.47±3.84	89.89±2.79	89.60±2.20
Half-width (ms)	3.38±0.51	3.35±0.69	0.84±0.06	0.79±0.06	0.84±0.04	0.79±0.05	0.78±0.03	0.78±0.03
C_m (pF)	21.30±0.78	19.96±1.18	43.30±4.27	42.72±8.65	55.53±3.24	49.96±3.22	66.92±3.52	73.23±3.68
R_{in} (GΩ)	2.40±0.17	2.35±0.18	0.79±0.14	0.97±0.16	0.39±0.03	0.36±0.03	0.29±0.03	0.25±0.03
RMP (mV)	-37.74±1.98	-36.25±4.08	-58.84±4.26	-57.50±3.04	-67.64±1.13	-69.21±1.53	-68.45±1.58	-73.18±1.84

AP: Action potential; C_m: Membrane capacitance; R_{in}: Input resistance; RMP: resting membrane potential. Statistical significances are represented in the respective figures.

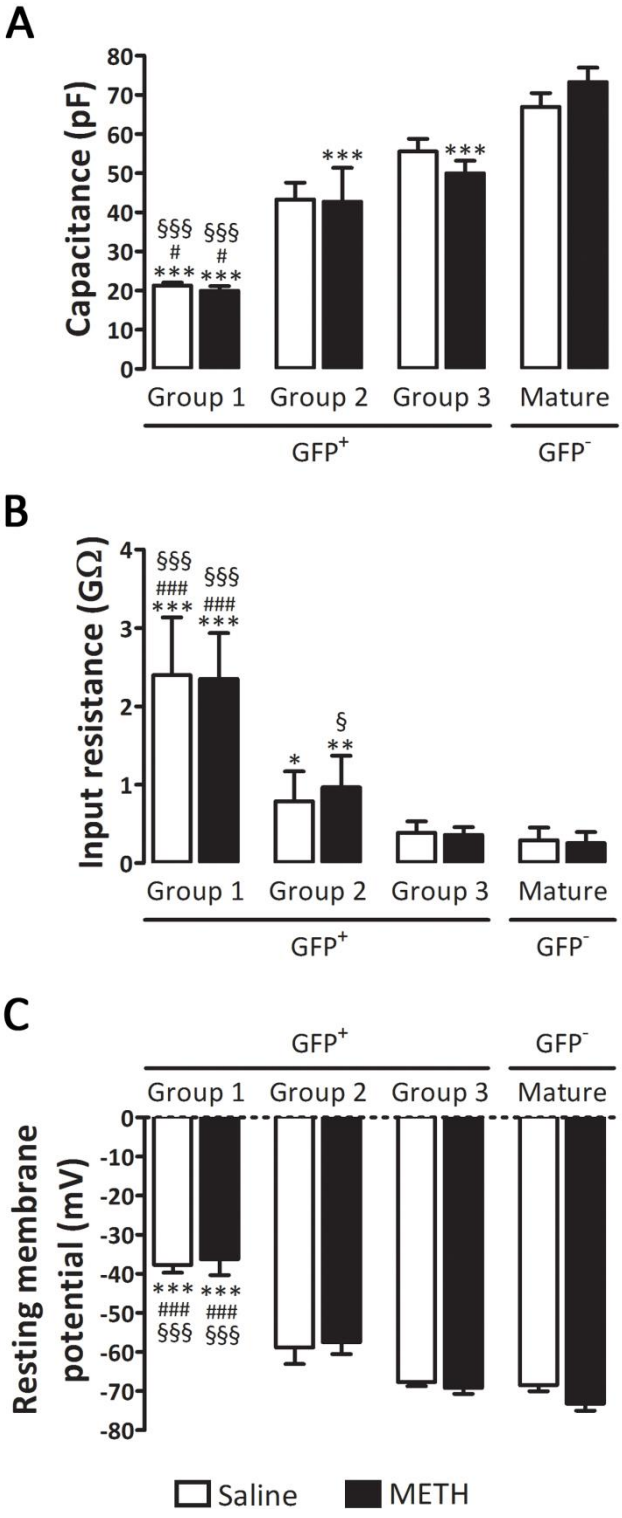

Figure 4.10 – METH does not change passive membrane properties in GFP$^+$ and mature cells. Data are expressed as mean + SEM (n = 3 – 14). *P < 0.05, **P < 0.01 and ***P < 0.001, significantly different from mature cells of the correspondent group using Bonferroni's multiple comparison post-hoc test. $^{\#}P$ < 0.05, and $^{\#\#\#}P$ < 0.001 significantly different from group 2 GFP$^+$ cells using Bonferroni's multiple comparison post-hoc test. $^{\S\S\S}P$ < 0.001, significantly different from group 3 GFP$^+$ cells using Bonferroni's multiple comparison post-hoc test.

4.4.4. Methamphetamine induces LTP in group 3 GFP^+ cells and strengthens LTP in mature neurons

Although some studies have pointed that METH induces cognitive deficits (Simon et al., 2000; Thompson et al., 2004), other showed that METH can improve memory performance (Cao et al., 2013; Silber et al., 2006). Also, learning and memory could be related to changes in synaptic strength in the hippocampus (Morris et al., 1986; Green et al., 1990) and integration of immature neurons into preexistent DG circuitries has been indicated to participate in memory processes (Kee et al., 2007; Garthe et al., 2009), and, immature neurons exhibit enhanced synaptic plasticity, depending on the developmental stage (Ge et al., 2007a). We therefore aimed to clarify if chronic treatment with METH affects synaptic plasticity of both immature and mature DG neurons. For that, evoked EPSCs were recorded from GFP^+ (groups 1, 2 and 3) and GFP^- (mature) cells, and LTP was induced by TBS paradigm. MPP stimulation failed to induce EPSCs in group 1 GFP^+ cells. In contrast, both group 2 (Figure 4.12) and group 3 GFP^+ (Figure 4.13) cells displayed reliable EPSCs following MPP stimulation. Given the paucity of responses of group 1 cells, we focused our analysis of synaptic plasticity onto DG neurons belonging to GFP^+ neurons of group 2 and 3, and GFP^- mature granule cells.

MPP stimulation was identified according to the paired-pulse ratio (PPR) and EPSC amplitude after wash in with the selective $mGlu_2$ receptor agonist, DCG-IV. Indeed, it has been previously reported that MPP and LPP show paired-pulse depression and facilitation, respectively (Colino and Malenka 1993). Moreover, MPP, but not LPP, presynaptic terminals express $mGlu_2$ receptors (Macek et al., 1996; Chiu and Castillo, 2008; Shigemoto et al., 1997). MPP characterization was performed regularly and figure 4.11 represents a mature neuron from a saline-treated mouse showing lack of paired-pulse facilitation both in baseline and after TBS (Figure 4.11 A). DCG-IV strongly and abruptly decreased EPSC amplitude (Figure 4.11 B), shifting PPR towards facilitation, consistent with a presynaptic effect of the drug.

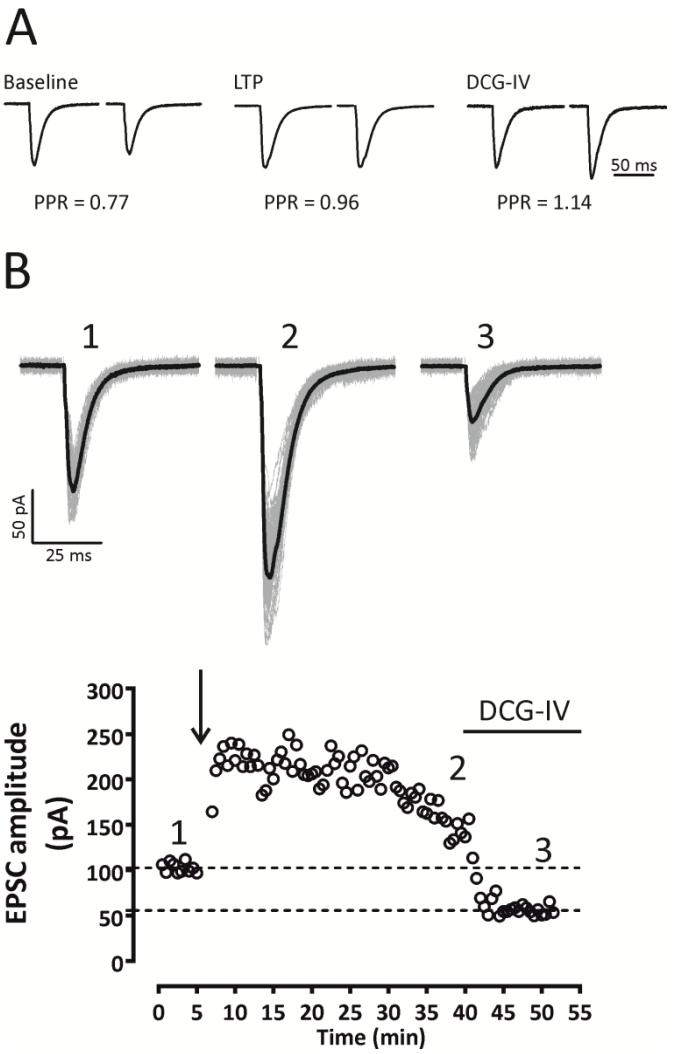

Figure 4.11 – Characterization of MPP stimulation. Bipolar electrodes were placed in the middle molecular layer to stimulate MPP fiber terminals from the medial EC. (A) Normalized EPSCs from paired-pulse responses after MPP stimulation in baseline, 25-30 min after TBS and after DCG-IV (1 µM) perfusion. (B) Representative time-course EPSCs in (1) baseline, (2) after LTP induction and (3) after DCG-IV perfusion of a mature neuron, from a saline-injected mouse.

GFP^+ DG neurons identified as group 2 represent a relatively small sample in both animal groups (Figure 4.8). At the time of writing the thesis, only few cells from saline- and METH-treated animals were stable enough to be recorded long-term (n = 3 cells from 3 mice *vs.* n = 6 cells from 6 mice, saline *vs.* METH). However, although these experiments are still ongoing, we noticed a trend of a higher LTP magnitude in METH-treated animals (Figure 4.12). Further experiments will be fundamental to reach a firm conclusion of METH-induced effects on synaptic plasticity in this immature cell population.

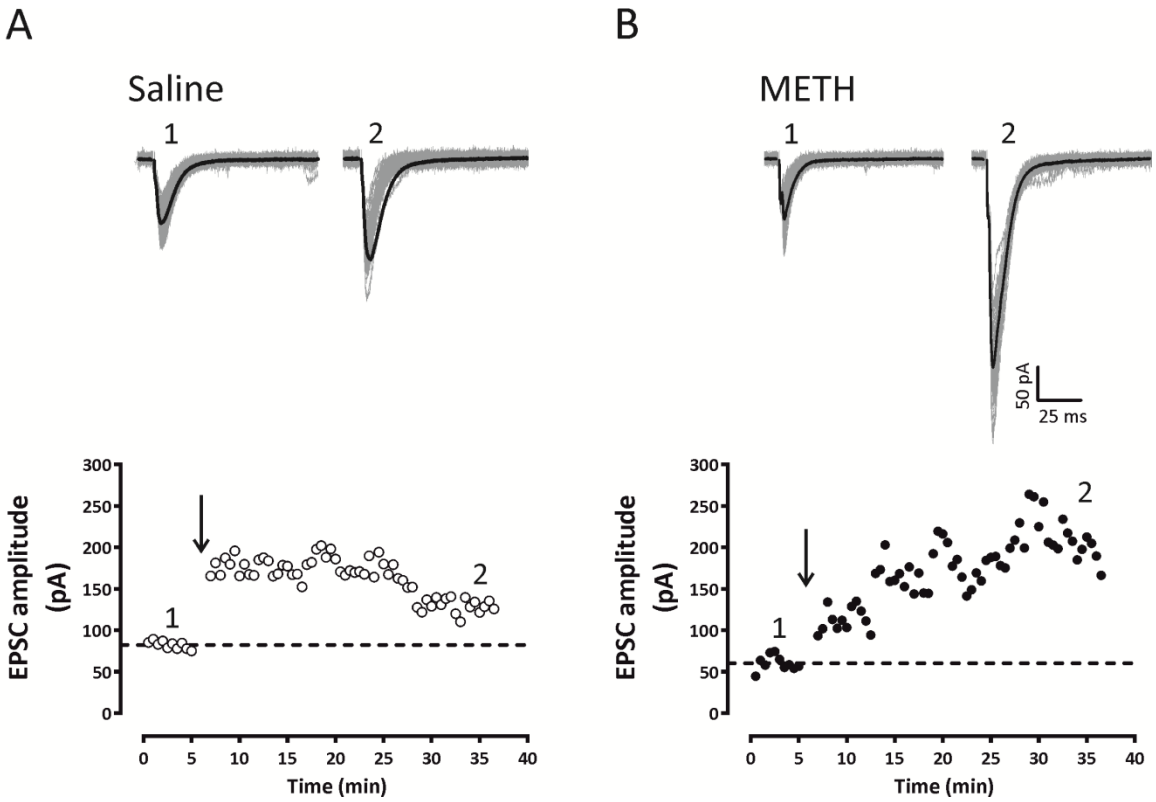

Figure 4.12 – Group 2 GFP$^+$ cells exhibit LTP. (A and B) Representative EPSCs traces (top) and time-course of evoked EPSCs from group 2 cells in (A) saline and (B) METH-injected mice (1) before and (2) after TBS stimulation.

Additionally, we found that group 3 cells from saline-treated animals exhibited a transient increase in EPSCs in response to TBS. This increase of synaptic strength could not be considered an LTP, as it was not sustained for longer than 10-15 min (EPSCs in baseline: 96.21 ± 11.39 pA; EPSCs in the last 5 min after TBS: 109.80 ± 17.25 pA, paired *t* test; Figure 4.13 A and C). Interestingly, however, METH increased the amplitude of EPSCs immediately after TBS (EPSCs in baseline: 64.80 ± 5.69 pA; EPSCs in the last 5 min after TBS: 105.20 ± 9.42 pA, $P < 0.001$, paired *t* test) and this potentiation lasted throughout the experiment, *i.e.*, METH treatment promoted the expression of LTP in group 3 GFP$^+$ cells by METH (Figure 4.13 B and C). LTP magnitude was assessed by comparing post-TBS EPSCs in the last 5 min with EPSCs from baseline. No difference in synaptic strength was detected in neurons originating from saline-treated mice (EPSCs in baseline: 100.00 + 14.06%; EPSCs in the last 5 min after TBS: 123.40 + 12.75% of baseline). By contrast, a stronger LTP magnitude was found in group 3 neurons recorded from METH-treated animals (EPSCs in baseline: 100.00 + 12.04%; EPSCs in the last 5 min after TBS: 165.40 + 8.97% of baseline; $P < 0.01$; Figure 4.13 D).

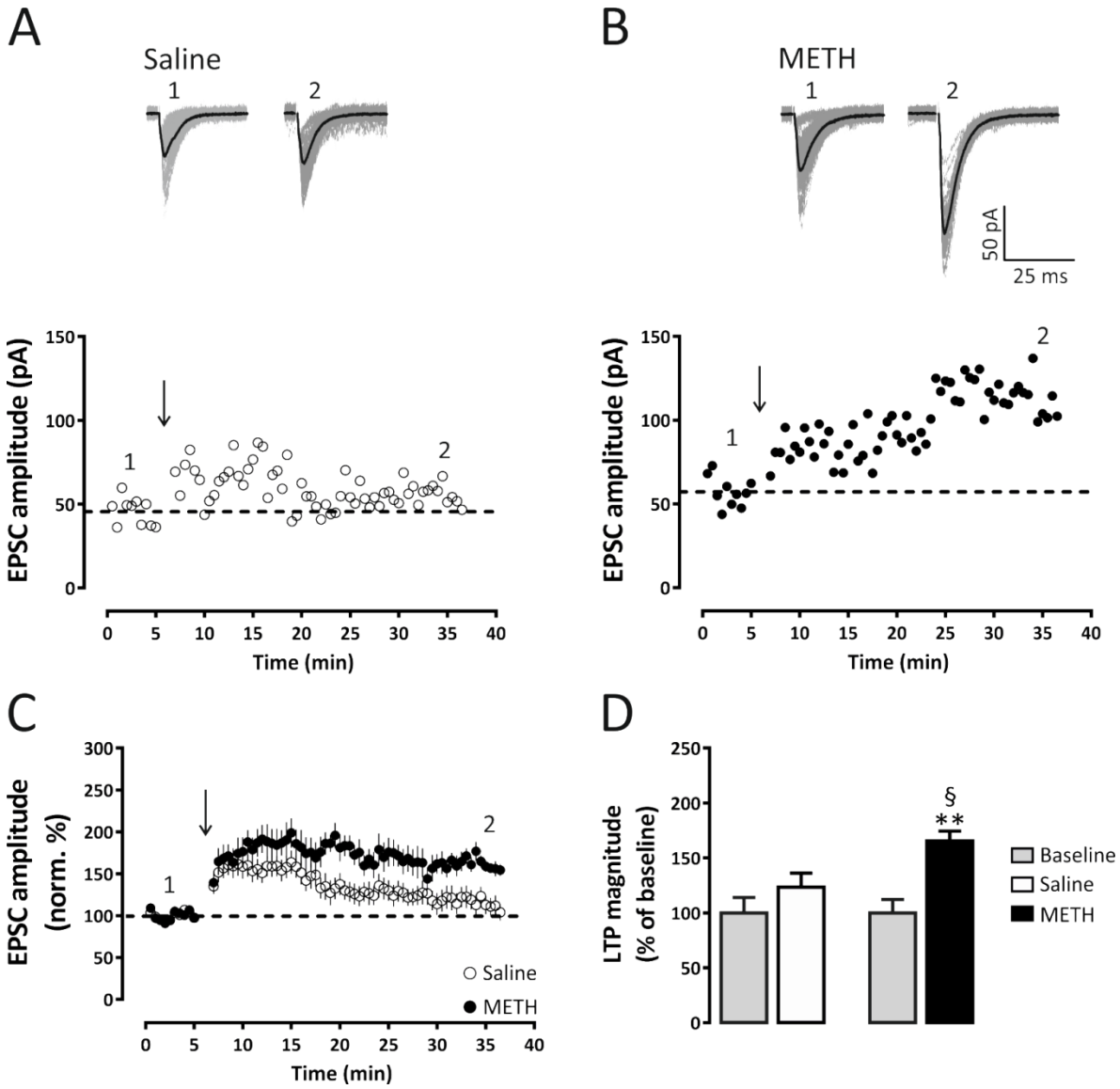

Figure 4.13 – METH induces LTP in group 3 GFP$^+$ cells. (A and B) Representative traces (top) of evoked EPSCs in (1) baseline and (2) after TBS, and time course of EPSCs (bottom) in (A) saline and (B) METH. (C) Average time-course of EPSCs from group 3 cells in saline and METH-injected mice (1) before and (2) after TBS stimulation. (D) LTP magnitude is higher in group 3 cells from mice injected with METH. Data are expressed as mean ± SEM from 13 cells in saline group and 7 cells from METH group. $^{**}P < 0.01$, significantly different from respective baseline using Mann Whitney post-hoc test. $^{§}P < 0.01$, significantly different from saline using Mann Whitney post-hoc test.

In GFP$^-$ mature neurons, TBS application increased EPSC amplitude in both saline (EPSCs in baseline: 138.90 ± 18.44 pA; EPSCs in the last 5 min after TBS: 191.10 ± 28.50 pA, $P < 0.05$, paired *t* test; Figure 4.14 A) and METH group (EPSCs in baseline: 128.20 ± 15.75 pA; EPSCs in the last 5 min after TBS: 234.90 ± 23.35 pA, $P < 0.001$, paired *t* test; Figure 4.14 B). Remarkably, however, METH induced a significantly stronger LTP (EPSCs in baseline: 100.00 + 6.62%; EPSCs in

the last 5 min after TBS: 193.60 + 14.69% of baseline; Figure 4.14 C) in comparison to saline group (EPSCs in baseline: 100.00 + 16.82%; EPSCs in the last 5 min after TBS: 142.40 + 13.66% of baseline; $P < 0.001$; Figure 4.14 D).

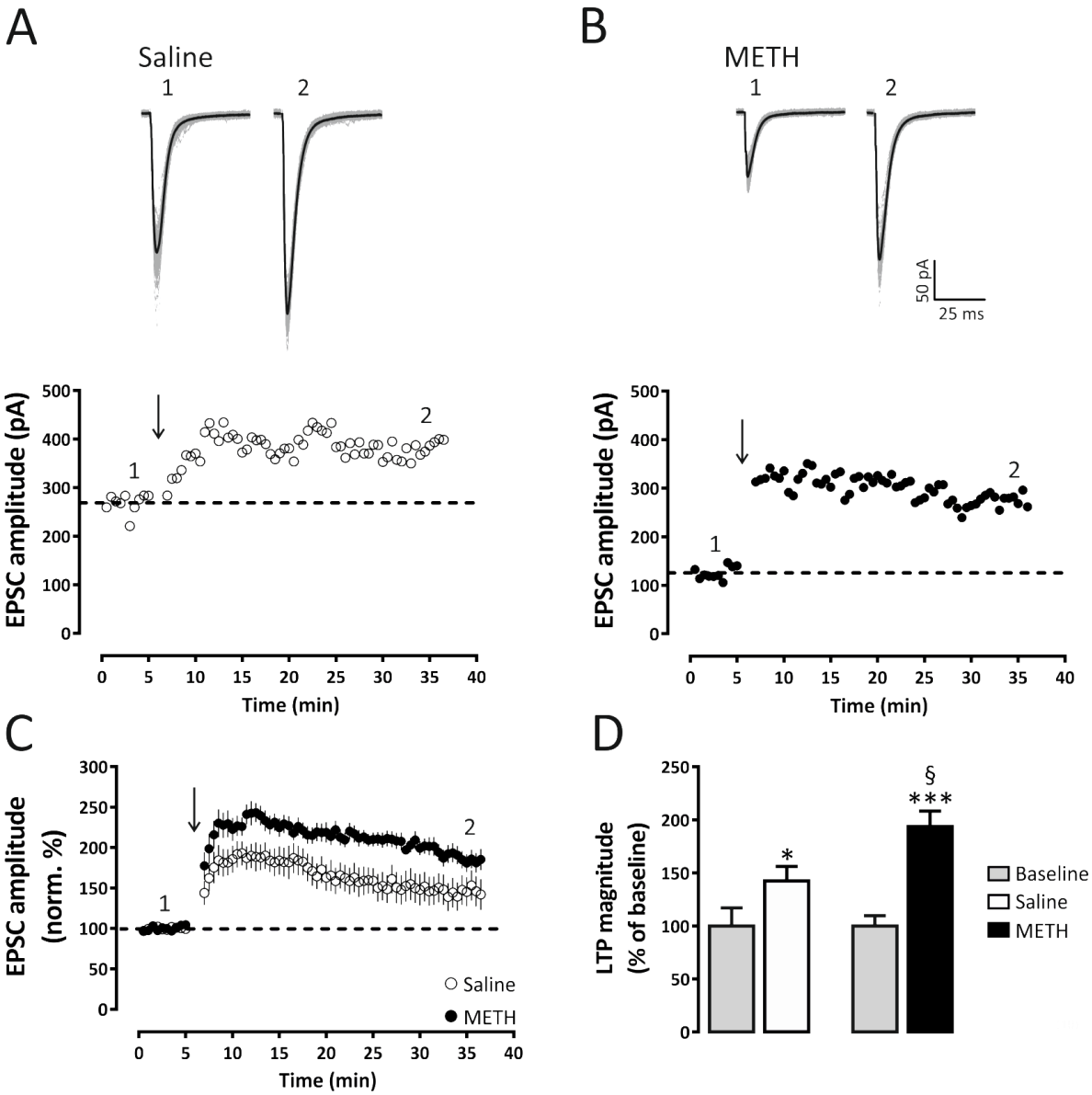

Figure 4.14 – METH increases LTP in DG mature cells. (A and B) Representative traces (top) of evoked EPSCs in (1) baseline and (2) after TBS, and time course of EPSCs (bottom) in (A) saline and (B) METH. (C) Average time-course of EPSCs from mature cells in saline and METH-injected mice (1) before and (2) after TBS stimulation. (D) LTP magnitude obtained between 25 and 30 min after TBS is higher in mature cells from mice injected with METH. Data are expressed as mean ± SEM from 12 cells in saline group and 10 cells from METH group. *$P < 0.05$ and ***$P < 0.001$, significantly different from respective baseline using Mann Whitney post-hoc test. $^{§}P < 0.05$, significantly different from saline using Mann Whitney post-hoc test.

Overall, GFP$^+$ cells responded differently to extracellular stimulation of the MPP as well as after the application of TBS. In detail, group 1 GFP$^+$ cells did not display at all, or displayed very small and unreliable evoked EPSCs, whereas group 2 cells exhibited evoked EPSCs and LTP (Figure 4.12). Group 3 GFP$^+$ cells exhibited only medium-term potentiation in saline group, but not LTP (Figures 4.13 and 4.15). Remarkably, METH treatment induced a large and sustained LTP in this cell group. Regarding mature DGCs, METH generated a larger LTP than in saline-treated mice (Figures 4.14 and 4.15). Figure 4.15 summarizes LTP magnitude in both group 3 GFP$^+$ cells and mature DGCs.

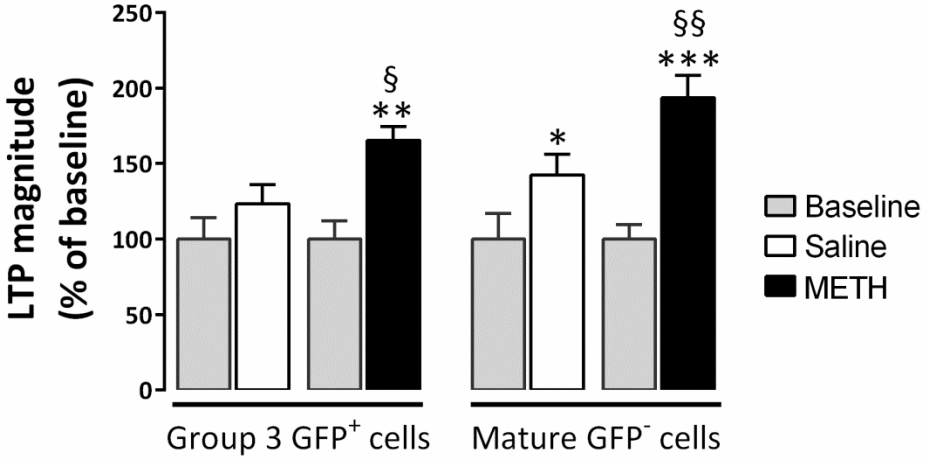

Figure 4.15 – METH induces LTP in GFP$^+$ (group 3) and increases LTP strength GFP$^-$ (mature) cells. Bar graph representing EPSCs and/or LTP magnitude in group 3 and mature cells. Data are expressed as mean % of baseline + SEM. *P < 0.05, **P < 0.01 and ***P < 0.001, significantly different from respective baseline using Mann Whitney post-hoc test. $^{§}P$ < 0.05 and $^{§§}P$ < 0.01, significantly different from respective saline.

4.5. Discussion

In the present study we found that chronic administration of METH (2 mg/kg, once a day for 7 days, i.p.) to G42 mice enhanced the differentiation of immature DGCs, without changing the number of GFP$^+$ cells. This enhanced differentiation was paralleled by increased synaptic plasticity in group 3 GFP$^+$ cells and mature neurons (GFP$^-$ cells). Chronic METH administration neither modified firing nor passive membrane properties in all groups of cells.

The G42 or GAD67-GFP mouse line has been considered to be a useful tool to study fast-spiking PV-positive interneurons mainly in the neocortex (Chattopadhyaya et al., 2004). Interestingly, GFP$^+$ cells in the DG of the mouse hippocampus are immature DGCs and not PV interneurons, as DGCs transiently express a GABAergic phenotype during their development

towards a more mature stage (Cabezas et al., 2012, 2013). These GFP^+ cells exhibit the typical profile of immature neurons presenting only one or few overshooting APs (Figure 4.6; Cabezas et al., 2012). Moreover, GFP^+ cells in the DG are restricted to Prox1, a marker of granule cells, at all postnatal ages (P1-P180) as well as DCX (a protein expressed in immature neurons) and/or the neuronal marker NeuN at P20-P30 mice (Cabezas et al., 2013). Also, these cells express calretinin that is transiently expressed in immature neurons, but not calbindin, confirming their immature neuronal identity (Cabezas et al., 2013). Therefore, the GAD67-GFP mouse line can be also used as a good model to study hippocampal neurogenesis. So, taking advantage of these mice characteristics, we observed that the population of GFP^+ cells expressing NeuN was more prevalent than those that expressed only DCX. GFP^+ cells that express both DCX and NeuN are fewer when compared to the other two populations, exclusively $NeuN^+$ or DCX^+ DG granule cells (≈20% less than DCX-expressing and 40-50% less than NeuN-expressing GFP^+ cells). Nonetheless, this represents an interesting population with a short-term transitory phenotype. Interestingly, 7-day treatment of METH decreased the population of GFP^+ cells that presented the most immature phenotype (DCX), and increased the number of NeuN-expressing GFP cells (Figure 4.5). Indeed, these results lead us to conclude that METH enhances differentiation of these specific immature neurons since it did not change the total number of GFP^+ cells. Mandyam and collaborators (2008) related a human recreational pattern of METH use with a self-administration protocol in rats (0.05 mg/kg/infusion METH, twice a week for 28 days) and observed that differentiation of proliferating cells was enhanced. We suggest that the administration protocol used in the present work may be similar to what is considered recreational drug intake.

In the present work, GFP^+ cells exhibited a range of firing patterns characteristic of immature neurons, indicating at least three different maturational stages: Group 1 – GFP^+ cells that fire a single AP; Group 2 – GFP^+ cells that fired few spikes, but cannot sustain repetitive firing of fully-blown APs; and Group 3 – GFP^+ cells that fired APs repeatedly, thus resembling mature GFP^- DGCs. Importantly, AP properties also differ among the 3 groups such as a progressive increase in AP peak and AP amplitude from group 1 to group 3 GFP^+ cells, without changing, however, AP area. Additionally, group 1 cells presented lower C_m and higher R_{in} that increased and decreased, respectively, upon maturation of these cells. Also, these cells presented significantly more depolarized RMP than groups 2 and 3 GFP^+ cells, and mature neurons. Interestingly, we further observed that group 1 GFP^+ cells failed to present postsynaptic responses upon extracellular stimulation, which we considered as silent neurons.

Moreover, group 3 GFP^+ cells present similar AP kinetics and passive membrane properties as of mature GFP^- DGCs. Our data is in line with other studies that characterized functionally newborn DGCs using both retroviral-mediated expression of GFP (Espósito et al., 2005; Mongiat et al., 2009; Vivar et al., 2012; Zhao et al., 2006) or transgenic mouse lines (Overstreet-Wadiche et al., 2006; Spampanato et al., 2012). Specifically, Mongiat and collaborators (2009) revealed that 19 day-old immature DGCs upon depolarizing steps generate a single AP, present lower C_m and have more depolarized membrane potentials than older neurons. Interestingly, these neurons presented short dendrites and few dendritic branches, and displayed none or relatively modest evoked excitatory currents. This lead us to predict that cells belonging to group 1 are younger than 19 days, but older than 15 days since GFP begins to be expressed in 2 week-old neurons (Cabezas et al., 2013). Regarding group 2 GFP^+ cells, we believe that they are around the third week of development as they show comparable AP firing and R_{in} with 22 day-old neurons (Mongiat et al., 2009). Accordingly, their dendrites are more complex than group 1 cells (Figure 4.7 B; Zhao et al., 2006) and they show reliable stimulations in response to MPP stimulation (Figure 4.12; Mongiat et al., 2009). Group 3 GFP^+ cells present a mature-like AP firing (Figure 4.6) and longer dendrites (Figure 4.7 C) that, compared to retroviral-mediated labeling of immature neurons, resemble 28 day-old neurons (Zhao et al., 2006; Mongiat et al., 2009). Little is known about the effect of METH on the intrinsic properties of immature and mature DGCs, and herein we showed that METH does not interfere with AP kinetics or passive membrane properties, leading us to conclude that METH accelerates differentiation of GFP^+ cells (Figure 4.5) without changing, however, their intrinsic functional properties (Figure 4.8 and 4.9; Table 1).

It has been well characterized that DGCs exhibit LTP or synaptic strength in response to trains of presynaptic stimulation (Bliss and Lømo, 1973). Importantly, this enhancement of synaptic responses is currently considered to be the cellular substrate for learning and memory (Morris et al., 1986; Green et al., 1990). To date, no information is available regarding the effect of METH on synaptic plasticity of immature neurons, although it has been shown that chronic exposure to METH (5 mg/kg, i.p) can decrease LTP in CA1 pyramidal cells (Hori et al., 2010). The same effect of decreased LTP in CA1 cells was observed after administration with a higher dose of METH (10 mg/kg, twice a day for 5 days, i.p.; Swant et al., 2010). Intriguingly, a higher dose of METH (24 mg/kg, i.p.) for 14 days did not induce any effect in LTP of CA1 cells, but there was a decrease after 21 days of drug abstinence, which was associated with poorer spatial memory performance (North et al., 2013).

Little is known about the effect of psychostimulants on synaptic plasticity of the DG. Interestingly, offspring rats exposed to nicotine from embryonic day 3 until weaning showed

increased LTP in the DG, without changes of cell proliferation or survival of proliferating cells (Mahar et al., 2012). Importantly, neurogenesis plays an active role in memory processes as immature neurons are recruited to integrate circuits responsible for memory formation (Kee et al., 2007). Likewise, ablation of neurogenesis induces significant cognitive deficits (Garthe et al., 2009). Integration of newborn neurons into existent neuronal circuitries is accomplished following newborn DG granule neurons' dendritic and axonal elongation towards the molecular layer and the hilus, respectively (Zhao et al., 2006; Toni et al., 2008). As a result, dendritic and axonal development allow immature neurons to form synaptic connections, receiving inputs from the EC (Mongiat et al., 2009) and send outputs to CA3 pyramidal, interneurons or mossy cells, respectively (Toni et al., 2008). In the present study we observed that cells belonging to group 2 and group 3 DGCs receive excitatory inputs from MPP fibers generating EPSCs (Figure 4.12 and 4.13). Moreover, group 2 (Figure 4.12) and group 3 (Figure 4.13) GFP^+ cells as well as mature neurons (Figure 4.14) were able to undergo LTP in response to TBS at MPP fibers. Nevertheless, one disadvantage of using G42 mice in synaptic plasticity studies is that group 2 and group 3 GFP^+ cells are difficult to be distinguished solely based on their fluorescence, as they share the same localization within the granule cell layer, in contrast to group 1 cells, which are easily identified by their small soma and specific localization in the inner granule cell layer, adjacent to the hilus. Moreover, group 2 GFP^+ cells are less common than group 3 neurons, thus the probability to patch a group 2 cell is much smaller. Therefore, we cannot provide any conclusion on this group due to its low sampling. This study will be completed in the next following months.

Importantly, we found that group 3 GFP^+ cells from saline-injected mice, exhibited a transient (10-15 min) potentiation of synaptic transmission in response to TBS (Figure 4.13). Interestingly, METH treatment switched this transient form of plasticity into a fully-blown LTP. In addition, we observed that LTP of glutamatergic synapses onto mature (GFP^-) DGCs was strongly enhanced by METH exposure (Figures 4.14 and 4.15). Although we cannot provide a mechanism for this METH-induced enhancement of synaptic plasticity, but it has been recently shown by Padgett and collaborators (2012) that a single dose of METH (2 mg/kg, i.p.) decreased $GABA_B$ mediated activation of G protein-gated inwardly rectifying potassium channels (GIRK) in GABAergic neurons in the ventral tegmental area, both at 24 h and 7 days after METH administration. According to the authors this decrease was a result of a METH-induced internalization of $GABA_B$ receptor-GIRK complex (Padgett et al., 2012). In fact, $GABA_B$ receptors are present in DGCs dendrites where they control cell excitability (Scanziani, 2000). Therefore, we can hypothesize that group 3 GFP^+ cells LTP at MPP pathway may be inhibited in normal

conditions by $GABA_B$ receptor activation. METH probably reduced $GABA_B$ receptor-mediated currents, resulting in enhanced LTP expression. Likewise, METH induced stronger LTP in mature, or GFP^- cells, which may also involve a similar mechanism of action. Another possible mechanism underlying the enhanced LTP after METH treatment could be a differential expression of specific subunits of NMDA receptors. Indeed, it was shown that the same dose of METH used here (2 mg/kg, i.p), but administered for 14 days, increased hippocampal GluN2 protein levels, a subunit of NMDA receptors required for LTP (Yamamoto et al., 2006). Also, proteins important for NMDA receptor transport in dendrites, like kinesin family member 17 (Setou et al., 2000), are up-regulated in the hippocampus after chronic exposure to METH (2 mg/kg for 14 days), suggesting that METH enhances integration of NMDA receptors in dendritic membranes (Yamamoto et al., 2006). Finally, Ge and collaborators (2007a) demonstrated that GluN2B subunits are required for enhanced synaptic plasticity in 1 month-old immature neurons. It is therefore possible that GluN2B subunits may be less expressed in NMDA receptors at synapses of group 3 GFP^+ cells. Further experiments are required to prove the role of $GABA_B$ and/or NMDA receptors in favoring and strengthening synaptic plasticity in group 3 and mature DGCs.

LTP is the current cellular mechanism proposed to underlie learning and memory. Accordingly, moving Fischer rats from their home cages to different environments produced an increase of exploratory behavior that resulted in an increase of field EPSP in the DG, which suggests a link between enhanced synaptic plasticity with acquisition of new memories (Green et al., 1990). Previously, Morris and co-workers (1986) showed that NMDA receptors are crucial for DG LTP and for hippocampal-dependent place learning, suggesting that LTP induction is important for memory performance. Along with these lines (Morris et al., 1986; Green et al., 1990) it is tempting to speculate that the enhanced LTP following METH administration will result in improved memory learning. Hippocampal-dependent memory experiments, such as Morris water maze, should be addressed to confirm this hypothesis directly. Accordingly, mice injected once with 1 mg/kg METH exhibited an improvement in memory consolidation (Cao et al., 2013). Similarly, 0.42 mg/kg METH given in two sessions, 2 weeks apart, to human volunteers showed improved psychomotor ability (Silber et al., 2006).

In conclusion, the present work shows that chronic administration with a low dose of METH favored differentiation of immature neurons and enhanced LTP in group 3 GFP^+ immature neurons. Also, METH increased LTP amplitude in mature DGCs. Although METH produces a “positive” effect on neurogenesis and synaptic plasticity, this drug is highly addictive and it alters hippocampal homeostasis, likely converting these “positive” effects into malign and dysfunctional effects to cognitive performance.

Chapter 5

General discussion

5. General discussion

With the present thesis we aimed at studying neurogenesis in the DG as resident stem cells generate new neurons that are recruited to integrate the preexistent circuitries contributing to cognition (Kee et al., 2007; Garthe et al., 2009). Moreover, it is well known that METH enhances or impairs memory performance according to the amount and frequency of exposure (Cao et al., 2013; Ito et al., 2007). Thus, we investigated the effect of METH on different stages of neuronal development along the neural stem cell lineage: stem cells, differentiating cells and immature and mature DGCs.

Our major findings show that METH can induce DG stem cell death depending on the concentration. Importantly, even a single nontoxic concentration of METH was able to decrease DG stem cell self-renewal capacities and the number of mature neurons. Additionally, a chronic exposure to a low dose of METH accelerated the differentiation of immature neurons as well as enhanced LTP. Furthermore, NPY revealed to be a promising therapeutic tool against the negative impact of METH on hippocampal neurogenesis.

In chapter 2, we suggest the involvement of MAPK pathway, a well-known mediator in cell proliferation (Heo et al., 2006), on DG self-renewal impairment induced by METH. Overall, we found that METH reduced the activity of EGFR, confirmed by the down-regulation of the phosphorylation levels of this receptor, and also decreased pERK1/2 levels. Furthermore, METH induced alterations in downstream targets such as mediators of the cell cycle. In fact, we verified that METH delayed the transition from G0/G1 to the S phase and increased the number of cells in the quiescence state. This effect was confirmed by the down-regulation of cyclin E, a protein involved in the progression through G1 phase and initiation of DNA replication, and thereby limiting the progression of the cell cycle. On the other hand, METH did not induce any effect in p21 or p27, which confirms that METH selectively targets the MAPK pathway. In fact, the only evidence available that studies the effect of METH on cell cycle showed that self-administration of this drug may arrest cell cycle of DG proliferating cells in the G1 phase (Yuan et al., 2011). As METH was able to decrease self-renewal, we further explored its influence in DG stem cell-fate division. Indeed, through characterization of the phenotype of cells that derived from the division of one stem cell, we verified that METH decreased self-renewal symmetric cell division while increased pairs of cells that are committed to differentiate. This last effect resulted from the activation of NMDA receptors. In general, these receptors negatively regulate neurogenesis by reducing proliferation (Cameron et al., 1995; Nacher et al., 2003), but activation of these receptors in radial glia-like cells enhances the expression of NeuroD, a downstream regulator of neuronal differentiation, and consequently increases neurogenesis (Deisseroth et al., 2004). In

fact, we predict that METH activated NMDA receptors that triggered differentiation of DG stem cells. Accordingly, we revealed that METH increased DCX expression in DG neurospheres, an effect that correlates with data from cell-fate division. In fact, Mandyam and collaborators (2008) verified an increase of DCX^+ neurons in rat DG after self-administration with METH that mimics the recreational pattern of human use. In summary, METH interferes with DG stem cell proliferation due to a delay in cell progression (G0/G1-to-S phase), which involves the down-regulation of pEGFR, pERK1/2 and cyclin E. In addition, METH impairs DG cell division towards self-renewal *via* NMDA receptor signaling thereby promoting neuronal differentiation (Figure 5.1).

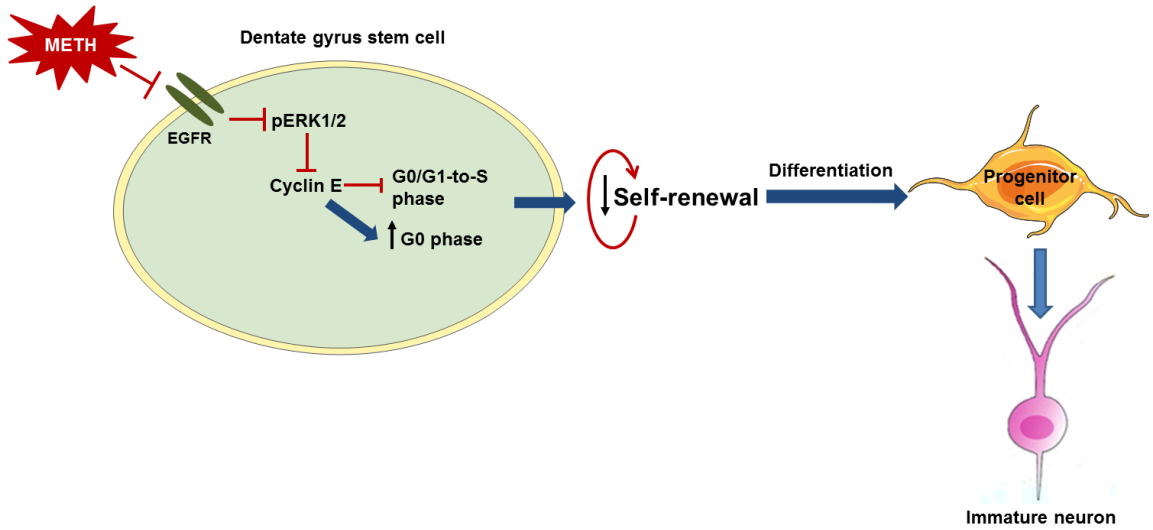

Figure 5.1 – Schematic representation of the effect of METH in DG stem cell properties. METH down-regulates the phosphorylation levels of EGFR and ERK1/2, compromising DG cell proliferation as observed by down-regulation of cyclin E levels. As a result, METH increases the population of quiescent cells and delays the transition from G0/G1 to S phase of the cell cycle. These effects may result in the decrease of DG stem cell self-renewal under METH exposure. The impairment of self-renewal can lead DG stem cells to differentiate as observed by the cell fate division towards differentiation and the increase of DCX expression in neurospheres.

In chapter 3, the toxic effect of METH in DG-derived neurosphere cultures was investigated, and we demonstrated that the glutamatergic system is involved in this effect. Indeed, METH increased glutamate release in these cultures that in turn activated NMDA receptors, resulting in an increased cell death. Moreover, we observed that METH did not have any effect on cell proliferation, but decreased the number of mature neurons in these cultures, even at a nontoxic concentration. Interestingly, we described above that METH decreased self-renewal and triggered neuronal differentiation by increasing immature neurons in DG

neurospheres. Here, on the other hand, we observed that METH decreased the number of mature neurons, so we can deduce that METH may also compromise neuronal survival. In fact, DG-derived neurosphere cultures were devoid of EGF and bFGF-2 in contrast to self-renewal studies where EGF and FGF were present at low concentration and thereby conferring survival to these cells. So, we may predict that neurons from DG-derived neurosphere cultures hardly survived against METH due to low paracrine-/autocrine-induced protection. Afterwards, we aimed to identify a possible therapeutic target against the noxious effects induced by METH. We chose NPY based on previous facts that stated a protective role for NPY against excitotoxicity (Silva et al., 2003a) and METH insults (Thiriet et al., 2005; Gonçalves et al., 2012). Herein, NPY protected DG cells from the toxicity induced by METH by preventing the increased glutamate release and thereby apoptotic events, as well as by preventing the decrease of mature neurons. Besides, NPY increased cell proliferation and neuronal differentiation *via* Y_1 receptors, which corroborated with previous findings in the SGZ (Howell et al., 2003, 2005; Decressac et al., 2011) and SVZ (Agasse et al., 2008; Decressac et al., 2009). With these results, we can also hypothesize that NPY could prevent the effects of METH on self-renewal as well, specifically by preventing the down-regulation of pERK1/2 as it was verified by others that NPY increases phosphorylation of ERK1/2 (Cheung et al., 2012; Howell et al., 2005). In conclusion, NPY revealed to be a promising factor in protecting DG cells against the harmful effect induced by METH.

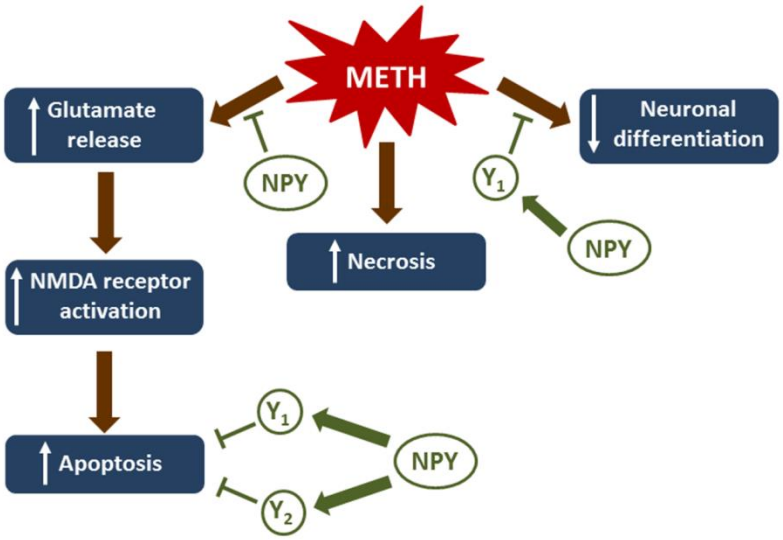

Figure 5.2 – Schematic representation of METH-induced toxicity in DG-derived neurosphere cultures. METH increases glutamate release that in turn will overactivate NMDA receptors leading to apoptosis. In contrast, NPY prevents METH-induced glutamate release and METH-induced apoptosis *via* activation of Y_1 or Y_2 receptors. Also, METH triggers cell death by necrosis. The number of mature neurons is reduced by METH and NPY is able to counteract this effect through Y_1 receptors.

After revealing that METH affects DG cell self-renewal and survival of mature neurons, we asked if METH could affect the development on immature neurons, specifically looking to their neurogenic and functional properties (Chapter 4). Our major findings show that METH (2 mg/kg, once a day for 7 days) accelerated maturation of newborn neurons as well as enhanced LTP. Indeed, we verify that chronic administration of METH decreased the number of GFP^+ cells that co-express DCX while it increased those that co-expressed NeuN, though accelerating differentiation of GFP^+ neurons (Figure 5.3). Indeed, we were able to confirm that METH triggered differentiation of these cells as it did not alter the density of GFP^+ cells and was not toxic to these immature neurons. These results go in line with our previous data where we show that stem cells from DG neurospheres exposed to METH underwent differentiation. We can conclude that a nontoxic concentration or dose of METH promotes differentiation of stem cells or immature neurons, respectively. Other major finding in the present work was that METH induces LTP in group 3 GFP^+ cells in contrast to the medium-term potentiation found in saline-injected mice (Figure 5.3). To explain these observations we suggest that METH may induce GluN2 subunit expression alterations in NMDA receptors as they are required for LTP. In fact, the same dose of METH was able to increase GluN2 protein levels in the hippocampus (Yamamoto et al., 2006), and GluN2B was shown to mediate enhanced synaptic plasticity in 1 month-old immature neurons (Ge et al., 2007a). As a result, we suggest that group 3 GFP^+ cells may have less GluN2B expression in NMDA receptors and METH may increase it. Another mechanism that may be involved in METH-induced LTP is the inhibition of $GABA_B$ receptors as their main function is to regulate neuronal excitability, and METH at the same dose decreased currents mediated by this receptor in the ventral tegmental area (Padgett et al., 2012). In contrast to what were observed in group 3 cells, mature DGCs were able to sustain LTP and METH increased the strength in synaptic plasticity (Figure 5.3). In summary, the enhanced maturation of immature neurons and generation of LTP strength suggest that the METH regiment used in the present work may improve memory performance. Indeed, it has been demonstrated in both humans (Silber et al., 2006) and rodents (Cao et al., 2013) that METH can improve cognitive deficits (Figure 5.3).

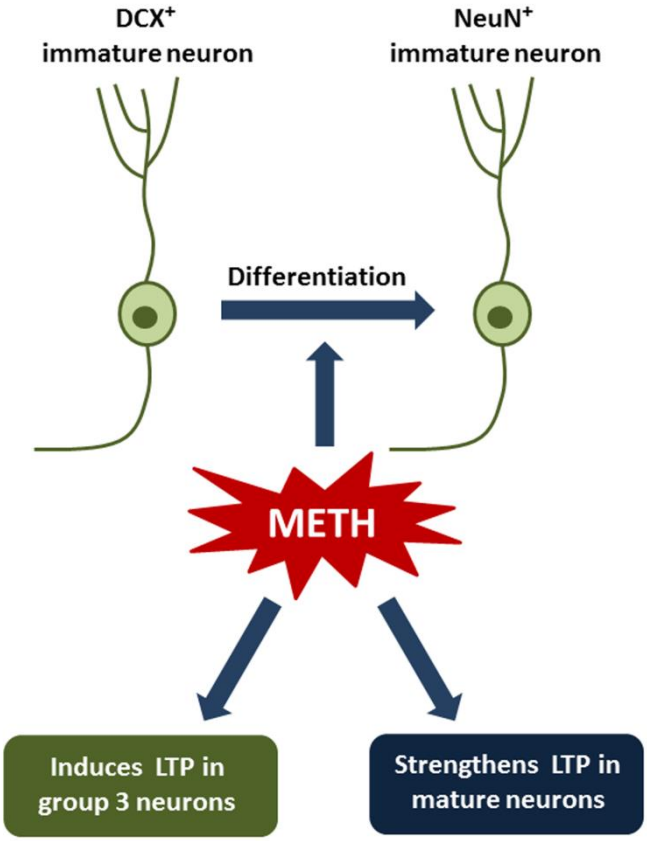

Figure 5.3 – Schematic representation of the effect of a chronic administration of METH in DG neurogenesis of G42 mice. METH accelerates differentiation of immature DG neurons. Moreover, METH induces and strengths LTP in group 3 GFP^+ cells and mature neurons, respectively.

In conclusion, with the present thesis it is possible to conclude that METH is able to decrease DG stem cell self-renewal, to promote neuronal differentiation and to enhance LTP in immature DGCs. Additionally, NPY seems to be a promising therapeutic tool under conditions of METH neurotoxicity.

Chapter 6

References

Abrous DN, Adriani W, Montaron MF, Aurousseau C, Rougon G, Le Moal M, Piazza PV (2002). Nicotine self-administration impairs hippocampal plasticity. J. Neurosci. 22: 3656–3662.

Agasse F, Bernardino L, Kristiansen H, Christiansen SH, Ferreira R, Silva B, Grade S, Woldbye DP, Malva JO (2008). Neuropeptide Y promotes neurogenesis in murine subventricular zone. Stem Cells 26: 1636–1645.

Aizenman E, McCord MC, Saadi RA, Hartnett KA, He K (2010). Complex role of zinc in methamphetamine toxicity in vitro. Neuroscience 171: 31–39.

Albertson TE, Derlet RW, Van Hoozen BE (1999). Methamphetamine and the expanding complications of amphetamines. West J. Med. 170: 214–219. Review.

Allen J, Novotný J, Martin J, Heinrich G (1987). Molecular structure of mammalian neuropeptide Y: analysis by molecular cloning and computer-aided comparison with crystal structure of avian homologue. Proc. Natl. Acad. Sci. U. .S A. 84: 2532–2536.

Allen JM (1990). Molecular structure of neuropeptide Y. Ann. N. Y. Acad. Sci. 611: 86–98.

Álvaro AR, Rosmaninho-Salgado J, Ambrósio AF, Cavadas C (2009). Neuropeptide Y inhibits [Ca2+]i changes in rat retinal neurons through NPY Y1, Y4, and Y5 receptors. J. Neurochem. 109: 1508–1515.

Álvaro AR, Rosmaninho-Salgado J, Santiago AR, Martins J, Aveleira C, Santos PF, Pereira T, Gouveia D, Carvalho AL, Grouzmann E, Ambrósio AF, Cavadas C (2007). NPY in rat retina is present in neurons, in endothelial cells and also in microglial and Müller cells. Neurochem. Int. 50: 757–763.

Ammar DA, Eadie DM, Wong DJ, Ma YY, Kolakowski LF Jr, Yang-Feng TL, Thompson DA (1996). Characterization of the human type 2 neuropeptide Y receptor gene (NPY2R) and localization to the chromosome 4q region containing the type 1 neuropeptide Y receptor gene. Genomics 38: 392–398.

Arvidsson A, Kokaia Z, Lindvall O (2001). N-methyl-D-aspartate receptor-mediated increase of neurogenesis in adult rat dentate gyrus following stroke. Eur. J. Neurosci. 14: 10–18.

Ashton RS, Conway A, Pangarkar C, Bergen J, Lim KI, Shah P, Bissell M, Schaffer DV (2012). Astrocytes regulate adult hippocampal neurogenesis through ephrin-B signaling. Nat. Neurosci. 15: 1399–1406.

Azuma A, Huang P, Matsuda A, Plunkett W (2001). 2'-C-cyano-2'-deoxy-1-beta-D-arabino-pentofuranosylcytosine: a novel anticancer nucleoside analog that causes both DNA strand breaks and G(2) arrest. Mol. Pharmacol. 59: 725–731.

Babu H, Cheung G, Kettenmann H, Palmer TD, Kempermann G (2007). Enriched monolayer precursor cell cultures from micro-dissected adult mouse dentate gyrus yield functional granule cell-like neurons. PLoS One 2: e388.

Baker E, Hort YJ, Ball H, Sutherland GR, Shine J, Herzog H (1995). Assignment of the human neuropeptide Y gene to chromosome 7p15.1 by nonisotopic in situ hybridization. Genomics 26: 163–164.

Balasubramaniam A, Sheriff S, Rigel DF, Fischer JE (1990). Characterization of neuropeptide Y binding sites in rat cardiac ventricular membranes. Peptides 11: 545–550.

Balasubramaniam AA (1997). Neuropeptide Y family of hormones: receptor subtypes and antagonists. Peptides 18: 445–457. Review.

Baptista S (2009). The effect of methamphetamine on dentate gyrus neurogenesis: role of neuropeptide Y. Master thesis

Barria A, Malinow R (2005). NMDA receptor subunit composition controls synaptic plasticity by regulating binding to CaMKII. Neuron 48: 289–301.

Barros LF, Hermosilla T, Castro J (2001). Necrotic volume increase and the early physiology of necrosis. Comp. Biochem. Physiol. A Mol. Integr. Physiol. 130: 401–409.

Bayazitov IT, Richardson RJ, Fricke RG, Zakharenko SS (2007). Slow presynaptic and fast postsynaptic components of compound long-term potentiation. J. Neurosci. 27: 11510–11521.

Beaulieu JM, Gainetdinov RR (2011). The physiology, signaling, and pharmacology of dopamine receptors. Pharmacol. Rev. 63: 182–217. Review.

Benarroch EE (2009). Neuropeptide Y: its multiple effects in the CNS and potential clinical significance. Neurology 72: 1016–1020.

Bento AR, Baptista S, Malva JO, Silva AP, Agasse F (2011). Methamphetamine exerts toxic effects on subventricular zone stem/progenitor cells and inhibits neuronal differentiation. Rejuvenation Res. 14: 205–214.

Berglund MM, Lundell I, Eriksson H, Söll R, Beck-Sickinger AG, Larhammar D (2001). Studies of the human, rat, and guinea pig Y4 receptors using neuropeptide Y analogues and two distinct radioligands. Peptides 22: 351–356.

Berglund MM, Schober DA, Esterman MA, Gehlert DR (2003). Neuropeptide Y Y4 receptor homodimers dissociate upon agonist stimulation. J. Pharmacol. Exp. Ther. 307: 1120–1126.

Bernardino L, Agasse F, Silva B, Ferreira R, Grade S, Malva JO (2008). Tumor necrosis factor-alpha modulates survival, proliferation, and neuronal differentiation in neonatal subventricular zone cell cultures. Stem Cells 26: 2361–2371.

Bernardino L, Eiriz MF, Santos T, Xapelli S, Grade S, Rosa AI, Cortes L, Ferreira R, Bragança J, Agasse F, Ferreira L, Malva JO (2012). Histamine stimulates neurogenesis in the rodent subventricular zone. Stem Cells 30: 773–784.

Bernardino L, Xapelli S, Silva AP, Jakobsen B, Poulsen FR, Oliveira CR, Vezzani A, Malva JO, Zimmer J (2005). Modulator effects of interleukin-1beta and tumor necrosis factor-alpha on AMPA-induced excitotoxicity in mouse organotypic hippocampal slice cultures. J. Neurosci. 25: 6734–6744.

Bhisikar SM, Kokare DM, Nakhate KT, Chopde CT, Subhedar NK (2009). Tolerance to ethanol sedation and withdrawal hyper-excitability is mediated via neuropeptide Y Y1 and Y5 receptors. Life Sci. 85: 765–772.

Blanco-Calvo E, Rivera P, Arrabal S, Vargas A, Pavón FJ, Serrano A, Castilla-Ortega E, Galeano P, Rubio L, Suárez J, Rodriguez de Fonseca F (2014). Pharmacological blockade of either cannabinoid CB1 or CB2 receptors prevents both cocaine-induced conditioned locomotion and cocaine-induced reduction of cell proliferation in the hippocampus of adult male rat. Front. Integr. Neurosci. 7: 106.

Bliss TV, Lomo T (1973). Long-lasting potentiation of synaptic transmission in the dentate area of the anaesthetized rabbit following stimulation of the perforant path. J. Physiol. 232: 331–356.

Boku S, Nakagawa S, Masuda T, Nishikawa H, Kato A, Kitaichi Y, Inoue T, Koyama T (2009). Glucocorticoids and lithium reciprocally regulate the proliferation of adult dentate gyrus-derived neural precursor cells through GSK-3beta and beta-catenin/TCF pathway. Neuropsychopharmacology 34: 805–815.

Bowyer JF (1995). The role of hyperthermia in amphetamine's interactions with NMDA receptors, nitric oxide, and age to produce neurotoxicity. Ann. N. Y. Acad. Sci. 765: 309–310.

Bowyer JF, Ali S (2006). High doses of methamphetamine that cause disruption of the blood-brain barrier in limbic regions produce extensive neuronal degeneration in mouse hippocampus. Synapse 60: 521–532.

Bowyer JF, Davies DL, Schmued L, Broening HW, Newport GD, Slikker W Jr, Holson RR (1994). Further studies of the role of hyperthermia in methamphetamine neurotoxicity. J. Pharmacol. Exp. Ther. 268: 1571–1580.

Bowyer JF, Robinson B, Ali S, Schmued LC (2008). Neurotoxic-related changes in tyrosine hydroxylase, microglia, myelin, and the blood-brain barrier in the caudate-putamen from acute methamphetamine exposure. Synapse 62: 193–204.

Brandt MD, Jessberger S, Steiner B, Kronenberg G, Reuter K, Bick-Sander A, von der Behrens W, Kempermann G (2003). Transient calretinin expression defines early postmitotic step of neuronal differentiation in adult hippocampal neurogenesis of mice. Mol. Cell Neurosci. 24: 603–613.

Broqua P, Wettstein JG, Rocher MN, Gauthier-Martin B, Junien JL (1995). Behavioral effects of neuropeptide Y receptor agonists in the elevated plus-maze and fear-potentiated startle procedures. Behav. Pharmacol. 6: 215–222.

Brown JM, Hanson GR, Fleckenstein AE (2000). Methamphetamine rapidly decreases vesicular dopamine uptake. J. Neurochem. 74: 2221–2223.

Brown JM, Quinton MS, Yamamoto BK (2005). Methamphetamine-induced inhibition of mitochondrial complex II: roles of glutamate and peroxynitrite. J. Neurochem. 95: 429–436.

Bruel-Jungerman E, Veyrac A, Dufour F, Horwood J, Laroche S, Davis S (2009). Inhibition of PI3K-Akt signaling blocks exercise-mediated enhancement of adult neurogenesis and synaptic plasticity in the dentate gyrus. PLoS One 4: e7901.

Burrows KB, Gudelsky G, Yamamoto BK (2000). Rapid and transient inhibition of mitochondrial function following methamphetamine or 3,4-methylenedioxymethamphetamine administration. Eur. J. Pharmacol. 398: 11–18.

Caberlotto L, Fuxe K, Sedvall G, Hurd YL (1997). Localization of neuropeptide Y Y1 mRNA in the human brain: abundant expression in cerebral cortex and striatum. Eur. J. Neurosci. 9: 1212–1225.

Cabezas C, Irinopoulou T, Cauli B, Poncer JC (2013). Molecular and functional characterization of GAD67-expressing, newborn granule cells in mouse dentate gyrus. Front. Neural Circuits. 7: 60.

Cabezas C, Irinopoulou T, Gauvain G, Poncer JC (2012). Presynaptic but not postsynaptic GABA signaling at unitary mossy fiber synapses. J. Neurosci. 32: 11835–11840.

Cabrele C, Langer M, Bader R, Wieland HA, Doods HN, Zerbe O, Beck-Sickinger AG (2000). The first selective agonist for the neuropeptide YY5 receptor increases food intake in rats. J. Biol. Chem. 275: 36043–36048.

Cadet JL, Krasnova IN (2009). Molecular bases of methamphetamine-induced neurodegeneration. Int. Ver. Neurobiol. 88: 101–119. Review.

Cadet JL, Sheng P, Ali S, Rothman R, Carlson E, Epstein C (1994). Attenuation of methamphetamine-induced neurotoxicity in copper/zinc superoxide dismutase transgenic mice. J. Neurochem. 62: 380–383.

Caldwell J, Dring LG, Williams RT (1972). Metabolism of (14 C)methamphetamine in man, the guinea pig and the rat. Biochem. J. 129: 11–22.

Cameron HA, McEwen BS, Gould E (1995). Regulation of adult neurogenesis by excitatory input and NMDA receptor activation in the dentate gyrus. J. Neurosci. 15: 4687–4692.

Camodeca N, Breakwell NA, Rowan MJ, Anwyl R (1999). Induction of LTD by activation of group I mGluR in the dentate gyrus in vitro. Neuropharmacology 38: 1597–1606.

Campbell RE, ffrench-Mullen JM, Cowley MA, Smith MS, Grove KL (2001). Hypothalamic circuitry of neuropeptide Y regulation of neuroendocrine function and food intake via the Y5 receptor subtype. Neuroendocrinology 74: 106–119.

Campbell RE, Smith MS, Allen SE, Grayson BE, Ffrench-Mullen JM, Grove KL (2003). Orexin neurons express a functional pancreatic polypeptide Y4 receptor. J. Neurosci. 23: 1487–1497.

Cao G, Zhu J, Zhong Q, Shi C, Dang Y, Han W, Liu X, Xu M, Chen T (2013). Distinct roles of methamphetamine in modulating spatial memory consolidation, retrieval, reconsolidation and the accompanying changes of ERK and CREB activation in hippocampus and prefrontal cortex. Neuropharmacology 67: 144–154.

Catlow BJ, Badanich KA, Sponaugle AE, Rowe AR, Song S, Rafalovich I, Sava V, Kirstein CL, Sanchez-Ramos J (2010). Effects of MDMA ("ecstasy") during adolescence on place conditioning and hippocampal neurogenesis. Eur. J. Pharmacol. 628: 96–103.

Cerdá-Reverter JM, Larhammar D (2000). Neuropeptide Y family of peptides: structure, anatomical expression, function, and molecular evolution. Biochem. Cell Biol. 78: 371–392. Review.

Chattopadhyaya B, Di Cristo G, Higashiyama H, Knott GW, Kuhlman SJ, Welker E, Huang ZJ (2004). Experience and activity-dependent maturation of perisomatic GABAergic innervation in primary visual cortex during a postnatal critical period. J. Neurosci. 24: 9598–9611.

Chetty S, Friedman AR, Taravosh-Lahn K, Kirby ED, Mirescu C, Guo F, Krupik D, Nicholas A, Geraghty AC, Krishnamurthy A, Tsai MK, Covarrubias D, Wong AT, Francis DD, Sapolsky RM, Palmer TD, Pleasure D, Kaufer D (2014). Stress and glucocorticoids promote oligodendrogenesis in the adult hippocampus. Mol. Psychiatry.

Cheung A, Newland PL, Zaben M, Attard GS, Gray WP (2012). Intracellular nitric oxide mediates neuroproliferative effect of neuropeptide y on postnatal hippocampal precursor cells. J. Biol. Chem. 287: 20187–20196.

Chevaleyre V, Siegelbaum SA (2010). Strong CA2 pyramidal neuron synapses define a powerful disynaptic cortico-hippocampal loop. Neuron 66: 560–572.

Chiu CQ, Castillo PE (2008). Input-specific plasticity at excitatory synapses mediated by endocannabinoids in the dentate gyrus. Neuropharmacology 54: 68–78.

Choi JH, Yoo KY, Lee CH, Park JH, Yan BC, Kwon SH, Seo JY, Cho JH, Hwang IK, Won MH (2012). Comparison of neurogenesis in the dentate gyrus between the adult and aged gerbil following transient global cerebral ischemia. Neurochem. Res. 37: 802–810.

Christie BR, Abraham WC (1992). NMDA-dependent heterosynaptic long-term depression in the dentate gyrus of anaesthetized rats. Synapse 10: 1–6.

Chronwall BM, DiMaggio DA, Massari VJ, Pickel VM, Ruggiero DA, O'Donohue TL (1985). The anatomy of neuropeptide-Y-containing neurons in rat brain. Neuroscience 15: 1159–1181.

Clelland CD, Choi M, Romberg C, Clemenson GD Jr, Fragniere A, Tyers P, Jessberger S, Saksida LM, Barker RA, Gage FH, Bussey TJ (2009). A functional role for adult hippocampal neurogenesis in spatial pattern separation. Science 325: 210–213.

Coelho-Santos V, Gonçalves J, Fontes-Ribeiro C, Silva AP (2012). Prevention of methamphetamine-induced microglial cell death by TNF-α and IL-6 through activation of the JAK-STAT pathway. J. Neuroinflammation 9: 103.

Coles-Takabe BL, Brain I, Purpura KA, Karpowicz P, Zandstra PW, Morshead CM, van der Kooy D (2008). Don't look: growing clonal versus nonclonal neural stem cell colonies. Stem Cells 26: 2938–2944.

Colino A, Malenka RC (1993). Mechanisms underlying induction of long-term potentiation in rat medial and lateral perforant paths in vitro. J. Neurophysiol. 69: 1150–1159.

Crawford JT, Roberts DC, Beveridge TJ (2003). The group II metabotropic glutamate receptor agonist, LY379268, decreases methamphetamine self-administration in rats. Drug Alcohol Depend. 132: 414–419.

Criscione L, Rigollier P, Batzl-Hartmann C, Rüeger H, Stricker-Krongrad A, Wyss P, Brunner L, Whitebread S, Yamaguchi Y, Gerald C, Heurich RO, Walker MW, Chiesi M, Schilling W, Hofbauer KG, Levens N (1998). Food intake in free-feeding and energy-deprived lean rats is mediated by the neuropeptide Y5 receptor. J. Clin. Invest. 102: 2136–2145.

Crowley WR, Ramoz G, Keefe KA, Torto R, Kalra SP, Hanson GR (2005). Differential effects of methamphetamine on expression of neuropeptide Y mRNA in hypothalamus and on serum leptin and ghrelin concentrations in ad libitum-fed and schedule-fed rats. Neuroscience 132: 167–173.

Cruickshank CC, Dyer KR (2009). A review of the clinical pharmacology of methamphetamine. Addiction 104: 1085–1099. Review.

Dabe EC, Majdak P, Bhattacharya TK, Miller DS, Rhodes JS (2013). Chronic D-amphetamine administered from childhood to adulthood dose-dependently increases the survival of new neurons in the hippocampus of male C57BL/6J mice. Neuroscience 231: 125–135.

Darby K, Eyre HJ, Lapsys N, Copeland NG, Gilbert DJ, Couzens M, Antonova O, Sutherland GR, Jenkins NA, Herzog H (1997). Assignment of the Y4 receptor gene (PPYR1) to human chromosome 10q11.2 and mouse chromosome 14. Genomics 46: 513–515.

Darcy MJ, Trouche S, Jin SX, Feig LA (2014). Ras-GRF2 mediates long-term potentiation, survival, and response to an enriched environment of newborn neurons in the hippocampus. Hippocampus, 1–13.

de la Torre R, Farre M, Navarro M, Pacifici R, Zuccaro P, Pichini S (2004). Clinical pharmacokinetics of amphetamine and related substances: monitoring in conventional and non-conventional matrices Clin. Pharmacokinet. 43: 157–185. Review.

de Quidt ME, Emson PC (1986). Distribution of neuropeptide Y-like immunoreactivity in the rat central nervous system-II. Immunohistochemical analysis. Neuroscience 18: 545–618.

Decimo I, Bifari F, Krampera M, Fumagalli G (2012). Neural stem cell niches in health and diseases. Curr. Pharm. Des. 18: 1755–1783. Review.

Decressac M, Prestoz L, Veran J, Cantereau A, Jaber M, Gaillard A (2009). Neuropeptide Y stimulates proliferation, migration and differentiation of neural precursors from the subventricular zone in adult mice. Neurobiol. Dis. 34: 441–449.

Decressac M, Wright B, David B, Tyers P, Jaber M, Barker RA, Gaillard A (2011). Exogenous neuropeptide Y promotes in vivo hippocampal neurogenesis. Hippocampus 21: 233–238.

Deisseroth K, Singla S, Toda H, Monje M, Palmer TD, Malenka RC (2004). Excitation-neurogenesis coupling in adult neural stem/progenitor cells. Neuron 42: 535–552.

Deng W, Aimone JB, Gage FH (2010). New neurons and new memories: how does adult hippocampal neurogenesis affect learning and memory? Nat. Rev. Neurosci. 11: 339–350. Review.

Deng W, Saxe MD, Gallina IS, Gage FH (2009). Adult-born hippocampal dentate granule cells undergoing maturation modulate learning and memory in the brain. J. Neurosci. 29: 13532–13542.

Deng X, Cai NS, McCoy MT, Chen W, Trush MA, Cadet JL (2002). Methamphetamine induces apoptosis in an immortalized rat striatal cell line by activating the mitochondrial cell death pathway. Neuropharmacology 42: 837–845.

Di Monte DA, Royland JE, Jakowec MW, Langston JW (1996). Role of nitric oxide in methamphetamine neurotoxicity: protection by 7-nitroindazole, an inhibitor of neuronal nitric oxide synthase. J. Neurochem. 67: 2443–2450.

Dolphin AC, Errington ML, Bliss TV (1982). Long-term potentiation of the perforant path in vivo is associated with increased glutamate release. Nature 297: 496–498.

Domínguez-Escribà L, Hernández-Rabazam V, Soriano-Navarrom M, Barciam JA, Romero FJ, García-Verdugo JM, Canales JJ (2006). Chronic cocaine exposure impairs progenitor proliferation but spares survival and maturation of neural precursors in adult rat dentate gyrus. Eur. J. Neurosci. 24: 586–594.

Doods H, Gaida W, Wieland HA, Dollinger H, Schnorrenberg G, Esser F, Engel W, Eberlein W, Rudolf K (1999). BIIE0246: a selective and high affinity neuropeptide Y Y(2) receptor antagonist. Eur. J. Pharmacol. 384: R3–R5.

Dumont Y, Quirion R (2006). An overview of neuropeptide Y: pharmacology to molecular biology and receptor localization. EXS 7–33.

Dumont Y, Thakur M, Beck-Sickinger A, Fournier A, Quirion R (2004). Characterization of a new neuropeptide Y Y5 agonist radioligand: [125I][cPP(1-7), NPY(19-23), Ala31, Aib32, Gln34]hPP. Neuropeptides 38: 163–174.

Dyzma M, Boudjeltia KZ, Faraut B, Kerkhofs M (2010~). Neuropeptide Y and sleep. Sleep Med. Rev. 14: 161–165.

Ehninger D, Kempermann G (2008). Neurogenesis in the adult hippocampus. Cell Tissue Res. 331: 243–250. Review.

Eisch AJ, Barrot M, Schad CA, Self DW, Nestler EJ (2000). Opiates inhibit neurogenesis in the adult rat hippocampus. Proc. Natl. Acad. Sci. U S A 97: 7579–7584.

El Bahh B, Balosso S, Hamilton T, Herzog H, Beck-Sickinger AG, Sperk G, Gehlert DR, Vezzani A, Colmers WF (2005). The anti-epileptic actions of neuropeptide Y in the hippocampus are mediated by Y and not Y receptors. Eur. J. Neurosci. 22: 1417–1430.

Enwere E, Shingo T, Gregg C, Fujikawa H, Ohta S, Weiss S (2004). Aging results in reduced epidermal growth factor receptor signaling, diminished olfactory neurogenesis, and deficits in fine olfactory discrimination. J. Neurosci. 24, 8354–8365.

Espósito MS, Piatti VC, Laplagne DA, Morgenstern NA, Ferrari CC, Pitossi FJ, Schinder AF (2005). Neuronal differentiation in the adult hippocampus recapitulates embryonic development. J. Neurosci. 25: 10074–10086.

Eva C, Serra M, Mele P, Panzica G, Oberto A (2006). Physiology and gene regulation of the brain NPY Y1 receptor. Front. Neuroendocrinol. 27: 308–339. Review.

Farfel GM, Vosmer GL, Seiden LS (1992). The N-methyl-D-aspartate antagonist MK-801 protects against serotonin depletions induced by methamphetamine, 3,4-methylenedioxymethamphetamine and p-chloroamphetamine. Brain Res. 595: 121–127.

Farioli-Vecchioli S, Saraulli D, Costanzi M, Pacioni S, Cinà I, Aceti M, Micheli L, Bacci A, Cestari V, Tirone F (2008). The timing of differentiation of adult hippocampal neurons is crucial for spatial memory. PLoS Biol 6: e246.

Fernando RN, Eleuteri B, Abdelhady S, Nussenzweig A, Andäng M, Ernfors P (2011). Cell cycle restriction by histone H2AX limits proliferation of adult neural stem cells. Proc. Natl. Acad. Sci. U. S. A. 108: 5837–5842.

Ferreira R, Xapelli S, Santos T, Silva AP, Cristóvão A, Cortes L, Malva JO (2010). Neuropeptide Y modulation of interleukin-1{beta} (IL-1{beta})-induced nitric oxide production in microglia. J. Biol Chem. 285: 41921-34.

Filippov V, Kronenberg G, Pivneva T, Reuter K, Steiner B, Wang LP, Yamaguchi M, Kettenmann H, Kempermann G (2003). Subpopulation of nestin-expressing progenitor cells in the adult murine hippocampus shows electrophysiological and morphological characteristics of astrocytes. Mol. Cell Neurosci. 23: 373–382.

Fitzmaurice PS, Tong J, Yazdanpanah M, Liu PP, Kalasinsky KS, Kish SJ (2006). Levels of 4-hydroxynonenal and malondialdehyde are increased in brain of human chronic users of methamphetamine. J. Pharmacol. Exp. Ther. 319: 703–709.

Fleckenstein AE, Metzger RR, Beyeler ML, Gibb JW, Hanson GR (1997). Oxygen radicals diminish dopamine transporter function in rat striatum. Eur. J. Pharmacol. 334: 111–114.

Fleckenstein AE, Volz TJ, Riddle EL, Gibb JW, Hanson GR (2007). New insights into the mechanism of action of amphetamines. Annu. Ver.Pharmacol. Toxicol. 47: 681–698. Review.

Flora G, Lee YW, Nath A, Maragos W, Hennig B, Toborek M (2002). Methamphetamine-induced TNF-alpha gene expression and activation of AP-1 in discrete regions of mouse brain: potential role of reactive oxygen intermediates and lipid peroxidation. Neuromolecular Med. 2: 71–85.

Frankel PS, Alburges ME, Bush L, Hanson GR, Kish SJ (2007). Brain levels of neuropeptides in human chronic methamphetamine users. Neuropharmacology 53: 447–454.

Fuhlendorff J, Gether U, Aakerlund L, Langeland-Johansen N, Thøgersen H, Melberg SG, Olsen UB, Thastrup O, Schwartz TW (1990). [Leu31, Pro34]neuropeptide Y: a specific Y1 receptor agonist. Proc. Natl. Acad. Sci. U. S. A. 87: 182–186.

Fukazawa Y, Saitoh Y, Ozawa F, Ohta Y, Mizuno K, Inokuchi K (2003). Hippocampal LTP is accompanied by enhanced F-actin content within the dendritic spine that is essential for late LTP maintenance in vivo. Neuron 38: 447–460.

Gage FH(2000). Mammalian neural stem cells. Science. 287: 1433–1438. Review.

Gampe K, Brill MS, Momma S, Götz M, Zimmermann H (2011). EGF induces CREB and ERK activation at the wall of the mouse lateral ventricles. Brain Res. 1376: 31–41.

Gao J, Ghibaudi L, Hwa JJ (2004). Selective activation of central NPY Y1 vs. Y5 receptor elicits hyperinsulinemia via distinct mechanisms. Am. J. Physiol. Endocrinol. Metab. 287: E706–E711.

Gariboldi M, Conti M, Cavaleri D, Samanin R, Vezzani A (1998). Anticonvulsant properties of BIBP3226, a non-peptide selective antagonist at neuropeptide Y Y1 receptors. Eur. J. Neurosci. 10: 757–759.

Garthe A, Behr J, Kempermann G (2009). Adult-generated hippocampal neurons allow the flexible use of spatially precise learning strategies. PLoS One 4: e5464.

Ge S, Goh EL, Sailor KA, Kitabatake Y, Ming GL, Song H (2006). GABA regulates synaptic integration of newly generated neurons in the adult brain. Nature 439: 589–593

Ge S, Pradhan DA, Ming GL, Song H (2007b). GABA sets the tempo for activity-dependent adult neurogenesis. Trends Neurosci. 30: 1–8. Review.

Ge S, Yang CH, Hsu KS, Ming GL, Song H (2007a). A critical period for enhanced synaptic plasticity in newly generated neurons of the adult brain. Neuron 54: 559–566.

Gebara E, Sultan S, Kocher-Braissant J, Toni N (2013). Adult hippocampal neurogenesis inversely correlates with microglia in conditions of voluntary running and aging. Front. Neurosci. 7: 145.

Genc K, Genc S, Kizildag S, Sonmez U, Yilmaz O, Tugyan K, Ergur B, Sonmez A, Buldan Z (2003). Methamphetamine induces oligodendroglial cell death in vitro. Brain Res. 982: 125–130.

Gerald C, Walker MW, Criscione L, Gustafson EL, Batzl-Hartmann C, Smith KE, Vaysse P, Durkin MM, Laz TM, Linemeyer DL, Schaffhauser AO, Whitebread S, Hofbauer KG, Taber RI, Branchek TA, Weinshank RL (1996). A receptor subtype involved in neuropeptide-Y-induced food intake. Nature 382: 168–171.

Ginawi OT, Al-Majed AA, Al-Suwailem AK (2005). Ondansetron, a selective 5-HT3 antagonist, antagonizes methamphetamine-induced anorexia in mice. Pharmacol. Res. 51: 255–9.

Glaum SR, Miller RJ, Rhim H, Maclean D, Georgic LM, MacKenzie RG, Grundemar L (1997). Characterization of Y3 receptor-mediated synaptic inhibition by chimeric neuropeptide Y-peptide YY peptides in the rat brainstem. Br. J. Pharmacol. 120: 481–487.

Gluck MR, Moy LY, Jayatilleke E, Hogan KA, Manzino L, Sonsalla PK (2001). Parallel increases in lipid and protein oxidative markers in several mouse brain regions after methamphetamine treatment. J. Neurochem. 79: 152–160.

Gonçalves J, Baptista S, Martins T, Milhazes N, Borges F, Ribeiro CF, Malva JO, Silva AP (2010). Methamphetamine-induced neuroinflammation and neuronal dysfunction in the mice hippocampus: preventive effect of indomethacin. Eur. J. Neurosci. 31: 315–326.

Gonçalves J, Ribeiro CF, Malva JO, Silva AP (2012a). Protective role of neuropeptide Y Y_2 receptors in cell death and microglial response following methamphetamine injury. Eur. J. Neurosci. 36: 3173–3183.

Gonçalves J, Baptista S, Olesen MV, Fontes-Ribeiro C, Malva JO, Woldbye DP, Silva AP (2012b). Methamphetamine-induced changes in the mice hippocampal neuropeptide Y system: implications for memory impairment. J. Neurochem. 123: 1041–1053.

Gonçalves J, Baptista S, Silva AP (2014). Psychostimulants and brain dysfunction: A review of the relevant neurotoxic effects. Neuropharmacology 15.

Gonçalves J, Martins T, Ferreira R, Milhazes N, Borges F, Ribeiro CF, Malva JO, Macedo TR, Silva AP (2008). Methamphetamine-induced early increase of IL-6 and TNF-alpha mRNA expression in the mouse brain. Ann. N. Y. Acad. Sci. 1139: 103–111.

Grandt D, Schimiczek M, Rascher W, Feth F, Shively J, Lee TD, Davis MT, Reeve JR Jr, Michel MC (1996). Neuropeptide Y 3-36 is an endogenous ligand selective for Y2 receptors. Regul. Pept. 67: 33–37.

Green EJ, McNaughton BL, Barnes CA (1990). Role of the medial septum and hippocampal theta rhythm in exploration-related synaptic efficacy changes in rat fascia dentata. Brain Res. 529: 102–108.

Gregor P, Feng Y, DeCarr LB, Cornfield LJ, McCaleb ML (1996). Molecular characterization of a second mouse pancreatic polypeptide receptor and its inactivated human homologue. J. Biol Chem. 271: 27776–27781.

Gross NB, Duncker PC, Marshall JF (2011). Cortical ionotropic glutamate receptor antagonism protects against methamphetamine-induced striatal neurotoxicity. Neuroscience 199: 272–283.

Grouzmann E, Buclin T, Martire M, Cannizzaro C, Dörner B, Razaname A, Mutter M (1997). Characterization of a selective antagonist of neuropeptide Y at the Y2 receptor. Synthesis and pharmacological evaluation of a Y2 antagonist. J. Biol. Chem. 272: 7699–7706.

Grundemar L, Wahlestedt C, Reis DJ (1991). Long-lasting inhibition of the cardiovascular responses to glutamate and the baroreceptor reflex elicited by neuropeptide Y injected into the nucleus tractus solitarius of the rat. Neurosci. Lett. 122: 135–139.

Gu Y, Arruda-Carvalho M, Wang J, Janoschka SR, Josselyn SA, Frankland PW, Ge S (2012). Optical controlling reveals time-dependent roles for adult-born dentate granule cells. Nat. Neurosci. 15: 1700–1706.

Hadlock GC, Chu PW, Walters ET, Hanson GR, Fleckenstein AE (2010). Methamphetamine-induced dopamine transporter complex formation and dopaminergic deficits: the role of D2 receptor activation. J. Pharmacol. Exp. Ther. 335: 207–212.

Haga Y, Sakamoto T, Shibata T, Nonoshita K, Ishikawa M, Suga T, Takahashi H, Takahashi T, Takahashi H, Ando M, Murai T, Gomori A, Oda Z, Kitazawa H, Mitobe Y, Kanesaka M, Ohe T, Iwaasa H, Ishii Y, Ishihara A, Kanatani A, Fukami T (2009). Discovery of trans-N-[1-(2-fluorophenyl)-3-pyrazolyl]-3-oxospiro[6-azaisobenzofuran-1(3H),1'-cyclohexane]-4'-carboxamide, a potent and orally active neuropeptide Y Y5 receptor antagonist. Bioorg. Med. Chem. 17: 6971–6982.

Haglund L, Swanson LW, Köhler C (1984). The projection of the supramammillary nucleus to the hippocampal formation: an immunohistochemical and anterograde transport study with the lectin PHA-L in the rat. J. Comp. Neurol. 229: 171–185.

Hansel DE, Eipper BA, Ronnett GV (2001). Regulation of olfactory neurogenesis by amidated neuropeptides. J. Neurosci. Res. 66: 1–7.

Hardingham GE, Bading H (2010). Synaptic versus extrasynaptic NMDA receptor signalling: implications for neurodegenerative disorders. Nat. Rev. Neurosci. 11: 682–696. Review.

Harris EW, Cotman CW (1986). Long-term potentiation of guinea pig mossy fiber responses is not blocked by N-methyl D-aspartate antagonists. Neurosci. Lett. 70: 132–137.

Hattiangady B, Rao MS, Shetty GA, Shetty AK (2005). Brain-derived neurotrophic factor, phosphorylated cyclic AMP response element binding protein and neuropeptide Y decline as early as middle age in the dentate gyrus and CA1 and CA3 subfields of the hippocampus. Exp Neurol. 195: 353–371.

Haughey NJ, Nath A, Chan SL, Borchard AC, Rao MS, Mattson MP (2002). Disruption of neurogenesis by amyloid beta-peptide, and perturbed neural progenitor cell homeostasis, in models of Alzheimer's disease. J. Neurochem. 83: 1509–1524.

Hayashi Y, Shi SH, Esteban JA, Piccini A, Poncer JC, Malinow R (2000). Driving AMPA receptors into synapses by LTP and CaMKII: requirement for GluR1 and PDZ domain interaction. Science 287: 2262–2267.

Heo JS, Lee YJ, Han HJ (2006). EGF stimulates proliferation of mouse embryonic stem cells: involvement of Ca2+ influx and p44/42 MAPKs. Am. J. Physiol. Cell Physiol. 290: C123–C133.

Hernández-Rabaza V, Domínguez-Escribà L, Barcia JA, Rosel JF, Romero FJ, García-Verdugo JM, Canales JJ (2006). Binge administration of 3,4-methylenedioxymethamphetamine ("ecstasy") impairs the survival of neural precursors in adult rat dentate gyrus. Neuropharmacology 51: 967–973.

Herzog H, Darby K, Ball H, Hort Y, Beck-Sickinger A, Shine J (1997). Overlapping gene structure of the human neuropeptide Y receptor subtypes Y1 and Y5 suggests coordinate transcriptional regulation. Genomics 41: 315–319.

Hildebrandt K, Teuchert-Noodt G, Dawirs RR (1999). A single neonatal dose of methamphetamine suppresses dentate granule cell proliferation in adult gerbils which is restored to control values by acute doses of haloperidol. J. Neural Transm. 106: 549–558.

Hipskind PA, Lobb KL, Nixon JA, Britton TC, Bruns RF, Catlow J, Dieckman-McGinty DK, Gackenheimer SL, Gitter BD, Iyengar S, Schober DA, Simmons RM, Swanson S, Zarrinmayeh H, Zimmerman DM, Gehlert DR (1997). Potent and selective 1,2,3-trisubstituted indole NPY Y-1 antagonists. J. Med. Chem. 40: 3712–3714.

Hori N, Kadota MT, Watanabe M, Ito Y, Akaike N, Carpenter DO (2010). Neurotoxic effects of methamphetamine on rat hippocampus pyramidal neurons. Cell. Mol. Neurobiol. 30: 849–856.

Horner KA, Gilbert YE, Cline SD (2011). Widespread increases in malondialdehyde immunoreactivity in dopamine-rich and dopamine-poor regions of rat brain following multiple, high doses of methamphetamine. Front. Syst. Neurosci. 5: 27.

Horner KA, Westwood SC, Hanson GR, Keefe KA (2006). Multiple high doses of methamphetamine increase the number of preproneuropeptide Y mRNA-expressing neurons in the striatum of rat via a dopamine D1 receptor-dependent mechanism. J. Pharmacol. Exp. Ther. 319: 414–421.

Howell OW, Doyle K, Goodman JH, Scharfman HE, Herzog H, Pringle A, Beck-Sickinger AG, Gray WP (2005). Neuropeptide Y stimulates neuronal precursor proliferation in the post-natal and adult dentate gyrus. J. Neurochem. 93: 560–570.

Howell OW, Scharfman HE, Herzog H, Sundstrom LE, Beck-Sickinger A, Gray WP (2003). Neuropeptide Y is neuroproliferative for post-natal hippocampal precursor cells. J. Neurochem. 86: 646–659.

Hu S, Cheeran MC, Sheng WS, Ni HT, Lokensgard JR, Peterson PK (2006). Cocaine alters proliferation, migration, and differentiation of human fetal brain-derived neural precursor cells. J. Pharmacol. Exp. Ther. 318: 1280–1286.

Hu Y, Bloomquist BT, Cornfield LJ, DeCarr LB, Flores-Riveros JR, Friedman L, Jiang P, Lewis-Higgins L, Sadlowski Y, Schaefer J, Velazquez N, McCaleb ML (1996). Identification of a novel hypothalamic neuropeptide Y receptor associated with feeding behavior. J. Biol. Chem. 271: 26315–26319.

Ishikawa A, Kadota T, Kadota K, Matsumura H, Nakamura S (2005). Essential role of D1 but not D2 receptors in methamphetamine-induced impairment of long-term potentiation in hippocampal-prefrontal cortex pathway. Eur. J. Neurosci. 22: 1713–1719.

Ito Y, Takuma K, Mizoguchi H, Nagai T, Yamada K (2007). A novel azaindolizinone derivative ZSET1446 (spiro[imidazo[1,2-a]pyridine-3,2-indan]-2(3H)-one) improves methamphetamine-induced impairment of recognition memory in mice by activating extracellular signal-regulated kinase 1/2. J. Pharmacol. Exp. Ther. 320: 819–827.

Itzhak Y, Gandia C, Huang PL, Ali SF (1998). Resistance of neuronal nitric oxide synthase-deficient mice to methamphetamine-induced dopaminergic neurotoxicity. J. Pharmacol. Exp. Ther. 284: 1040–1047.

Iversen L (2006). Neurotransmitter transporters and their impact on the development of psychopharmacology. Br. J. Pharmacol. 1:S82–88. Review.

Jacques D, Tong Y, Shen SH, Quirion R (1998). Discrete distribution of the neuropeptide Y Y5 receptor gene in the human brain: an in situ hybridization study. Brain Res. Mol. Brain Res. 61: 100–107.

Jayanthi S, Deng X, Bordelon M, McCoy MT, Cadet JL (2001). Methamphetamine causes differential regulation of pro-death and anti-death Bcl-2 genes in the mouse neocortex. FASEB J. 15: 1745–1752.

Jayanthi S, Deng X, Noailles PA, Ladenheim B, Cadet JL (2004). Methamphetamine induces neuronal apoptosis via cross-talks between endoplasmic reticulum and mitochondria-dependent death cascades. FASEB J. 18: 238–251.

Jessberger S, Clark RE, Broadbent NJ, Clemenson GD Jr, Consiglio A, Lie DC, Squire LR, Gage FH (2009). Dentate gyrus-specific knockdown of adult neurogenesis impairs spatial and object recognition memory in adult rats. Learn. Mem. 16: 147–154.

Jessberger S, Zhao C, Toni N, Clemenson GD Jr, Li Y, Gage FH (2007). Seizure-associated, aberrant neurogenesis in adult rats characterized with retrovirus-mediated cell labeling. J. Neurosci. 27: 9400–9407.

Jin K, Sun Y, Xie L, Batteur S, Mao XO, Smelick C, Logvinova A, Greenberg DA (2003). Neurogenesis and aging: FGF-2 and HB-EGF restore neurogenesis in hippocampus and subventricular zone of aged mice. Aging Cell 2: 175–183.

Kalasinsky KS, Bosy TZ, Schmunk GA, Reiber G, Anthony RM, Furukawa Y, Guttman M, Kish SJ (2001). Regional distribution of methamphetamine in autopsied brain of chronic human methamphetamine users. Forensic Sci. Int. 116: 163–169.

Kalechstein AD, Newton TF, Green M (2003). Methamphetamine dependence is associated with neurocognitive impairment in the initial phases of abstinence. J. Neuropsychiatry Clin. Neurosci. 15: 215–220.

Kanatani A, Mashiko S, Murai N, Sugimoto N, Ito J, Fukuroda T, Fukami T, Morin N, MacNeil DJ, Van der Ploeg LH, Saga Y, Nishimura S, Ihara M (2000). Role of the Y1 receptor in the regulation of neuropeptide Y-mediated feeding: comparison of wild-type, Y1 receptor-deficient, and Y5 receptor-deficient mice. Endocrinology 141: 1011–1016.

Kandel E, Schwartz J, Jessel T (1991). Principles of neural science. McGraw Hill 4th edition, Chapter 9, 150–170.

Kannangara TS, Eadie BD, Bostrom CA, Morch K, Brocardo PS, Christie BR (2014). GluN2A-/- Mice Lack Bidirectional Synaptic Plasticity in the Dentate Gyrus and Perform Poorly on Spatial Pattern Separation Tasks. Cereb. Cortex.

Kask A, Rägo L, Harro J (1998). Evidence for involvement of neuropeptide Y receptors in the regulation of food intake: studies with Y1-selective antagonist BIBP3226. Br. J. Pharmacol. 124: 1507–1515.

Kee N, Teixeira CM, Wang AH, Frankland PW (2007). Preferential incorporation of adult-generated granule cells into spatial memory networks in the dentate gyrus. Nat. Neurosci. 10: 355–362.

Kelleher RJ 3rd, Govindarajan A, Jung HY, Kang H, Tonegawa S (2004). Translational control by MAPK signaling in long-term synaptic plasticity and memory. Cell 116: 467–479.

Kempermann G, Kuhn HG, Gage FH (1997). More hippocampal neurons in adult mice living in an enriched environment. Nature 386: 493–495.

Kheirbek MA, Tannenholz L, Hen R (2012). NR2B-dependent plasticity of adult-born granule cells is necessary for context discrimination. J. Neurosci. 32: 8696–8702.

Kish SJ (2008). Pharmacologic mechanisms of crystal meth. CMAJ. 178: 1679–1682. Review.

Kishi T, Aschkenasi CJ, Choi BJ, Lopez ME, Lee CE, Liu H, Hollenberg AN, Friedman JM, Elmquist JK (2005). Neuropeptide Y Y1 receptor mRNA in rodent brain: distribution and colocalization with melanocortin-4 receptor. J. Comp. Neurol. 482: 217–243.

Kitayama T, Yoneyama M, Tamaki K, Yoneda Y (2004). Regulation of neuronal differentiation by N-methyl-D-aspartate receptors expressed in neural progenitor cells isolated from adult mouse hippocampus. J. Neurosci. Res. 76: 599–612.

Kiyatkin EA, Brown PL, Sharma HS (2007). Brain edema and breakdown of the blood-brain barrier during methamphetamine intoxication: critical role of brain hyperthermia. Eur. J. Neurosci. 26: 1242–1253.

Klette KL, Kettle AR, Jamerson MH (2006). Prevalence of use study for amphetamine (AMP), methamphetamine (MAMP), 3,4-methylenedioxy-amphetamine (MDA), 3,4-methylenedioxy-methamphetamine (MDMA), and 3,4-methylenedioxy-ethylamphetamine (MDEA) in military entrance processing stations (MEPS) specimens. J. Anal. Toxicol. 30: 319–322.

Klongpanichapak S, Govitrapong P, Sharma SK, Ebadi M (2006). Attenuation of cocaine and methamphetamine neurotoxicity by coenzyme Q10. Neurochem. Res. 31: 303–311.

Kohara K, Pignatelli M, Rivest AJ, Jung HY, Kitamura T, Suh J, Frank D, Kajikawa K, Mise N, Obata Y, Wickersham IR, Tonegawa S (2014). Cell type-specific genetic and optogenetic tools reveal hippocampal CA2 circuits. Nat. Neurosci. 17: 269–279.

Kohl Z, Winner B, Ubhi K, Rockenstein E, Mante M, Münch M, Barlow C, Carter T, Masliah E, Winkler J (2012). Fluoxetine rescues impaired hippocampal neurogenesis in a transgenic A53T synuclein mouse model. Eur. J. Neurosci. 35: 10–19.

Kokoeva MV, Yin H, Flier JS (2005). Neurogenesis in the hypothalamus of adult mice: potential role in energy balance. Science 310: 679–683.

Kokoeva MV, Yin H, Flier JS (2007). Evidence for constitutive neural cell proliferation in the adult murine hypothalamus. J. Comp. Neurol. 505: 209–220.

Krasnova IN, Cadet JL (2009). Methamphetamine toxicity and messengers of death. Brain Res. Rev. 60: 379–407. Review.

Kronenberg G, Reuter K, Steiner B, Brandt MD, Jessberger S, Yamaguchi M, Kempermann G (2003). Subpopulations of proliferating cells of the adult hippocampus respond differently to physiologic neurogenic stimuli. J. Comp. Neurol. 467: 455–463.

Lamprecht R, LeDoux J (2004). Structural plasticity and memory. Nat. Rev. Neurosci. 5: 45–54. Review.

Laplagne DA, Espósito MS, Piatti VC, Morgenstern NA, Zhao C, van Praag H, Gage FH, Schinder AF (2006). Functional convergence of neurons generated in the developing and adult hippocampus. PLoS Biol. 4: e409.

Larhammar D, Salaneck E (2004). Molecular evolution of NPY receptor subtypes. Neuropeptides 38: 141–151. Review.

LaVoie MJ, Hastings TG (1999). Dopamine quinone formation and protein modification associated with the striatal neurotoxicity of methamphetamine: evidence against a role for extracellular dopamine. J. Neurosci. 19: 1484–1491.

Le Belle JE, Orozco NM, Paucar AA, Saxe JP, Mottahedeh J, Pyle AD, Wu H, Kornblum HI (2011). Proliferative neural stem cells have high endogenous ROS levels that regulate self-renewal and neurogenesis in a PI3K/Akt-dependant manner Cell Stem Cell 8: 59–71.

Lee CT, Chen J, Hayashi T, Tsai SY, Sanchez JF, Errico SL, Amable R, Su TP, Lowe RH, Huestis MA, Shen J, Becker KG, Geller HM, Freed WJ (2008). A mechanism for the inhibition of neural progenitor cell proliferation by cocaine. PLoS Med. 5: e117.

Lee YW, Hennig B, Yao J, Toborek M (2001). Methamphetamine induces AP-1 and NF-kappaB binding and transactivation in human brain endothelial cells. J. Neurosci. Res. 66: 583–591.

Lin LY, Di Stefano EW, Schmitz DA, Hsu L, Ellis SW, Lennard MS, Tucker GT, Cho AK (1997). Oxidation of methamphetamine and methylenedioxymethamphetamine by CYP2D6. Drug Metab. Dispos. 25: 1059–1064.

Liu X, Tilwalli S, Ye G, Lio PA, Pasternak JF, Trommer BL (2000). Morphologic and electrophysiologic maturation in developing dentate gyrus granule cells. Brain Res. 856: 202–212.

Liu YB, Lio PA, Pasternak JF, Trommer BL (1996). Developmental changes in membrane properties and postsynaptic currents of granule cells in rat dentate gyrus. J. Neurophysiol. 76: 1074–1088.

Lledo PM, Alonso M, Grubb MS (2006). Adult neurogenesis and functional plasticity in neuronal circuits. Nat. Rev. Neurosci. 7: 179–193. Review.

Macek TA, Winder DG, Gereau RW 4th, Ladd CO, Conn PJ (1996). Differential involvement of group II and group III mGluRs as autoreceptors at lateral and medial perforant path synapses. J. Neurophysiol. 76: 3798–3806.

Madsen TM, Kristjansenm PE, Bolwig TG, Wörtwein G (2003). Arrested neuronal proliferation and impaired hippocampal function following fractionated brain irradiation in the adult rat. Neuroscience 119: 635–642.

Maeda K, Sugino H, Hirose T, Kitagawa H, Nagai T, Mizoguchi H, Takuma K, Yamada K (2007). Clozapine prevents a decrease in neurogenesis in mice repeatedly treated with phencyclidine. J. Pharmacol. Sci. 103: 299–308.

Maglóczky Z, Acsády L, Freund TF (1994). Principal cells are the postsynaptic targets of supramammillary afferents in the hippocampus of the rat. Hippocampus 4: 322–334.

Mahar I, Bagot RC, Davoli MA, Miksys S, Tyndale RF, Walker CD, Maheu M, Huang SH, Wong TP, Mechawar N (2012). Developmental hippocampal neuroplasticity in a model of nicotine replacement therapy during pregnancy and breastfeeding. PLoS One 7: e37219.

Malva JO, Xapelli S, Baptista S, Valero J, Agasse F, Ferreira R, Silva AP (2012). Multifaces of neuropeptide Y in the brain--neuroprotection, neurogenesis and neuroinflammation. Neuropeptides 46: 299–308.

Mandyam CD, Wee S, Crawford EF, Eisch AJ, Richardson HN, Koob GF (2008). Varied access to intravenous methamphetamine self-administration differentially alters adult hippocampal neurogenesis. Biol. Psychiatry 64: 958–965.

Mandyam CD, Wee S, Eisch AJ, Richardson HN, Koob GF (2007). Methamphetamine self-administration and voluntary exercise have opposing effects on medial prefrontal cortex gliogenesis. J. Neurosci. 27: 11442–11450.

Mark KA, Quinton MS, Russek SJ, Yamamoto BK (2007). Dynamic changes in vesicular glutamate transporter 1 function and expression related to methamphetamine-induced glutamate release. J. Neurosci. 27: 6823–6831.

Mark KA, Soghomonian JJ, Yamamoto BK (2004). High-dose methamphetamine acutely activates the striatonigral pathway to increase striatal glutamate and mediate long-term dopamine toxicity. J. Neurosci. 24: 11449–11456.

Martins T, Baptista S, Gonçalves J, Leal E, Milhazes N, Borges F, Ribeiro CF, Quintela O, Lendoiro E, López-Rivadulla M, Ambrósio AF, Silva AP (2011). Methamphetamine transiently increases the blood-brain barrier permeability in the hippocampus: role of tight junction proteins and matrix metalloproteinase-9. Brain Res. 1411: 28–40.

Martins T, Burgoyne T, Kenny BA, Hudson N, Futter CE, Ambrósio AF, Silva AP, Greenwood J, Turowski P (2013). Methamphetamine-induced nitric oxide promotes vesicular transport in blood-brain barrier endothelial cells. Neuropharmacology 65: 74–82.

Mashiko S, Ishihara A, Iwaasa H, Sano H, Oda Z, Ito J, Yumoto M, Okawa M, Suzuki J, Fukuroda T, Jitsuoka M, Morin NR, MacNeil DJ, Van der Ploeg LH, Ihara M, Fukami T, Kanatani A (2003). Characterization of neuropeptide Y (NPY) Y5 receptor-mediated obesity in mice: chronic intracerebroventricular infusion of D-Trp(34)NPY. Endocrinology 144: 1793–1801.

Matsumoto M, Nomura T, Momose K, Ikeda Y, Kondou Y, Akiho H, Togami J, Kimura Y, Okada M, Yamaguchi T (1996). Inactivation of a novel neuropeptide Y/peptide YY receptor gene in primate species. J. Biol. Chem. 271: 27217–27220.

Mazumder S, DuPree EL, Almasan A (2004). A dual role of cyclin E in cell proliferation and apoptosis may provide a target for cancer therapy. Curr. Cancer Drug Targets 4: 65–75.

Melega WP, Cho AK, Harvey D, Laćan G (2007). Methamphetamine blood concentrations in human abusers: application to pharmacokinetic modeling. Synapse 61: 216–220.

Michel MC (1991). Receptors for neuropeptide Y: multiple subtypes and multiple second messengers. Trends Pharmacol. Sci. 12: 389–394. Review.

Michel MC, Beck-Sickinger A, Cox H, Doods HN, Herzog H, Larhammar D, Quirion R, Schwartz T, Westfall T (1998). XVI. International Union of Pharmacology recommendations for the nomenclature of neuropeptide Y, peptide YY, and pancreatic polypeptide receptors. Pharmacol. Rev. 50: 143–150. Review.

Minakata H, Taylor JW, Walker MW, Miller RJ, Kaiser ET (1989). Characterization of amphiphilic secondary structures in neuropeptide Y through the design, synthesis, and study of model peptides. J. Biol. Chem. 264: 7907–7913.

Minth CD, Andrews PC, Dixon JE (1986). Characterization, sequence, and expression of the cloned human neuropeptide Y gene. J. Biol. Chem. 261: 11974–11979.

Minth CD, Bloom SR, Polak JM, Dixon JE (1984). Cloning, characterization, and DNA sequence of a human cDNA encoding neuropeptide tyrosine. Proc. Natl. Acad. Sci. U. S. A. 81: 4577–4581.

Mirecki A, Fitzmaurice P, Ang L, Kalasinsky KS, Peretti FJ, Aiken SS, Wickham DJ, Sherwin A, Nobrega JN, Forman HJ, Kish SJ (2004). Brain antioxidant systems in human methamphetamine users. J. Neurochem. 89: 1396–1408.

Mizuno M, Malta RS Jr, Nagano T, Nawa H (2004). Conditioned place preference and locomotor sensitization after repeated administration of cocaine or methamphetamine in rats treated with epidermal growth factor during the neonatal period. Ann. N. Y. Acad. Sci. 1025: 612–618.

Molosh AI, Sajdyk TJ, Truitt WA, Zhu W, Oxford GS, Shekhar A (2013). NPY Y1 receptors differentially modulate GABAA and NMDA receptors via divergent signal-transduction pathways to reduce excitability of amygdala neurons. Neuropsychopharmacology 38: 1352–1364.

Mongiat LA, Espósito MS, Lombardi G, Schinder AF (2009). Reliable activation of immature neurons in the adult hippocampus. PLoS One 4: e5320.

Monje ML, Toda H, Palmer TD (2003). Inflammatory blockade restores adult hippocampal neurogenesis. Science 302: 1760–1765.

Monnet FP, Fournier A, Debonnel G, de Montigny C (1992). Neuropeptide Y potentiates selectively the N-methyl-D-aspartate response in the rat CA3 dorsal hippocampus. I. Involvement of an atypical neuropeptide Y receptor. J. Pharmacol. Exp. Ther. 263: 1212–1218.

Morris RG, Anderson E, Lynch GS, Baudry M (1986). Selective impairment of learning and blockade of long-term potentiation by an N-methyl-D-aspartate receptor antagonist, AP5. Nature 319: 774–776.

Nacher J, Alonso-Llosa G, Rosell DR, McEwen BS (2003). NMDA receptor antagonist treatment increases the production of new neurons in the aged rat hippocampus. Neurobiol. Aging 24: 273–284.

Nakashiba T, Cushman JD, Pelkey KA, Renaudineau S, Buhl DL, McHugh TJ, Rodriguez Barrera V, Chittajallu R, Iwamoto KS, McBain CJ, Fanselow MS, Tonegawa S (2012). Young dentate granule cells mediate pattern separation, whereas old granule cells facilitate pattern completion. Cell 149: 188–201.

Neve KA, Seamans JK, Trantham-Davidson H. Dopamine receptor signaling (2004). J. Recept. Signal Transduct. Res. 24: 165–205. Review.

Neves G, Cooke SF, Bliss TV (2008). Synaptic plasticity, memory and the hippocampus: a neural network approach to causality. Nat. Rev. Neurosci. 9: 65–75. Review.

North A, Swant J, Salvatore MF, Gamble-George J, Prins P, Butler B, Mittal MK, Heltsley R, Clark JT, Khoshbouei H (2013). Chronic methamphetamine exposure produces a delayed, long-lasting memory deficit. Synapse 67: 245–257.

Nowakowski RS, Lewin SB, Miller MW (1989). Bromodeoxyuridine immunohistochemical determination of the lengths of the cell cycle and the DNA-synthetic phase for an anatomically defined population. J. Neurocytol. 18: 311–318.

O'Connor RM, Finger BC, Flor PJ, Cryan JF (2010). Metabotropic glutamate receptor 7: at the interface of cognition and emotion. Eur. J. Pharmacol. 639: 123–131. Review.

O'Dell SJ, Weihmuller FB, Marshall JF (1993). Methamphetamine-induced dopamine overflow and injury to striatal dopamine terminals: attenuation by dopamine D1 or D2 antagonists. J. Neurochem. 60: 1792–1799.

Okahisa Y, Ujike H, Kotaka T, Morita Y, Kodama M, Inada T, Yamada M, Iwata N, Iyo M, Sora I, Ozaki N, Kuroda S (2009). Association between neuropeptide Y gene and its receptor Y1 gene and methamphetamine dependence. Psychiatry Clin. Neurosci. 63: 417–422.

Okuyama N, Takagi N, Kawai T, Miyake-Takagi K, Takeo S (2004). Phosphorylation of extracellular-regulating kinase in NMDA receptor antagonist-induced newly generated neurons in the adult rat dentate gyrus. J. Neurochem. 88: 717–725.

O'Mara SM, Rowan MJ, Anwyl R (1995). Metabotropic glutamate receptor-induced homosynaptic long-term depression and depotentiation in the dentate gyrus of the rat hippocampus in vitro. Neuropharmacology 34: 983–989.

Ortiz AA, Milardo LF, DeCarr LB, Buckholz TM, Mays MR, Claus TH, Livingston JN, Mahle CD, Lumb KJ (2007). A novel long-acting selective neuropeptide Y2 receptor polyethylene glycol-conjugated peptide agonist reduces food intake and body weight and improves glucose metabolism in rodents. J. Pharmacol. Exp. Ther. 323: 692–700.

Overstreet-Wadiche LS, Bensen AL, Westbrook GL (2006). Delayed development of adult-generated granule cells in dentate gyrus. J. Neurosci. 26: 2326–2334.

Padgett CL, Lalive AL, Tan KR, Terunuma M, Munoz MB, Pangalos MN, Martínez-Hernández J, Watanabe M, Moss SJ, Luján R, Lüscher C, Slesinger PA (2012). Methamphetamine-evoked depression of GABA(B) receptor signaling in GABA neurons of the VTA. Neuron 73: 978–989.

Papadopoulos GC, Parnavelas JG, Cavanagh ME (1987). Extensive co-existence of neuropeptides in the rat visual cortex. Brain Res. 420: 95–99.

Paredes MF, Greenwood J, Baraban SC (2003). Neuropeptide Y modulates a G protein-coupled inwardly rectifying potassium current in the mouse hippocampus. Neurosci. Lett. 340: 9–12.

Parker RM, Herzog H (1999). Regional distribution of Y-receptor subtype mRNAs in rat brain. Eur. J. Neurosci. 11: 1431–1448.

Pastrana E, Silva-Vargas V, Doetsch F (2011). Eyes wide open: a critical review of sphere-formation as an assay for stem cells. Cell Stem Cell 8: 486–498. Review.

Perez JA Jr, Arsura EL, Strategos S 1999). Methamphetamine-related stroke: four cases. J. Emerg. Med. 17: 469–471.

Picard M (2011). Pathways to aging: the mitochondrion at the intersection of biological and psychosocial sciences. J. Aging Res. 2011: 814096.

Pla P, Orvoen S, Saudou F, David DJ, Humbert S (2014). Mood disorders in Huntington's disease: from behavior to cellular and molecular mechanisms. Front. Behav. Neurosci. 8: 135. Review.

Pöschel B, Manahan-Vaughan D (2005). Group II mGluR-induced long term depression in the dentate gyrus in vivo is NMDA receptor-independent and does not require protein synthesis. Neuropharmacology 1: 1–12.

Price MG, Yoo JW, Burgess DL, Deng F, Hrachovy RA, Frost JD Jr, Noebels JL (2009). A triplet repeat expansion genetic mouse model of infantile spasms syndrome, Arx(GCG)10+7, with interneuronopathy, spasms in infancy, persistent seizures, and adult cognitive and behavioral impairment. J. Neurosci. 29: 8752–8763.

Prickaerts J, Koopmans G, Blokland A, Scheepens A (2004). Learning and adult neurogenesis: survival with or without proliferation? Neurobiol. Learn. Mem. 81: 1–11.

Rabaneda LG, Carrasco M, López-Toledano MA, Murillo-Carretero M, Ruiz FA, Estrada C, Castro C (2008). Homocysteine inhibits proliferation of neuronal precursors in the mouse adult brain by impairing the basic fibroblast growth factor signaling cascade and reducing extracellular regulated kinase 1/2-dependent cyclin E expression. FASEB J. 22: 3823–3835.

Ramirez SH, Potula R, Fan S, Eidem T, Papugani A, Reichenbach N, Dykstra H, Weksler BB, Romero IA, Couraud PO, Persidsky Y (2009). Methamphetamine disrupts blood-brain barrier function by induction of oxidative stress in brain endothelial cells. J. Cereb. Blood Flow Metab. 29: 1933–1945.

Raposinho PD, Broqua P, Hayward A, Akinsanya K, Galyean R, Schteingart C, Junien J, Aubert ML (2000). Stimulation of the gonadotropic axis by the neuropeptide Y receptor Y1 antagonist/Y4 agonist 1229U91 in the male rat. Neuroendocrinology 71: 2–7.

Recinto P, Samant AR, Chavez G, Kim A, Yuan CJ, Soleiman M, Grant Y, Edwards S, Wee S, Koob GF, George O, Mandyam CD (2012). Levels of neural progenitors in the hippocampus predict memory impairment and relapse to drug seeking as a function of excessive methamphetamine self-administration. Neuropsychopharmacology 37: 1275–1287.

Redrobe JP, Dumont Y, Herzog H, Quirion R (2004). Characterization of neuropeptide Y, Y(2) receptor knockout mice in two animal models of learning and memory processing. J. Mol. Neurosci. 22: 159–166.

Richardson HN, Chan SH, Crawford EF, Lee YK, Funk CK, Koob GF, Mandyam CD (2009). Permanent impairment of birth and survival of cortical and hippocampal proliferating cells following excessive drinking during alcohol dependence. Neurobiol. Dis. 36: 1–10.

Riddle EL, Fleckenstein AE, Hanson GR (2006). Mechanisms of methamphetamine-induced dopaminergic neurotoxicity. AAPS J. 8: E413–E418. Review.

Rimondini R, Thorsell A, Heilig M (2005). Suppression of ethanol self-administration by the neuropeptide Y (NPY) Y2 receptor antagonist BIIE0246: evidence for sensitization in rats with a history of dependence. Neurosci. Lett. 375: 129–133.

Rocher C, Gardier AM (2001). Effects of repeated systemic administration of d-Fenfluramine on serotonin and glutamate release in rat ventral hippocampus: comparison with methamphetamine using in vivo microdialysis. Naunyn. Schmiedebergs Arch. Pharmacol. 363: 422–428.

Rodrigo C, Zaben M, Lawrence T, Laskowski A, Howell OW, Gray WP (2010). NPY augments the proliferative effect of FGF2 and increases the expression of FGFR1 on nestin positive postnatal hippocampal precursor cells, via the Y1 receptor. J. Neurochem. 113: 615–627.

Rose PM, Fernandes P, Lynch JS, Frazier ST, Fisher SM, Kodukula K, Kienzle B, Seethala R (1995). Cloning and functional expression of a cDNA encoding a human type 2 neuropeptide Y receptor. J. Biol. Chem. 270: 22661–22664.

Ruscheweyh R, Forsthuber L, Schoffnegger D, Sandkühler J (2007). Modification of classical neurochemical markers in identified primary afferent neurons with Abeta-, Adelta-, and C-fibers after chronic constriction injury in mice. J. Comp Neurol. 502: 325–336.

Rush AM, Wu J, Rowan MJ, Anwyl R (2002). Group I metabotropic glutamate receptor (mGluR)-dependent long-term depression mediated via p38 mitogen-activated protein kinase is inhibited by previous high-frequency stimulation and activation of mGluRs and protein kinase C in the rat dentate gyrus in vitro. J. Neurosci. 22: 6121–6128.

Sahay A, Scobie KN, Hill AS, O'Carroll CM, Kheirbek MA, Burghardt NS, Fenton AA, Dranovsky A, Hen R (2011). Increasing adult hippocampal neurogenesis is sufficient to improve pattern separation. Nature 472: 466–470.

Sajdyk TJ, Vandergriff MG, Gehlert DR (1999). Amygdalar neuropeptide Y Y1 receptors mediate the anxiolytic-like actions of neuropeptide Y in the social interaction test. Eur. J. Pharmacol. 368: 143–147.

Salomoni P, Calegari,F (2010). Cell cycle control of mammalian neural stem cells: putting a speed limit on G1. Trends Cell Biol. 20: 233–243.

Sanai N, Tramontin AD, Quiñones-Hinojosa A, Barbaro NM, Gupta N, Kunwar S, Lawton MT, McDermott MW, Parsa AT, Manuel-García Verdugo J, Berger MS, Alvarez-Buylla A (2004). Unique astrocyte ribbon in adult human brain contains neural stem cells but lacks chain migration. Nature 427: 740–744.

Sandoval V, Hanson GR, Fleckenstein AE (2000). Methamphetamine decreases mouse striatal dopamine transporter activity: roles of hyperthermia and dopamine. Eur. J. Pharmacol. 409: 265–271.

Santos T, Ferreira R, Maia J, Agasse F, Xapelli S, Cortes L, Bragança J, Malva JO, Ferreira L, Bernardino L (2012). Polymeric nanoparticles to control the differentiation of neural stem cells in the subventricular zone of the brain. ACS Nano 6: 10463–10474.

Scanziani M (2000). GABA spillover activates postsynaptic GABA(B) receptors to control rhythmic hippocampal activity. Neuron 25: 673–681.

Schaefers AT, Teuchert-Noodt G, Bagorda F, Brummelte S (2009). Effect of postnatal methamphetamine trauma and adolescent methylphenidate treatment on adult hippocampal neurogenesis in gerbils. Eur. J. Pharmacol. 616: 86–90.

Schinder AF, Olson EC, Spitzer NC, Montal M (1996). Mitochondrial dysfunction is a primary event in glutamate neurotoxicity. J. Neurosci. 16: 6125–6133.

Schmidt-Hieber C, Jonas P, Bischofberger J (2004). Enhanced synaptic plasticity in newly generated granule cells of the adult hippocampus. Nature 429: 184–187.

Schultz W (2007). Multiple dopamine functions at different time courses. Annu. Rev. Neurosci. 30: 259–88. Review.

Schwartzberg M, Unger J, Weindl A, Lange W (1990). Distribution of neuropeptide Y in the prosencephalon of man and cotton-head tamarin (Saguinus oedipus): colocalization with somatostatin in neurons of striatum and amygdala. Anat. Embryol. (Berl). 181: 157–166.

Setou M, Nakagawa T, Seog DH, Hirokawa N (2000). Kinesin superfamily motor protein KIF17 and mLin-10 in NMDA receptor-containing vesicle transport. Science 288: 1796–1802.

Sharma HS, Ali SF (2006). Alterations in blood-brain barrier function by morphine and methamphetamine. Ann. N. Y. Acad. Sci. 1074: 198–224.

Shigemoto R, Kinoshita A, Wada E, Nomura S, Ohishi H, Takada M, Flor PJ, Neki A, Abe T, Nakanishi S, Mizuno N (1997). Differential presynaptic localization of metabotropic glutamate receptor subtypes in the rat hippocampus. J. Neurosci. 17: 7503–7522.

Shoblock JR, Welty N, Nepomuceno D, Lord B, Aluisio L, Fraser I, Motley ST, Sutton SW, Morton K, Galici R, Atack JR, Dvorak L, Swanson DM, Carruthers NI, Dvorak C, Lovenberg TW, Bonaventure P (2010). In vitro and in vivo characterization of JNJ-31020028 (N-(4-{4-[2-(diethylamino)-2-oxo-1-phenylethyl]piperazin-1-yl}-3-fluorophenyl)-2-pyridin-3-ylbenzamide), a selective brain penetrant small molecule antagonist of the neuropeptide Y Y(2) receptor. Psychopharmacology (Berl) 208: 265–277.

Silber BY, Croft RJ, Papafotiou K, Stough C (2006). The acute effects of d-amphetamine and methamphetamine on attention and psychomotor performance. Psychopharmacology (Berl) 187: 154–169.

Silva AP (2003). Neurotoxicity and neuroprotection in the hippocampus: Role of neuropeptide Y receptors. *Ph.D Thesis*.

Silva AP, Carvalho AP, Carvalho CM, Malva JO (2001). Modulation of intracellular calcium changes and glutamate release by neuropeptide Y1 and Y2 receptors in the rat hippocampus: differential effects in CA1, CA3 and dentate gyrus. J. Neurochem. 79: 286–296.

Silva AP, Carvalho AP, Carvalho CM, Malva JO (2003b). Functional interaction between neuropeptide Y receptors and modulation of calcium channels in the rat hippocampus. Neuropharmacology 44: 282–292.

Silva AP, Lourenço J, Xapelli S, Ferreira R, Kristiansen H, Woldbye DP, Oliveira CR, Malva JO (2007). Protein kinase C activity blocks neuropeptide Y-mediated inhibition of

glutamate release and contributes to excitability of the hippocampus in status epilepticus. FASEB J. 21: 671–681.

Silva AP, Martins T, Baptista S, Gonçalves J, Agasse F, Malva JO (2010). Brain injury associated with widely abused amphetamines: neuroinflammation, neurogenesis and blood-brain barrier. Curr. Drug Abuse. Rev. 3: 239–254. Review.

Silva AP, Pinheiro PS, Carvalho AP, Carvalho CM, Jakobsen B, Zimmer J, Malva JO (2003a). Activation of neuropeptide Y receptors is neuroprotective against excitotoxicity in organotypic hippocampal slice cultures. FASEB J. 17: 1118–1120.

Silva AP, Xapelli S, Grouzmann E, Cavadas C (2005a). The putative neuroprotective role of neuropeptide Y in the central nervous system. Curr. Drug. Targets CNS Neurol. Disord. 4: 331–347. Review.

Silva AP., Xapelli S, Pinheiro PS, Ferreira R, Lourenço J, Cristóvão A, Grouzmann E, Cavadas C, Oliveira CR, Malva JO (2005b). Up-regulation of neuropeptide Y levels and modulation of glutamate release through neuropeptide Y receptors in the hippocampus of kainate-induced epileptic rats. J. Neurochem. 93: 163–170.

Simões PF, Silva AP, Pereira FC, Marques E, Grade S, Milhazes N, Borges F, Ribeiro CF, Macedo TR (2007). Methamphetamine induces alterations on hippocampal NMDA and AMPA receptor subunit levels and impairs spatial working memory. Neuroscience 150: 433–441.

Simon SL, Domier C, Carnell J, Brethen P, Rawson R, Ling W (2000). Cognitive impairment in individuals currently using methamphetamine. Am. J. Addict. 9: 222–231.

Smith KJ, Butler TR, Prendergast MA (2010). Inhibition of sigma-1 receptor reduces N-methyl-D-aspartate induced neuronal injury in methamphetamine-exposed and-naive hippocampi. Neurosci. Lett. 481: 144–148.

Snyder JS, Glover LR, Sanzone KM, Kamhi JF, Cameron HA (2009). The effects of exercise and stress on the survival and maturation of adult-generated granule cells. Hippocampus 19: 898–906.

Snyder JS, Soumier A, Brewer M, Pickel J, Cameron HA (2011). Adult hippocampal neurogenesis buffers stress responses and depressive behaviour. Nature 476: 458–461.

Song H, Stevens CF, Gage FH (2002). Astroglia induce neurogenesis from adult neural stem cells. Nature 417: 39–44.

Song J, Zhong C, Bonaguidi MA, Sun GJ, Hsu D, Gu Y, Meletis K, Huang ZJ, Ge S, Enikolopov G, Deisseroth K, Luscher B, Christian KM, Ming GL, Song H (2012). Neuronal circuitry

mechanism regulating adult quiescent neural stem-cell fate decision. Nature 489: 150–154.

Sørensen G, Jensen M, Weikop P, Dencker D, Christiansen SH, Loland CJ, Bengtsen CH, Petersen JH, Fink-Jensen A, Wörtwein G, Woldbye DP (2012). Neuropeptide Y Y5 receptor antagonism attenuates cocaine-induced effects in mice. Psychopharmacology (Berl) 222: 565–577.

Soscia SJ, Harrington ME (2005). Neuropeptide Y does not reset the circadian clock in NPY Y2-/- mice. Neurosci. Lett. 373: 175–178.

Spalding KL, Bergmann O, Alkass K, Bernard S, Salehpour M, Huttner HB, Boström E, Westerlund I, Vial C, Buchholz BA, Possnert G, Mash DC, Druid H, Frisén J (2013). Dynamics of hippocampal neurogenesis in adult humans. Cell 153: 1219–1227.

Spampanato J, Sullivan RK, Turpin FR, Bartlett PF, Sah P (2012). Properties of doublecortin expressing neurons in the adult mouse dentate gyrus. PLoS One 7: e41029.

Sparrow AM, Lowery-Gionta EG, Pleil KE, Li C, Sprow GM, Cox BR, Rinker JA, Jijon AM, Peňa J, Navarro M, Kash TL, Thiele TE (2012). Central neuropeptide Y modulates binge-like ethanol drinking in C57BL/6J mice via Y1 and Y2 receptors. Neuropsychopharmacology 37: 1409–1421.

Sriram K, Miller DB, O'Callaghan JP (2006). Minocycline attenuates microglial activation but fails to mitigate striatal dopaminergic neurotoxicity: role of tumor necrosis factor-alpha. J. Neurochem. 96: 706–718.

Stanić D, Brumovsky P, Fetissov S, Shuster S, Herzog H, Hökfelt T (2006). Characterization of neuropeptide Y2 receptor protein expression in the mouse brain. I. Distribution in cell bodies and nerve terminals. J. Comp. Neurol. 499: 357–390.

Stanić D, Mulder J, Watanabe M, Hökfelt T (2011). Characterization of NPY Y2 receptor protein expression in the mouse brain. II. Coexistence with NPY, the Y1 receptor, and other neurotransmitter-related molecules. J. Comp. Neurol. 519: 1219–1257.

Steiner B, Zurborg S, Hörster H, Fabel K, Kempermann G (2008). Differential 24 h responsiveness of Prox1-expressing precursor cells in adult hippocampal neurogenesis to physical activity, environmental enrichment, and kainic acid-induced seizures. Neuroscience 154: 521–529.

Sudai E, Croitoru O, Shaldubina A, Abraham L, Gispan I, Flaumenhaft Y, Roth-Deri I, Kinor N, Aharoni S, Ben-Tzion M, Yadid G (2011). High cocaine dosage decreases neurogenesis in the hippocampus and impairs working memory. Addict. Biol. 16: 251–260.

Sugaya Y, Maru E, Kudo K, Shibasaki T, Kato N (2010). Levetiracetam suppresses development of spontaneous EEG seizures and aberrant neurogenesis following kainate-induced status epilepticus. Brain Res. 1352: 187–199.

Suh H, Consiglio A, Ray J, Sawai T, D'Amour KA, Gage FH (2007). In vivo fate analysis reveals the multipotent and self-renewal capacities of Sox2+ neural stem cells in the adult hippocampus. Cell Stem Cell 1: 515–528.

Swanson DM, Wong VD, Jablonowski JA, Shah C, Rudolph DA, Dvorak CA, Seierstad M, Dvorak LK, Morton K, Nepomuceno D, Atack JR, Bonaventure P, Lovenberg TW, Carruthers NI (2011). The discovery and synthesis of JNJ 31020028, a small molecule antagonist of the Neuropeptide Y Y_2 receptor. Bioorg. Med. Chem. Lett. 21: 5552–5556.

Swant J, Chirwa S, Stanwood G, Khoshbouei H (2010). Methamphetamine reduces LTP and increases baseline synaptic transmission in the CA1 region of mouse hippocampus. PLoS One 5: e11382.

Sweatt JD (2001). The neuronal MAP kinase cascade: a biochemical signal integration system subserving synaptic plasticity and memory. J. Neurochem. 76: 1–10. Review.

Taffe MA, Kotzebue RW, Crean RD, Crawford EF, Edwards S, Mandyam CD (2010). Long-lasting reduction in hippocampal neurogenesis by alcohol consumption in adolescent nonhuman primates. Proc. Natl. Acad. Sci. U. S. A. 107: 11104–11109.

Takayasu T, Ohshima T, Nishigami J, Kondo T, Nagano T (1995). Screening and determination of methamphetamine and amphetamine in the blood, urine and stomach contents in emergency medical care and autopsy cases. J. Clin. Forensic. Med. 2: 25–33.

Tasan RO, Nguyen NK, Weger S, Sartori SB, Singewald N, Heilbronn R, Herzog H, Sperk G (2010). The central and basolateral amygdala are critical sites of neuropeptide Y/Y2 receptor-mediated regulation of anxiety and depression. J. Neurosci. 30: 6282–6290.

Tashiro A, Makino H, Gage FH (2007). Experience-specific functional modification of the dentate gyrus through adult neurogenesis: a critical period during an immature stage. J. Neurosci. 27: 3252–3259.

Tata DA, Yamamoto BK (2007). Interactions between methamphetamine and environmental stress: role of oxidative stress, glutamate and mitochondrial dysfunction. Addiction 1: 49–60. Review.

Tata DA, Yamamoto BK (2008). Chronic stress enhances methamphetamine-induced extracellular glutamate and excitotoxicity in the rat striatum. Synapse 62: 325–336.

Tatemoto K (1982a). Neuropeptide Y: complete amino acid sequence of the brain peptide. Proc. Natl. Acad. Sci. U. S. A. 79: 5485–5489.

Tatemoto K, Carlquist M, Mutt V (1982b). Neuropeptide Y-a novel brain peptide with structural similarities to peptide YY and pancreatic polypeptide. Nature 296: 659–660.

Teuchert-Noodt G, Dawirs RR, Hildebrandt K (2000). Adult treatment with methamphetamine transiently decreases dentate granule cell proliferation in the gerbil hippocampus. J. Neural Transm. 107: 133–143.

Thiriet N, Agasse F, Nicoleau C, Guégan C, Vallette F, Cadet JL, Jaber M, Malva JO, Coronas V (2011). NPY promotes chemokinesis and neurogenesis in the rat subventricular zone. J. Neurochem. 116: 1018–1027.

Thiriet N, Deng X, Solinas M, Ladenheim B, Curtis W, Goldberg SR, Palmiter RD, Cadet JL (2005). Neuropeptide Y protects against methamphetamine-induced neuronal apoptosis in the mouse striatum. J. Neurosci. 25: 5273–5279.

Thomas DM, Dowgiert J, Geddes TJ, Francescutti-Verbeem D, Liu X, Kuhn DM (2004). Microglial activation is a pharmacologically specific marker for the neurotoxic amphetamines. Neurosci. Lett. 367: 349–354.

Thomas GM, Huganir RL (2004). MAPK cascade signalling and synaptic plasticity. Nat. Rev. Neurosci. 5: 173–183. Review.

Thompson PM, Hayashi KM, Simon SL, Geaga JA, Hong MS, Sui Y, Lee JY, Toga AW, Ling W, London ED (2004). Structural abnormalities in the brains of human subjects who use methamphetamine. J. Neurosci. 24: 6028–6036.

Tian C, Murrin LC, Zheng JC (2009). Mitochondrial fragmentation is involved in methamphetamine-induced cell death in rat hippocampal neural progenitor cells. PLoS One 4: e5546.

Tocharus J, Khonthun C, Chongthammakun S, Govitrapong P (2010). Melatonin attenuates methamphetamine-induced overexpression of pro-inflammatory cytokines in microglial cell lines. J. Pineal. Res. 48: 347–352.

Toni N, Laplagne DA, Zhao C, Lombardi G, Ribak CE, Gage FH, Schinder AF (2008). Neurons born in the adult dentate gyrus form functional synapses with target cells. Nat. Neurosci. 11: 901–907.

Toth PT, Bindokas VP, Bleakman D, Colmers WF, Miller RJ (1993). Mechanism of presynaptic inhibition by neuropeptide Y at sympathetic nerve terminals. Nature 364: 635–639.

Tozuka Y, Fukuda S, Namba T, Seki T, Hisatsune T (2005). GABAergic excitation promotes neuronal differentiation in adult hippocampal progenitor cells. Neuron 47: 803–815.

Tsien JZ, Huerta PT, Tonegawa S (1996). The essential role of hippocampal CA1 NMDA receptor-dependent synaptic plasticity in spatial memory. Cell 87: 1327–1338.

United Nations Office on Drugs and Crime (UNODC). World Drug Report 2011. United Nations Publication; 2011.

Urbach A, Redecker C, Witte OW (2008). Induction of neurogenesis in the adult dentate gyrus by cortical spreading depression. Stroke 39: 3064–3072.

van Praag H, Schinder AF, Christie BR, Toni N, Palmer TD, Gage FH (2002). Functional neurogenesis in the adult hippocampus. Nature 415: 1030–1034.

Vanderheyden PM, Van Liefde I, De Backer JP, Vauquelin G (1997). Non-competitive binding of the nonpeptide antagonist BIBP3226 to rat forebrain neuropeptide Y1 receptors. Eu.r J. Pharmacol. 331: 275–284.

Venkatesan A, Uzasci L, Chen Z, Rajbhandari L, Anderson C, Lee MH, Bianchet MA, Cotter R, Song H, Nath A (2011). Impairment of adult hippocampal neural progenitor proliferation by methamphetamine: role for nitrotyrosination. Mol. Brain 4: 28.

Vivar C, Potter MC, Choi J, Lee JY, Stringer TP, Callaway EM, Gage FH, Suh H, van Praag H (2012). Monosynaptic inputs to new neurons in the dentate gyrus. Nat. Commun. 3: 1107.

Voisin T, Goumain M, Lorinet AM, Maoret JJ, Laburthe M (2000). Functional and molecular properties of the human recombinant Y4 receptor: resistance to agonist-promoted desensitization. J. Pharmacol. Exp. Ther. 292: 638–646.

Wan CP, Lau BH (1995). Neuropeptide Y receptor subtypes. Life Sci. 56: 1055–1064. Review.

Westwood SC, Hanson GR (1999). Effects of stimulants of abuse on extrapyramidal and limbic neuropeptide Y systems. J. Pharmacol. Exp. Ther. 288: 1160–1166.

Wieland HA, Engel W, Eberlein W, Rudolf K, Doods HN (1998). Subtype selectivity of the novel nonpeptide neuropeptide Y Y1 receptor antagonist BIBO 3304 and its effect on feeding in rodents. Br. J. Pharmacol. 125: 549–555.

Wolak ML, DeJoseph MR, Cator AD, Mokashi AS, Brownfield MS, Urban JH (2003). Comparative distribution of neuropeptide Y Y1 and Y5 receptors in the rat brain by using immunohistochemistry. J. Comp. Neurol. 464: 285–311.

Woldbye DP, Angehagen M, Gøtzsche CR, Elbrønd-Bek H, Sørensen AT, Christiansen SH, Olesen MV, Nikitidou L, Hansen TV, Kanter-Schlifke I, Kokaia M (2010). Adeno-associated viral vector-induced overexpression of neuropeptide Y Y2 receptors in the hippocampus suppresses seizures. Brain 133: 2778–2788.

Woldbye DP, Larsen PJ, Mikkelsen JD, Klemp K, Madsen TM, Bolwig TG (1997). Powerful inhibition of kainic acid seizures by neuropeptide Y via Y5-like receptors. Nat. Med. 3: 761–764.

Woldbye DP, Nanobashvili A, Sørensen AT, Husum H, Bolwig TG, Sørensen G, Ernfors P, Kokaia M (2005). Differential suppression of seizures via Y2 and Y5 neuropeptide Y receptors. Neurobiol. Dis. 20: 760–772.

Wu CW, Ping YH, Yen JC, Chang CY, Wang SF, Yeh CL, Chi CW, Lee HC (2007). Enhanced oxidative stress and aberrant mitochondrial biogenesis in human neuroblastoma SH-SY5Y cells during methamphetamine induced apoptosis. Toxicol. Appl. Pharmacol. 220: 243–251.

Wu J, Wang Y, Rowan MJ, Anwyl R (1998). Evidence for involvement of the cGMP-protein kinase G signaling system in the induction of long-term depression, but not long-term potentiation, in the dentate gyrus in vitro. J. Neurosci. 18: 3589–3596.

Xapelli S, Agasse F, Sardà-Arroyo L, Bernardino L, Santos T, Ribeiro FF, Valero J, Bragança J, Schitine C, de Melo Reis RA, Sebastião AM, Malva JO (2013). Activation of type 1 cannabinoid receptor (CB1R) promotes neurogenesis in murine subventricular zone cell cultures. PLoS One 8: e63529.

Xapelli S, Silva AP, Ferreira R, Malva JO (2007). Neuropeptide Y can rescue neurons from cell death following the application of an excitotoxic insult with kainite in rat organotypic hippocampal slice cultures. Peptides 28: 288–294.

Xiao Z, Kong Y, Yang S, Li M, Wen J, Li L (2007). Upregulation of Flk-1 by bFGF via the ERK pathway is essential for VEGF-mediated promotion of neural stem cell proliferation. Cell Res. 17: 73–79.

Xu JC, Bernreuther C, Cui YF, Jakovcevski I, Hargus G, Xiao MF, Schachner M (2011). Transplanted L1 expressing radial glia and astrocytes enhance recovery after spinal cord injury. J. Neurotrauma 28: 1921–1937.

Yamaguchi M, Suzuki T, Seki T, Namba T, Juan R, Arai H, Hori T, Asada T (2004). Repetitive cocaine administration decreases neurogenesis in adult rat hippocampus. Ann. N. Y. Acad. Sci. 1025: 351–362.

Yamaguchi T, Kuraishi Y, Minami M, Nakai S, Hirai Y, Satoh M (1991). Methamphetamine-induced expression of interleukin-1 beta mRNA in the rat hypothalamus. Neurosci. Lett. 128: 90–92.

Yamamoto BK, Moszczynska A, Gudelsky GA (2010). Amphetamine toxicities: classical and emerging mechanisms. Ann. N. Y. Acad. Sci. 1187: 101–121. Review.

Yamamoto BK, Zhu W (1998). The effects of methamphetamine on the production of free radicals and oxidative stress. J. Pharmacol. Exp. Ther. 287: 107–114.

Yamamoto H, Imai K, Kamegaya E, Takamatsu Y, Irago M, Hagino Y, Kasai S, Shimada K, Yamamoto T, Sora I, Koga H, Ikeda K (2006). Repeated methamphetamine

administration alters expression of the NMDA receptor channel epsilon2 subunit and kinesins in the mouse brain. Ann. N. Y. Acad. Sci. 1074: 97–103.

Yamamoto H, Kitamura N, Lin XH, Ikeuchi Y, Hashimoto T, Shirakawa O, Maeda K (1999). Differential changes in glutamatergic transmission via N-methyl-D-aspartate receptors in the hippocampus and striatum of rats behaviourally sensitized to methamphetamine. Int. J. Neuropsychopharmacol 2: 155–163.

Yassa MA, Stark CE (2011). Pattern separation in the hippocampus. Trends Neurosci. 34: 515–525.

Yeckel MF, Kapur A, Johnston D (1999). Multiple forms of LTP in hippocampal CA3neurons use a common postsynaptic mechanism. Nat. Neurosci. 2: 625–633.

Yoshihara T, Honma S, Mitome M, Honma K (1996). Methamphetamine stimulates the release of neuropeptide Y and noradrenaline from the paraventricular nucleus in rats. Brain Res. 707: 119–121.

Yuan CJ, Quiocho JM, Kim A, Wee S, Mandyam CD (2011). Extended access methamphetamine decreases immature neurons in the hippocampus which results from loss and altered development of neural progenitors without altered dynamics of the S-phase of the cell cycle. Pharmacol. Biochem. Behav. 100: 98–108.

Zakharenko SS, Zablow L, Siegelbaum SA (2001). Visualization of changes in presynaptic function during long-term synaptic plasticity. Nat. Neurosci. 4: 711–717.

Zhao C, Teng EM, Summers RG Jr, Ming GL, Gage FH (2006). Distinct morphological stages of dentate granule neuron maturation in the adult mouse hippocampus. J. Neurosci. 26: 3–11.

Zheng W, Zhuge Q, Zhong M, Chen G, Shao B, Wang H, Mao X, Xie L, Jin K (2013). Neurogenesis in Adult Human Brain after Traumatic Brain Injury. J. Neurotrauma 30: 1872–1880.

Ziemek R, Schneider E, Kraus A, Cabrele C, Beck-Sickinger AG, Bernhardt G, Buschauer A (2007). Determination of affinity and activity of ligands at the human neuropeptide Y Y4 receptor by flow cytometry and aequorin luminescence. J. Recept. Signal Transduct. Res. 27: 217–233.

Zou C, Kumaran S, Markovic S, Walser R, Zerbe O (2008). Studies of the structure of the N-terminal domain from the Y4 receptor - a G protein-coupled receptor – and its interaction with hormones from the NPY family. Chembiochem. 9: 2276–2284.